University of Alberta

Definition of the degeneration phenotype in Light-Induced Retinal Degeneration in Rats, a model system of human retinal dystrophy

Michelle Louise Patterson ©

A thesis submitted to the Faculty of Graduate Studies and Research in partial fulfillment of the requirements for the degree of Doctor of Philosophy

in

Molecular Biology and Genetics

Department of Biological Sciences
Edmonton, AB

Fall 2005

Library and
Archives Canada

Published Heritage
Branch

395 Wellington Street
Ottawa ON K1A 0N4
Canada

Bibliothèque et
Archives Canada

Direction du
Patrimoine de l'édition

395, rue Wellington
Ottawa ON K1A 0N4
Canada

0-494-08713-7

Your file Votre référence
ISBN:
Our file Notre reference
ISBN:

NOTICE:
The author has granted a non-exclusive license allowing Library and Archives Canada to reproduce, publish, archive, preserve, conserve, communicate to the public by telecommunication or on the Internet, loan, distribute and sell theses worldwide, for commercial or non-commercial purposes, in microform, paper, electronic and/or any other formats.

The author retains copyright ownership and moral rights in this thesis. Neither the thesis nor substantial extracts from it may be printed or otherwise reproduced without the author's permission.

AVIS:
L'auteur a accordé une licence non exclusive permettant à la Bibliothèque et Archives Canada de reproduire, publier, archiver, sauvegarder, conserver, transmettre au public par télécommunication ou par l'Internet, prêter, distribuer et vendre des thèses partout dans le monde, à des fins commerciales ou autres, sur support microforme, papier, électronique et/ou autres formats.

L'auteur conserve la propriété du droit d'auteur et des droits moraux qui protège cette thèse. Ni la thèse ni des extraits substantiels de celle-ci ne doivent être imprimés ou autrement reproduits sans son autorisation.

In compliance with the Canadian Privacy Act some supporting forms may have been removed from this thesis.

While these forms may be included in the document page count, their removal does not represent any loss of content from the thesis.

Conformément à la loi canadienne sur la protection de la vie privée, quelques formulaires secondaires ont été enlevés de cette thèse.

Bien que ces formulaires aient inclus dans la pagination, il n'y aura aucun contenu manquant.

Canada

Abstract:

Light-induced retinal degeneration in rats (LIRD) is a well-studied model of human retinal degeneration, which employs the use of intense light to induce photoreceptor apoptosis. LIRD is known to involve the bleaching of rhodopsin, the induction of an oxidative stress environment, changes in gene expression and photoreceptor cell loss via apoptosis. To identify and characterize the some molecular changes associated with LIRD, a cDNA library was constructed from light-treated rat retinae representing the active execution phase of cell death. Differential cross screening identified numerous genes induced or repressed during LIRD. Bioinfomatic characterization of these genes demonstrated that the molecular changes in LIRD represent a global cellular response of ubiquitously expressed genes.

One novel gene, showing repression following light exposure, demonstrated significant homology to the yeast diphthamide methyltransferase (Dph5). Dph5 modifies EF-2, resulting in an increased sensitivity to ADP-ribosylation, EF-2 inactivation, and termination of translation. Gene and protein structure of the rat Dph was determined, and comparisons with known orthologs demonstrated a high degree of sequence conservation. Using a yeast cell line lacking Dph5, we were able to demonstrate that a lack of Dph5 expression was associated with an increased sensitivity to an oxidative stress environment. The increased cell loss in response to oxidative stress was the result of apoptotic cell death as determined by transmission electron microscopy.

In addition, several of proteins encoded by the LIRD genes contained putative caspase cut sites, and/or were known targets of the caspase cascade. Analysis of the various members of the caspase cascade demonstrated that numerous branches of the

cascade were proteolytically activated during LIRD and were localized to the photoreceptor cell layer. The activation of the caspases was demonstrated to coincide with changes in photoreceptor cell gene expression and to precede DNA fragmentation indicative of apoptotic cell death.

These results have provided novel information in regards to the underlying mechanism associated with apoptosis in LIRD, and have demonstrated that cell death in this system is the result of complex cellular changes and regulation of gene expression at the transcriptional, translational and post-translational levels.

ACKNOWLEDGEMENTS

There are numerous people who contributed to this thesis, directly and indirectly. I would like to thank:

My amazing husband Gerry: for your love, support, encouragement and sense of humor through all of this. You are my rock, and my best friend. I couldn't have done this without you.

My parents, Al and Louise Chambers; my grandparents, John and Cecelia Asher; and the rest of my family (Frank and Karen Patterson; Mary, John and Angela Emmons; Craig, Sarah, Brooke, and Josh Chambers; Lorraine and Paul Delano; Danielle Chambers and Clint Olson; Shannon Patterson and Randy Paquette) and all of my wonderful friends: for your continued love and support, and faith that I could do this.

Dr. Jack Von Borstel: for your kindness, enthusiasm for science, and for kindly pestering my everyday in the hall until I agreed to do this.

Ron Koss: for being one of the kindest people at U of A, for being wonderful to work with and for all of your time and effort that made the yeast TEM work possible. Thank you for always being my friend and cheering squad.

Dr. Daniel Organisciak, Ruth Darrow, and Linda Barsalou: for providing rat retinal tissue and much appreciated guidance and support throughout this project. Thank you so much!

Dr. Rakesh Bhatnagar, Jack Scott and Randy Mandryk of the Microscopy Unit/ Bio-DiTRL, for your invaluable technical support and knowledge, and patience as you taught me the finer points of microscopy.

Laith Dabbagh at the Cross-Cancer Institute: for your very generous help with sectioning of rat retinae for immunohistochemistry.

Pat Murray and Lisa Ostafichuk in the Molecular Biology Service Unit: for the countless hours of sequencing that made this project possible.

Gwen Jewitt, Michelle Green and Chesceri Mason: for always being there to help, especially in a crisis.

Members of the Wong lab, past and present: for making my time in the lab productive, and enjoyable. Thank you for all your help.

Dr. David McLaughlin and Dr. Christina Popesu at Grant MacEwan College: for your assistance in statistical analysis of the data from this project.

For my friends and colleagues at Grant MacEwan College: for your encouragement, patience, and support over the last few years. And for giving me the opportunity to prove myself as an instructor.

My committee: Dr. Ian MacDonald, Dr. Roseline Godbout, Dr. William Stell, and Dr. John Bell: for your time, effort, and attention to detail in reading through my thesis, and for your guidance and support through out this project. I especially want to thank Dr. Roseline Godbout for going above and beyond the duties of a committee member, for spending hours helping me edit and revise my thesis, and for always being so kind and encouraging. I can't thank you enough.

And last but not least, my "tyrant of a boss" Dr. Paul Wong: Thank you for your generosity, kindness and patience, your never ending supply of chocolate in the lab; your sense of humor, your unique perspective, and for always being there to listen, guide and challenge me. Thank you for letting me stand on my own, make my own decisions, and learn from my mistakes. Thank you for making this a positive and worth while experience. But mostly, thank you for being a truly kind hearted and wonderful person. It has been a pleasure to work with you! Thank you.

TABLE OF CONTENTS PAGE...

Chapter 1. Introduction 2

1.A. INTRODUCTION 2

1.A-1. The mammalian eye 2

1.A-2. Types and spatial organization of cells of the mammalian retina 2

1.A-3. Photoreceptor cells 6

1.A-4. Phototransduction 7

1.A-5. Retinitis pigmentosa and macular degeneration 10

1.A-6. Apoptosis in retinal degeneration 13

1.A-7. Animal models of retinal disease 15

1.B. LIGHT-INDUCED RETINAL DAMAGE (LIRD) 17

1.B-1. LIRD: Background and current state of knowledge 18

1. B-1a. Role of rhodopsin bleaching in LIRD 18

1.B-1b. The role of oxidative stress in LIRD 22

1.B-1c. The role of differential gene expression 26

1.B-1d. Other factors affecting LIRD 29

1.B-1d-i. Interactions between cell populations during LIRD 29

1.B-1d-ii. Genetic background 30

1.C. PROJECT DESIGN 31

1.C-1. Practical considerations in experimental design 31

1.C-1a. Nature of light exposure used in current study 31

1.C-1b. Rearing conditions 35

1.C-1b-i. Changes in rhodopsin levels and organization 37

1.C-1b-ii. Changes in gene expression of phototransduction-related genes 37

1.C-1b-iii. Changes in levels of oxidative-stress related factors 38

1.C-1b.iv. Changes in OS membrane structure and composition 38

1.C-1c. Use of rats during LIRD 39

1.C-1d. Time of light exposure 40

1.C-2.Prelimary studies 40

1.C-3. Rationale for the use of LIRD in the study of retinal disease 43

1.C-3a. Similarities between photoreceptor cell loss in LIRD and human retinal dystrophy 43

1.C-3b. Advantages of the use of LIRD over other models of retinal dystrophy 45

1.C-3c. Advantages and disadvantages of using dark-reared controls in LIRD 47

1D. DEFINITION OF THE DEGENERATION PHENOTYPE IN LIGHT-INDUCED RETINAL DEGENERATION IN RATS, A MODEL SYSTEM OF HUMAN RETINAL DYSTROPHY 48

1.D-1. Focus of thesis 48

1.D-1a. Objectives 48

1.D-1b. Hypothesis 49

1.D-2. Experimental approach and rationale 49

1.B-2a. Chapter 3: Activation of members of the caspase cascade in the rod outer segments by intense green light-induced retinal degeneration 49

1.B.-2b Chapter 4: Identification and bioinformatic characterization of differentially expressed LIRD genes 50

1.D-2c. Chapter 5: Identification of a novel rat diphthamide methyltransferase, which plays a role in oxidative stress-induced cell death 50

Chapter 2. Materials and Methods 51

2.A. PREPARATION OF ANIMALS 52

2.B. ISOLATION OF NUCLEIC ACID 54

2.B-1. Isolation of RNA 54

2.B-1a. Isolation of total RNA 54

2.B-1b. Isolation of mRNA 55

2.B-2. Isolation of DNA 56

2.B-2a. Isolation of genomic DNA from blood 56

2.B-2b. Isolation of genomic DNA from tissue 57

2.B-2c. Isolation of plasmid DNA 57

2.B-2d. Isolation of PCR products 58

2.B-2e. Isolation of cDNA 60

2.C. ISOLATION OF PROTEINS 60

2.D. QUANTIFICATION OF NUCLEIC ACID AND PROTEINS 61

2.D-1. Quantification of nucleic acids 61

2.D-1a. Quantification of nucleic acids using a spectrophotomer 61

2.D-1b. Quantification of nucleic acids on ethidium bromide plates 62

2.D-2. Quantification of Proteins 62

2.E. CONSTRUCTION OF A cDNA LIBRARY 63

- 2.E-1. First strand cDNA synthesis 63
- 2.E-2. Second strand cDNA synthesis 66
- 2.E-3. Blunting the cDNA termini 67
- 2.E-4. Ligating EcoR1 adaptors 67
- 2.E-5. Phosphorylating the EcoR1 ends 68
- 2.E-6. Digestion with Xho 68
- 2.E-7. Size fractionation of cDNA 68
- 2.E-8. Ligating cDNA into the Uni-ZAP XR vector 69
- 2.E-9. Packaging the Phage 70
- 2.E-10. Plating of the cDNA library 72
- 2.E-11. Amplification of the cDNA library 73
- 2.E-12. Isolation of individual plaques 74
- 2.E-13. Making of phagemids and clone stocks 74
- 2.F. TRANSFORMATIONS 75
  - 2.F-1. Transformation of bacterial cells 75
    - 2.F-1a. Construction of competent cells 75
    - 2.F-1b. Transformation of bacterial competent cells with plasmid DNA 76

2.G. cDNA SYNTHESIS 76

2.H. HYBIDIZATION USING RADIOACTIVELY LABELED DNA PROBES 79

- 2.H-1. Radioactive labeling of probes 79
- 2.H-2. Hybridization of membranes 80

2.I. SCREENING OF THE EXECUTION PHASE cDNA LIBRARY 81

2.I-1. Primary Screen 81

  2.I-1a. Plaque lifts 81

  2.I-1b. Differential screening of plaque lifts 84

2.I-2. Secondary screen of execution phase library 84

2.I-3 Tertiary screen of the execution phase library 85

2.J. POLYMERASE CHAIN REACTION 85

2.J-1. Designing PCR primers 85

2.J-2. Polymerase Chain Reaction using Taq polymerase 86

2.J-3. Polymerase Chain Reaction using Platinum Pfx polymerase 88

2.J-4. Polymerase Chain Reaction Amplification Cycle 88

2.K. ELECTROPHORESIS 88

2.K-1. Electrophoresis of DNA 88

  2.K-1a. Alkaline gel electrophoresis for the analysis of cDNA 88

  2.K-1b. Standard gel electrophoresis 89

2.K-2. Electrophoresis of RNA 90

  2.K-2a. Preparation of formaldehyde gels 90

  2.K-2b Preparation of RNA samples 90

  2.K-2c. Running of formaldehyde gels 90

2.K-3. Electrophoresis of proteins 91

  2.K-3a. Preparation of SDS polyacrylamide gels (PAGE) 91

  2.K-3b. Preparation of samples 92

  2.K-3c. Running of SDS-PAGE gels 92

2.L. SOUTHERN BLOT ANALYSIS 92

2.L-1. Southern blot transfer 92

2.L-2. Southern blot analysis 93

2.M. NORTHERN BLOT ANALYSIS 93

2.M-1. Northern blot transfer 93

2.M-2 Northern blot analysis 94

2.N. WESTERN BLOT ANALYSIS 95

2.N-1. Western blot transfer 95

2.N-2. Western blot analysis of proteins 95

2.O. DNA SEQUENCING 96

2.O-1. Manual DNA Sequencing 96

2.O-1a. Preparation of samples 96

2.O-1b. Preparation of polyacrylamide sequencing gels 98

2.O-2. Automated DNA sequencing 99

2.P. BIOINFORMATIC ANALYSIS 99

2.P-1. Key web-sites used for bioinformatic analysis 99

2.P-2. Development of Sitefind program 100

2.Q. IMMUNOFLUORESCENCE 100

2.Q-1. Isolation of optic cups 100

2.Q-2. Fixation 102

2.Q-3. Cryosectioning of the rat retina 102

2.Q-4. Immunohistochemisty on frozen sections 103

2.Q-5. Haematoxylin and acidified eosin staining of sections 103

2.R. FUNCTIONAL ANALYSIS OF THE YEAST *DPH5* GENE 104

2.R-1. Oxidative stress assay on wild-type and mutant yeast cells 104

2.S. TRANSMISSION ELECTRON MICROSCOPY OF YEAST CELLS 106

2.S-1. Fixation of yeast cells 107

2.S-2. Sectioning for TEM 107

2.S-3. Visualization of sections 107

Chapter 3. Activation of members of the caspases cascade in the rod outer segments by intense green that light-induces retinal degeneration 108

3.A. INTRODUCTION 109

3.B. RESULTS 111

3.B-1. Defining the treatment profile 111

3.C-2. Activation of initiator caspases 112

3.C-3. Activation of caspase 3 and cleavage of downstream targets 116

3.C-4. Localization of caspases and their targets in the normal and light-treated retina 118

3.D. DISCUSSION 123

Chapter 4. Identification and bioinformatic characterization of differentially expressed LIRD genes 133

4.A. INTRODUCTION 134

4.B. RESULTS 136

4.B-1. Construction and preliminary characterization of the 8-hour execution phase cDNA library 136

4.B-2. Primary screening of the execution phase cDNA library 136

4.B-3. Secondary and tertiary screening of the putative differentially expressed clones 137

4.B-4. Confirmation of the differential status of isolated clones by Northern blot analysis 140

4.B-5. Sequence analysis of the differentially expressed clones isolated from the execution phase library 143

4.B-6. Identification of mouse and human orthologs of rat LIRD clones 148

4.B-7. Comparison of chromosomal locations of human LIRD gene orthologs to those of known retinal disease genes 149

4.B-8. Analysis of LIRD gene expression 158

4.B-9. Analysis of LIRD gene function 163

4.B-10. Analysis of ubiquitinylation and phototransduction associated genes 172

4.C. DISCUSSION 177

4.C-1. Differential gene expression during LIRD 177

4.C-2. *In silico* functional analysis of LIRD clones 184

4.C-2a. Kinases, phosphatases and their regulators 184

4.D-2b. Cytoskeleton components 186

4.C-2c. Energy metabolism 188

4.C-2d. Transcriptional Regulators 192

4.C-2e. Ribosomal binding proteins, splicing factors and translational regulators 195

4.C-2f. Chaperone and heat shock proteins 196

4.C-2g. Vesicle transport 198

4.C-2h. Ubiquitinylation 199

4.C-2i. Phototransduction 202

4.C-3. Summary 207

Chapter 5. Identification of a novel rat diphthamide methyltransferase, which plays a role in oxidative stress-induced cell death 209

5.A. INTRODUCTION 210

5.B. RESULTS 213

- 5.B-1. Isolation of the putative rat diphthamide methyltransferase gene 213
- 5.B-2. Bioinformatic analysis of the putative rat ORF and putative protein 217
- 5.B-3. Determining the rat gene structure 218
- 5.B-4. Analysis of the rat promoter and UTR sequence 227
- 5.B-5. Potential for alternate splicing of the rat gene 232
- 5.B-6. Determining the role of diphthamide methyltransferase during oxidative stress induced cell death 235
- 5.B-7. Transmission Electron Microscopy of yeast cells oxidative stress-induced cell death 239

5.C. DISCUSSION 239

Chapter 6. Summary 250

6.A. Defining the molecular phenotype in LIRD 251

6.B. Mechanisms of gene regulation 252

6.C. Degeneration in LIRD is the result of a global response 253

6.D. Changes in gene expression at the translational level in LIRD 255

6.E. Changes in gene expression at the level of protein function 257

6.F. Conclusion 258

6.G Future directions 259

- 6.G-1. Analysis of the role of caspases in LIRD 259
- 6.G-2. Analysis of differential gene expression during LIRD 260

6.G-3. Characterization of DPH5 in photoreceptor cell loss 261

Bibliography 263

LIST OF TABLES

Chapter 2

Table 2.1. Specific information regarding plasmids used in the course of this study

Table 2.2. Specific information regarding the PCR primers utilized in this study

Table 2.3. Specific information regarding antibodies used in the course of this study for immunohistochemistry and Western analysis

Table 2.4. Web-sites used for the bioinformatic analysis of the isolated differentially expressed clones

Chapter 4

Table 4.1. Sequence analysis of clones differentially expressed between 8-hour retinae and dark-reared control

Table 4.2. Comparison of the human chromosomal locations of known retinal disease genes with human orthologs of the LIRD genes

Table 4.3. Percentages of clones/orthologs expressed in specific tissues

Table 4.4. Functional analysis of the LIRD genes

LIST OF FIGURES

Chapter 1

Figure 1.1. Representational cross-section of the human eye

Figure 1.2. Cross-section through the mammalian retina

Figure 1.3. The Phototransduction Cascade

Figure 1.4. Human retinal dystrophy

Figure 1.5. Morphological changes associated with the progression of apoptosis

Figure 1.6. Key players in the progression of light-induced retinal degeneration

Figure 1.7. Reduction of light-induced photoreceptor cell death by antioxidant pre-treatment

Figure 1.8. Absorption spectrum of rat photoreceptors versus transmission of green Plexiglas filter #2092

Figure 1.9. Loss of photoreceptor cells following light exposure

Figure 1.10. Definition of the molecular phenotype of light-induced retinal degeneration

Chapter 2

Figure 2.1. Light damage chamber used to induce green light induced retinal degeneration

Figure 2.2. Overview of construction of the execution phase cDNA library using the lambda ZAP-cDNA synthesis kit, and lambda ZAP cDNA Gigapack III Gold Cloning kit

Figure 2.3. Cloning vectors used in library synthesis

Figure 2.4. Overview of cDNA probe synthesis using a combination of 5' and 3' RACE

Figure 2.5. Screening of the execution phase cDNA library

Figure 2.6. Confirmation of genotype of *DPH5* deletion mutant and wildtype yeast strains

Chapter 3

Figure 3.1. Extent of photoreceptor dysfunction in the light-treated retina

Figure 3.2. Cellular caspases can be activated through internal or external signaling mechanisms

Figure 3.3. Activation of upstream caspases following exposure to green light

Figure 3.4. Proteolytic processing of downstream targets

Figure 3.5. Localization of activated caspases in dark-reared and 8-hour light-treated retinae

Figure 3.6. Western blot analysis of purified outer segments performed to detect the presence of caspases and PARP

Chapter 4

Figure 4.1. Representative results from the screening of the 8-hour cDNA library

Figure 4.2. Representative results from the secondary screening of differentially expressed clones isolated from the 8-hour library

Figure 4.3. Northern analysis of differentially expressed clones

Figure 4.4. Degree of identity between rodent and human orthologs of the isolated LIRD clones

Figure 4.5. Percentage of genes on each human chromosome that represent a retinal disease associated gene

Figure 4.6. Functional analysis of the LIRD genes

Figure 4.7. Northern blot analysis of phototransduction-related LIRD genes

Figure 4.8. Northern blot analysis of genes associated with ubiquitinylation

Chapter 5

Figure 5.1. Formation of EF-2 diphthamide

Figure 5.2. Identification of clone 28-2 as a dark-enriched EST using a PCR-based secondary and tertiary screen

Figure 5.3. Northern blot analysis of expression levels of the rat *DPH5* gene over the course of LIRD

Figure 5.4. Alignment of the rat *DPH5* mRNA sequence with known orthologs

Figure 5.5. Alignment of the putative rat DPH5 protein sequence with that of known orthologs

Figure 5.6. Summary of the rat *DPH5* gene structure

Figure 5.7. Alignment of rat, mouse and human promoter sequences

Figure 5.8. Percent survival of wild-type and DPH5 mutant yeast cells treated with varying concentrations of acetic acid

Figure 5.9. Percent survival of wild-type and DPH5 mutant yeast following treatment with varying concentrations of H_2O_2

Figure 5.10. Transmission Electron Microscopy of wild-type and dph5 mutant cells treated with acetic acid

Figure 5.11. Analysis of dph5 mutant yeast cells treated with 10 mM H_2O_2 for characteristic signs of apoptosis

Figure 5.12. Transmission Electron Microscopy of wild-type and dph5 mutant cells treated with H_2O_2

LIST OF SYMBOLS, NOMENCLATURE, AND ABBREVIATIONS

β-APP	β-amyloid precursor protein
°C	Degrees Celcius
Aamp	Angio-associated migratory protein
ABCR	ATP-binding cassette transporter, retina-specific
ADP	Adenosine diphosphate
AIF	Apoptosis inducing factor
Akr1d1	Aldo-keto reductase family 1, member D1
AKT	v-akt murine thymoma viral oncogene homolog 1
Aldoc	Aldolase C, fructose-biphosphate
AMPA	Alpha-amino-3-hydroxy-5-methyl-4-isoxazole propionate
Ant2	Adenine nucleotide translocator 2
AP-1	Activator protein-1
Apaf1	Apoptotic protease activating factor 1
ATF4	Activating transcription factor 4
ATP	Adneine triphosphate
Bad	BCL2-antagonist of cell death
Bag	BCL2-associated athanogene
Bak	BCL2-antagonist/killer 1
Bax	BCL2-associated X protein
Bcl-2	B-cell leukemia/lymphoma 2
Bcl-w	Bcl-2-like-2
Bcl-xl/xs	Bcl-2 associated X protein long isoform/short isoform
BDNF	Brain-derived neurotrophic factor
bFGF	Basic fibroblast growth factor
BLAST	Basic Local Alignment Search Tool
bp	Base pair
CaLB motif	Calcium and lipid binding motif
CBP	CREB binding protein
Ccl-2	Chemokine, CC motif receptor-2

Ccr-2	C-C chemokine receptor 2
Cct4	Chaperonin subunit 4 delta
cDNA	complementary DNA
c-fos	Cellular Finkel-Biskis-Jinkins (FBJ) murine osteosarcoma virus oncogene homolog
CFU	Colony forming units
cGMP	Cyclic guanosine mono-phosphate
CHO	Chinese hamster ovary
Cited2	Cbp/p300-interacting transactivator, with Glu/Asp-rich carboxy-terminal domain, 2
Ckap1	Cytoskeleton-associated protein 1
c-myc	Cellular myelocytomatosis oncogene
CNIB	Canadian National Institute for the Blind
CNTF	Ciliary neurotrophic factor
CoA	Co-enzyme A
Copb2	Coatamer protein complex beta prime
Copg1	Coatomer protein complex, subunit gamma
Cox6a1	Cytochrome c oxidase, subunit VIa, polypeptide 1
CREB3L2	cAMP responsive element binding protein 3-like 2
Crybb2	Crystallin, beta B2
CTP	Cytosine triphoshate
DAP5	Death associated protein 5
DHA	Decosohexanoic acid
DMTU	Dimethylthiourea
DNA	Deoxyribonucleic acid
DNase	DNA nuclease
Dph2L	Diphthamide methyltransferase 2-like
Dph5	Yeast Diphthamide methyltransferase 5
E2F	E2F transcription factor 1
EAAT1	Excitatory amino acid transporter
EAT/mcl-1	Myeloid cell leukemia sequence 1

ECM	Extracellular matrix
eEF	Eukaryotic Elongation factor
Eef1d	Eukaryotic translation elongation factor 1 delta guanine nucleotide exchange protein
EF-2	Elongation factor-2
eIF	Eukaryotic Initiation factor
ELOVL4	Elongation of very long chain fatty acids-like 4
EMBL-EBI	European Molecular Biology Laboratories - European Bioinfomatics Institute
ENaC	Epithelial Na+ channel
Epb4.1l1	Erythrocyte protein band 4.1-like 1
ERG	Electroretinograph
EST	Expressed sequence tag
E-value	Expectation value
FADD	Fas-associated death domain
Fas	Fas antigen
FasL	Fas ligand
GADD34	Growth arrest and DNA damage inducible 4
GDNF	Glial cell derived neurotrophic factor
GDP	Guanine diphosphate
GFAP	Glial fibrillary acidic protein
GIMP	GNU Image manipulation program
GluR1	Glutamamte receptor 1
Grifin	Galectin-related inter-fiber protein
GSH	Glutathione reduced
GSSH	Glutathione oxidized
GTP	Guanine triphosphate
GTPase	GTP binding protein (hydrolyase)
Guca1a	Guanylate cyclase activator 1a retina
H2O2	Hydrogen peroxide
Hif-1	Hypoxia inducible factor 1

His	Histidine
Hk1	Hexokinase 1
Hmgcl	3-hydroxy-3-methylglutaryl CoA lyase
HNF-4	Hepatocyte nuclear factor 4
HO-1	Heme-oxygenase-1
Hr	Hour
Hrmt1l2	Heterogeneous nuclear ribonucleoproteins methyltransferase-like 2
HSP	Heat shock proteins
IAP	Inhibitor of apoptosis protein
IL-9	Interlukin 9
INL	Inner nuclear layer
IRBP	Interphotoreceptor retinol-binding protein
IRES	Internal ribosome entry site
ITGAV	Integrin, alpha V
Kb	Kilobase
Kda	Kilodalton
KEGG	Kyoto Encyclopedia of Genes and Genomes
Laptm4b	Lysosomal-associated protein transmembrane 4B
Leu	Leucine
LHON	Leber optic atrophy
LIRD	Light-Induced Retinal Degeneration
MAP1B	Microtubule-associated protein 1B
MAPK	Mitogen associated protein kinase
MAT	Mating type loci
MBSU	Molecular Biology Sequencing Unit
MD	Macular degeneration
Mertk	Mer tyrosine kinase protooncogene
Met	Methionine
mi	microphthalmia
MMLV-RT	Moloney-Murine leukemia virus reverse transcriptase
MRF’	Minus restriction

mRNA	Messenger RNA
MSS4	Mammalian suppressor of Sec4
mt-Co1	Cytochrome c oxidase subunit 1
Myo15	Myosin XV
Myo1b	Myosin IB
NAD+	Nicotinamide adenine dinucleotide
NADH4L	NADH dehydrogenase 4L, mitochondrial
NADP/H	Nicotinamide adenine dinucleotide phosphate
NCBI	National Center for Biotechnology Information
NDUFB4	NADH dehydrogenase (ubiquinone) 1 beta subcomplex, 4
Nedd4	Neural precursor cell expressed, developmentally down-regulated 4
NFκβ	Nuclear factor of kapp beta
NGF	Nerve growth factor
Nkx2-5	Homeobox protein NK-2 homolog E
NT-3	Neurotrophin-3
Nurr77	Orphan nuclear receptor 77
Oct-1	Octamer binding transcription factor 1
OD	Optical density
OMIM	Online Mendelian Inheritance in Man
ORF	Open reading frame
p53	Tumor protein 53
$P75^{NTR}$	p75 neurotrophin receptor
Pafah1b3	Platelet-activating factor acetylhydrolase, isoform 1b, alpha1 subunit
PARP	Poly (ADP-ribose) polymerase
Pax4	Paired box gene 4
PCR	Polymerase chain reaction
PD	Parkinson's disease
Pdc	Phosducin
PDE	Phosphodiesterase
PEGASUS	Zinc finger protein, subfamily 1A, 5
PERK	Pancreatic EIF-2 alpha kinase

PERL	Practical extraction and reporting language
PFU	Plaque forming units
Pgk1	Phosphoglycerate kinase 1
PGP9.5	Ubiquitin carboxyl terminal esterase L1
PND	Post-natal day
Ppp2r5c	Protein phosphatase 2, regulatory subunit B B56, gamma isoform
Pqbp1	Polyglutamine binding protein 1
PR	Photoreceptor
Psme3	Proteaseome prosome, macropain 28 subunit, 3
PTP	Permeability transition pore
PY motif	Proline/Tryptophan motif
QH_2	Ubiquinone
RABIF	RAB interacting factor, also MSS4
RACE	Rapid amplification of cDNA ends
RAIDD	RIP associated protein with death domain
Raly	Similar to hnRNP-associated with lethal yellow
Ras	Ras oncogene
RCS	Royal College of Surgeons
Rd	Retinal degeneration
Rdh	Retinol dehydrogenase
Rdh11	Retinol dehydrogenase 11
rDPH	Rat Diphthamide methyltransferase
Rds	Retinal degeneration slow
RHO	Rhodopsin
RhoC	Ras homolog 9 RhoC
RIKEN	RIKEN Genome Sciences Center
RIP	Receptor interacting protein
RIS	Rod inner segment
RNA	Ribonucleic acid
RNase	RNA nuclease
ROS	Rod outer segment

RP	Retinitis pigmentosa
RPE	Retinal pigment epithelium
Rpl4	Ribosomal protein L4
Rpl5	Ribosomal protein L5
RPS10	Ribosomal protein S10
Rps16	Ribosomal protein S16
Rps27a	Ribosomal protein S27a
rRNA	Ribosomal RNA
SAGE	Serial analysis of gene expression
Sfrs6	Splicing factor, arginine/serine-rich 6
SGLT1	Sodium-coupled glucose transporter
Slc25a5	Solute carrier family 25 mitochondrial carrier; adenine nucleotide translocator, member 5
Sncg	Synuclein, gamma
SOD	Superoxide dismutase
TBP	TATA binding protein
TBPL	TATA box binding protein like
TEM	Transmission electron microscopy
TF	Transcription factor
Tlk2	Tousled-like kinase 2
Tpi1	Triosephosphate isomerase 1
TRB2	Tribbles homolog 2
TrkC	Tyrosine kinase receptor C
tRNA	Transfer RNA
TRPM-2	Testosterone-repressed prostate message 2
TTP	Thymine triphosphate
TUNEL	Terminal UTP nick end labeling
Ubb	Ubiquitin B
Ube2e3	Ubiquitin-conjugating enzyme E2E 3
UchL1	Ubiquitin carboxyl terminal hydroxylase L1
Unc119h	Unc119 homolog C. elegans (HRG4 = human; RRG4 = rat)

Ura	Uracil
USUHS	Uniformed Services University of the Health Sciences
UTR	Untranslated region
UV	Ultra-violet
v/v	volume/volume
VDAC	Voltage dependent anion channel
VEGF	Vascular endothelial growth factor
w/v	weight/volume
XIAP	X-linked inhibitor of apoptosis protein

Chapter 1

Introduction

1.A. INTRODUCTION

1.A-1. The mammalian eye

The mammalian eye is composed of a complex array of cells whose intricate interactions are necessary for the reception and amplification of visual stimuli (Hart, 1992; Cohen, 1992; Nicholls *et al*, 1992) (Figure 1.1). Light, in the visible (400-750 nm) and ultraviolet range (300-400 nm) passes through the cornea, and enters the interior of the eye through the pupil (Hemmingsen and Douglas, 1970). The iris regulates the opening of the pupil and hence, the amount of light entering the eye. The iris also regulates the depth of focus of the eye and minimizes spherical abortions resulting from the spherical shape of the lens. The light then passes through the lens, which focuses the light onto the neural retina and photoreceptor cells. In humans, only visible light can pass through the lens, while in rats up to 50% of ultraviolet A light, in addition to visible light, can pass through the lens (Gorgels and van Norren, 1992). The light signal is converted into an electro-chemical signal within the photoreceptor cells of the retina. This signal is then passed through the retina, along the optic nerve to the brain where the signal is interpreted into a visual image.

1.A-2. Types and spatial organization of cells of the mammalian retina

The retina itself is composed of several highly organized cell layers, which interact through synaptic connections to transmit visual information (Figure 1.2; Hart, 1992; Cohen, 1992; Nicholls *et al*, 1992). The most posterior portion of the retina (most distal from the cornea) contains the retinal pigment epithelium (RPE). The RPE itself is

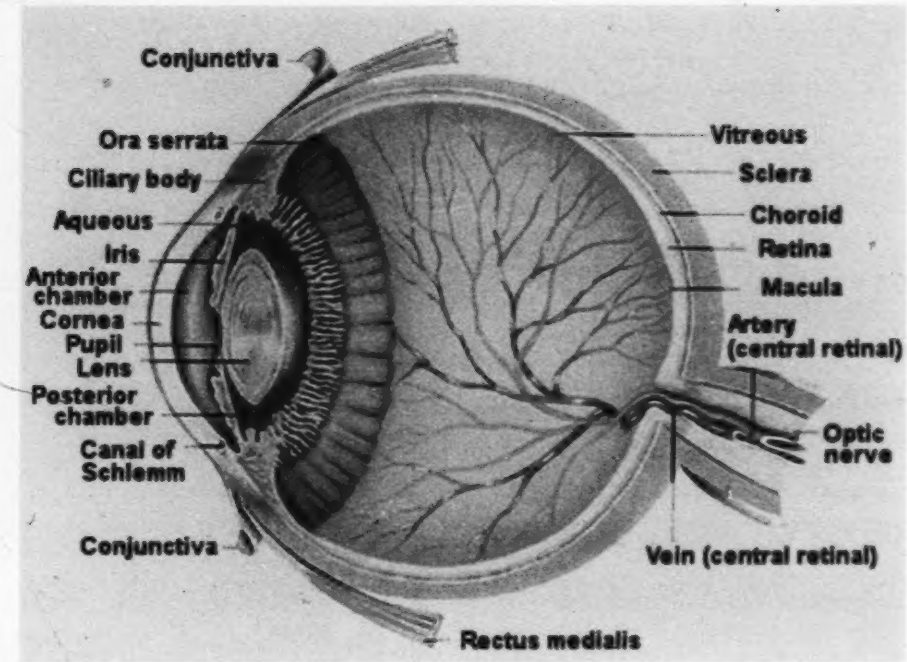
Conjunctiva
Ora serrata
Ciliary body
Aqueous
Iris
Anterior chamber
Cornea
Pupil
Lens
Posterior chamber
Canal of Schlemm
Conjunctiva
Vitreous
Sclera
Choroid
Retina
Macula
Artery (central retinal)
Optic nerve
Vein (central retinal)
Rectus medialis

Figure 1.1. Representational cross-section of the human eye. Adapted from "The Discovery Fund for Eye Research" web-site, 2004.

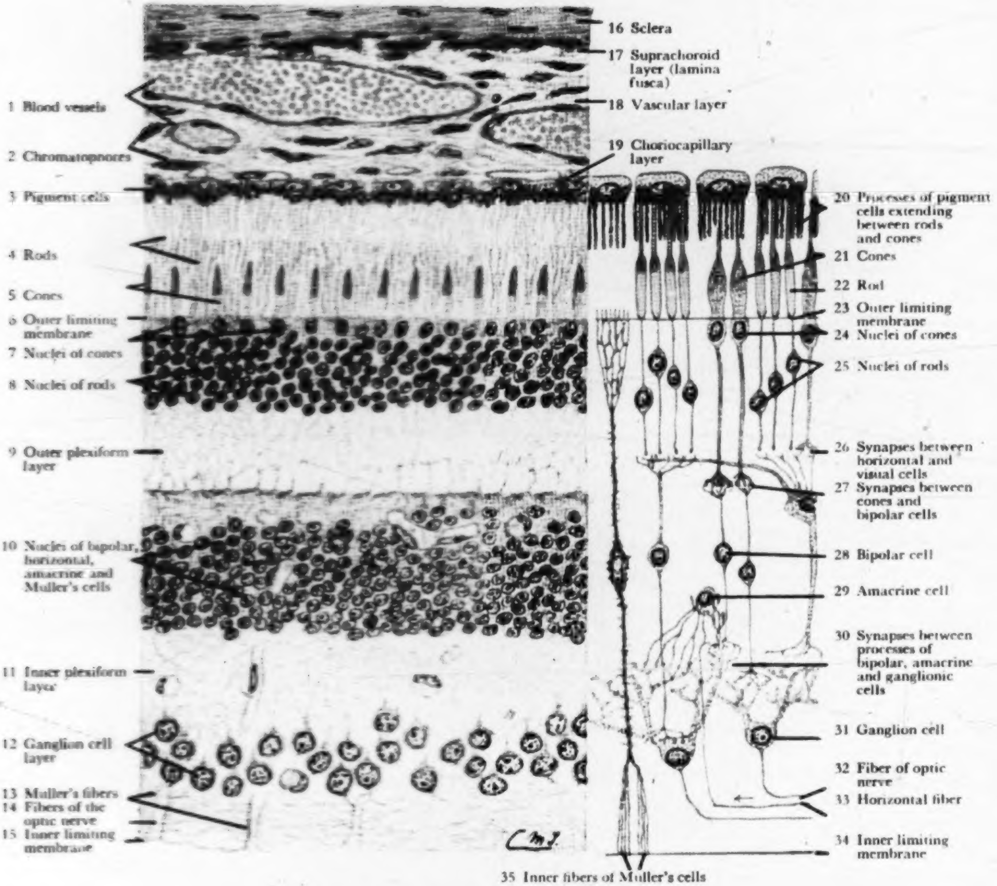
1 Blood vessels
2 Chromatophores
3 Pigment cells
4 Rods
5 Cones
6 Outer limiting membrane
7 Nuclei of cones
8 Nuclei of rods
9 Outer plexiform layer
10 Nuclei of bipolar, horizontal, amacrine and Muller's cells
11 Inner plexiform layer
12 Ganglion cell layer
13 Muller's fibers
14 Fibers of the optic nerve
15 Inner limiting membrane
16 Sclera
17 Suprachoroid layer (lamina fusca)
18 Vascular layer
19 Choriocapillary layer
20 Processes of pigment cells extending between rods and cones
21 Cones
22 Rod
23 Outer limiting membrane
24 Nuclei of cones
25 Nuclei of rods
26 Synapses between horizontal and visual cells
27 Synapses between cones and bipolar cells
28 Bipolar cell
29 Amacrine cell
30 Synapses between processes of bipolar, amacrine and ganglionic cells
31 Ganglion cell
32 Fiber of optic nerve
33 Horizontal fiber
34 Inner limiting membrane
35 Inner fibers of Muller's cells
CMJ

Layers of the retina and choroid in detail.

Stain: hematoxylin-eosin. 400×.

Figure 1.2. Cross-section through the human retina. Hematoxylin-eosin staining of the human retina (400X magnification). Image adapted from DiFiore (1967).

not directly involved in the conversion of the light signal to an electro-chemical signal, but it plays a key role in the recovery of the photoreceptor cells following the light signal. The RPE also aids in the passage of nutrients and wastes between the photoreceptor cells and the choroid layer, facilitating the maintenance and survival of the neural retina.

Lying just anterior to the RPE is the outer segment (OS) of the light-sensing photoreceptor cells. The OS consists of stacks of tightly packed discs containing visual pigments, which absorb light photons and activate the phototransduction cascade. It is through the phototransduction cascade of events that the light signal is converted into an electro-chemical signal. This signal then passes through the inner segment (IS) of the photoreceptor cell, which contains the cellular organelles, such as the Golgi apparatus, endoplasmic reticulum, and mitochondria, and is the site of active cell metabolism. Anterior to the IS is the outer nuclear layer (ONL) containing the nuclei of the photoreceptor cells. The light-induced electro-chemical signal produced in the photoreceptor cells is passed to the more anterior bipolar cells through synaptic connections that comprise the outer plexiform layer (OPL). The cell bodies of the bipolar cells lie within the inner nuclear layer (INL). As well, Müller cells, the major glial cells of the retina, extend processes posteriorly from their cell bodies within the INL to form tight junctions with the photoreceptor cells. The electro-chemical signal is passed from the bipolar cells to the ganglion cells through synaptic connections that comprise the inner plexiform layer (IPL). The long axonal processes of the ganglion cells (in the ganglion cell layer, GCL) converge at a central point within the retina where they form the optic nerve. This structure carries the light-induced signal to the brain where it is interpreted to produce a visual image.

Aside from these vertical signaling connections, there are also numerous lateral connections in the retina. Lateral connections made between the photoreceptor cells are mediated by horizontal cells, while amacrine cells form lateral connections at the sites of synapsis between bipolar and ganglion cells. Interplexiform cells receive input from both bipolar and amacrine cells, and signal to horizontal cells, potentially adjusting retinal sensitivity to light. Whereas the vertical signaling within the retina denotes how much light is detected, the lateral signaling within the retina provides information regarding contrast of light detected between areas of the retina, and temporal changes in light detection.

1.A-3. Photoreceptor cells

There are two major classes of photoreceptor cells within the mammalian retina, rods and cones. Rods account for the majority of the human and rodent photoreceptor cells, while cones account for 5% (Hecht, 1987) and 1% (LaVail, 1976) of the human and rat retina, respectively. Rods, which absorb light in the blue and green range (peak absorbance at 496 nm), are responsible for general light detection and night vision. In rats, rods tend to have smaller nuclei (less than 5.5 μm in diameter) and heterochromatin contained within a central mass within the nucleus (LaVail, 1976). Cone cells facilitate visual acuity and color vision. In humans and other primates there are three classes of cones cells that absorb light in either the blue (peak absorbance at 420 nm), green (peak absorbance at 530 nm), or red (peak absorbance at 560 nm) regions of the light spectrum. In rodents such as the rat, there are two classes of photoreceptors that detect blue-UV (approximately 7% of rat cones, peak absorbance at 359 nm) and green (approximately

93% of rat cones) peak absorbance at 510 nm) light (Szel, 1992; Radlwimmer, 1998; Jacobs *et al*, 1991; 2001; Rat behavior web-site). In rats, cone cells can be distinguished from rod cells by their slightly larger nuclei (greater than 5.5 µm in diameter), which are ovoid in shape and contains multiple small clumps of heterochromatin (LaVail, 1976). In humans, the cones are found predominantly in the central macula region of the retina, and centermost fovea, regions responsible for maximal visual acuity. Rodents lack a macula and fovea region and have their cone cells more evenly distributed throughout the retina, though their nuclei are restricted in the outer one third to one half of the ONL (LaVail, 1976).

1.A-4. Phototransduction

A photoreceptor in the dark is in a depolarized state, and consequently releases neurotransmitters from its synaptic terminal to the neighboring bipolar cells (Hart, 1992; Cohen, 1992; Nicholls *et al*, 1992). When a depolarized photoreceptor cell is exposed to light, several key events occur that mediate phototransduction (summarized in Figure 1.3) and lead to the conversion of a light stimulus to an electro-chemical stimulus. Photo-pigments in the OS of the photoreceptor cells; specifically rhodopsin, the visual pigment in rod cells; or red, blue, or green opsin in cone cells; absorb light. In all cases, the visual pigment consists of an opsin protein bound to a retinalaldehyde molecule. Light results in an isomerization of the retinal from an 11-cis retinal molecule form to an active all-trans retinal form. The active photo-pigment then activates the trimeric G-protein transducin, which in turn activates guanosine monophosphate (cGMP) phosphodiesterase (PDE). Activation of PDE results in a decrease in the levels of cGMP, the subsequent closing of

Figure 1.3. The Phototransduction Cascade. Photons of light are absorbed by the photopigment rhodopsin, which consists of an opsin protein and an 11-cis-retinal molecule. The 11-cis-retinal is converted to all-trans-retinal via several intermediates, including metarhodopsin II. This represents the active or bleached form of the rhodopsin molecule, as indicated by the red star. Metarhodopsin II binds to the trimeric G-protein transducin, facilitating the exchange of GTP for GDP, on the transducin molecule. Binding of GTP signals the dissociation of the β- and γ-transducin subunits, leaving the activated α-transducin subunit bound to GTP. The active α-transducin is indicated by the red star. A single metarhodopsin II molecule can facilitate the activation of up to 800 transducin molecules (Purves *et al*, 2001), and therefore, functions as one of the initial amplification steps in the transduction of the visual signal. The activation of transducin (Tα:GTP) molecules catalyzes the activation of phosphodiesterase (PDE) through the binding of two Tα:GTP to the two γ subunits PDE. This results in the activation of the α- and β-subunits of PDE, which functions to decrease the levels of cyclic GMP (cGMP) in the cell. As well, free cellular calcium ions form a complex with the enzyme guanylate cyclase which converts GTP to cGMP. Inactivation of this enzyme by Ca++ results in a further decrease in cGMP levels in the cell. In an unstimulated cell, cGMP interacts with cGMP-gated cation channels, keeping them open, facilitating a net influx of sodium and calcium ions, resulting in a continuous depolarization of the photoreceptor cell. When levels of cGMP drop in response to a light stimulus, these ion channels close, resulting in an increased photoreceptor membrane potential and a subsequent hyperpolarization of the cell. This signals a decrease in the levels of the neurotransmitter glutamate released by the rods to the retinal bipolar cells, leading to subsequent changes in polarization of these cells.

Closing of the cation channels lowers the concentration of free calcium in the cell. This allows for the reactivation of guanylate cyclase (as indicated by the red star), which facilitates a net increase in the levels of cGMP in the cell. This allows ion channels to reopen, and returns the cell to a depolarized state. Meanwhile, the GTPase activity of transducin hydrolyzes the GTP to GDP, resulting in the release and subsequent inactivation of PDE. The metarhodopsin II is then phosphorylated by rhodopsin kinase, and phosphorylated opsin molecule is bound by arrestin/S- antigen, preventing further rounds of transducin activation by the visual pigment. The all-trans-retinal molecule dissociates from the opsin protein and is transported to the cytosol of the photoreceptor cell by the ATP binding cassette transporter ABCR, where the all-trans-retinal is reduced to all-trans-retinol by NADPH-dependent all-trans-retinol dehydrogenase. The all-trans-retinol is bound by the carrier protein IRBP (interphotoreceptor retinoid-binding protein). and this complex diffuses to the retinal pigment epithelium (RPE) Here, in conjunction with retinol binding proteins such as retinaldehyde-binding protein (CRALBP), retinol binding protein (CRBP), and the RPE65 (and lecithin:retinol acyltransferase, the all-trans-retinol is converted to 11-cis-retinol (esterification reaction). The 11-cis-retinol is converted to 11-cis-retinal (through an oxidation reaction mediated by NAD- and NADP-dependent 11-cis retinol dehydrogenases), which will then be transported back to the photoreceptor cells (via IRBP) where it will join with opsin (which has been dephosphorylated by protein phosphatase 2A) and reform rhodopsin. This regenerated rhodopsin is now ready to repeat the signal transduction cascade in response to a visual stimulus.

Image self-made from literature (reviewed by McBee *et al*, 2001; Saari, 1992; Oyster, 1999).

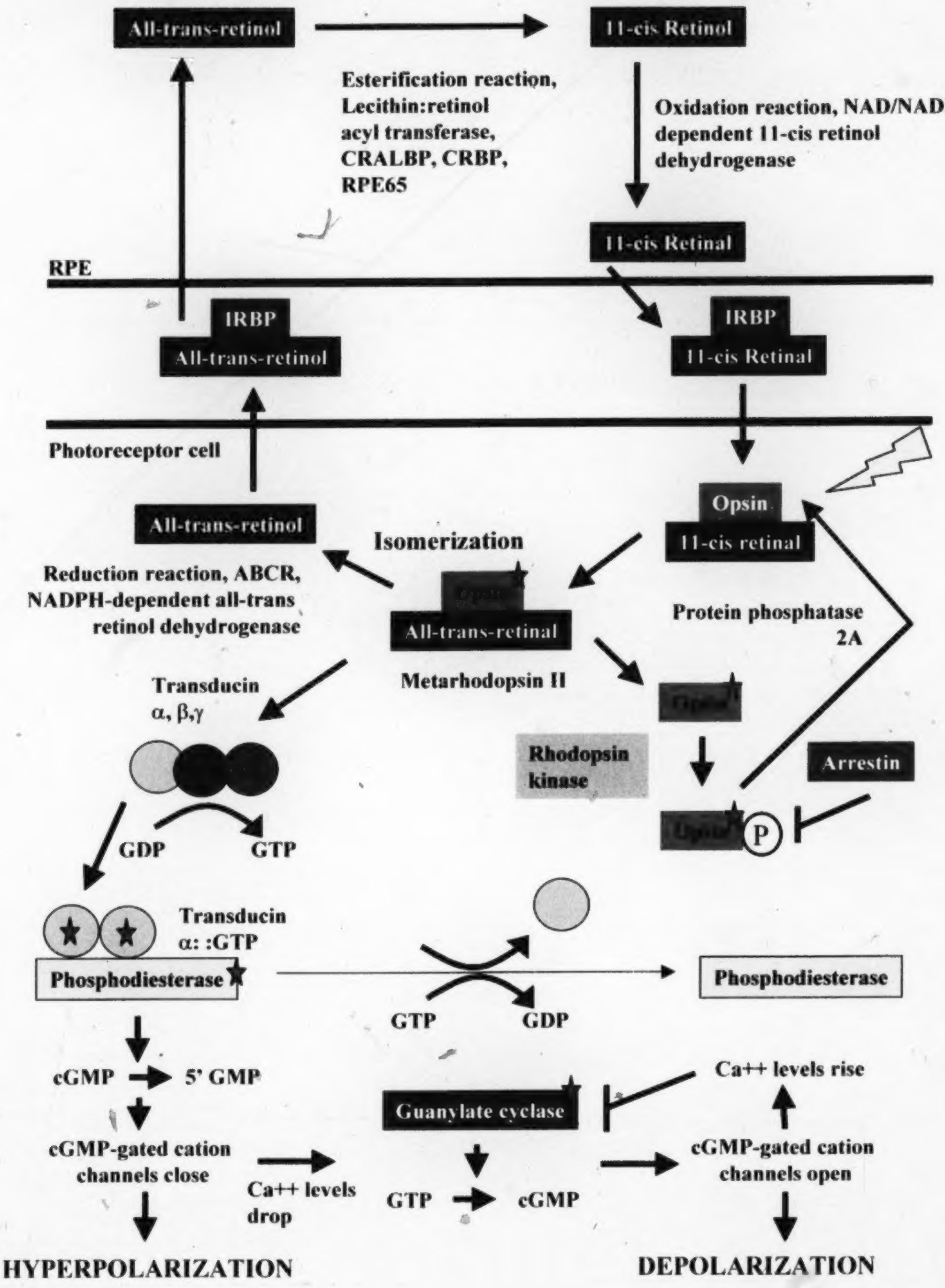
All-trans-retinol
11-cis Retinol
Esterification reaction, Lecithin:retinol acyl transferase, CRALBP, CRBP, RPE65
Oxidation reaction, NAD/NADP-dependent 11-cis retinol dehydrogenase
11-cis Retinal
RPE
IRBP
All-trans-retinol
IRBP
11-cis Retinal
Photoreceptor cell
All-trans-retinol
Isomerization
Opsin
11-cis retinal
Reduction reaction, ABCR, NADPH-dependent all-trans retinol dehydrogenase
Opsin
All-trans-retinal
Metarhodopsin II
Protein phosphatase 2A
Transducin α, β,γ
Opsin
Rhodopsin kinase
Arrestin
Opsin
P
GDP
GTP
Transducin α: :GTP
Phosphodiesterase
Phosphodiesterase
GTP
GDP
cGMP
5' GMP
Ca++ levels rise
Guanylate cyclase
cGMP-gated cation channels close
Ca++ levels drop
GTP
cGMP
cGMP-gated cation channels open
HYPERPOLARIZATION
DEPOLARIZATION

cGMP-gated cation channels, hyperpolarization of the photoreceptor cell, and decrease in neurotransmitter release to the bipolar cells. This results in a change in membrane polarity of the bipolar, and subsequently ganglion cells, and the transmission of the visual signal to the visual cortex of the brain.

The phototransduction cascade is inactivated through the inhibitory activities of arrestin and rhodopsin kinase. These molecules inhibit the interaction of the active photo-pigment with transducin, subsequently leading to the inactivation of PDE, the opening of the cGMP gated cation channels, and a return to a depolarized state. The activated retinal molecule dissociates from the opsin protein, and is transported to the RPE where it is regenerated back to the 11-cis retinal form. The inactive retinal is transported back to the OS where it can re-initiate the phototransduction cascade.

1.A-5. Retinitis pigmentosa and macular degeneration

The intricate interactions of the phototransduction cascade and the overall function and integrity of the photoreceptor cell are critical, not only to mediate vision, but also for the survival of the cell itself. An imbalance in any of the biological events occurring within the photoreceptor can lead to a dysfunctional state and potentially degeneration of the retina if the dysfunction is widespread. Two main classes of retinal degeneration are of medical significance in the human retina. These include retinitis pigmentosa (RP), which involves degeneration of the peripheral retina, and primarily affects the rod photoreceptor cells, and macular degeneration (MD), which is characterized by the degeneration of the cone-rich macula in the central retina.

Retinitis pigmentosa is a heterogeneous group of disorders, both genetically and clinically (Steele, 1994; Wong, 1994). There are X-linked, autosomal dominant, and autosomal recessive forms of the disease, although 50% of the cases have an unidentified genetic basis. It is estimated that one in 2,500 Canadians is affected with RP, and that this family of disorders affects over three million people worldwide (CNIB web-site, July, 1998; Foundation Fighting Blindness web-site, July 2005). Symptoms include impaired light adaptation, night blindness, diminished visual fields, and loss of peripheral vision, with the final outcome of legal blindness occurring between 30 and 60 years of age (Figure 1.4B; Steele, 1994 and Wong, 1994).

Macular degeneration, on the other hand, is characterized by a gradual loss of central vision due to retinal cone cell death (Humphries *et al*, 1994; Mah *et al*, 1998; Foundation Fighting Blindness web-site, July 2004). Disease pathology also includes irregularities in the RPE and eventual degeneration of both the RPE and cone photoreceptors in the region of the macula (Figure 1.4C). Diseases of the macula account for 80% of the diseases leading to blindness worldwide (Mah *et al*, 1998). Macular degeneration is known to cause visual loss in over 2.1 million Canadians (CNIB web-site, July, 1998), with 78,000 new cases diagnosed each year (CNIB web-site, July 2004). Lipofuscin deposits (the residual products of oxidative damage to cellular lipids) in the RPE characterize macular degeneration. Oxidative damage, resulting from high levels of oxidative stress, has been documented in cases of macular degeneration (Eye Disease Case-Control Study Group Disease, 1992; West *et al*, 1994). Other studies suggest that dietary antioxidants could slow the accumulation of oxidative damage, and hence slow the progression of macular disease (Taylor *et al*, 1992).

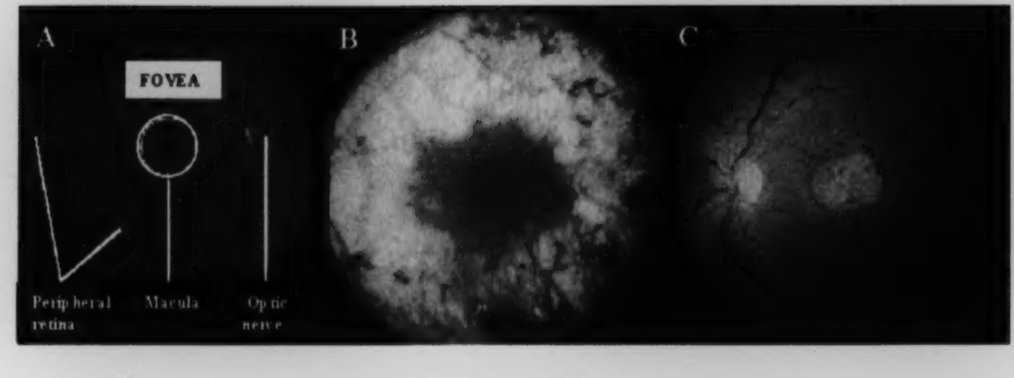

Figure 1.4. Human retinal dystrophy. (A) Fundus photograph of a normal human retina indicating the peripheral retina, macular region with the central fovea, and the optic nerve. (B) Fundus photograph of a retina from a patient with retinitis pigmentosa, showing extensive loss of cells from the peripheral retina. (C) Fundus photographs of a retina from a patient with macular degeneration. Degeneration of the cone rich central macular region is evident. Images courtesy of Dr. Ian MacDonald, University of Alberta.

1.A-6. Apoptosis in retinal degeneration

Apoptosis is defined as an active process of gene-directed cellular self-destruction (Kerr and Harmon, 1991; Bursch *et al*, 1990). The first morphological observation is a condensation of the chromatin within the cell nucleus (Figure 1.5B). Gel electrophoresis of DNA at this stage shows a characteristic ladder as the DNA is cleaved into large 300,000 to 600,000 bp fragments, followed by further fragmentation into multinucleosomal fragments. This nuclear condensation is followed by a breakdown of cell:cell interactions mediated by extracellular matrix (ECM) remodeling. Next is the condensation of the cytoplasm of the apoptotic cell, facilitated by the disruption of contacts with neighboring cells and a disruption of the cytoskeleton. This results in a characteristic blebbing of the cell membrane, which leads to the formation of apoptotic bodies containing fragments of the dying cell (Figure 1.5C). The apoptotic bodies provide new epitopes, normally hidden within the cell, that are now exposed to promote phagocytosis by neighboring healthy cells (Figure 1.5D) or macrophages that infuse the tissue (Figure 1.5E).

In contrast, necrotic cell death is characterized by cellular swelling, disintegration of organelles and the plasma membrane, and chromatin clumping (Syntichaki and Tavernarakis, 2002). Unlike apoptosis, necrosis does not require de novo mRNA and protein synthesis, and is associated with random cleavage of the DNA. As well, the release of cellular components into the extracellular environment, due to disruption of the plasma membrane, is often associated with an inflammatory response as antigens normal hidden within a cell are detected by the immune system.

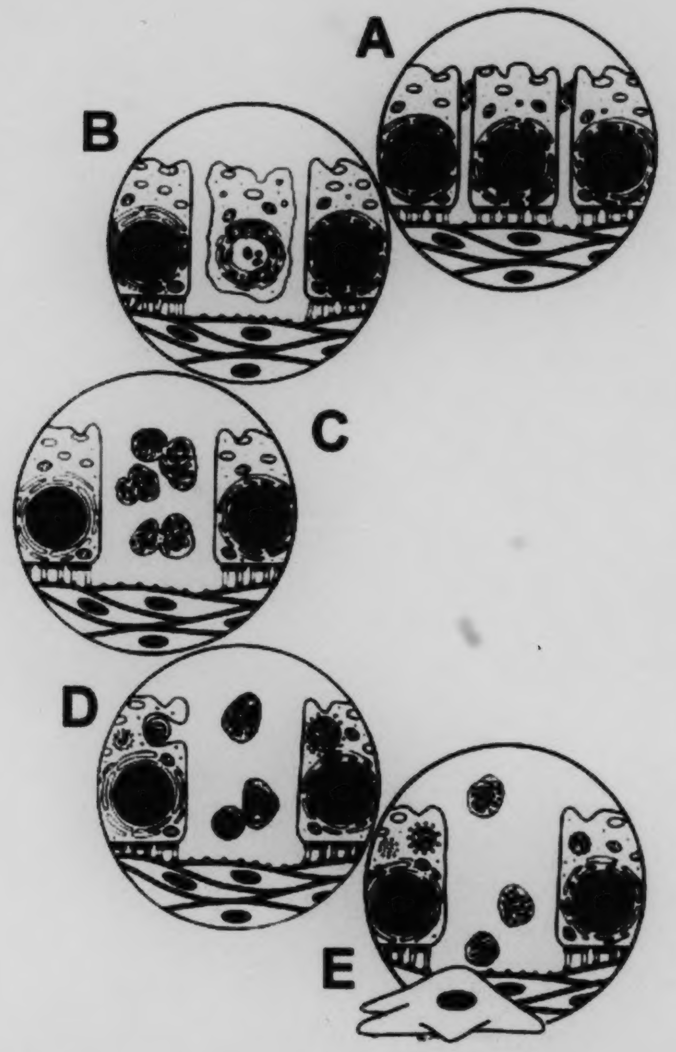

Figure 1.5. Morphological changes associated with the progression of apoptosis. (A) Normal tissue morphology showing normal cell structure, cell-cell and cell-basal lamina connections. (B) Following the induction of the apoptotic pathway, nuclear and cytoplasmic condensation begins. Cells lose normal attachments to neighboring cells and the basal lamina. (C) Membrane blebbing results in the formation of apoptotic bodies. (D) Neighboring cells remove the apoptotic bodies via phagocytosis. (E) Phagocytic cells enter the apoptotic environment to clear remaining debris. Image courtesy of Dr. Paul Wong, University of Alberta.

Apoptosis has been shown to play a role in human retinal disease (reviewed by Wong, 1994; Nickells and Zack, 1996). TUNEL (terminal dUTP nick end labeling) analysis of retinae from patients with various forms of retinitis pigmentosa shows TUNEL-positive cells in the photoreceptor cell layer, indicating DNA fragmentation (Milam and Li, 1995). Morphological analysis of these TUNEL-positive photoreceptor cells showd the morphology characteristics of apoptotic cell death including condensed nuclei and disorganized inner and outer segments. Analyses of many animal models of RP have demonstrated that the predominantly rod-specific degeneration observed is the result of apoptosis (Chang *et al*, 1993; Li *et al*, 1985, Abler *et al*, 1996; Portera-Calliau *et al*, 1994, Tso *et al*, 1994, Smith *et al*, 1995).

1.A-7. Animal models of retinal disease

There are over 80 genetic animal models currently being used for the study of photoreceptor degeneration including those in rodents, bird (Fite *et al*, 1993), frog (Moritz *et al*, 1999), fruit fly (Lee and Montell, 2004), rabbits (Lawwill, 1973), ground squirrels (Collier and Zigman, 1989), miniature pigs (Dureau *et al*, 1996), trout (Allen and Hallows, 1997), monkeys (Sperling *et al*, 1980a) and zebrafish (Li and Dowling, 1998). These models show photoreceptor cell loss as a result of mutations in key photoreceptor cell genes, and subsequent cellular dysfunction. Some of the best studied examples of these include the RCS (Royal College of Surgeon) rat, the vitiligo mouse, rd (retinal degeneration) 1 mouse, the Rds (retinal degeneration slow)/peripherin/rd2 mouse, and several rodent models containing mutant or knocked out forms of rhodopsin or various members of the phototransduction cascade (for review see Fauser *et al*, 2002; Chang *et al*, 2002; Remé *et al*, 1998b).

While there are many models of RP, there are few animal models for MD. Many of these models rely on exogenous alterations such as diet, age and light exposure to mimic the features of MD (Dithmar *et al*, 2001; Cousins *et al*, 2002; Majji *et al*, 2000). Several genetic models have recently been developed including an ABCR (ATP-binding cassette transporter, retina-specific) knock-out mouse (Weng *et al*, 1999), a transgenic mouse line expressing a mutant cathepsin D (Rakoczy *et al*, 2002), and mice lacking Ccl-2 (Chemokine, CC motif receptor-2, a monocyte chemoattractant protein) or its receptor Ccr-2 (C-C chemokine receptor 2) (Ambati *et al*, 2003).

These model systems of MD, as well as those used to study RP, are useful to study photoreceptor cell dystrophy in general. As proper function of the retina requires complex interactions between different cell types, understanding the events that lead to dysfunction of one cell type can provide insight into the mechanisms leading to degeneration of a different cell type. An example of this lies in the disease gene responsible for recessive Stargardt macular dystrophy, which encodes a retinal ATP binding cassette transporter (ABCA4), believed to be involved in the transport of essential molecules in or out of the photoreceptor. Though ABCA4 is localized in the rod inner segment (RIS), Stargardt macular dystrophy primarily affects the cone cells within the macula. Similarly, the identification of a mutation in ELOVL4 (Elongation of very long chain fatty acids-like 4), a member of the fatty acid elongase family of enzymes, has been identified as the underlying genetic cause of Stargardt-like macular dystrophy (Zhang *et al*, 2001; Lagali *et al*, 2000). This gene has been shown to be expressed throughout the inner segments of the photoreceptor cell layer in mice (Zhang *et al*, 2003; Mandel *et al*, 2004), while patients with this dystrophy show defects restricted to the macula and RPE (Lagali *et al*, 2000). As well, in some cases of Retinitis pigmentosa induced by rod-specific mutations in rhodopsin, there is a spread in retinal dystrophy from the pheripheral retinal to the cones of the macula (To *et al*, 2000).

Therefore, dysfunction and/or degeneration in one cell type can lead to subsequent dysfunction and degeneration of another cell type. This idea points to complex cell:cell interactions and global tissue response to cellular dysfunction as a contributing factor in disease pathology and progression.

1.B. LIGHT-INDUCED RETINAL DAMAGE (LIRD)

Unlike genetic models, light-induced retinal degeneration in rodents is an acquired model of retinal dystrophy. Noell *et al* (1966) published one of the first accounts of the effects of intense light exposure on photoreceptor cells. After treating rats with experimental light conditions, an irreversible reduction in the amplitudes of electroretinographic response (ERG) was observed, indicating a loss of photoreceptor responsiveness and viability. Key morphological changes resulting from light exposure affected both the visual cell and/or the RPE. The ONL of the rod photoreceptors began to degrade, causing a thinning of the ONL that continued for different lengths of time, depending on experimental conditions used. The cells of the inner nuclear layer generally maintained their normal appearance.

Based on these observations, Noell *et al* proposed three hypotheses pertaining to the mechanism underlying this phenomenon: (1) the action of light on a visual pigment leads to oxidation of the cellular environment, (2) exposure to intense light adversely affects the metabolic state of a photoreceptor cell, and (3) a toxic product is produced through the light-mediated events that cause inherent damage to the cell (reviewed by Organisciak and Winkler, 1994). Research over the past four decades has established extensive support for Noell's hypotheses and has provided an understanding of some of the key players in LIRD (summarized in Figure 1.6). It is important to point out that though numerous cellular changes have be associated with LIRD, there are limited data supporting a direct cause and effect relationship between the majority of these changes and the progression of LIRD. Additional research will be required to identify which factors play a causative role in LIRD, and which factors are altered merely as a consequence of other functional or molecular alterations. As current research is still at the stage of identifying potential players, it will require considerable work to tie these numerous factors together into a workable model of cell loss in LIRD.

1.B-1. LIRD: Background and current state of knowledge

LIRD is known to involve the bleaching of rhodopsin, the development of oxidative stress and photoreceptor cell loss via apoptosis. As apoptosis is known to involve *de novo* transcription and translation, changes in gene expression are also important in photoreceptor cell loss in LIRD.

1. B-1a. Role of rhodopsin bleaching in LIRD

Biochemical analysis in rats has demonstrated a correlation between sensitivity to light and levels of rhodopsin in the OS of photoreceptor cells (Organisciak *et al*, 1991b).

Figure 1.6. Key players in the progression of light-induced retinal degeneration. Photoreceptor cell loss induced by exposure to intense light is known to involve a variety of genetic and environmental factors that augment cell death. The bleaching of rhopdosin is an early event, and is believed to act as a trigger for the apoptotic pathway activated as a result of phototoxicity. As a result of, or in conjunction with, this extensive bleaching, the production of an oxidative stress environment, changes in gene expression, and photoreceptor cell loss occur. The rate and extent of the occurrence of these events are regulated by several exogenous factors such as diet (including the levels of dietary anti-oxidants), light exposure history, the nature of the light exposure (intensity, wavelength and exposure times), and the presence of pupil dilation. Endogenous factors such as body temperature, the point within the animals circadian cycle that the light exposure occurs, genetic background, species, pigmentation, age, the levels of stress and sex hormones, and the level of cellular anti-oxidant factors, DHA, rhodopsin and members of the phototransduction cascade affect the extent of cell death in response to light. The changes in gene expression lead to not only the induction of the apoptotic pathway and survival response within the affected cell, but affect function of other cell populations within the retina including the RPE, Müller cells, glial cells, as well as other photoreceptor cell populations. Image self-made based on literature.

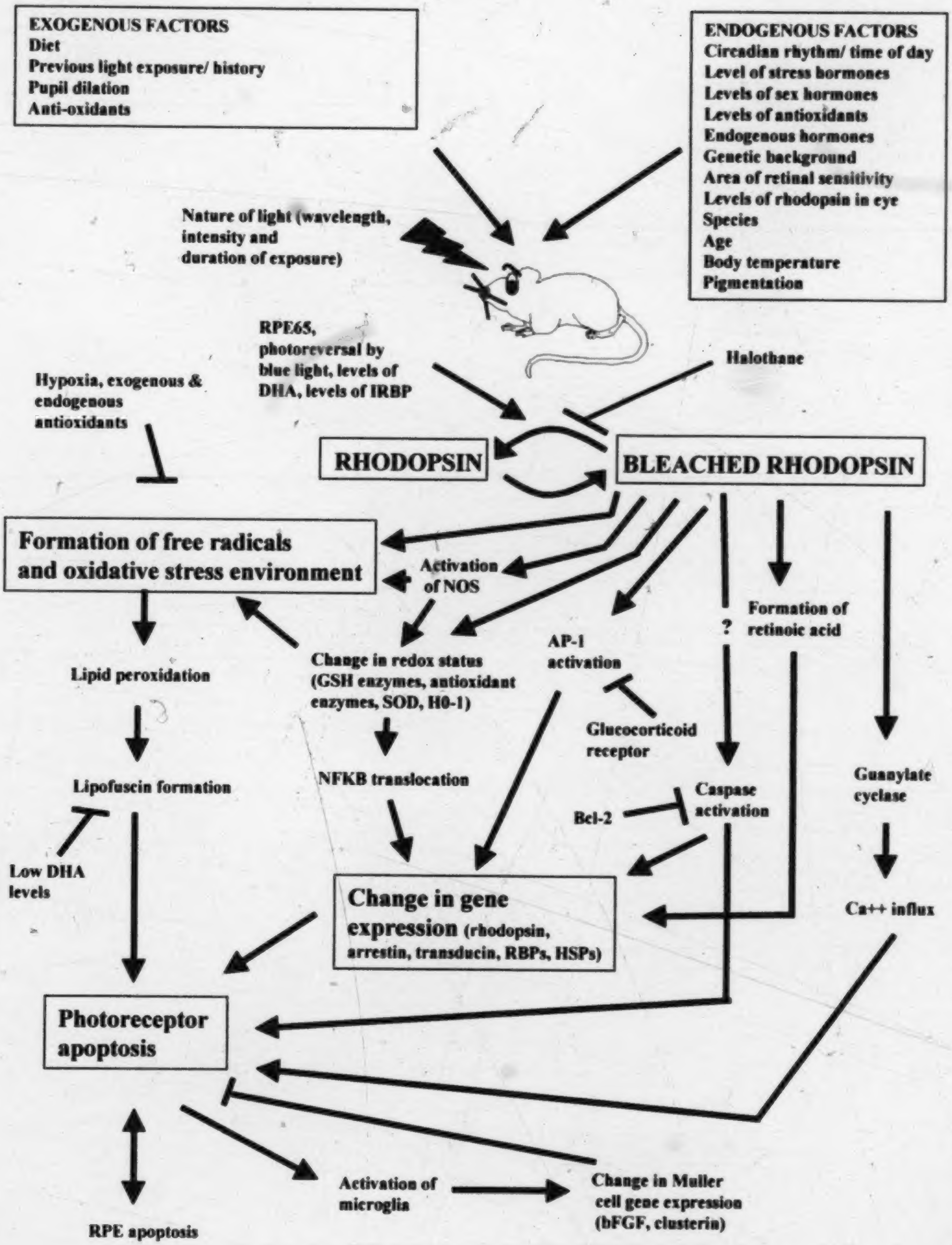
EXOGENOUS FACTORS
Diet
Previous light exposure/ history
Pupil dilation
Anti-oxidants
ENDOGENOUS FACTORS
Circadian rhythm/ time of day
Level of stress hormones
Levels of sex hormones
Levels of antioxidants
Endogenous hormones
Genetic background
Area of retinal sensitivity
Levels of rhodopsin in eye
Species
Age
Body temperature
Pigmentation
Nature of light (wavelength, intensity and duration of exposure)
RPE65, photoreversal by blue light, levels of DHA, levels of IRBP
Halothane
Hypoxia, exogenous & endogenous antioxidants
RHODOPSIN
BLEACHED RHODOPSIN
Formation of free radicals and oxidative stress environment
Activation of NOS
?
Formation of retinoic acid
Lipid peroxidation
Change in redox status (GSH enzymes, antioxidant enzymes, SOD, H0-1)
AP-1 activation
Glucocorticoid receptor
Lipofuscin formation
NFKB translocation
Bcl-2
Caspase activation
Guanylate cyclase
Low DHA levels
Change in gene expression (rhodopsin, arrestin, transducin, RBPs, HSPs)
Ca++ influx
Photoreceptor apoptosis
RPE apoptosis
Activation of microglia
Change in Muller cell gene expression (bFGF, clusterin)

Rhodopsin knock-out mice were shown to be resistant to light-induced photoreceptor cell loss (Grimm *et al*, 2000c), as well as to have altered photoreceptor cell morphology (Lem *et al*, 1999). In addition, cyclic-reared rats fed diets deficient in vitamin-A (retinol), a precursor of retinaldehyde, were also protected against light-induced damage (Noell *et al*, 1971a, b; 1979). Dark-reared vitamin A-deficient animals not exposed to light maintained normal ERG patterns and rhodopsin levels, while their cyclic-reared counterparts lost rhodopsin continuously. As a result, only cyclic-reared vitamin A-deficient rats were protected against light-damage, owing to the reduced levels of rhodopsin. Interestingly, Katz *et al* (1993) demonstrated that dietary depletion of retinoid precursors of rhodopsin led to cell death, and that this effect was amplified if the deficient animals were exposed to intense light. Therefore, both elevated and insufficient levels of rhodopsin lead to increased sensitivity to light.

It is not just the levels of rhodopsin that affect sensitivity to light in LIRD, but rather the amount of bleached rhodopsin. Mice lacking the gene *RPE65* are resistant to LIRD (Redmond *et al*, 1998; Grimm *et al*, 2000c; Grimm *et al*, 2001). *RPE*65 is an RPE-expressed gene that functions in the synthesis of 11 cis-retinal, facilitating rhodopsin regeneration after bleaching, Differences in rhodopsin regeneration rates, as a result of sequence variation in RPE65, have been shown to underlie strain-specific differences in sensitivity to light damage in mice (Wenzel *et al*, 2001a). Strains of transgenic mice with mutations in *RPE65* that result in slow rhodopsin regeneration demonstrated low sensitivity to light-induced retinal cell loss, due to the low levels of rhodopsin available for bleaching. In addition, pre-treatment of mice and rats with halothane, an anesthetic drug that competes with 11 cis-retinal for binding to free opsin, inhibits the regeneration of bleached rhodopsin and protects against white light-induced phototoxic injury (Keller *et al*, 2001). Therefore, high amount of bleached rhodopsin, owing to elevated rhodopsin levels, or to defective rhodopsin regeneration, promotes the progression of LIRD.

Though the mechanism in which bleached rhodopsin leads to cell death in LIRD is not known, it is proposed that exposure to light causes excessive rhodopsin bleaching, that in turn releases retinol, that may build up to toxic levels within the cell (Noell *et al*, 1971a, b; 1979). Alternatively, Fain *et al* (1993) proposed that a high level of free opsin released following rhodopsin bleaching may continuously activate the phototransduction cascade. This continuous activation of phototransduction may result in the depletion of energy stores in the cell, which may lead to dysfunction in other critical events within the photoreceptor, including protein synthesis, disc shedding, and cellular metabolism. This large-scale disruption of photoreceptor cell function may lead to cell death.

1.B-1b. The role of oxidative stress in LIRD

There is considerable evidence that oxidative stress plays a significant role in light-induced pathology. Cellular levels of hydrogen peroxide increase with the progression of LIRD (Yamashita *et al*, 1992). In addition, the cellular redox regulators thioredoxin and glutathione (GSH) are also altered during LIRD, showing a close association between the redox state of a cell and levels of oxidative stress (Tanito *et al*, 2002a, b).

The level of ascorbic acid, an antioxidant normally present in the retina, is shown to decrease after exposure to intense light (Organisciak *et al*, 1984; Tso *et al*, 1984). This decrease in retinal ascorbic acid concentrations is more pronounced in dark-reared rats than in cyclic-reared animals. Supplementation of rats with ascorbic acid prior to light-treatment is shown to reduce, but not abolish, light-induced damage (Li *et al*, 1985; Organisciak *et al*, 1984, 1985). Biochemical analysis of these rats demonstrates that higher levels of rhodopsin remain in the retinae of ascorbic-acid supplemented animals before light exposure, but not after (Organisciak *et al*, 1985; Penn *et al*, 1987a). In addition, pre-treatment with the exogenous anti-oxidant dimethylthiourea (DMTU), has also been shown to provide almost complete protection against retinal damage in cyclic-reared rats, and partial protection in dark-reared rats (Figure 1.7, Organisciak *et al*, 1992b). This protective role of DMTU may be associated with the fact that there is reduced rhodopsin loss in animals treated with DMTU prior to or during light exposure. Therefore, studies using both DMTU and ascorbic acid suggest a link between rhodopsin levels and oxidative stress.

The levels of rhodopsin bleaching may directly affect the levels of oxidative stress. Bleaching of rhodopsin leads to lipid peroxidation in cultured amphibian rod cells as a result of 470-490 nm light, in a mechanism independent of activation of the phototransduction cascade (Demontis *et al*, 2002). Demontis *et al* (2002) propose that 470-490 nm light leads to a cis to trans isomerization of rhodopsin and results in the formation of free retinol, which has been shown to induce the formation of oxidative free radicals (Delmelle *et al*, 1977). In addition, blue light has been shown to inhibit cytochrome c oxidase while activating prostaglandin G/H synthase, an event that is further linked to the formation of free radicals within the retina and subsequent lipid peroxidation (Grimm *et al*, 2001).

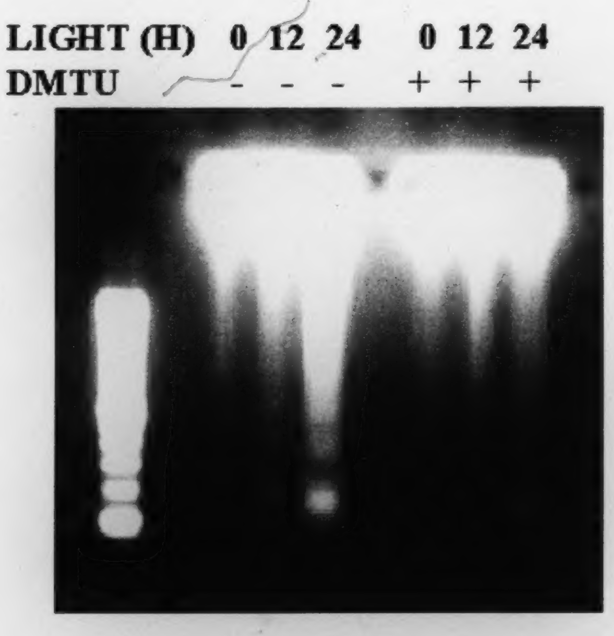

Figure 1.7. Reduction of light-induced photoreceptor cell death by antioxidant pre-treatment. Treatment of rats with the antioxidant DMTU prior to 12 or 24 hours of light treatment significantly reduces photoreceptor apoptosis as indicated by the decrease in DNA fragmentation observed following gel electrophoresis. Adapted from Organisciak *et al*

Lipid peroxidation, as a result of increased oxidative free radical production, is known to occur during LIRD (Wiegand *et al*, 1983; Organisciak *et al*, 1984, 1992a; b; Penn *et al*, 1987b). Levels of docosohexanoic acid (DHA), the predominant polyunsaturated fatty acid in the ROS, decrease in the light-treated retina (Organisciak *et al*, 1985). Light-induced loss of DHA is linked to increased levels of toxic lipid-conjugated dienes, derived from lipid hydroperoxides produced in the OS. Anderson *et al* (1985) proposed that lipid-conjugated dienes and toxic aldehydes, produced from DHA following lipid peroxidation, bind to primary amino groups of cellular components leading to their loss of function, and cause metabolic dysfunction and subsequent cell death. As such, dietary depletion of DHA has been shown to decrease the susceptibility of OS to light-mediated damage, as there is less DHA to be converted into lipid-conjugated dienes following light exposure (Bush *et al*, 1991). Conflicting results demonstrate that age-related declines in the levels of DHA correlate with the increased susceptibility to light observed in cyclic-reared rats, a feature shared with some cases of age-related macular degeneration (Organisciak *et al*, 1998; Bush *et al*, 1991). These conflicting data can be accounted for by the probability that there is a different response to light in cells lack DHA due to dietary depletion, (as cells have adapted to its absence), and in cells in which DHA decreases over time.

The role of DHA in the formation of lipid-conjugated dienes is demonstrated by antioxidant treatments during LIRD. Ascorbate and DMTU treatment prior to light exposure has protective effects on DHA, preventing its loss due to lipid peroxidation after light exposure (Organisciak *et al*, 1985, 1992a; b). In addition, animals raised under cyclic light conditions have high levels of endogenous anti-oxidants in the retina, coupled with low levels of DHA, and these levels seem to be affected by the intensity of light used in the rearing conditions (Penn *et al*, 1987b).

Organisciak *et al* (1977) proposed that the cellular levels of DHA and rhodopsin are closely integrated in mediating light-sensitivity. They suggested that increased packing of rhodopsin in a DHA lipid matrix plays a role in increasing the susceptibility of these rats to light. This close interaction is reinforced by the observation that DHA appears to migrate between the rod photoreceptors and the RPE at the same rate as retinol (Bush *et al*, 1991). In addition, low levels of DHA result in a slow rate of rhodopsin regeneration, and hence a low level of light-induced cell death (Bicknell *et al*, 2002; Grimm *et al*, 2001).

1.B-1c. The role of differential gene expression

Changes in gene expression are critical for the progression through the apoptotic pathway (Bursch *et al*, 1990) and several studies have demonstrated that the global inhibition of transcription and translation can inhibit the progression of apoptosis (Naora, 1995; Yonish-Rouach, 1995). As cell death in LIRD is known to occur through apoptotic cell loss (Organisciak *et al*, 1985; 1989; 1992b, Wong *et al*, 2001; Abler *et al*, 1996; Shahinfar *et al*, 1991), changes in the expression of photoreceptor cell genes are not unexpected.

AP-1 (activator protein-1), a transcriptional activator known to play a role in apoptosis in numerous systems including LIRD (reviewed in Remé *et al*, 1998a, b), is a heterodimer commonly consisting of c-fos and c-jun. Studies in c-fos knock-out mice have suggested that AP-1 activation is essential for apoptosis in LIRD (Wenzel *et al*, 2000), although this requirement appears to depend on the intensity of light used (Hao *et al*, 2002), and the genetic background of the mice studied (Wenzel *et al*, 2003). Interestingly, the levels of c-fos are known to be altered simply by handling the animals, and c-fos knock-out mice have significant morphological defects that may affect interpretation of data (Grimm *et al*, 2000b; Wenzel *et al*, 2001b). In addition, hypoxia, which inhibits light damage, does not act through AP-1, suggesting that several other factors may be playing a role in the regulation of apoptosis (Grimm *et al*, 2002). Retinoic acid, a potent regulator of gene expression under a variety of conditions, can potentially be produced by the oxidation of all-trans retinal following intense light exposure (reviewed by Remé *et al*, 1998a). In addition, Oct-1 (octamer binding transcription factor 1), known to regulate several housekeeping genes, is down regulated following light exposure, and as a result may affect normal cell function during apoptosis (Hafezi *et al*, 1999b). Ribosomal binding proteins, known regulators of gene expression at the translational level, also show altered expression during LIRD (Stepczynski, 2001; Grewal and Stepczynski *et al*, 2004). In addition, alternate splicing of the transcript encoding the GluR1 subunit of the AMPA (alpha-amino-3-hydroxy-5-methyl-4-isoxazole propionate)-type glutamate receptor occurs during LIRD (Harada *et al*, 1998).

As expected, members of the phototransduction cascade also affect sensitivity to intense light exposure. For example, exposure to high intensity light requires transducin for light-induced photoreceptor cells loss and is associated with activation of AP-1, while exposure to low intensity light is transducin independent and does not involve the activation of AP-1, suggesting that the underlying mechanisms involved in responding to light of varying intensities may differ (Hao *et al*, 2002)). In addition, numerous members of the phototransduction cascade are repressed following the induction of LIRD in arrestin/rhodopsin kinase mice (Choi *et al*, 2001). Results in our lab in light-treated wild-type rats support these findings, in addition to showing an increase in *c-fos* and *c-jun* during LIRD.

Numerous genes involved in a stress response including DNA repair enzymes (Gordon *et al*, 2002), heat shock proteins, and crystallin chaperones (MacDonald, 2003; Kutty *et al*, 1995; Sakaguchi *et al*, 2003) have been shown to be induced during the progression of LIRD. Heme-oxygenase-1 (*HO-1*), a gene known to be expressed during periods of high oxidative stress, is induced following intense light treatment (Kutty *et al*, 1995). Similarly, clusterin, a Müller cell-expressed lipid binding protein shown to be associated with apoptosis, is induced to high levels in both cyclic- and dark-reared animals following light exposure (Wong *et al*, 1994a, b; 2001). Pre-treatment of these animals with DMTU delays the induction of clusterin and HO-1, suggesting a relationship between the degree of oxidative stress and the response to cell damage.

In addition, several "apoptotic genes" have been found to play a role in LIRD, such as EAT/mcl-1 (myeloid cell leukemia sequence 1) (Shinoda *et al*, 2001). Results in our laboratory, and others, have shown activation of the members of the caspase cascade during LIRD in rats (Liu *et al*, 1999; Chen *et al*, 1996; Katai *et al*, 1999; Grimm *et al*, 2000; Wu *et al*, 2003). This contrasts with studies in mice that suggest that LIRD in this species is caspase-independent (Donovan *et al*, 2001; Donovan and Cotter, 2002). As well, members of the Bcl-2 family, including Bcl-2 itself, and Bcl-xl have been shown to have a protective role in LIRD (Wu *et al*, 2003).

1.B-1d. Other factors affecting LIRD

1.B-1d-i. Interactions between cell populations during LIRD: There are extensive cell:cell interactions occurring within the retina. Loss of photoreceptor cells in light-treated rats is followed by a loss of the associated RPE and vice versa (La Vail *et al*, 1987; 1992a; Keller *et al*, 2001). In addition, though cone cells generally survive during LIRD (Cicerone, 1976; Kuwabara *et al*, 1976; LaVail, 1976; Rapp *et al*, 1990), the small subset of cone cells that perish (0% in the peripheral retina and less than 40% in the posterior retina; LaVail, 1976) shows a morphology indicative of necrosis (Cortina *et al* 2003). This light-induced necrosis of cone cells likely occurs as a result of the loss of cell:cell interactions with the rod cells, or due to interactions with damaged rod cells.

The involvement of Müller cells in the photoreceptor cell response to LIRD has also been demonstrated. In addition to clusterin (see previous section), several growth factors are also induced in response to light damage. These include bFGF (basic fibroblast growth factor), BDNF (brain-derived neurotrophic factor), NT-3 (neurotrophin-3) and CNTF (ciliary neurotrophic factor), all of which are known to promote cell survival in states of phototoxicity (Gao and Hollyfield, 1996; LaVail *et al*, 1992b). The NT-3 receptor trkC (tyrosine kinase receptor C) has been localized to photoreceptor and Müller cells, while the p75^{NTR} NT-3 receptor is restricted to microglial cells (Harada *et al*, 2000). Both BDNF and CNTF can protect photoreceptor cells which lack the required receptors for these molecules, suggesting an indirect mechanism of action (Harada *et al*, 2000; Kirsch *et al*, 1997). Harada *et al* (2002) have proposed that damaged photoreceptors release signals that activate microglia which then migrate from the inner to the outer retina. The activated microglia secrete a variety of trophic factors that induce

Müller cells to change their trophic factor expression patterns. Microglial secretion of NGF (nerve growth factor) will signal to the Müller cells to reduce their secretion of bFGF. The lack of bFGF signals photoreceptors to initiate the apoptotic pathway. On the other hand, if the microglia secrete CNTF or GDNF (glial cell-derived neurotrophic factor), this stimulates BDNF secretion from the Müller cells, which will auto-stimulate the Müller cells to increase bFGF secretion to the photoreceptor cells, promoting photoreceptor cell survival. Therefore, this complex interaction between microglial, Müller and photoreceptor cells may play an important role in regulating cell death and survival following the onset of LIRD. In support of this model, Hafezi *et al* (1997a) have observed an influx of microglial into the light-treated retina within 24 hours of light treatment, likely in response to the initial damage to the photoreceptor cells.

1.B-1d-ii. Genetic background: Within a particular species there can also be significant difference in response to LIRD. LaVail *et al* (1987) demonstrated that different strains of mice displayed different sensitivity to light-induced photoreceptor cell loss. Recently, sequence variation in RPE65 has been shown to account for some of this strain variability, with mice containing an altered form of RPE65 having a slowed rhodopsin regeneration rate and a reduced sensitivity to bright light exposures (Wenzel *et al*, 2001a). This variation in RPE65 in these strains also appears to affect the mechanism of photoreceptor cell loss, as a lack of c-fos protects wild-type mice from light damage but has no effect on RPE65-knock-out mice (Wenzel *et al*, 2003). In addition to RPE65, several variable quantitative trait loci have been identified in different strains of mice that affect light damage sensitivity (Danciger *et al*, 2003), though the identities of these loci are unknown.

Even within transgenic lines carrying the same genetic mutations within a given gene, the response to LIRD can vary greatly. In rats carrying mutant forms of rhodopsin, the strain P23H (pro23his) sub-strain 2 showed photoreceptor cell loss restricted to the superior hemisphere, while strain P23H sub-strain 3 showed photoreceptor and RPE loss along the entire vertical median (Vaughan *et al*, 2003). Even more extreme differences were observed in S-antigen/transducin double knock-out mice; 6 out of 18 litter mates displayed high sensitivity to light, while the remaining 12 were resistant to light damage (Hao *et al*, 2002). Therefore, as seen with retinal degeneration in humans, genetic background can play a significant role in the susceptibility and progression of LIRD in rodent models.

1.C. PROJECT DESIGN

1.C-1. Practical considerations in experimental design

1.C-1a. Nature of light exposure used in current study

In order to elucidate the molecular changes associated with light-induced retinal degeneration in rats we chose to utilize green light-induced retinal degeneration. Light exposures were performed in Plexiglas chambers, known to have an approximately 100 nm band pass, transmitting 490-580 nm light and resulting in an illuminance of approximately 1200 lux within the chamber (Figure 1.8, Ogranisciak, 2003). The Plexiglas chambers absorb UV light, thus preventing conjunctivitis, and blue-UV cone

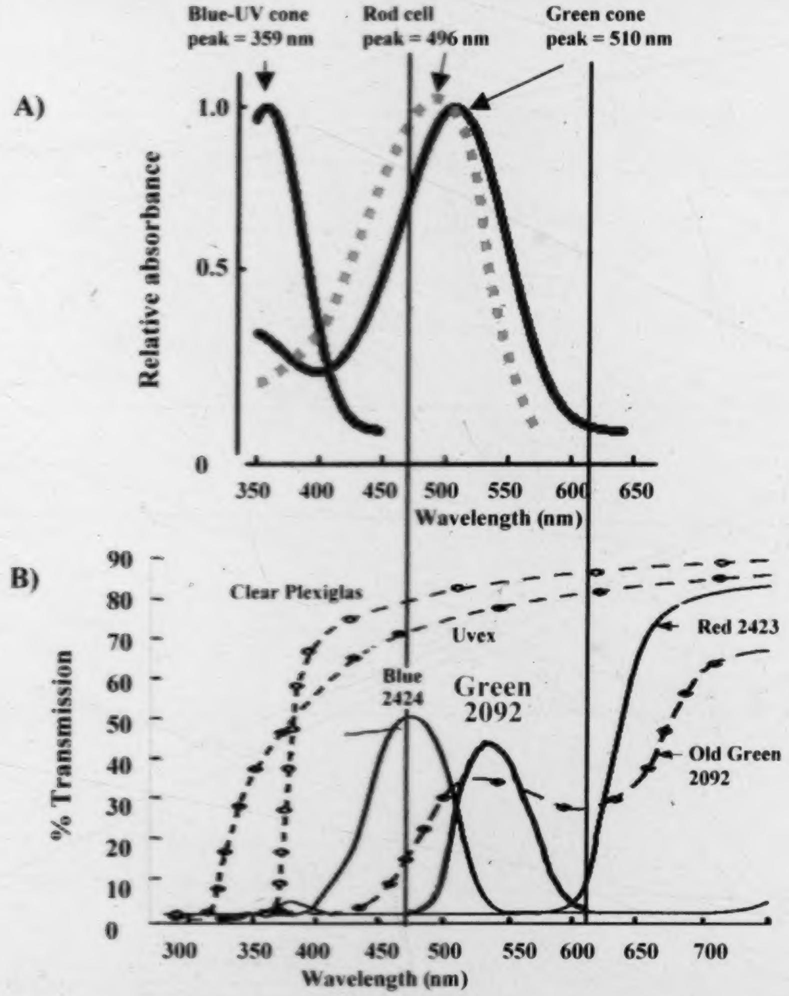

Absorption spectrum of rat photoreceptors versus transmission of green Plexiglas filter #2092

Figure 1.8. Absorption spectrum of rat photoreceptors versus transmission of green Plexiglas filter #2092. (A) Representation of the absorbance functions of rat rod photoreceptors (Berg *et al*, 2002), and rat blue-UV and green cone photoreceptors (Jacobs *et al*, 2001). (B) Transmission spectrum of green Plexiglas #2092 filters used during light-exposures in current study (adapted from Organisciak, 2003). Area between solid purple lines show region of overlap between transmission and absorption spectrums. Image compiled from those in Berg *et al*, 2002; Jacobs *et al*, 2001; and Organisciak, 2003.

cell response (Organisciak and Winkler, 1994), which may confound results. The treatments used were designed to induce 50% of rhodopsin bleaching within 5 minutes, though inferior regions of the retina are less vulnerable than superior retina (reviewed by Organisciak, 2003). Conditions used have been shown to induce rod photoreceptor cell death within 1-6 days following light exposures. By 10 to14 days after exposure cell death is complete, as is cellular repair of surviving cells.

Wavelength of light, exposure times and light intensity have all been shown to affect the duration and rate of photoreceptor cell death in LIRD (Noell, *et al* 1966; Wong *et al*, 2001; Organisciak *et al*, 2003; Specht *et al*, 1999). In rodents, green light (490-580 nm) corresponds to the absorption spectrum of rhodopsin and results in activation of the phototransduction cascade (Noell *et al*, 1966; Williams *et al*, 1983) in both rod photoreceptors and green light-sensitive cones (Figure 1.8). As rhodopsin orgreen cone opsin are the only target molecule, only one pathway should be affected in these cells. Though both cell types respond to green light, histological analysis of the green light-treated retina demonstrated that the rod photoreceptor cells primarily degenerate, while the cone cells prevailed (Cicerone, 1976; Kuwabara and Funahashi, 1976; LaVail, 1976; Rapp *et al*, 1990). Evidence of cone survival is based on ERG response patterns, and histological analysis of light treated retinae. Though the green-light sensitive cones will respond to the intense green light exposure, the proportion of cone cells in the rat retina is less than 1%, and hence it is assumed that the cone response will have a minimal effect on the results obtained. Therefore, the use of green light allows for the analysis of a primarily rod photoreceptor cell degeneration. Analysis of rod cell death has shown DNA fragmentation ladders and morphological characteristics indicative of apoptotic cell death (Organisciak *et al*, 1995; Remé *et al*, 1995; Kuwabara *et al*, 1976).

Other studies have used intense blue light (420-460 nm) exposure in rodents to study LIRD. Blue light induces damage to the both rod and blue-UV light sensitive cone photoreceptors as well as to the neighboring RPE (Ham and Mueller, 1976; Noell *et al*, 1966). Interestingly, blue light appears to have a more detrimental effect on photoreceptor cells than green light, and leads to high levels of rod cell loss, likely due to a process known as photochemical reversal of bleaching (Grimm *et al*, 2000a; 2001). The process is believed to occur when metarhodopsin II, an intermediate formed following rhodopsin bleaching, absorbs photons of light, and as a result is converted back to 11-cis retinal. As the metarhodopsin II is still attached to the opsin protein at the time of this conversion back to 11-cis retinal, the regeneration back to an unbleached state is very rapid. By reversing the bleaching of rhodopsin through this RPE-independent mechanism, blue light maintains a high level of unbleached rhodopsin which increases sensitivity to light damage. Therefore, unlike green light-induced cell loss, blue light appears to induce photoreceptor cell death by a mechanism independent of activation of the phototransduction cascade (Remé *et al*, 2003).

Broad spectrum white light, which encompasses all wavelengths within the visible spectrum, and is used by a variety of groups investigating LIRD (Grimm *et al*, 2000b; Hafezi *et al*, 1997a; Donovan and Cotter, 2001, 2002), includes the combined effects of both blue and green light. UVA (ultra-violet A) light (325-350 nm), on the other hand, also induces photoreceptor cell degeneration, although the RPE is not affected (Rapp *et al*, 1990; 1992; Ham and Mueller, 1976).

Moderate intensity green light (~1200 lux) was chosen to further limit the response to light the photoreceptor cells. Exposures of 1000 lux for 2 hours lead to changes evident throughout the photoreceptor cell (Szczesny *et al*, 1995). Low intensity exposures of 400-800 lux for 2 hours lead to changes in only the rod outer segments (Bush *et al*, 1991), while exposures of 3000 lux for 2 hours affect the photoreceptor cells of the central retina as well as the RPE (Hafezi *et al*, 1997a). (Note: One lux represents the light from 0.0929 footcandles or the amount of illumination that would be produced by one candle positioned in the exact center of a sphere one foot in diameter, with the candle giving off equal illumination to all points within the sphere [Word IQ dictionary web-site]).

Continuous light was used in this study, to which dark-reared rats were shown to be more vulnerable to intense light exposures than their cyclic-reared counterparts (Figure 1.9; Organisciak *et al*, 1989; Noell *et al*, 1966; Birch *et al*, 1980). Exposure to intermittent light was found to increase the intensity of the photoreceptor damage (Organisciak *et al*, 1989). Cyclic-reared rats showed a lower degree of degeneration than dark-reared rats when the two groups were exposed to intermittent light.

1.C-1b. Rearing conditions

Rats, being nocturnal animals, are normally exposed to cycles of approximately 12 hours of visible light and 12 hours of darkness. Alterations in the amount of light that a rat is exposed to lead to numerous changes in the protein composition and morphology of the photoreceptor cells. The photoreceptor cells will undergo several changes that will allow for the absorption of more or fewer photons depending on the light flux available.

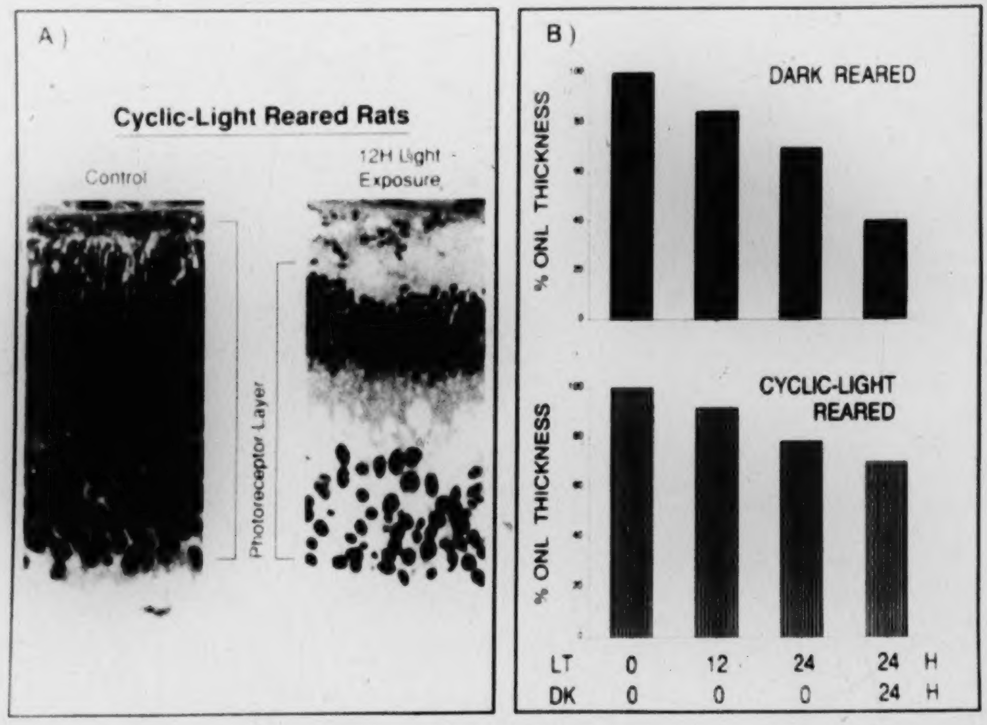

Figure 1.9. Loss of photoreceptor cells following light exposure. Cyclic- and dark-reared rats were exposed to intense green light for 12 or 24 hours, followed by a 0 to 24 hour dark-recovery period. (A) Retinal histology showing a decrease in thickness of the ON, indicating loss of photoreceptor cells following 12 hours of light. (B) Measurements of ONL thickness (as percent of un-treated control retinae), demonstrating increased sensitivity of dark reared rat retinae to varying light exposure as compared their cyclic reared counterparts. Figure adapted from Organisciak *et al*, 1985; 1989.

These changes may be the result of what is known as photostasis (Penn and Williams, 1986), where the retina requires that a certain number of photons of light per day be absorbed for proper photoreceptor cell function. An expansion of the photostasis concept is the Equivalent Light hypothesis (Fain and Lisman, 1993, Lisman and Fain, 1995). This hypothesis proposes that through continuous or excessive light exposure, or genetic mutations, constitutive activation of the phototransduction cascade represents a state that exceeds the photon absorption requirements of the cell and leads to stress within the cell. This will lead to apoptosis if the cell is not able to up-regulate protective mechanisms that allow it to deal with the increased stress levels. Therefore, the rearing conditions-induced changes in the photoreceptor cell (described below) can have significant effects on the susceptibility of photoreceptor cells to damage induced by intense light exposure.

1.C-1b-i. Changes in rhodopsin levels and organization: In order to maximize the absorption of photons in a dark environment, dark-reared animals increase the amount of rhodopsin per eye, and organize this rhodopsin more tightly in the discs of the rod OS (ROS, Noell *et al*, 1971a, b; Organisciak *et al*, 1977). In cyclic-reared rats, which are exposed to higher levels of light, and as such are more at risk of exceeding their daily photon requirements, the levels of rhodopsin is reduced and the rhodopsin present is less densely packed into the OS. As a result, the outer segments of cyclic-reared rod cells are shorter and more disorganized than their dark-reared counterparts (Penn *et al*, 1987a; Kaldi *et al*, 2003; Noell *et al*, 1971 a, b; Organisciak *et al*, 1977).

1.C-1b-ii. Changes in gene expression of phototransduction-related genes: In addition to changes in the levels of rhodopsin, changes are also seen in the expression of genes associated with phototransduction as a result of rearing conditions. Biochemical protein analysis demonstrated that levels of α-transducin increase in a dark environment, while arrestin (S-antigen) levels decrease (Organisciak *et al*, 1991; 1999a; Farber *et al*, 1991). The opposite holds true in a cyclic environment. Other protein components of the phototransduction pathway, such as the cGMP (cyclic guanosine mono-phosphate)-PDEγ complex, remain unchanged under the different rearing conditions.

1.C-1b-iii. Changes in levels of oxidative-stress related factors: In a normal cyclic-reared animal, a high level of metabolism and oxygen tension within the retina, coupled with high levels of polyunsaturated fatty acids in the OS, result in high levels of oxidative stress in the normal retina (Organisciak and Winkler, 1994). In dark-reared animals, increased levels of rhodopsin and proteins involved in phototransduction make these animals more vulnerable to light levels, but also place them more at risk to the effects of light-induced oxidative stress than cyclic-reared animals. Anti-oxidant factors such as vitamin C, vitamin E/ascorbate, glutathione (GSH), GSH peroxidases, GSH S-transferase and GSH reductase, all of which affect the redox levels within a cell are induced in dark-reared animals (Penn *et al*, 1987b; Kaldi *et al*, 2003; Tanito *et al*, 2002a, b). As well, levels of the enzyme superoxide dismutase (SOD), which converts oxygen radicals to hydrogen peroxide, have been shown to decrease in cyclic-reared rats, but remain unchanged in dark-reared rats (Yamashita *et al*, 1992).

1.C-1b.iv. Changes in OS membrane structure and composition: Dark-rearing conditions alter rod outer segment tip shedding and phagocytosis by RPE, and OS length as a result of rhodopsin packing and activity of the phototransduction cascade. As a result, the levels of docosahexaenoic acid (DHA) and cholesterol, major constituents of the photoreceptor OS are increased in dark-reared rats (Penn *et al*, 1987a; Kaldi *et al*, 2003; Noell *et al*, 1971a, b; Organisciak *et al*, 1977).

1.C-1c. Use of rats during LIRD

Male Sprague-Dawley rats at 61 days of age were used for control and experimental groups in this study. Rats were chosen over mice, as rats appear to be significantly more vulnerable to LIRD than mice (Penn *et al*, 1985; Organisciak and Winkler, 1994). In addition to differences in sensitivity, differences between the response to LIRD have also been observed between mouse and rats. Studies in rats show loss of both photoreceptor cells and the overlying RPE, while studies in mice show loss restricted to the photoreceptor cell layer even under similar treatment conditions (La Vail *et al*, 1987; Keller *et al*, 2001). Sprague-Dawley rats were chosen over other strains of rats, as they are albinos. This is important as pigmentation provides a protective function, and hence albino rodents are significantly more vulnerable than their pigmented counterparts (Rapp and Williams, 1980a, 1980b; LaVail 1980; Rapp and Willaims, 1979; Semple-Rowland and Dawson, 1987).

Increased age has been shown to increase susceptibility to LIRD (O'Steen *et al*, 1974). The use of 61day old rats allows for the exposure of mature photoreceptors, which mimics RP conditions. As well, rats less than 25 days old are significantly less vulnerable than adult rats (Noell, 1980). Male rats were used exclusively in this study as hormone levels have also been shown to play a role in phototoxic sensitivity (O'Steen, 1980, 1982). The involvement of the adrenal and pituitary glands and their respective hormones appears to play a role in the stress response to light damage, possibly through the regulation of prolactin levels (O'Steen *et al*, 1982).

1.C-1d. Time of light exposure

All light exposures in this study were performed at 9 am. Time of day in which light exposure was administered was significant as there appears to be a circadian effect to phototoxic sensitivity. Animals treated with intense light at night (1 a.m.) are more vulnerable than those treated during the day (5 p.m.) (Organisciak *et al*, 2000; Vaughan *et al*, 2002). Interestingly, cyclic-reared animals are more vulnerable to night treatments than dark-reared animals (Organisciak *et al*, 2000). Therefore, there are likely internal diurnal regulated factors that promote cell death versus cell survival that peak at night. Though 1 am light-treatments give the maximal levels of photoreceptor cell loss in dark-reared animals (Organisciak *et al*, 2000), 9 am was chosen as a exposure start time for the convenience of those individuals performing the light treatments on the rats.

1.C-2.Prelimary studies

To quantify the molecular progression of LIRD, the expression profiles of several key genes was determined (Wong *et al*, 2001). Analysis of *IRBP* (Interphotoreceptor retinol-binding protein), a photoreceptor specific gene involved in retinol transport between the photoreceptor cells and the RPE, was used as a marker of normal photoreceptor cell function (Pepperberg *et al*, 1993; Wong *et al*, 2001). *IRBP* mRNA expression levels decreased after a 4-8 hour light exposure, and showed a partial recovery during the dark-recovery period. The initial loss of *IRBP* expression correlates with a loss of photoreceptor function as the cells begin to enter an apoptotic pathway. The recovery of *IRBP* expression correlates with the recovery of normal photoreceptor function in a sub-population of photoreceptor cells during the dark recovery period following treatment. Heme-oxygenase I (*HO-1*) expression was examined as a marker of oxidative stress in the light-treated retina (Stocker, 1990). *TRPM-2* (testosterone-repressed prostate message 2)/clusterin mRNA levels were analyzed to illustrate the active response of surviving cells to the cell death occurring in neighboring cells. After 8 hours of intense light exposure, the induction of *HO-1* became apparent, suggesting the presence of an oxidative stress environment. Following the induction of *HO-1* expression is the induction of clusterin, again first apparent after 8 hours of light exposure. This correlates with the time point where the first morphological signs of apoptosis become apparent. Levels of *HO-1* and clusterin are also very high during the initial recovery period, followed by a decrease in *HO-1* levels as recovery proceeds. The decline in *HO-1* suggests a decreased oxidative environment later in the recovery period, while the continued clusterin expression during this period suggests a role in further cell recovery.

Based on the expression profile of *IRBP, HO-1*, and clusterin, the degeneration profile was divided into distinct phases (Figure 1.10; Wong *et al*, 2001). The 4 hour treatment regime represents the commitment phase, where it is proposed that there is an expression of genes that commit the photoreceptor cell to the apoptotic pathway, accompanied by a reduction in expression of genes involved in normal metabolism.

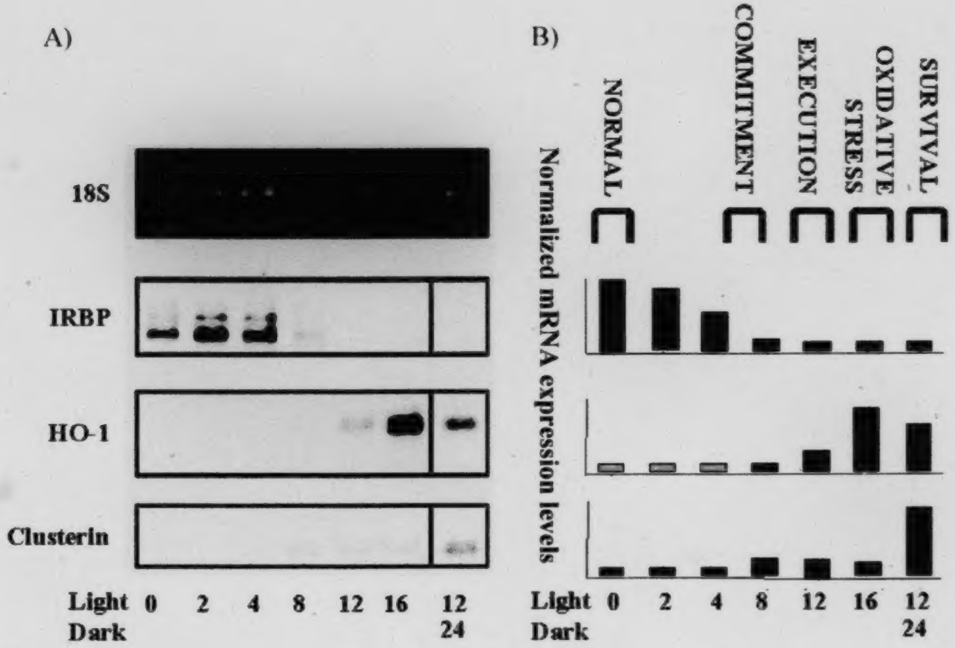

Figure 1.10. Definition of the molecular phenotype of light-induced retinal degeneration. (A) Northern blot analysis of IRBP, HO-1, and clusterin expression was performed on control retinae, and retinae treated with light for 2, 4, 8, 12, and 16 hours prior to enucleation. An additional treatment duration of 12 hours followed by a 24-hour dark recovery period was also performed. Expression levels of mRNA for IRBP, HO-1 and clusterin were normalized by comparison to 18S ribosomal RNA levels and are illustrated on the graph. IRBP expression was used as an indicator of normal photoreceptor function. HO-1 expression was used as an indicator of an oxidative stress environment. Clusterin expression was used as an indicator of a Muller cell survival response to an apoptotic environment. Based on these gene expression profiles, the apoptotic pathway observed in LIRD was divided into the commitment, execution, oxidative stress, and survival phases. Refer to text for phase description. (B) Relative levels of mRNA expression normalized to 18S ribosomal to account for loading differences between lanes. Figure adapted from Wong *et al*, 2001.

Treatment of the rat retina for 8 hours represents the execution phase where there is likely the induction of genes involved in the process of apoptosis itself. The 16 hour treatment represents the stress phase where there is induction of genes in response to a high oxidative stress environment. The 12 hour light treatment followed by the 24 hour dark recovery period represents the survival phase where the induction of genes involved in cell survival become apparent.

1.C-3. Rationale for the use of LIRD in the study of retinal disease

1.C-3a. Similarities between photoreceptor cell loss in LIRD and human retinal dystrophy

Light-induced retinal damage can be used as a model system for the study of both retinitis pigmentosa and macular degeneration. The rod-specific degeneration that is seen in RP is mimicked following exposure to intense green light. Similarly, the loss of DHA, seen following light exposure, is also observed in some patients with RP (Bush *et al*, 1991). Dietary supplementation with DHA has been shown to slow the progression of photoreceptor cell loss in a patient with Stargardt-like macular degeneration (MacDonald *et al*, 2004).

As previously discussed, rhodopsin is the primary photopigment affected following exposure to green light, and the involvement of rhodopsin in degeneration is a feature shared by the rhodopsin knock-out mouse model of RP and some forms of human RP (Grimm *et al*, 2000; NCBI OMIM web-site, entry 180380, rhodopsin, July 2004). In humans, defects in the rhodopsin gene are a causative factor accounting for over 15% of all cases of retinitis pigmentosa, with over 70 known disease-causing mutations previously identified (NCBI [National Center for Biotechnology Information] OMIM [Online Mendelian Inheritance in Man] web-site, entry 180380, rhodopsin, July 2005). As well, levels of α-transducin and arrestin are altered following light exposure, stressing the important role of changes to the phototransduction cascade in retinal pathology. This is shared with the rd mouse model of RP, in which alterations in the β-subunit of PDE result in problems in the phototransduction cascade, and subsequent cell death of the photoreceptor cells.

Macular degeneration, in contrast to RP, is a disease primarily of the cone photoreceptors located within the central macular and fovea region of the human retina. Though rodents, like other non-primate mammals, lack a macula and central fovea, it is still feasible to study macular degeneration in rodent models. This is largely due to the similarity in rod:cone ratios in the rodent retinae and the human peripheral retinae outside of the central 20° that comprises the macula (Osterberg, 1935). As well, the use of the light-induced model in the study of macular disease is based on the known interactions between rod and cone photoreceptors, as well as the involvement of oxidative stress in the pathology of both macular degeneration and LIRD. As in Stargardt macular dystrophy, where a rod dysfunction is believed to lead to a cone-specific degeneration (Allkiments *et al*, 1997; Steele, 1994), cone cell death in LIRD is believed to be a secondary effect to the dysfunction in the rod cells (Cortina *et al* 2003; Ham *et al*, 1976; Noell *et al*, 1966; Organisciak and Winkler, 1994).

Like LIRD, the direct interaction between photoreceptor cells and the RPE has also been demonstrated in human retinal dystrophies where defects in rod cell proteins such as ABCR or ELOVL4 affect cones and subsequently the RPE within the macular region (Allkiments *et al*, 1997; Zhang *et al*, 2001). Similarly, defects in RPE65, known to affects rod and cone photoreceptors in LIRD, affects rod cells in autosomal recessive retinitis pigmentosa (Morimura *et al*, 1998).

Similarly, the accumulation of lipofuscin in the macular region, a characteristic of macular dystrophies, is believed to be associated with lipid oxidation in a highly oxidative environment (Mah *et al*, 1998, and Taylor *et al*, 1992). The protective effects of DMTU and ascorbate during light exposure demonstrate the causative role of an oxidative environment in light-induced pathology. As well, clusterin expression is induced in both light-treated retinae and retinae of patients with RP (Jomary *et al*, 1999), suggesting a Müller cell response in both cases.

In addition, the use of light to induce photoreceptor cell loss is supported by experimental and epidemiological evidence that suggests that light may be an important factor in the etiology of age-related macular degeneration and retinitis pigmentosa (Beatrice *et al*, 2003; Taylor *et al*, 1990, Cruickshanks *et al*, 1993; Simons *et al*, 1993; Cideciyan *et al*, 1998, Cruickshanks *et al*, 2001). This role of light as a cofactor in photoreceptor cell loss due primarily to genetic mutations is also observed in animal models of RP and MD (Sanyal and Hawkins, 1986; Wang *et al*, 1997; Chen J *et al*, 1999; Chen CK *et al*, 1999; LaVail *et al*, 1999; Organisciak *et al*, 1999a).

1.C-3b. Advantages of the use of LIRD over other models of retinal dystrophy

The use of LIRD in the study of retinal degeneration is different from the previously described models of RP. First, in genetic animal models degeneration begins shortly after birth, often before the photoreceptors fully develop. As the majority of human retinopathies have onset in later life (Mah *et al*, 1998), the analysis of mature photoreceptor cells in the light-induced model provides advantages over systems where apoptotic cell death in photoreceptors is studied shortly after birth. Second, exposure of wild-type rats to intense light in LIRD allows the analysis of the resulting photoreceptor dysfunction and apoptosis in a normal genetic background. As the animals utilized are wild-type, their photoreceptor cells develop normally, allowing the study of the effect of light-exposure on mature photoreceptors. Third, LIRD provides an element of control that is not possible in genetic models of retinal degeneration. In genetic-based animal models, the genetic lesion affects normal cell function and leads to photoreceptor cell death. The rate of apoptosis and the final outcome of cell death are entirely under the "control" of the cell itself. In contrast, LIRD allows the experimenter to alter the rate and extent of cell death by simply altering exposure times and light intensities. The induction of a slow apoptotic response for example, allows for the fine analysis of the molecular changes occurring during cell death. In contrast, the induction of only marginal damage allows for the analysis of repair and survival responses. Thus, this model system allows for the detailed characterization of the normal retinal response to experimentally induced conditions, which is not possible in other models of retinal disease.

Finally, LIRD has an advantage over photoreceptor culture systems in which cell death is induced. As the retina consists of numerous different inter-dependent cell types, the response to a given stimulus in a cell culture system is limited to events associated with one cell type and therefore is not representative of a whole retinal response. As LIRD is performed on intact retina, a more complete response to light, and accompanying photoreceptor dysfunction, is observed as all cell types are present and able to mediate their effect. LIRD has an advantage over knock-out models of retinal dystrophy as well. Often the deletion of a single gene can affect numerous different pathways in a cell, leading to abnormal responses to experimental conditions. For example, photoreceptor cells in both c-fos and rhodopsin knock-out mice have significant structural alterations that may affect experimental results (Grimm *et al*, 2000b; Wenzel *et al*, 2001b; Lem *et al*, 1999). In addition, the variable response to LIRD of arrestin/transducin double knock-outs litter mates which contain the same genetic defect (Hao *et al*, 2002), suggests potential problems in the use of such systems to study physiological events.

1.C-3c. Advantages and disadvantages of using dark-reared controls in LIRD

Because of changes in photoreceptor structure and composition that result from dark-rearing conditions, dark-reared rats do not represent normal photoreceptor cells. Regardless, dark-reared rats were chosen for use in this study over cyclic-reared rats as dark-reared rats are two to three times more vulnerable to light damage than their cyclic-reared counter parts (reviewed by Organisciak, 2003; Organisciak *et al*, 1985; 1989; Noell *et al*, 1966; Birch *et al*, 1980). Dark-reared animals require an 8 hour exposure at 2200 lux of green light for a 50% loss in photoreceptors, while cyclic-reared animals require a 24 hour exposure for the same degree of damage (Figure 1.9; adapted from Organisciak *et al*, 1985).

Dark-rearing conditions helped to normalize the retinae of the rats used prior to treatment. Normalization of subjects during cyclic-rearing conditions is difficult, as there is often unavoidable variation in lighting conditions between cages in animal care facilities, and during transit from animal suppliers. As the OS of the retina is recycled through the RPE every 9-10 days, a minimum of two weeks acclimation is required regardless of dark- or cyclic-light rearing conditions to ensure all subjects have comparable retinal environments (Organisciak, 2003).

As dark-reared rats were used for light-treatments, untreated dark-reared rats were also used as controls. Though cyclic-reared rats have normal photoreceptors, their use as controls in this study would have confounded the interpretation of the results as both light exposures, and photoreceptor cell morphology and composition, would have varied between control and experimental groups. The use of dark-reared controls allows for the analysis of only the effect of light exposure in the experimental group. Therefore, as abnormal photoreceptor cell are used in this study, caution must be used when comparing the results obtained to normal cyclic-reared rats, or human cases of retinal degeneration.

1D. DEFINITION OF THE DEGENERATION PHENOTYPE IN LIGHT-INDUCED RETINAL DEGENERATION IN RATS, A MODEL SYSTEM OF HUMAN RETINAL DYSTROPHY.

1.D-1. Focus of thesis

1.D-1a. Objectives

The work described in this thesis was initiated with the objective of identifying and characterizing some of the molecular events involved in photoreceptor dysfunction in LIRD. Determining how these molecular factors affect the photoreceptor cell may provide insight into the mechanisms underlying photoreceptor degeneration in various human retinopathies such as retinitis pigmentosa and macular degeneration.

1.D-1b. Hypothesis

This work was based on the hypothesis that the retinal degenerative phenotype in LIRD can be defined at the molecular level and that it reflects an altered gene expression pattern when compared to untreated control retinae. The molecular changes that occur during LIRD will include alterations in the expression of genes that are either induced or repressed following intense light exposure. In addition, molecular changes will occur in both the dying and the surviving cells of the retina. Therefore, the results described here will represent the combined global response of a mixed population of cells within the light-treated retinae.

1.D-2. Experimental approach and rationale

1.B-2a. Chapter 3: Activation of members of the caspase cascade in the rod outer segments by intense green light-induced retinal degeneration

This chapter describes the characterization of the caspase family of pro-apoptotic regulators during the progression of LIRD. Northern blot analysis of known photoreceptor genes involved in phototransduction was used to determine the approximate time-line of photoreceptor dysfunction following intense light exposure. Gel electrophoresis was used to analyze the extent of DNA fragmentation, a known marker of apoptotic cell death, to establish a correlation between the onset of photoreceptor cell dysfunction and active apoptotic cell death. Western blot analysis was used to demonstrate proteolytic processing and potential activation of various members of the caspase cascade. In addition, immunohistochemistry was used to determine the localization of active caspases within the light-treated retina.

1.B.-2b Chapter 4: Identification and bioinformatic characterization of differentially expressed LIRD genes

This chapter describes the construction and screening of a cDNA library representing the molecular environment of the active execution phase of LIRD. Genes that demonstrated differences in expression between dark-reared control retinae and light-treated retina were isolated and preliminary characterization of these genes was performed. Northern blot analysis confirmed the differential status of the identified genes, and sequence analysis was used to determine clone identity. Extensive bioinformatic characterization of the identified genes included nucleotide and protein analysis of rat, mouse and human orthologs, analysis of specific tissue expression, and "*in silico*" functional analysis.

1.D-2c. Chapter 5: Identification of a novel rat diphthamide methyltransferase, which plays a role in oxidative stress-induced cell death

This chapter describes the isolation and characterization of a differentially expressed gene encoding a putative DPH5 diphthamide methyltransferase. A combination of sequence and bioinformatic analysis was used to determine the rat gene structure. In addition, bioinformatic analysis of the rat promoter sequence provided insight into the factors potentially regulating the expression of this gene in LIRD. The yeast ortholog of DPH5 was used in an oxidative stress sensitivity assay to determine the potential role of DPH5 in oxidative stress-induced cell death. In addition, transmission electron microscopy (TEM) was used to analyze yeast undergoing oxidative stress for morphology characteristic of apoptotic cell death.

Chapter 2

Materials and Methods

2.A. PREPARATION OF ANIMALS

Treated rat retinae used in the course of this study were generously provided by Dr. Daniel Organisciak, Linda Barsalou, and Ruth Darrow at Wright State University (Dayton, OH). Weanling male albino Sprague-Dawley rats were obtained from Harlan Inc. (Indianapolis, IN) and kept in darkness until the age of 60 days. At 61 days of age, rats (in groups of 2-3) were exposed to intense visible light for 0, 4, 8, or 16 hours prior to isolation of retinae. An additional time point of 12 hours of light treatment followed by 24 hours of dark recovery prior to enucleation was also performed. Light exposures were started at 9 a.m. and performed in green #2092 Plexiglas chambers (1/8" wall thickness, Dayton Plastics, Dayton OH) transmitting 490-580 nm light (green light). The chambers were surrounded by 7-12" circular 32W fluorescent bulbs (G.E. "Cool white" FC 12T9-CW), which provided 360° light exposure with an illuminance of approximately 1200 lux, and results in a corneal irradiance of 170-200 $\mu W/cm^2$ (Figure 2.1) (Noell, 1966; Organisciak *et al*, 1995; Organisciak, 2003; Wong *et al*, 2001). Rats were killed in carbon dioxide saturated chambers and retinae were excised and flash frozen in plastic vials on dry ice. The retinae were stored at –80°C until use. RPE contamination was estimated to be approximately 2-3% of the tissue quantity isolated, based on visual inspection (Linda Barsalou, personal communication). For each treatment condition, retinae from 6-8 animals were pooled. In all cases, the animals were cared for in accordance with the guidelines defined by the National Institute of Health Guide for the care and use of laboratory animals.

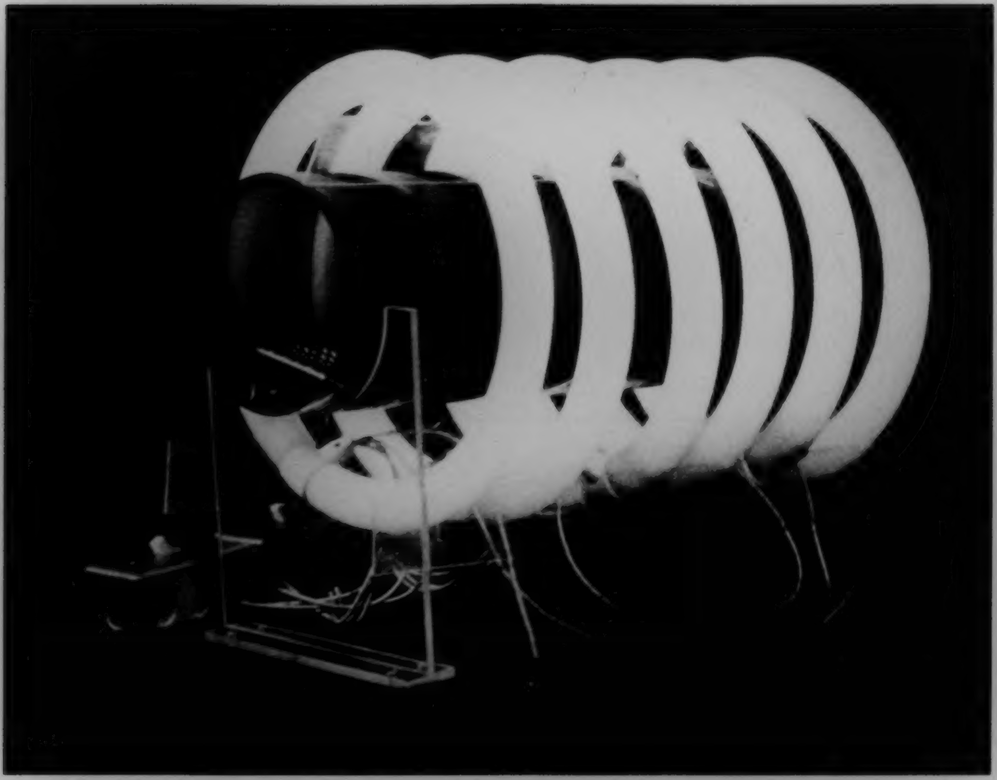

Figure 2.1. Light damage chamber used to induce green light induced retinal degeneration. Chamber specifications include: green #2092 Plexiglas chambers (Dayton Plastics, Dayton OH) transmitting 490-580 nm light (green light) with fluorescent bulbs with an illuminance of approximately 1200 lux. Treatments were performed on groups of 2-3 rats at a time.

2.B. ISOLATION OF NUCLEIC ACID.

2.B-1. Isolation of RNA

2.B-1a. Isolation of total RNA. All tubes, equipment, and items used in the process of RNA extraction were cleaned and autoclaved to ensure that they were as RNase free as possible. For the initial setup, the Polytron probe (Kinematica Polytron PT3100, Brinkmann Instruments, Mississauga, ON) was washed once in 100% ethanol, twice in DEPC-treated water (0.1% DEPC, autoclaved), and once with Trizol (Invitrogen, Burlington, ON). Between each sample, the probe was washed with 3 washes of DEPC-treated water.

Approximately 2 ml of Trizol was added to a 50 ml polypropylene tube containing 6 to 8 frozen rat retinae (2 ml per 100 mg of tissue). Tissues were homogenized with the Polytron at 23,000 rpm in short 30 second bursts until tissue was completely homogenized. Tissue was stored on ice between bursts. The homogenate was then placed on ice. Chloroform (0.1 ml per 1 ml of homogenate) was added, and the tubes were mixed with vigorous shaking for at least 15 seconds. The samples were divided into two 1.5 ml polypropylene tubes and incubated on ice for 15 minutes to 1 hour. The samples were then centrifuged at 13,000 rpm at 4°C for 30 minutes. The aqueous phase was isolated and transferred to a new 1.5 ml tube, and the organic layer was saved and used for protein isolation (Section 2.C). An equal volume of cold isopropanol (analytical grade) was added to the aqueous phase and the samples were stored at –20°C overnight. The samples were then centrifuged at 13,000 rpm at 4°C for 30 minutes. The supernatant was removed and the pellet washed with 1 ml of cold 70% ethanol in DEPC-treated water. The pellet was spun at 13,000 rpm at 4°C for 15 minutes. The supernatant was then decanted and the tube was inverted and the pellet was allowed to dry for approximately 10 minutes. The pellet was resuspended in 30-100 µl of DEPC-treated water depending on pellet size. The RNA was then flash frozen on dry ice and stored at –80°C until use.

2.B-1b. Isolation of mRNA. Poly(A+) RNA was isolated from total RNA using Oligotex Spin Columns (Qiagen, Mississauga, Ontario). DEPC-treated water (0.1% DEPC, autoclaved) was added to total RNA to a final volume of 250 µl. An equal volume of 2X binding buffer (20 mM Tris-HCl pH 7.5, 1000 mM NaCl, 2 mM EDTA, 0.2% SDS) and 15 µl of the Oligotex suspension {oligo dT_{30} primer linked to latex particles [10% w/v Oligotex particles, 10 mM Tris-HCl pH 7.5, 500 mM NaCl, 1 mM EDTA, 1% SDS, 0.1% NaN_3]} were then added. The mixture was incubated at 65°C for 3 minutes to disrupt secondary structure of the RNA, and then left at room temperature for 10 minutes at room temperature to allow for hybridization between the poly(A) tails of the mRNA and the Oligotex particles. The mixture was centrifuged at 14,000 g for 2 minutes and the supernatant was removed. The pellet was resuspended in 400 µl of wash buffer (10 mM Tris-HCl pH 7.5, 150 mM NaCl, 1 mM EDTA), and the solution was added to the spin column and centrifuged for 30 seconds at 14,000 g. Another 400 µl of wash buffer was added to the column and centrifuged as before. The mRNA was eluted twice with 20 µl of 70°C elution buffer (5 mM Tris-HCl pH 7.5). The mRNA was quantified using the ethidium bromide plate assay described in section 2.D-1b.

2.B-2. Isolation of DNA

2.B-2a. Isolation of genomic DNA from blood. Genomic DNA from blood was isolated using the protocol of Madisen *et al* (1987). Lysis buffers were pre-warmed to 37°C. Blood samples (5-15 ml in 0.5 M EDTA pH 8.0) were centrifuged at 2500 rpm for 5 minutes. The plasma layer was removed to 2-3 mm above the buffy coat and the buffy coat and half of the red blood cells were transferred to a 50 ml polypropylene tube. Five volumes of red blood cell lysis buffer (0.14 M NH_4Cl, 0.17 M Tris-HCl pH 7.7) was added and the mixture was incubated at 37°C for 4 minutes, then centrifuged at 2500 rpm at 4°C for 10 minutes. The supernatant was removed, leaving 3-4 ml and the pelleted cells. Pellets were washed several times with 0.15 M NaCl The cells were resuspended in 2 ml TE buffer (10 mM Tris-HCl, 1 mM EDTA; pH 8.0), and the cells were lysed by resuspending in white cell lysis buffer (0.2 % SDS, 1 M NaCl, 40 mM EDTA, 0.1 M Tris-HCl; pH 8.0). The mixture was incubated overnight at 4°C. An equal volume of phenol:chloroform isoamyl alcohol (25:24:1, saturated with 10 mM Tris-HCl pH 8.0, 1 mM EDTA) was added, the mixture was mixed for 15 minutes on a rocking platform, and then was centrifuged at 2500 rpm for 10 minutes at 4°C. The aqueous phase was removed and extracted with an equal volume of phenol:chloroform isoamyl alcohol.. The aqueous layer was removed after centrifugation and extracted with an equal volume of chloroform for 15 minutes on a rocking platform. After a second chloroform extraction, the aqueous layer was mixed with 2.5 volumes of 100% ethanol, and 0.1 volume 3 M NaoAc, and precipitated overnight at -20°C. The DNA was spooled around a 100 µl pipette tip and washed with 70% ethanol. The DNA was allowed to dry and was resuspended in TE buffer.

2.B-2b. Isolation of genomic DNA from tissue. 500 mg of tissue (stored at -70°C) was allowed to thaw in 50 ml polypropylene tubes, and allowed to thaw. Using surgical scissors, the tissue was minced, and was then mixed with 5 ml of lysis buffer (10 mM Tris-HCl pH 8.0, 10 mM NaCl, 1 mM EDTA). The samples were incubated at 65°C for 15 minutes to inactivate endogenous DNAses. SDS, proteinase K, and RNAse A were added to final concentrations of 1%, 2 mg/ml and 0.3 mg/ml, respectively. The mixture was incubated at 50°C for a maximum of 4 hours, with gentle inversion every 30 minutes, until the tissue was digested and appeared stringy in appearance. The tissue was extracted twice with phenol:chloroform isoamyl alcohol (25:24:1, saturated with 10 mM Tris-HCl pH 8.0, 1 mM EDTA). After the second extraction, 300 µl of 3 M NaoAc was added per ml and the samples were re-extracted with chloroform and precipitated with 2.5 volumes of 100% ethanol. The DNA was precipitated overnight at -20°C. The DNA was spooled onto a sterile 100 µl pipette tip, and was washed in 70% ethanol. The DNA was dried for approximately 10 minutes, and was resuspended in TE buffer (10 mM Tris-HCl pH 8.0, 1 mM EDTA).

2.B-2c. Isolation of plasmid DNA. Plasmid DNA was isolated from transformed bacterial cells using a modified alkaline lysis protocol (Pan *et al*, 1994). Ten ml cultures of transformed host bacterial cells were grown overnight at 37°C. The cells were pelleted at 3700 rpm for 5 minutes, and the supernatant was discarded. The cells were resuspended in 200 µl Merlin I solution (50 mM Tris-HCl pH 7.5, 10 mM EDTA), and an equal volume of Merlin II solution (0.2 M NaOH, 1% SDS) was added, followed by inverting several times. Merlin III solution [200 µl; 1.25 M KoAc, 7.1% glacial acetic acid (v/v)] was added and the samples were mixed by inversion. The sample was centrifuged at 17,000 rpm for 5 minutes. Supernatant was isolated and transferred to a fresh tube containing 1 ml of Merlin IV solution (7 M guanidine HCl, 33.3 % Merlin III, 1.5 % [w/v] diatomaceous earth). After reaction mixing, the sample was loaded onto a PrepSep R Extraction Column containing an isolation frit (Fisher, Ottawa, ON). The columns were centrifuged at 3700 rpm for 5 minutes. Two ml of Merlin V solution (200 mM NaCl, 20 mM Tris-HCl pH 7.5, 5 mM EDTA, 50% ethanol) was added to each column and they were centrifuged as before. The columns were placed in fresh 1.5 ml eppendorf tubes and 30-50 µl of 70°C TE buffer (10 mM Tris-HCl pH 7.4, 1 mM EDTA) or distilled water was added to each column. After a 1 minute incubation the columns were centrifuged at 3700 rpm for 5 minutes and the plasmid DNA was recovered in the eppendorf tube. Plasmids were stored at 4°C for short term storage or at -20°C for long term storage. Specific information regarding individual plasmids is summarized in Table 2.1.

2.B-2d. Isolation of PCR products. DNA synthesized by Polymerase Chain Reaction (PCR) (Section 2.J) was resolved by electrophoresis (Section 2.K-1b). PCR products were excised from agarose gels using a clean scalpel blade under UV illumination, and purified using a QiaQuick Gel Extraction kit (Qiagen, Mississauga, ON). Specifically, excised gel fragments were weighed and dissolved at 50°C in 3 volumes of QG buffer. An equal volume of isopropanol was added, and the solution was mixed by inversion. The mixture was loaded onto extraction columns and the supernatant was removed by centrifuging at 15,000 rpm for 2 minutes, or by use of a QIAvac Vacuum Manifold and a

Clone Name	Insert	Species	Vector	Insert Size	MCS site	Source
pGA-1	glutaminase	rat	pGEM-1	629 bp	EcoR1	ATCC
HHCH67	SPARC	human	pBluescrip SK-	1200 bp	EcoR1	ATCC
pSVcmyc1	c-myc	mouse	pSV2	4800 bp	BamH1/Xba1	ATCC
pCAT41	catalase	human	pcD	2200 bp	Xho1	ATCC
pH2.3	HSP70	human	pAT153	2300 bp	BamH1/HindIII	ATCC
pCS14-19	ribosomal protein S14	human	pUC13	688 bp	Pst1	ATCC
pKER2	ERCC2	human	pKSV10	2400 bp	Kpn1	ATCC
pUC-Cathepsin G	cathepsin G	human	pUC9	3000 bp	EcoR1	ATCC
XHJ-12.4	Jun-D	mouse	pBluescript KS-	1670 bp	EcoR1	ATCC
465.2	Jun-B	mouse	pGEM-2	1917 bp	EcoR1	ATCC
JAC.1	Jun	mouse	pGEM-2	2600 bp	EcoR1	ATCC
zif/268	Egr-1	mouse	pBluescript KS+	3200 bp	EcoR1	ATCC
pTAM2.5-a	Plat	mouse	pBluescript KS+	2519 bp	EcoR1	ATCC
pGEM2MCSF10	CSFM	mouse	pGEM-2	4000 bp	EcoR1	ATCC
pTR1	STMY1	rat	pUN121	1700 bp	EcoR1	ATCC
pMusSpl-11	Spl-1	mouse	pBluescript SK+	2600 bp	EcoR1	ATCC
CD-3A	cathepsin D	mouse	pBluescript KS+	1900 bp	EcoR1	ATCC
FosB2L	FosB	mouse	pBluescript KS-	1225 bp	BamH1/EcoR1	ATCC
Nup475	Nup475	mouse	pGEM-2	1814 bp	EcoR1	ATCC
pDP1278	ribosomal protein S4, Y-linked	human	pBluescript SK+	883 bp	Not1	ATCC
pDP1294	ribosomal protein S4, X-linked	human	pBluescript SK+	900 bp	Not1	ATCC
p19E	ribosomal protein S3	human	pUC19	862 bp	EcoR1	ATCC
HFBCL27	ribosomal phosphoprotein P1	human	pBluescript SK-1		EcoR1	ATCC
pc-fos	Fos	mouse	pBR322	7100 bp	EcoR1/Sst1	ATCC
pCS24-1	ribosomal protein S24	human	pBR322	659 bp	Pst1	ATCC
36B4	ribosomal phosphoprotein P0	human	pBR322	1068 bp	Pst1	ATCC
pNur77	Nur77	human	pBluescript SK	2400 bp	EcoR1/Apa1	Dr. S. Smith/Osborne Laboratory, University of Massachusetts at Amherst
c-jun	c-jun	mouse	pGEM3z	332 bp	Sma1	Derek LeRoith, NIH
c-fos	c-fos	mouse	pGEM5zf-	300 bp	Nco1-Sal1	Derek LeRoith, NIH
AF025670	caspase 6	rat	pT7T3D-PAC	346 bp	n/a	ResGen
AF072124	caspase 7	rat	pT7T3D-PAC	1063 bp	n/a	ResGen
AF025671	caspase 2	rat	pT7T3D-PAC	771 bp	n/a	ResGen
AF064071	Apaf-1	mouse	pT7T3D-PAC	5152 bp	n/a	ResGen
D14819	recoverin	rat	pT7T3D-PAC	832 bp	n/a	ResGen

Table 2.1. Specific information regarding plasmids used in the course of this study. Plasmids were isolated using a modified alkaline lysis protocol, confirmed by sequence analysis and stored at either 4°C or -20°C until use. Specific plasmid information was received from the plasmid source and vector information was obtained from the ATCC vector database.

standard vacuum line (Qiagen, Mississauga, ON). 750 µl of QG buffer was run through the extraction column as before and the DNA within the column was washed using 750 µl of buffer PE. The buffer was removed by centrifugation as before, or by using the vacuum manifold. The column was centrifuged at 15,000 rpm for 2 minutes to remove any residual solution, and 30-50 µl of sterile distilled water was added. The column was placed into a clean 1.5 ml eppendorf tube, and the DNA was eluted by centrifuging at 15,000 rpm for 4 minutes.

2.B-2e. Isolation of cDNA. cDNA was isolated using the GlassMAX DNA Isolation Spin Cartridge System (GibcoBRL, Burlington, ON). Specifically, 4.5 volumes of DNA binding solution (6 M NaI) was added to the cDNA sample. 600 µl of the DNA/NaI mixture was added to a GlassMAX DNA Spin Cartridge, which was then centrifuged at 13,000 x g for 20 seconds. The solution was discarded, 0.4 ml of cold wash buffer (4% [v/v] wash buffer concentrate, 44.4% [v/v] water, and 53.1% [v/v] absolute ethanol) was added, and the cartridge was centrifuged as before. This wash step was repeated an additional two times. To remove all excess wash buffer, the cartridge was centrifuged at 13,000 x g for 1 minute. The cartridge was transferred to a 1.5 ml recovery tube and 40 µl of 65°C water was added. The cartridge was centrifuged at 13,000 x g for 1 minute to elute the cDNA.

2.C. ISOLATION OF PROTEINS

Proteins were isolated using TRIzol reagent (Gibco-BRL, Rockville, MD). 1.5 ml of isopropanol per 1 ml of Trizol reagent was added to the organic layer isolated during the RNA extraction step (Section 2.B-1a). Samples were mixed briefly by inversion and then incubated at room temperature for 10 minutes. The protein precipitate was then pelleted by centrifugation at 12,000 x g for 10 minutes at 4°C. The supernatant was then removed and the protein pellet was washed 3 times for 20 minutes in 0.3 M guanidine hydrochloride in 95% ethanol (approximately 2 ml per 1 ml Trizol initially used in the RNA extraction step). Following each wash step, the protein was pelleted by centrifugation at 7500 x g for 5 minutes at 4°C. Two ml of ethanol was added to the protein pellet, the solution was mixed by vortexing, and then was incubated at room temperature for 20 minutes. The protein was pelleted by centrifugation at 7500 x g for 5 minutes at 4°C. The supernatant was removed and the pellet was air dried for 10-15 minutes. The pellet was resuspended in 1% SDS followed by vortexing and heating to 50°C for 15 minutes. Any sediment that would not go into solution was removed by brief centrifugation at 10,000 x g for 10 minutes at 4 °C. Samples were divided into 500 µl aliquots, frozen on dry ice and stored at -80°C until used.

2.D. QUANTIFICATION OF NUCLEIC ACID AND PROTEINS

2.D-1. Quantification of nucleic acids

2.D-1a. Quantification of nucleic acids using a spectrophotomer. Nucleic acid was quantified using a Phippis Unicam PU 8610 UV/VIS Kinetics Spectrophotometer (Hellma Canada Ltd., Concord, ON). To determine RNA or DNA concentrations, OD readings were taken at an absorbance of 260 (1 OD unit = 50 µg/ml double stranded DNA, 40 µg/ml single stranded DNA or RNA, 20 µg/ml single stranded oligonucleotides) and the 260 nm/280 nm ratio was calculated to determine the purity of the nucleic acid (a ratio of 1.8-2 specifies pure nucleic acid).

2.D-1b. Quantification of nucleic acids on ethidium bromide plates. A 0.8% agarose solution (w/v) was prepared using Tris-acetate (TAE) buffer (50X = 2M Tris-HCl pH 8.0, 5.7% [w/v] glacial acetic acid, 50 mM EDTA). The solution was boiled to dissolve the agar and then cooled to 50°C. Ten µg of ethidium bromide was added, the mixture was swirled and then poured into 100 mm Petri plates. The agarose was allowed to solidify at room temperature.

A DNA standard series (200, 150, 100, 75, 50, 25, and 10 µg/µl) was constructed using lambda DNA HindIII ladder (Gibco-BRL, Rockville, MD) in 100 mM EDTA. Half a µl of each standard was dotted onto the agarose:ethidium bromide plate. Half a µl of each cDNA sample was also dotted onto the plates. Comparison to the DNA standards was used to approximate the concentration of cDNA produced in the construction of the execution phase cDNA library (Section 2.E).

This technique was also used to quantify RNA isolated from the Oligotex mRNA Spin columns (Qiagen. Mississauga, Ontario) (Section 2.B-1b). The 0.24-9.5 kb RNA ladder (Gibco-BRL, Rockville, MD) was used to construct a RNA standard series as above.

2.D-2. Quantification of Proteins. Proteins were quantified using the Bradford method designed to quantify 1 to 100 µg of proteins (Bradford, 1976, Smith, 1985). A set of protein standards (2.5 µg, 5 µg, 7.5 µg, and 10 µg) was made using various volumes of a

0.5 mg/ml BSA stock solution. To each of these, 0.15 M NaCl was added to a final volume of 100 µl. One ml of Coomassie brilliant blue solution (0.01% [w/v] Coomassie Brilliant Blue G-250, 5% absolute ethanol, 10% phosphoric acid (85%); filtered through Whatman No.1 filter paper; stored at 4°C) was added, and each standard was vortexed and allowed to stand for 2 minutes. The absorbance at 595 nm was determined using a spectrophotometer and a standard curve was drawn. To quantify the unknown protein samples, 2 µl of each sample was mixed with 98 µl of 0.15 M NaCl and 1 ml of Coomassie brilliant blue solution as above and a reading was taken on the spectrophotometer. Absorbance at 595 nm was then compared to the standard curve to determine the quantity of protein in the sample.

2.E. CONSTRUCTION OF A cDNA LIBRARY

The Stratagene lambda ZAP cDNA synthesis and lambda ZAP cDNA Gigapack III Gold Cloning kits (Stratagene, La Jolla, CA) were used in the synthesis of the 8 hour execution phase cDNA library. The procedure is summarized in Figure 2.2. All reaction buffers, enzymes, primers, control RNA and cloning vector were provided with the lambda ZAP cDNA synthesis and lambda ZAP cDNA Gigapack III Gold Cloning kit and were used according to manufacturer's specification.

2.E-1. First strand cDNA synthesis. The first strand synthesis reaction consisted of 5 µl of 10X first-strand buffer, 3 µl of first-strand methyl nucleotide mixture (consisting of 10 mM dATP, dTTP, dGTP and 5 mM 5-methyl dCTP), 2 µl of linker primer (1.4 µg/ul, 5'-GAGAGAGAGAGAGAGAGAACTAGTCTCGATTTTTTTTTTTTTTTTTT-3'), 5

Figure 2.2. Overview of construction of the execution phase cDNA library using the lambda ZAP-cDNA synthesis kit, and lambda ZAP cDNA Gigapack III Gold Cloning kit. First strand cDNA synthesis was performed using poly(A)+ RNA template isolated from 8-hour light-treated rat retinae. MMLV-reverse transcriptase was used to synthesizes the first strand cDNA off of a poly (A)+ specific linker primer. A mixture of dATP, dGTP, dTTP and 5-methyl dCTP was used in the cDNA synthesis. The incorporation of 5-methyl dCTP prevented restriction endonuclease digestion of the cDNA in subsequent digestion steps. The mRNA template was removed using RNase H digestion, and the small remaining mRNA fragments acted as primer sites from which DNA polymerase I synthesized the second cDNA strand. dTTP, dCTP, dGTP, and α^{32}P dATP (800 Ci/mmol) were incorporated into the second cDNA strand. The α^{32}P dATP allowed for the tracking of the cDNA in the subsequent steps. The double stranded cDNA was blunted using *Pfu* polymerase, and the cDNA was extracted using phenol-chloroform extraction and precipitated with ethanol. EcoR1 adaptors were added to the double stranded cDNA using blunt end ligation. The cDNA ends were phosphorylated using T4 polynucleotide kinase to allow for subcloning into the UniZAP XR vector in later steps. The cDNA was digested with Xho1 to produce a 5' Xho1 and a 3' EcoR1 sticky end that will allow for force directional cloning into the vector in later steps. The cDNA was size fractionated in Sepharose CL-2B gel filtration columns to remove free nucleotides and small cDNA fragments. Fragments containing potentially full length cDNA molecules were purified using phenol-chloroform extractions and ethanol precipitation. The cDNA was ligated into the Uni-ZAP XR vector and was packaged into viable lambda phage using the Gigapack III Gold packaging extract. The phage were stored in SM buffer containing chloroform until use. The phage were used to infect *E.coli* XL-1 Blue MRF' cells and were plated on NZY media. This plated cDNA library was then used for further analysis.

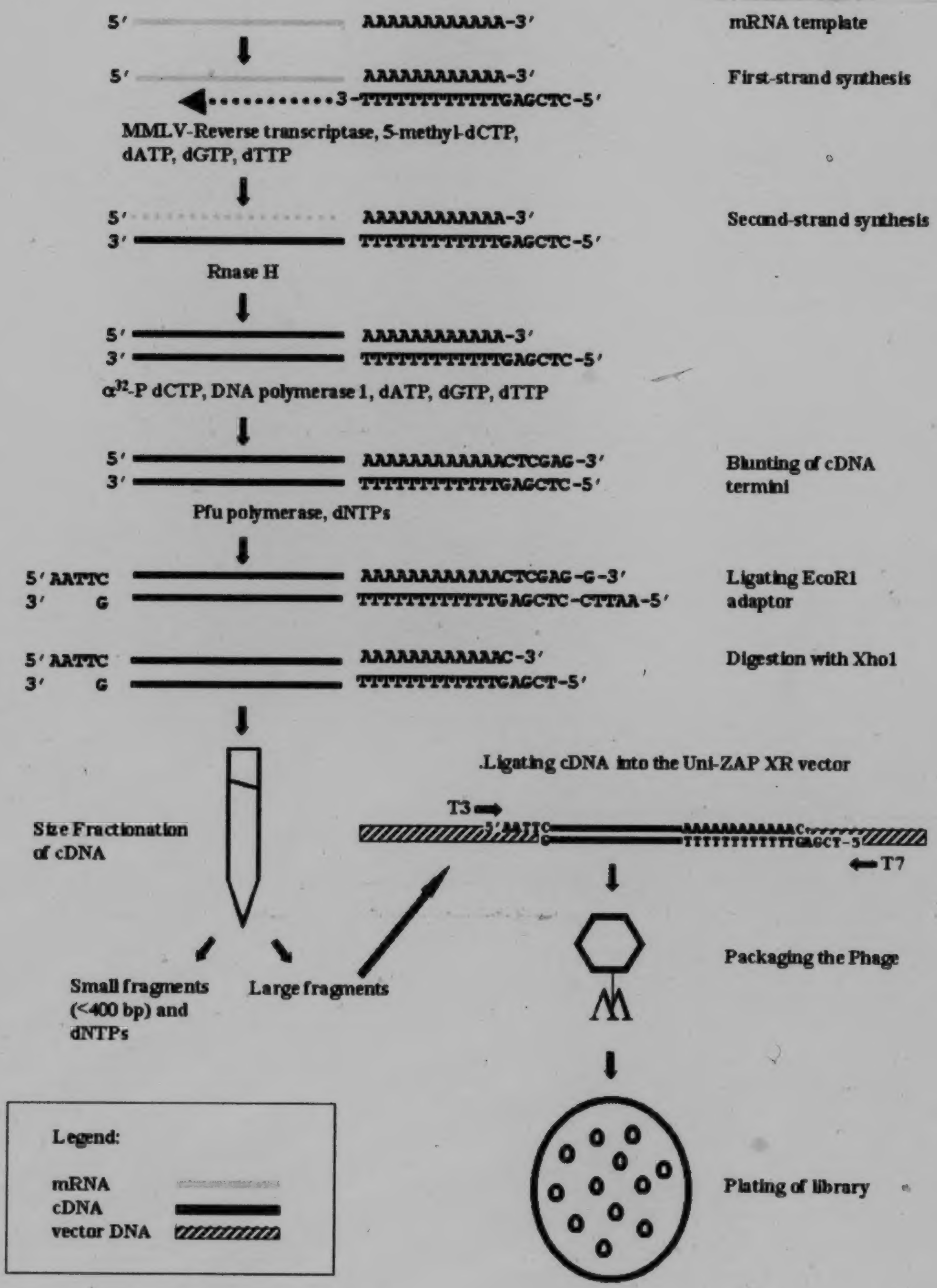
5′ AAAAAAAAAAAA-3′
mRNA template
5′ AAAAAAAAAAAA-3′
3-TTTTTTTTTTTTGAGCTC-5′
First-strand synthesis
MMLV-Reverse transcriptase, 5-methyl-dCTP, dATP, dGTP, dTTP
5′ AAAAAAAAAAAA-3′
3′ TTTTTTTTTTTTGAGCTC-5′
Second-strand synthesis
Rnase H
5′ AAAAAAAAAAAA-3′
3′ TTTTTTTTTTTTGAGCTC-5′
α32-P dCTP, DNA polymerase 1, dATP, dGTP, dTTP
5′ AAAAAAAAAAAACTCGAG-3′
3′ TTTTTTTTTTTTGAGCTC-5′
Blunting of cDNA termini
Pfu polymerase, dNTPs
5′ AATTC AAAAAAAAAAAACTCGAG-G-3′
3′ G TTTTTTTTTTTTGAGCTC-CTTAA-5′
Ligating EcoR1 adaptor
5′ AATTC AAAAAAAAAAAAC-3′
3′ G TTTTTTTTTTTTGAGCT-5′
Digestion with Xho1
.Ligating cDNA into the Uni-ZAP XR vector
T3
5′ AATTC
AAAAAAAAAAAAC
TTTTTTTTTTTTGAGCT-5′
T7
Size Fractionation of cDNA
Small fragments (<400 bp) and dNTPs
Large fragments
Packaging the Phage
Plating of library
Legend:
mRNA
cDNA
vector DNA

μg poly(A)$^+$ RNA (extracted from rat retinae treated with 8 hours of intense green light or Stratagene control RNA), 1 μl of RNase block inhibitor (40 units/μl), and DEPC-treated water to a final volume of 48.5 μl. The mixture was mixed gently and incubated at room temperature for 10 minutes to allow the primer to anneal. 1.5 μl Moloney Murine Leukaemia virus (MMLV)-reverse transcriptase (50 units/μl) was added, and 5 μl of the reaction was removed and added to a tube containing 0.5 μl of α^{32}P dATP (800Ci/mmol) (Amersham Biosciences, Piscataway, NJ). This acted as the first strand synthesis control. The reactions were incubated at 37°C for 1 hour. After 1 hour, the radioactive control tubes were stored at -20°C until the time when they were analyzed by alkaline gel electrophoresis (Section 2.K-1a).

2.E-2. Second strand cDNA synthesis. The first strand synthesis reaction mix was vortexed, spun down in a microcentrifuge and placed on ice. 20 μl of 10X second stand buffer, 6 μl of second strand dNTP mixture (containing 10 mM dATP, dGTP, dTTP and 26 mM dCTP), 114 μl of sterile distilled water, 2 μl of α^{32}P dATP (800Ci/mmol) (Amersham Biosciences, Piscataway, NJ), 2 μl of RNase H (1.5 units/μl), and 11 μl of DNA polymerase I (9.0 units/μl) were added to the first strand synthesis reaction mix. The second strand synthesis reaction mix was vortexed, spun in a microcentrifuge and incubated for 2.5 hours at 16°C. Following this incubation, the second strand synthesis reaction was placed on ice.

2.E-3. Blunting the cDNA termini. 23 µl of blunting dNTP mix (2.5 µl of dATP, dCTP, dGTP and dGTP) and 2 µl of cloned *Pfu* polymerase (2.5 units/µl) were added to the second strand reaction mixture, and the reaction was mixed, microcentrifuged and incubated at 72°C for a maximum of 30 minutes. 200 µl of phenol-chloroform [1:1 (v/v)] was added, the mixture was vortexed, and centrifuged for 2 minutes at room temperature. The aqueous layer, containing the cDNA, was transferred to a new tube, and an equal amount of chloroform was added. Following vortexing, the reaction was centrifuged for 2 minutes at room temperature and the aqueous layer was again transferred to a new tube. The cDNA was precipitated by adding 20 µl of 3 M NaoAc and 400 µl of 100% (v/v) ethanol, vortexed and then left overnight at -20°C. The next day, the reaction was centrifuged at maximum speed for 60 minutes at 4°C. The supernatant was removed and 15,000 rpm the pellet was gently washed in 500 µl of 70% (v/v) ethanol. Following centrifugation at 15,000 rpm for 2 minutes at 4°C, the supernatant was removed and the pellet was lyophilized.

2.E-4. Ligating EcoR1 adaptors. The pellet was resuspended in 9 µl of a solution of EcoR1 adapters (0.4 µg/µl). Resuspension was facilitated by incubating cDNA at 4°C for 30 minutes. To ensure that the cDNA was completely resuspended, the mixture was transferred to a new microfuge tube and the original tube was assayed for radioactivity using a Geiger counter. One µl of this mixture was removed and served as the second strand synthesis control. This aliquot was stored at -20°C until the time that it was analyzed by alkaline gel electrophoresis (Section 2.K-1a). To ligate the EcoR1 adapters to the cDNA, 1 µl of 10X ligase buffer, 1 µl of 10 mM ATP, and 1 µl of T4 DNA ligase

(4 units/μl) was added, and the mixture was incubated at 4°C for 2 days. The ligase was then heat inactivated at 70°C for 30 minutes. The reaction was centrifuged for 2 seconds and cooled to room temperature for 5 minutes.

2.E-5. Phosphorylating the EcoR1 ends. To phosphorylate the cDNA ends, 1 μl of 10X ligase buffer, 2 μl of 10 mM ATP, 6 μl of sterile water and 1 μl of T4 polynucleotide kinase (10 units/μl) were added. The reaction was mixed and incubated for 30 minutes at 37°C. The kinase was inactivated by heating to 70°C for 30 minutes, the reaction was centrifuged briefly, and the mixture was equilibrated to room temperature for 5 minutes.

2.E-6. Digestion with Xho1. The phosphorylated cDNA was digested with 3 μl of Xho1 (40 units/μl) for 1.5 hours at 37°C. 5 μl of 10X STE buffer (1 M NaCl, 200 mM Tris-HCl pH 7.5, 100 mM EDTA) and 125 μl of 100% (v/v) ethanol was added and the cDNA was precipitated overnight at -20°C. The cDNA was collected by centrifuging at 15,000 rpm for 60 minutes at 4°C. The supernatant was removed, the pellet was dried, and resuspended in 14 μl of 1X STE buffer. Column loading dye was added to the reaction mix to allow visualization during size fractionation.

2.E-7. Size fractionation of cDNA. The Sepharose CL-2B gel filtration media and 10X STE buffer was equilibrated to room temperature prior to use. The size fractionation column was assembled in a sterile 1 ml pipette with a small cotton plug at the bottom tip (achieved by trimming the cotton plug at the top of the pipette to 3-4 mm and then placing the pipette near the laboratory air valve to force the plug to the tip of the pipette).

The pipette was filled within 8 mm of the top with a uniform suspension of Sepharose CL-2B gel filtration media, avoiding air bubbles. The pipette was then attached to the tip of a 10 ml syringe using a 8 mm piece of connective tubing, and this column setup was attached to a ring stand using three-fingered clamps. 1X STE buffer was gently added to the top of the gel suspension until the syringe reservoir was filled with 10 ml of 1X STE buffer. The buffer was allowed to flow through the column, until approximately 50 µl remained above the gel. The cDNA sample (containing loading dye) was loaded, and fractions, consisting of 3 drops each (~100 µl) were collected, starting immediately. Fractions were isolated and assayed for the presence of radioactivity using a Geiger counter to determine the approximate fraction that contained free nucleotides. Fractions were isolated until no radioactivity was detected. Each tube was placed in a scintillation vial, and was counted using a scintillation counter. The radioactivity levels in each fraction was plotted and the presence of peaks of radioactivity were determined. The fractions that corresponded to the potential full-length cDNAs were separated into 2 pools. The fractions from the front half of the peak (which came off the column first) were pooled, as were those of the back half of the peak. Each pool was used to make a separate library. Eight µl from pool were isolated and saved for analysis by alkaline gel electrophoresis (Section 2.K-1a).

2.E-8. Ligating cDNA into the Uni-ZAP XR vector. Pooled cDNA was purified by adding an equal volume of phenol:chloroform (1:1 v/v), vortexing and centrifuging at 15,000 rpm for 2 minutes. The aqueous layer was isolated and an equal volume of chloroform was added to the sample. The sample was vortexed and centrifuged as before and the aqueous layer was again isolated. Two volumes of absolute ethanol was added to the sample and the cDNA was precipitated by incubating at -20°C overnight. The samples were centrifuged at 15,000 rpm for 60 minutes at 4°C. The supernatant was transferred to a new 1.5 ml tube and assayed for the presence of radioactivity using a Geiger counter. For efficient isolation of cDNA, the majority of the radioactivity should be found within the pellet. If this was the case, the supernatant was discarded and the pellet was washed with 200 µl of 80% (v/v) ethanol, and centrifuged for 2 minutes at room temperature. (If this was not the case, the supernatant was centrifuged again for 60 minutes at 4°C, and the presence of radioactivity was assayed for again). The ethanol wash was then discarded and the pellet was resuspended in 3.5-5 µl of sterile water, depending on whether the amount of radioactivity detected was below or above 30 counts per second (cps), respectively. (If several pellets were isolated from the same pooled sample, the same volume of water was used to resuspend all the pellets). The cDNA was quantified using the ethidium bromide plate method described in section 2.D-1b. One hundred ng of cDNA was mixed with 0.5 µl of 10X ligation buffer, 0.5 µl of 10 mM ATP (pH 7.5), 1 µl of the UniZAP XR vector (1 µg/µl) (Figure 2.3), water to a final volume of 4.5 µl, and 0.5 µl of T4 DNA ligase (4 units/µl). Ligation controls were performed as with the cDNA samples, using 1 µl of a test insert. The reactions were incubated at 4°C for 2 days.

2.E-9. Packaging the Phage. One tube of Gigapack III Gold Packaging extract per ligated cDNA sample was thawed and 4 µl of cDNA was immediately added to the extract. The contents were mixed by gentle stirring with a pipette tip. The packaging

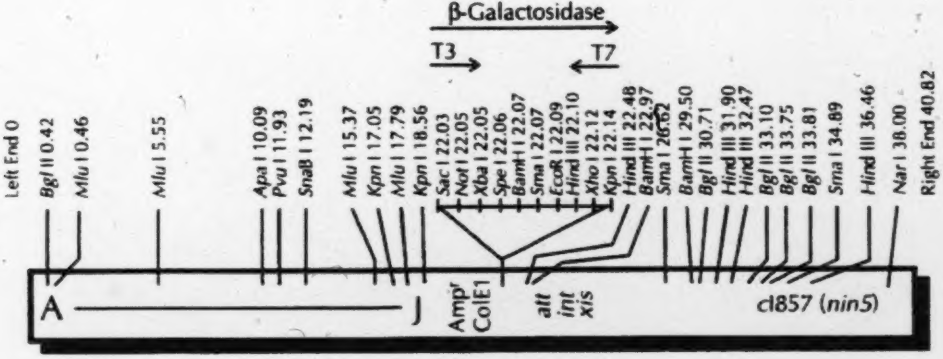
β-Galactosidase
T3
T7
Left End 0
Bgl II 0.42
Mlu I 0.46
Mlu I 5.55
Apa I 10.09
Pvu I 11.93
SnaB I 12.19
Mlu I 15.37
Kpn I 17.05
Mlu I 17.79
Kpn I 18.56
Sac I 22.03
Not I 22.05
Xba I 22.05
Spe I 22.06
BamH I 22.07
Sma I 22.07
EcoR I 22.09
Hind III 22.10
Xho I 22.12
Kpn I 22.14
Hind III 22.48
BamH I 22.97
Sma I 26.62
BamH I 29.50
Bgl II 30.71
Hind III 31.90
Hind III 32.47
Bgl II 33.10
Bgl II 33.75
Bgl II 33.81
Sma I 34.89
Hind III 36.46
Nar I 38.00
Right End 40.82
A
J
Amp^r
ColE1
att
int
xis
cI857 (nin5)

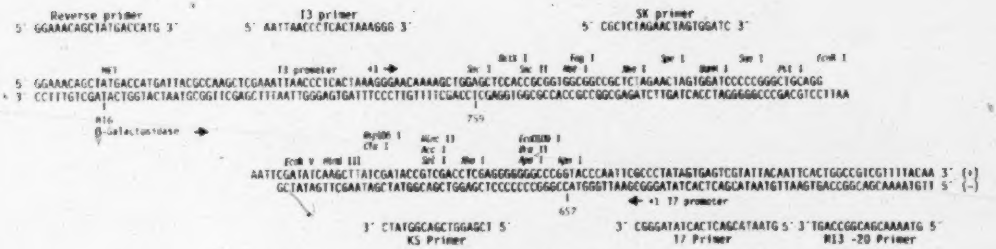
Reverse primer
5' GGAAACAGCTATGACCATG 3'
T3 primer
5' AATTAACCCTCACTAAAGGG 3'
SK primer
5' CGCTCTAGAACTAGTGGATC 3'
MET
T3 promoter
+1
Sac I
BssH II
Sac II
Eag I
Not I
Xba I
Spe I
BamH I
Sma I
Pst I
EcoR I
5' GGAAACAGCTATGACCATGATTACGCCAAGCTCGAAATTAACCCTCACTAAAGGGAACAAAAGCTGGAGCTCCACCGCGGTGGCGGCCGCTCTAGAACTAGTGGATCCCCCGGGCTGCAGG
3' CCTTTGTCGATACTGGTACTAATGCGGTTCGAGCTTTAATTGGGAGTGATTTCCCTTGTTTTCGACCTCGAGGTGGCGCCACCGCCGGCGAGATCTTGATCACCTAGGGGGCCCGACGTCCTTAA
816
759
β-Galactosidase
EcoR V
Hind III
Bsp106 I
Cla I
Hinc II
Acc I
Sal I
Xho I
EcoO109 I
Dra II
Apa I
Kpn I
AATTCGATATCAAGCTTATCGATACCGTCGACCTCGAGGGGGGGCCCGGTACCCAATTCGCCCTATAGTGAGTCGTATTACAATTCACTGGCCGTCGTTTTACAA 3' (+)
GCTATAGTTCGAATAGCTATGGCAGCTGGAGCTCCCCCCCGGGCCATGGGTTAAGCGGGATATCACTCAGCATAATGTTAAGTGACCGGCAGCAAAATGTT 5' (-)
657
+1 T7 promoter
3' CTATGGCAGCTGGAGCT 5'
KS Primer
3' CGGGATATCACTCAGCATAATG 5'
T7 Primer
3' TGACCGGCAGCAAAATG 5'
M13 -20 Primer

FIGURE 3 Circular map and polylinker sequence of the pBluescript SK(+/–) phagemid.

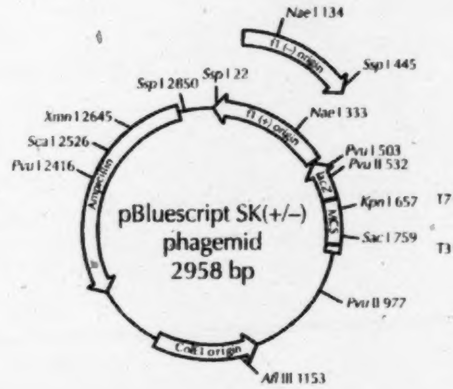
Nae I 134
f1 (–) origin
Ssp I 445
Ssp I 2850
Ssp I 22
f1 (+) origin
Nae I 333
Xmn I 2645
Sca I 2526
Pvu I 2416
Pvu I 503
Pvu II 532
Kpn I 657
T7
Sac I 759
T3
Pvu II 977
Ampicillin
lacZ
MCS
ColE1 origin
Afl III 1153
pBluescript SK(+/–)
phagemid
2958 bp

Figure 2.3. Cloning vectors used in library synthesis. A) Diagram of the Uni-ZAP XR insertion vector used in the synthesis of the execution phase cDNA library. cDNA samples were ligated into the EcoR1 and Xho1 restriction sites. B) Sequence of the Uni-ZAP XR and pBluescript SK (+/-) phagemid multiple cloning sites. C) Diagram of pBluescript SK (+/-) phagemid vector used to produce clone stocks of differentially expressed clones. (ZAP cDNA Synthesis kit, Stratagene, La Jolla, CA).

reaction was incubated for a maximum of 2 hours at room temperature (22°C). 500 μl of SM buffer (0.1 M NaCl, 8,1 mM $MgSO_4$, 50 mM Tris-HCl pH 7.5, 2% [w/v] gelatin), and 20 μl of chloroform were added, and the contents were gently mixed. The tube was briefly centrifuged to sediment cell debris. The packaged phage were stored at 4°C until used.

2.E-10. Plating of the cDNA library. A 50 ml culture of *E. coli* XL1-Blue MRF' in LB broth (1% bacto-tyrptone, 0.5% bacto-yeast extract, 0.17 M NaCl; pH 7.0) containing 10 mM $MgSO_4$ and 0.2% maltose (w/v) was started from a single colony. The culture was grown to an OD_{600} of 1.0, and the cells were spun down by centrifugation at 500 x g for 10 minutes. The supernatant was discarded and the cells were resuspended in 25 ml of 10 mM $MgSO_4$. The cells were further diluted to an OD_{600} of 0.5 with 10 mM $MgSO_4$. In order to determine the number of plaque forming units per μl of cDNA library, 0.1, 1 or 10 μl of the packaging reaction were mixed with 200 μl of *E. coli* XL1-Blue MRF' cells diluted in 10 mM $MgSO_4$. The phage and bacteria were incubated at 37°C for 15 minutes to give the phage sufficient time to adhere to the cells. 3 ml of 48°C molten NZY top agar (85.6 mM NaCl, 8.1 mM $MgSO_4$, 0.5% [w/v] yeast extract, 1% [w/v] casein hydrolysate, 0.7% agar or agarose; pH 7.5) was added to the phage and cells and the mixture was immediately poured onto NZY plates (85.6 mM NaCl, 8.1 mM $MgSO_4$, 0.5% [w/v] yeast extract, 1% [w/v] casein hydrolysate, 1.5% [w/v] agar; pH 7.5). Once the top agar solidified, the plates were incubated at 37°C overnight. The number of plaques were counted and the titer of the library was determined.

2.E-11. Amplification of the cDNA library. A 50 ml culture of *E. coli* XL1-Blue MRF' in LB broth (1% bacto-tryptone, 0.5% bacto-yeast extract, 0.17 M NaCl; pH 7.0) containing 10 mM $MgSO_4$ and 0.2% maltose (w/v) was started from a single colony. The culture was grown to an OD_{600} of 1.0, and the cells were spun down by centrifugation at 500 x g for 10 minutes. The cells were diluted to an OD_{600} of 0.5 in 10 mM $MgSO_4$ 600 µl of cells were mixed with aliquots of the cDNA library containing 5×10^4 pfu in a 15 ml polypropylene tube. The cells and bacteriophage mixture was incubated for 15 minutes at 37°C and 6.5 ml of 48°C NZY top agar (85.6 mM NaCl, 8.1 mM $MgSO_4$, 0.5% [w/v] yeast extract, 1% [w/v] casein hydrolysate, 0.7% agar or agarose; pH 7.5) was added. The mixture was then poured onto 150 mm plates containing NZY agar (85.6 mM NaCl, 8.1 mM $MgSO_4$, 0.5% [w/v] yeast extract, 1% [w/v] casein hydrolysate, 1.5% [w/v] agar; pH 7.5) and were allowed to solidify. The plates were incubated for 6-8 hours until plaques were 1-2 mm in diameter. Ten ml of SM buffer (0.1 M NaCl, 8,1 mM $MgSO_4$, 50 mM Tris-HCl pH 7.5, 2% [w/v] gelatin) was added and the plates were incubated overnight at 4°C on a shaking platform. The bacteriophage suspension was collected and pooled in 15 ml polypropylene tubes. The plates were rinsed with an additional 2 ml of SM buffer and the wash was added to the isolated suspension. Chloroform was added to a final concentration (v/v) of 5%, the solution was mixed, and was incubated at room temperature for 15 minutes. The cellular debris was removed by centrifugation at 500 x g. The supernatant was isolated and chloroform was added to a 0.3% (v/v) final concentration and 7% (v/v) dimethyl-sulfoxide (DMSO) was added. The solution was divided into 1 ml aliquots, frozen on dry ice and stored at -80°C.

2.E-12. Isolation of individual plaques. Individual plaques were isolated using sterile wide bore pasteur pipettes. Each isolated plaque was placed in a 1.5 ml microfuge tube containing 500 µl of SM buffer, with 100 µl of chloroform. The phage were allowed to diffuse out of the NZY agar plug into the buffer for 24 hours at 4°C prior to use.

2.E-13. Making of phagemids and clone stocks. Selected clones were made into phagemid stocks using the Single Clone excision protocol included with the Stratagene library kit. The phagemid vector used is shown in Figure 2.3C. Cultures of *E. coli* XL1-Blue MRF' and *E. coli* SOLR in LB broth (1% bacto-tyrptone, 0.5% bacto-yeast extract, 0.17 M NaCl; pH 7.0) containing 0.2% maltose (w/v) and 10 mM MgSO4 were grown overnight at 30°C. The cells were centrifuged at 1000 x g for 5 minutes and then resuspended to a OD_{600} of 1.0 in 10 mM MgSO4. The cells were combined with 250 µl of the selected phage stock (~1 x 10^5 pfu) and 1 µl of ExAssist helper phage (1 x 10^6 pfu/µl). The mixture was incubated at 37°C for 15 minutes, and 3 ml of LB broth was added, followed by incubation for 2.5-3 hours at 37°C with gentle shaking. The cells were heated to 65-70°C for 20 minutes and then centrifuged at 1000 x g for 15 minutes. The supernatant containing excised pBluescript phagemids was divided into aliquots, mixed with 7% DMSO (v/v) and frozen on dry ice.

To plate the excised phagemids, 0.5 µl of the phage was mixed with 200 µl of *E. coli* SOLR cells (OD_{600} of 1.0) grown as above. This mixture was incubated for 15 minutes at 37°C and 10 -100 µl of the mixture was plated out on LB plates containing ampicillin. The plates were then incubated overnight. A single colony was isolated and used to inoculate 10 ml of LB broth containing ampicillin. The phagemid was isolated using standard plasmid prep protocols (Section 2.B-2c).

2.F. TRANSFORMATIONS

2.F-1. Transformation of bacterial cells

2.F-1a. Construction of competent cells. Bacterial competent cells were made using the 18°C method described by Inoue *et al* (1990). A 5 ml overnight culture of *E. coli* XL1-Blue was prepared in LB broth (1% bacto-tryptone, 0.5% bacto-yeast extract, 0.17 M NaCl; pH 7.0) at 37°C. 0.5 ml of this culture was used to inoculate 50 ml of SOB media (2% bacto-tryptone, 0.5% yeast extract, 10 mM NaCl, 2.5 mM KCl, 10 mM $MgCl_2$, 10 mM $MgSO_4$; pH 6.8-7.0), and the culture was incubated at 18°C with vigorous agitation to an OD_{600nm} of 0.6. The culture was maintained at 4°C for all subsequent steps. The culture was centrifuged at 3000 rpm for 5 minutes. The pellet was resuspended in 80 ml of cold TB solution (10 mM PIPES [piperazine-N,N^1 –bis {2-ethanesufonic acid}], 15 mM $CaCl_2$, 250 mM KCl, 55 mM $MnCl_2$ pH to 6.7 with KOH, sterilized by filtration) by gentle swirling. The solution was incubated on ice for 10 minutes and then centrifuged at 3000 rpm for 5 minutes. The pellet was resuspended in 20 ml of TB solution, and DMSO was added dropwise with gentle swirling to a final concentration of 7%. Following incubation at 4°C for an additional 10 minutes the cells were flash frozen on dry ice in 0.5 ml aliquots. Transformation efficiency was determined by transformation with pBluescript SK$^-$, and the average efficiency obtained was 5 x 10^8 cfu/μg DNA.

2.F-1b. Transformation of bacterial competent cells with plasmid DNA. 150 µl of XL1-Blue *E. coli* competent cells were added to 100 ng of plasmid DNA. The mixture was incubated on ice for 10-20 minutes and then heat-shocked at 42°C for 90 seconds. The mixture was transferred to ice for 2 minutes, and 600 µl of 37°C LB broth was added. The cells were incubated at 37°C for 20 minutes and the cells were plated on LB plates containing antibiotic for selection (20-60 µg/ ml ampicillin, or 10-60 µg/ml tetracycline). If color selection was required, 50 µl of XGal ([5-bromo-4-chloro-3-indolyl-β-D-galactoside], 20 mg/ml in dimethylformamde) and 10 µl of IPTG (isopropylthio-β-D-galactoside, 200 mg/ml) were spread on the plate prior to the addition of the cells.

2.G. cDNA SYNTHESIS

Total cDNA population probes used for the primary and secondary screenings the cDNA library were constructed using the 5'- and the 3' RACE Systems for Rapid Amplification of cDNA ends (Gibco-BRL, Burlington, ON) (Figure 2.4). This technique was necessary to amplify the cDNAs as rat retinal tissues was only available in limited quantity. Fifty ng of poly(A+) RNA was mixed with 1 µM of Adapter primer in a volume of 12 µl. The mixture was heated at 70°C for 10 minutes, mixed with 2.5 µl of 10X PCR buffer (200 mM Tris-HCl pH 8.4, 500 mM KCl), 2.5 µl of 25 mM $MgCl_2$, 1 µl of 10 mM dNTPs, and 2.5 µl of 0.1M DTT. After pre-incubating at 42°C for 2-5 minutes, 1 µl of Superscript II reverse transcriptase (200 units/µl) was added and the mixture was incubated at 42°C for 50 minutes, followed by heat-shocking at 70°C for 15 minutes. The mixture was treated with 1 µl (2 units/µl) RNase H for 30 minutes at 37°C. The cDNA

Figure 2.4. Overview of cDNA probe synthesis using a combination of 5' and 3' RACE. Poly(A)+ RNA template was used to synthesize first strand cDNA using Superscript II Reverse Transcriptase. The enzyme extended the first strand cDNA off of a poly (T)+ adapter primer containing a 5' end sequence that corresponded to the sequence contained in the Abridged Universal Amplification primer (AUAP) used in the PCR amplification step. The mRNA template was removed by RNase H treatment. The single stranded cDNA molecule was isolated using the GlassMAX DNA isolation system. A 3' poly(C)+ tail was added to the first strand cDNA using terminal deoxynucleotidyl transferase. This single stranded tailed cDNA was then amplified by PCR using the AUAP primer and a 5' RACE Abridged Anchor primer that contained 3' sequence complimentary to the 3' poly (C)+ tail of the cDNA. The amplified cDNA was used quantified using a spectrophotometer and was analyzed by gel electrophoresis.

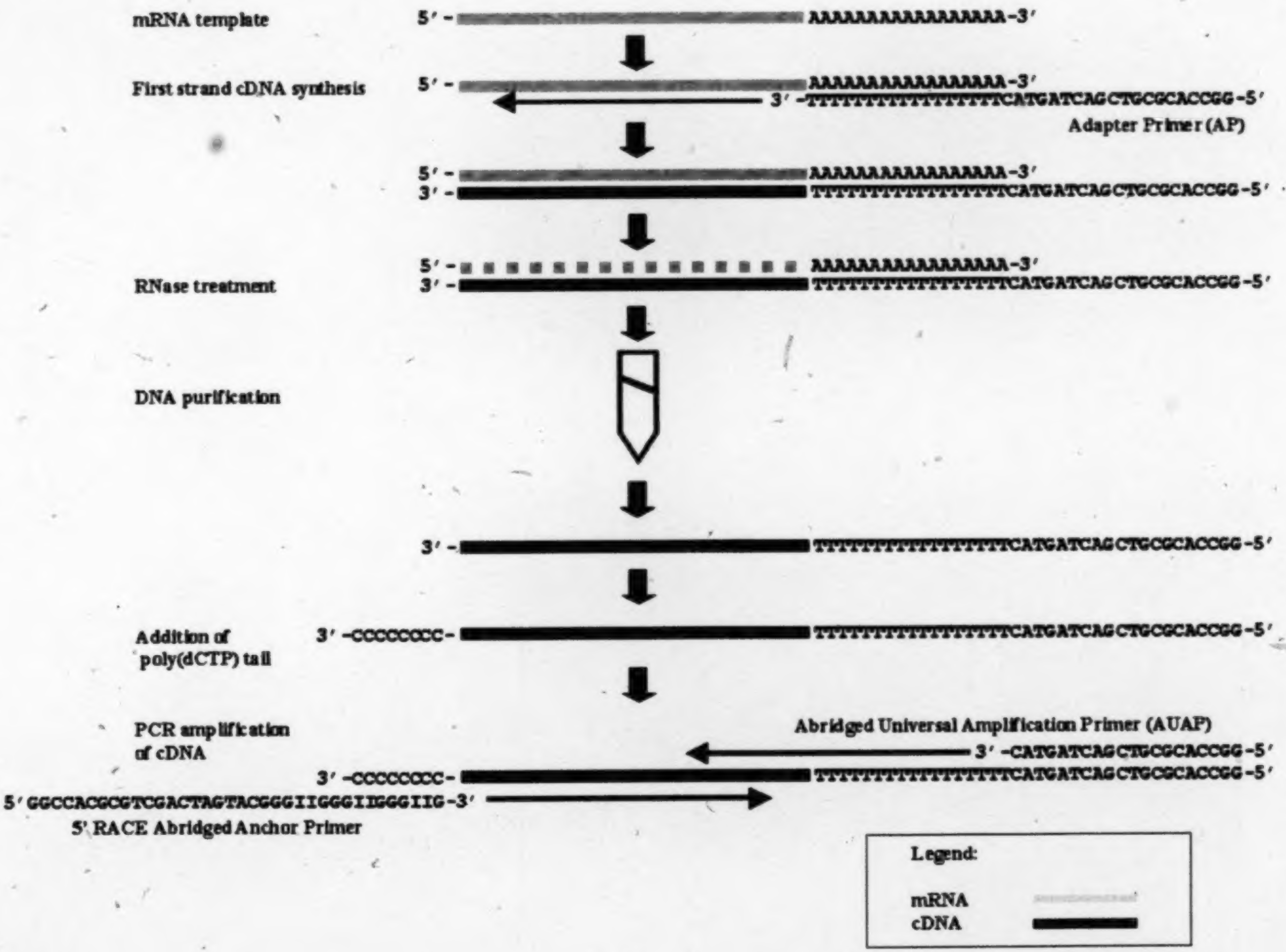
mRNA template
5′ -
AAAAAAAAAAAAAAAAA-3′
First strand cDNA synthesis
5′ -
AAAAAAAAAAAAAAAAA-3′
3′ -TTTTTTTTTTTTTTTTTCATGATCAGCTGCGCACCGG-5′
Adapter Primer (AP)
5′ -
3′ -
AAAAAAAAAAAAAAAAA-3′
TTTTTTTTTTTTTTTTTCATGATCAGCTGCGCACCGG-5′
RNase treatment
5′ -
3′ -
AAAAAAAAAAAAAAAAA-3′
TTTTTTTTTTTTTTTTTCATGATCAGCTGCGCACCGG-5′
DNA purification
3′ -
TTTTTTTTTTTTTTTTTCATGATCAGCTGCGCACCGG-5′
Addition of poly(dCTP) tail
3′ -CCCCCCCC-
TTTTTTTTTTTTTTTTTCATGATCAGCTGCGCACCGG-5′
PCR amplification of cDNA
Abridged Universal Amplification Primer (AUAP)
3′ -CATGATCAGCTGCGCACCGG-5′
3′ -CCCCCCCC-
TTTTTTTTTTTTTTTTTCATGATCAGCTGCGCACCGG-5′
5′ GGCCACGCGTCGACTAGTACGGGIIGGGIIGGGIIG-3′
5′ RACE Abridged Anchor Primer
Legend:
mRNA
cDNA

was isolated using a GlassMAX DNA isolation spin cartridge system (Section 2.B-2e; GibcoBRL, Burlington, ON). A poly(dCTP) tail was added to the single stranded cDNA by incubating the cDNA with 1 µl of terminal deoxynucleotidyl transferase (15 units/µl) in 5µl 5X tailing buffer (50 mM Tris-HCl, pH 8.4, 125 mM KCl, 7.5 mM $MgCl_2$), and 2.5 µl 2 mM dCTP. Following a 10 minute incubation at 37°C, the enzyme was inactivated by incubating at 65°C for 10 minutes. The tailed double-stranded DNA was amplified by PCR (Section 2.J-2) using a 5' RACE Abridged anchor primer (5' RACE Systems for Rapid Amplification of cDNA ends, Gibco-BRL, Burlington, ON), and a Abridged Universal Amplification primer (3' RACE Systems for Rapid Amplification of cDNA ends, Gibco-BRL, Burlington, ON). Refer to Figure 2.4 for primer sequences.

As later access to retinal tissue improved, secondary and tertiary screens were performed using unamplified total cDNA population probes constructed using the cDNA Synthesis System (GibcoBRL, Burlington, ON) or the Time saver cDNA Synthesis System (Amersham-Pharmacia, Piscataway, NJ) according to manufacturer's protocols. As the protocols were very similar to those used in the construction of the cDNA library (Section 2.E1-E2), they are not described in detail here. In all cases, cDNA probes were analyzed by gel electrophoresis (Section 2.K-1b) and were quantified using a spectrophotometer (Section 2.D1-a).

2.H. HYBIDIZATION USING RADIOACTIVELY LABELED DNA PROBES

2.H-1. Radioactive labeling of probes. Probes for screening the library (total cDNA populations) or for Northern blot or Southern blot analysis (PCR products derived from the inserted DNA from individual clones) were labeled using the Prime-It II Random

Primer Labeling System (Stratagene, La Jolla, CA), the Multiprime DNA labeling system (Amersham, Baie d'Urfe, QC), or the Random Primers DNA Labeling System (Invitrogen, Burlington, ON). In general, 25 ng of double stranded DNA (in sterile double distilled water to a volume of 23 µl) was denatured by boiling for 5 minutes, and then the DNA was cooled on ice. 1 mM of each dNTPs was added, omitting the dNTP that was being substituted for radioactive nucleotide. [For labeling of PCR products α-^{32}P dCTP (6000 Ci/mmol) was used, and therefore no dCTP was added. For labeling of total cDNA population probes, α-^{32}P dCTP (6000 Ci/mmol), α-^{32}P dATP (6000 Ci/mmol), and α-^{32}P dGTP (3000 Ci/mol) were used, and therefore only dTTP was added]. Primer buffer (5X = 0.67 M HEPES, 0.17 M Tris-HCl, 17 mM $MgCl_2$, 33 mM 2-mercaptoethanol, 1.33 mg/ml BSA, 18-27 OD units/ml oligodeoxyribonucleotide primers [hexamers]; pH 6.8) was added to a concentration of 1X. The contents were mixed briefly and the required (α-^{32}P) dNTP(s) and 3-5 units of Klenow polymerase were added. The reaction was incubated at room temperature for 1-12 hours. Five µl of stop buffer (0.5 M EDTA pH 8.0) was added and radio-labeled probe was isolated using Quick Spin Columns (G-50 Sephadex columns, Roche, Indianapolis, IN). Incorporated radioactivity was measured by Cerenkov scintillation counting of a 1 µl aliquot of the labeled probe. Sheared salmon sperm DNA was added to a final concentration of 20 µg/µl, and the probe was boiled for 5 minutes, followed by incubation on ice for 5 minutes prior to use.

2.H-2. Hybridization of membranes. Membranes were washed for 10 minutes in 2X SSC (20X SSC= 3 M NaCl, 180 mM sodium citrate; pH 7.0) at 65°C in a rotating hybridization oven, and then prehybridized for 3 hours in 65°C Hybrisol II hybridization solution (10% dextran sulfate, 1% SDS, 6X SSC, sheared salmon sperm DNA, modified Denhardt's solution; Serologicals Corporation, Norcross, GA). Radioactively-labeled total population cDNA probes were added at a concentration 2 x 10^6 cpm/ml of hybridization solution. The membranes were hybridized overnight at 65°C. The radioactive hybridization solution was discarded according to Occupational Health and Safety guidelines and the blots were washed at 65°C as follows: two washes of 2X SSC for 15 minutes, two washes of 2X SSC, 0.1% SDS for 20 minutes, and one wash of 0.1X SSC, 0.1% SDS for 10 minutes. The blots were rinsed in 2X SSC, placed on damp Whatman paper (soaked in 2X SSC), and wrapped in saran wrap. The membranes were exposed to Kodak X-OMAT autoradiography film at -70°C until the desired exposure was obtained. Autoradiographs were developed using a manual film processor.

2.I. SCREENING OF THE EXECUTION PHASE cDNA LIBRARY

2.I-1. Primary Screen

2.I-1a. Plaque lifts. The screening of the library is outlined in Figure 2.5. Phage were plated out to a concentration of ~400 plaque forming units (pfu)/ plate as described in section 2.E-10 using the unamplified cDNA library. Following an overnight incubation at 37°C, the plates were chilled for 2 hours at 4°C. Precut nylon membranes (NEM Research Products, Boston, MS) were nicked along the edge in three places for orientation purposes, and then were placed onto the NZY agar plates for 2 minutes, ensuring that no bubbles were caught between the membrane and agar surface. A sterile needle was used to poke three holes in the membrane to further aid in orientating the membrane to the plate. The location of both nicks and holes in the membranes were

Figure 2.5. Screening of the execution phase cDNA library. The 8 hour execution phase cDNA library was plated out to a concentration of ~400 pfu/plate. Phage from the library were transferred to duplicate nylon membranes and the phage DNA was denatured by an alkaline treatment. Following neutralization and cross-linking of the DNA to the membranes, the membranes were hybridized with dark reared cDNA or 8 hour cDNA populations radio-labelled with α^{32}P dATP, dGTP and dGTP. Phage that contained inserts that demonstrated differential expression between the two treatments were isolated using a wide-bore pasteur pipette and were stored in SM buffer containing chloroform. The phage inserts were amplified using PCR and the PCR products were resolved on duplicate agarose gels by electrophoresis. Southern transfer of the PCR products to duplicate GeneScreen Plus membranes was performed and the membranes were hybridized with dark reared or 8 hour cDNA populations as before. The plaques that represented PCR products that showed differential expression patterns between the two treatment conditions were plated out at low density on individual LB plates and 6 plaques were isolated from each plate. The phage DNA was amplified by PCR, resolved by electrophoresis and transferred to duplicate membranes as before. The membranes were hybrizided as before and phage that contained inserts that represented differentially expressed clones were isolated, stored in SM buffer containing chloroform, and used for further analysis.

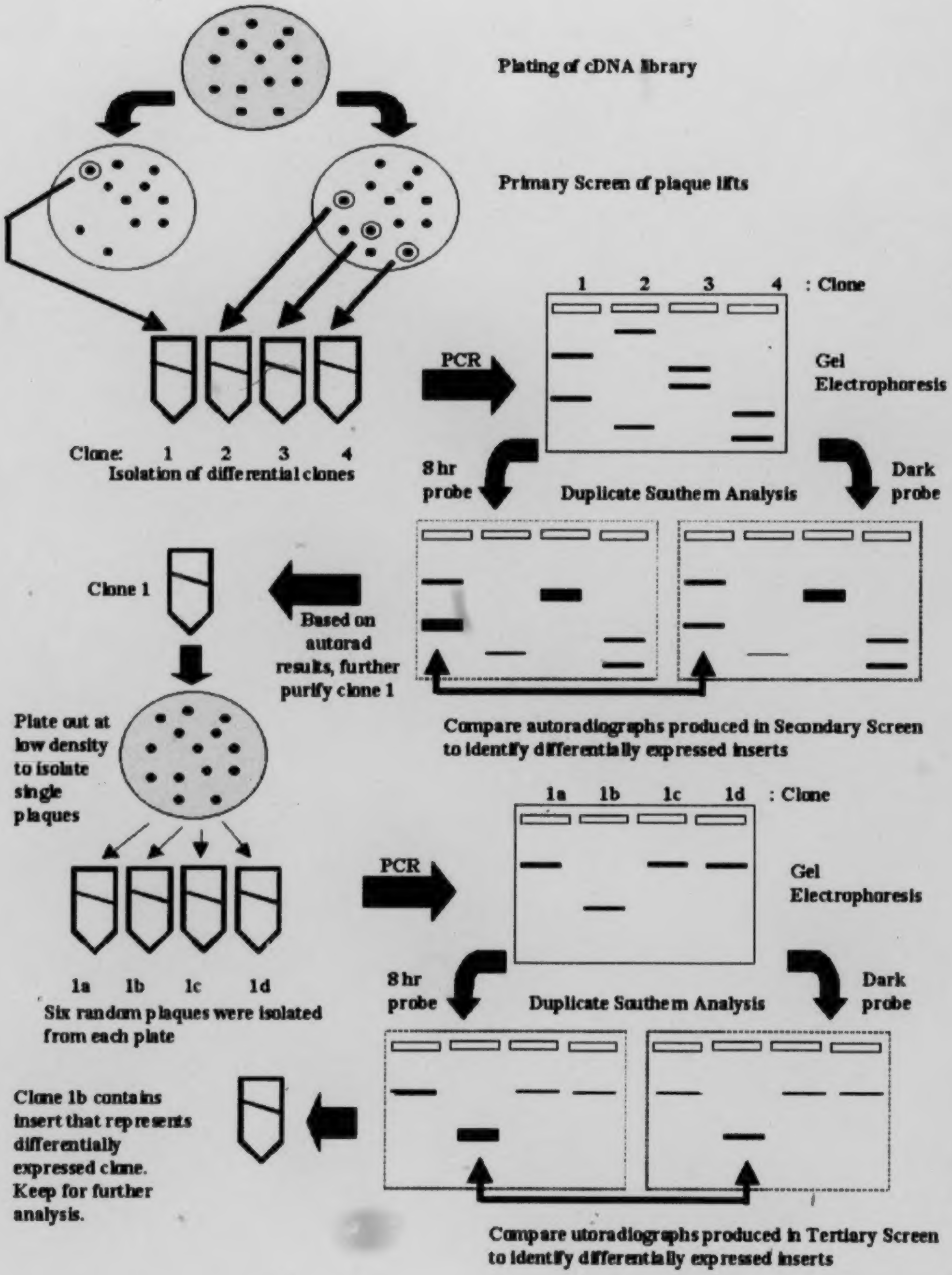
Plating of cDNA library
Primary Screen of plaque lifts
Clone: 1 2 3 4
Isolation of differential clones
1 2 3 4 : Clone
PCR
Gel Electrophoresis
8 hr probe
Duplicate Southern Analysis
Dark probe
Clone 1
Based on autorad results, further purify clone 1
Compare autoradiographs produced in Secondary Screen to identify differentially expressed inserts
Plate out at low density to isolate single plaques
1a 1b 1c 1d : Clone
PCR
Gel Electrophoresis
1a 1b 1c 1d
Six random plaques were isolated from each plate
8 hr probe
Duplicate Southern Analysis
Dark probe
Clone 1b contains insert that represents differentially expressed clone. Keep for further analysis.
Compare utoradiographs produced in Tertiary Screen to identify differentially expressed inserts

marked on the bottom of the agar plate. After the first membrane was removed, a second membrane was placed on the agar, marked as before, and allowed to adhere for 3 minutes. The DNA on the duplicate filters was denatured in 1.5 M NaCl and 0.5 M NaOH solution for 2 minutes. The filter were then neutralized by washing the membranes for 5 minute in a 1.5 M NaCl and 0.5 M Tris-HCl pH 8.0 solution for 5 minutes. The membranes were rinsed for 20 seconds in 2X SSC buffer (3 M NaCl, 0.18 M sodium citrate; pH 7.0) containing 0.2 M Tris-HCl pH 7.5. The excess solution was removed from the membranes by draining on Whatman 3MM Paper, and then the cDNA was cross-linked to the membranes using a UV Stratalinker 1800 (Stratagene, La Jolla, CA) for 30 seconds (auto cross-link setting). The membranes were stored at room temperature between 2 pieces of Whatman 3MM paper until use. The agar plates were stored at 4°C.

2.I-1b. Differential screening of plaque lifts. Each of the duplicate filters was hybridized with α-^{32}P-labeled cDNA obtained from the retinae of either dark-reared (control) animals or from 8-hour light-reared (experimental) animals. Hybridizations were performed as described in section 2.H-2, and autoradiographs were developed after a 2-3 day exposure at -70°C. Plaques representing clones that showed differential expression between the 8 hour and control cDNA probes were isolated and stored in 500 µl SM buffer containing 50 µl chloroform (as described in section 2.E-12).

2.I-2. Secondary screen of execution phase library. Polymerase chain reaction (described in detail in section 2.J-2) was performed on primary differentially-expressed clones isolated from the 8-hour cDNA library using T7 and T3 primers corresponding to the Lambda ZAP vector. Due to the high density of phage in the initial screen, several PCR products were often produced from each isolated phage sample, suggesting the presence of multiple unrelated phage. PCR products were resolved by gel electrophoresis (Section 2.K-1b) and transferred to duplicate GeneScreen Plus membranes (NEN Life Science Products, Boston, MA), by Southern blot transfer (Section 2.L-1). Membranes were hybridized using total control or 8-hour cDNA population probes as described in section 2.H-2. Analysis of the autoradiographs demonstrated which PCR products corresponded to inserts representative of differentially expressed genes.

2.I-3 Tertiary screen of the execution phase library. Plaque purification was used to isolate phage that generated PCR products that represented differentially expressed genes (Section 2.I-2). Individual plaques were isolated using the plating protocol described in section 2.E-10, using 1 µl of each phage mixture. Six individual plaques were isolated from each plate. In order to confirm that the individual plaque isolated consisted of a pure phage clone that represented a differentially expressed gene insert, the purified phage were amplified by PCR, resolved by gel electrophoresis, transferred to duplicate membranes and differentially cross-screened as described in section 2.I-2. The phage that contained inserts that represented differentially expressed genes were used for further analysis.

2.J. POLYMERASE CHAIN REACTION

2.J-1. Designing PCR primers. Template specific primers were designed with the following considerations: primers were in the range of 20-30 nucleotides long, depending on the AT content; primers were designed to avoid the formation of hairpin loops; the presence of multiple dCTP and dGTP nucleotides at the 3'-end of the primer was avoided; the presence of a dTTP at the 3'-end of the primer was avoided; both upstream and downstream primers were designed to have approximately the same melting and annealing temperatures (T_m=2°C [A+T] + 4°C [G+C]); and both the upstream and downstream primers were designed to have approximately equal numbers of dTTP/dATP and dGTP/dCTP nucleotides (approximately 40-60% GC content). If restriction enzyme sites were added to the primers, they were added to the 5'-end of the primer in addition to the required template-specific complementary sequence. Once the primers were designed, they were analyzed to ensure that upstream and downstream primers were not complementary to each other, and hence would not form primer dimers. As well, the primers were analyzed using "BLAST search for short nearly exact matches" (http://www.ncbi.nlm.nih.gov/BLAST/) to ensure that the primers were specific for the template of interest. Primers were synthesized by either Invitrogen (Burlington, ON), Qiagen (Mississauga, ON) or BioServe Technologies (Laurel, MD). Primers were resuspended to a concentration of either 40 μM or 400 μM in DEPC-treated water, and were stored at 4°C for short-term storage or at -20°C for long-term storage. Information regarding specific PCR primers is summarized in Table 2.2.

2.J-2. Polymerase Chain Reaction using Taq polymerase. One hundred μl PCR reactions were set up using Taq PCR buffer (10X PCR buffer = 0.2 M Tris-HCl pH 8.3, 0.2 M KCl, 15 mM $MgCl_2$, 2% [v/v] gelatin), 200 μM of each of dATP, dTTP, dGTP, PCR primers

Name	Sequence (5' to 3')	Company	target	species
pUC-1pr	gttttcccagtcacgac	BioServe	pUC cloning vector	n/a
pUC-2pr	caggaaacagctatgac	BioServe	pUC cloning vector	n/a
pBR322Pst-1	gctagagtaagtagtt	BioServe	pBR322 cloning vector-Pst1 site	n/a
pBR322Pst-2	aacgacgagcgtgac	BioServe	pBR322 cloning vector-Pst1 site	n/a
Nur77-1	acaactacagcacaggcta	BioServe	Nur77	mouse
Nur77-2	gtgtctctctgtgaccata	BioServe	Nur77	mouse
T7-1pr	taatacgactcactataggg	BioServe	lambda zap II cloning vector	n/a
T3-1pr	attaaccctcactaaaggga	BioServe	lambda zap II cloning vector	n/a
SP6pr	tatttaggtgacactatag	BioServe	pGEM cloning vector	n/a
S28pr-1	gttgcgctgagctt	BioServe	ribosomal binding protein S28	rat
S28pr-2	gagcatctcagttacg	BioServe	ribosomal binding protein S28	rat
pcat41.1	ggctactttgaggtcacaca	BioServe	catalase	rat
pcat41.2	cagcacgttcacatagaatgc	BioServe	catalase	rat
ups-1	gacagtcactgcgcacccac	BioServe	human rod photoreceptor protein ups	human
ups-2	ctggtcaagttccccacacag	BioServe	human rod photoreceptor protein ups	human
Xmn1 G strand non-palindromic adaptor	cgaaggggttcg	NEB		n/a
Ecolr1-Xmn1 non-palindromic adaptor	aattcgaaccccttcg	NEB		n/a
M13 reverse sequencing primer	caggaaacagctatgac	Invitrogen		n/a
M13 reverse	agcggataacaatttcacacagg	BioServe		n/a
HO-1s	aaggaggtgcacatccgtgca	BioServe	HO-1	rat
Ho-1a	atgttgagcaggaaggcggtc	BioServe	HO-1	rat
casp-9 up	gacatgatcgaggatattcagc	BioServe	caspase 9	rat
casp-9 down	caaacttgacactgcgtccag	BioServe	caspase 9	rat
casp8up	agttcctgtgcttggaccac	BioServe	caspase 8	rat
casp8down	gagtttgggtatgtcctcc	BioServe	caspase 9	rat
casp3-up	gaagcaagtcgatggactctg	BioServe	caspase 3	rat
casp3-down	gacacaatacacgggatctg	BioServe	caspase 4	rat
casp1-up	gagaagagagtcctgaaccag	BioServe	caspase 1	rat
casp1-down	catctccagagctgtgagat	BioServe	caspase 2	rat
ratbclxlr	catcaatggcaacccatcct	Dr. Martin Tenniswood	Bcl-xl	rat
ratbclxlf	ttgtctacgctttcccacgcaca	Dr. Martin Tenniswood	Bcl-xl	rat
ratbclxsr	aatggcaacccatcctggca	Dr. Martin Tenniswood	Bcl-xs	rat
ratbclxsf	tgagcccagcagaagtacacca	Dr. Martin Tenniswood	Bcl-xs	rat
ratbclxsr2	agctttgaacaggacactttg	Dr. Martin Tenniswood	Bcl-xs	rat
ratfaslr	ccagcacaccctctgaaaccaa	Dr. Martin Tenniswood	FasL	rat
ratfaslf	ttgccacacagcagcccaaa	Dr. Martin Tenniswood	FasL	rat
ratfasr	catccttgagccttgcacacga	Dr. Martin Tenniswood	Fas	rat
ratfasf	tgccggttgtcgatgcagtt	Dr. Martin Tenniswood	Fas	rat
ratbaxr	gacgcatccaccaagaagctga	Dr. Martin Tenniswood	Bax	rat
ratbaxf	aagtccagtgtccagcccatga	Dr. Martin Tenniswood	Bax	rat
ratbadr	ccagagtatgttccagatccca	Dr. Martin Tenniswood	Bad	rat
ratbadf	tggataatgcgcgtccaact	Dr. Martin Tenniswood	Bad	rat
ratbcl2r	tggcatcttctccttccagcct	Dr. Martin Tenniswood	Bcl-2	rat
ratbcl2f	aaaggcatcccagcctccgtta	Dr. Martin Tenniswood	Bcl-2	rat
adaptor primerv(AP)	ggccacgcgtcgactagtacttttttttttttttttt	GibcoBRL	mRNA poly(A+)	n/a
Abridged Universal Amplification Primer (AUAP)	ggccacgcgtcgactagtac	GibcoBRL	mRNA poly(A+):AP	n/a
5' RACE Abridged Anchor Primer	ggccacgcgtcgactagtacgggiigggiigggiig	GibcoBRL	poly(C+) tailed mRNA	n/a
DPH-up-BamH1	ccctggatccggaatgctttacttgatcgg	Qiagen	rDPH ORF	rat
DPHS-down-EcoR1	atgtgaattctcagatccatcagtactctgg	Qiagen	rDPH ORF	rat
DPHns-down-EcoR1	atgtgaattctcagatccatcagtactctgg	Qiagen	rDPH ORF	rat
28-2 Up	cggaatggtttacttgatcgg	Invitrogen	rDPH ORF	rat
28-2 Down NS	gagtccatcagtactctgg	Invitrogen	rDPH ORF	rat
28-2 Down S	tcagagtccatcagtactctgg	Invitrogen	rDPH ORF	rat
MLPR up	ggccatggaggtggag[illegible]	Invitrogen	RRG4 ORF	rat
MLPR Down NS	ggtcccgctgtaggaatag	Invitrogen	RRG4 ORF	rat
MLPR Down S	gggcagtgttggaggtcagg	Invitrogen	RRG4 ORF	rat
MRG-1 up	cggaaggactggaaatggc	Invitrogen	Mrg-1 ORF	rat
MRG-1 Down NS	acagctgactctgctgg	Invitrogen	Mrg-1 ORF	rat
MRG-1 Down S	gagtcaacagctgactctgc	Invitrogen	Mrg-1 ORF	rat

Table 2.2. Specific information regarding the PCR primers utilized in this study. Primers were resuspended in DEPC treated water to a final concentration of either 400 or 40 μM and were stored at 4°C for short term storage or at -20°C for long term storage.

and dCTP, 5 μM of each the upstream and downstream primers, 2.5 units of Taq polymerase, 1 μg template DNA, and water to 100 μl. In some cases, PCR was optimized by adjusting $MgCl_2$ concentration within the range of 1.5 mM – 5 mM, or by adding enhancer solutions such as 1X Qiagen Q-solution (5X stock, Qiagen, Mississauga, ON).

2.J-3. Polymerase Chain Reaction using Platinum Pfx polymerase. Platinum Pfx PCR was set up according to manufacturer's specifications (Invitrogen, Burlington, ON) as follows: 50 μl PCR reactions were set up using 1X Platinum Pfx PCR buffer (10X PCR buffer stock, Invitrogen, Burlington, ON), 0.3 mM of each of dATP, dTTP, dGTP, and dCTP, 1 mM $MgSO_4$, 0.3 μM each of the upstream and downstream primers, 1 unit of Pfx polymerase, 200 ng template DNA, and water to 50 μl. In some cases, PCR was optimized by adding 10X Pfx enhancer (Invitrogen, Burlington, ON) at a concentration of 0.5-3X.

2.J-4. Polymerase Chain Reaction Amplification Cycle. DNA was amplified by heating to 95°C for 5 minutes, followed by 30 cycles of: 95°C for 1 minute, 50-60°C (optimized for any given reaction) for 1 minute, 72°C for 3 minutes; and finally one cycle of 72°C for 6 minutes. The reactions were stored at 4°C until use. PCR products were resolved using gel electrophoresis (Section 2.K1-b) and purified by gel extraction (Section 2.B-2d).

2.K. ELECTROPHORESIS

2.K-1. Electrophoresis of DNA

2.K-1a. Alkaline gel electrophoresis for the analysis of cDNA. Alkaline gels were prepared by melting 0.8 g of agarose in 72 ml of boiling water. The mixture was cooled to

55°C, and 8 ml of 10X alkaline buffer (1.9 M NaOH, 2 ml of 125 mM EDTA) was added. The solution was mixed, immediately poured into an electrophoresis casting tray, and allowed to solidify. The cDNA samples and controls isolated from the first and second strand synthesis reactions were mixed with an equal volume of 2X alkaline loading buffer (2% glycerol [v/v], 4.6% saturated Bromophenol blue [v/v], and 25 mM NaOH), and loaded onto the alkaline gel. The gel was run at 100 mA in 1X alkaline buffer. The outside of the gel box was packed with ice to prevent overheating, as the alkaline buffer lacks the buffering capacity of conventional running buffers. Once electrophoresis was complete, the gel was dried down on a gel dryer and the gel was exposed to autoradiography film. The film was developed and analyzed after an appropriate exposure.

2.K-1b. Standard gel electrophoresis. 1% agarose gels were made by adding 1% [w/v] agarose to 1X TAE buffer (50X TAE=2 M Tris-HCl, 5.7% [v/v] glacial acetic acid, 50 mM EDTA; pH 8.0), or 0.5X TBE buffer (5X TBE= 0.45 M Tris-HCl, 2.25 M boric acid, 10 mM EDTA; pH 8.0) and boiling until the agarose was dissolved. The molten agarose was poured into an electrophoresis casting tray and allowed to solidify. DNA samples were mixed with 0.1 volume of 10X DNA loading dye (0.21% Bromophenol Blue, 0.21% Xylene Cyanol FF, 0.2 M EDTA; pH 8.0, and 50% glycerol). Samples were loaded into the wells in the agarose gel, and the DNA was resolved by running the gel at 100-150 volts in 1X TAE or 0.5 TBE buffer.

2.K-2. Electrophoresis of RNA

2.K-2a. Preparation of formaldehyde gels. Agarose (sufficient for a 1.0 to 1.2% gel) was added to milliQ water (72% of final gel volume), and the mixture was brought to a boil until the agarose was completely dissolved. After removing from heat, formaldehyde (18% of final gel volume), and 10X MOPS (10% of final gel volume; 200 mM 3-[N-morpholino]propane-sulfonic acid, 50 mM sodium acetate, and 10 mM EDTA; pH 6.5; Intergen, Purchase, NY) was added and mixed by gentle swirling. This mixture was immediately poured into a gel casting tray, and bubbles were removed using a Kim-Wipe. The tray was then covered to prevent exposure to drafts (which can lead to swirls and unevenness in the gels), and the gel was allowed to solidify for at least 3 hours. Once solidified, the gel was submerged in formaldehyde running buffer (8.3% formaldehyde, 10% 10X MOPS, 81.7% milliQ water) (Sambrook, 1989).

2.K-2b Preparation of RNA samples. Just prior to loading of the gel, total RNA was thawed on ice, and a 10 μg aliquot was taken. The volume was adjusted to 9 μl with DEPC-treated water. Thirty-two μl of RNA loading buffer (12.5 % 10X MOPS, 21.9% formaldehyde, 62.5% deionized formamide, 1 μg ethidium bromide) was added to each sample. The samples were heated in a 55°C water bath for 15 minutes. Five μl of 10X loading dye (Eppendorf, Westbury, NY) was added to each sample.

2.K-2c. Running of formaldehyde gels. After loading of samples, electrophoresis was performed at 150 V until samples had completely entered the gel. Electrophoresis was continued overnight (approximately 14 hours) at 25-30 V. The next morning the gels were soaked in milliQ water for 15 minutes and then images were taken at 302 and 360 nm using a Kodak Digital Science DC120 Zoom Digital Camera and Kodak ID Image Analysis Software (Eastman Kodak Co., Rochester, NY).

2.K-3. Electrophoresis of proteins

2.K-3a. Preparation of SDS polyacrylamide gels (PAGE). PAGE was performed using the BioRad Mini-Protean III apparatus (BioRad, Hercules, CA), according to the method of Laemmli (1970) and Ornstein (1964). Prior to use, all glass plates, combs and spacers were washed with 95% ethanol or methanol. A separating gel was prepared by mixing 13.2 ml of 10% polyacrylamide separating gel (0.28 M Tris-HCl pH 8.8, 75 mM SDS) and 15%-acrylamide-bis solution 19:1 [Hercules, CA]). The mixture was degassed using a standard vacuum line, and 100 µl of 10% ammonium persulfate (APS) and 10 µl of Temed was added. The solution was mixed and poured into the gel apparatus using a pasteur pipette, avoiding bubble formation. Isopropanol was layered onto the gel, and the gel was allowed to solidify. Once solid, the isopropanol was poured off and the gel was rinsed with water. Five ml of 10% stacking gel (125 mM Tris-HCl pH 6.8, 10 mM SDS, and 4% acrylamide-bis solution 19:1 [Biorad, Hercules, CA]) was degassed as above and 50 µl of APS and 10 µl of Temed was added. The solution was mixed and poured on top of the separating gel. The combs were immediately placed in the gel apparatus and the gel was allowed to solidify for at least 30 minutes. Prior to use, the combs were removed and the wells were rinsed out with distilled water to remove any unpolymerized acrylamide.

2.K-3b. Preparation of samples. 10 μg of each protein sample were mixed with 2X Laemmlli buffer (63 mM Tris-HCl pH 6.8, 10% [v/v] glycerol, 2% SDS, 0.025% [w/v] bromophenol blue, 32 mM β-mercaptoethanol), and boiled for 5 minutes to denature the proteins. The samples were stored on ice until loaded.

2.K-3c. Running of SDS-PAGE gels. Denatured proteins were loaded into the wells and electrophoresis was performed at 50-70 V in 1X Western blot running buffer (5X=0.12 M Tris-HCl, 0.96 M glycine, 17.3 mM SDS; pH 8.3-8.6) until the proteins lined up at the interface between the stacking and separating gels. Once the proteins had entered the separating gel, the voltage was increased to 150 V and electrophoresis was continued until the loading dye ran off the bottom of the gel (allowing for the visualization of proteins 8.5 kDa and higher). Kaleidoscope pre-stained protein standards (BioRad, Hercules, CA) were used.

2.L. SOUTHERN BLOT ANALYSIS

2.L-1. Southern blot transfer. Transfer of electrophoresed DNA in agarose gels onto GeneScreen Plus membrane (NEN Life Science Products, Boston, MA) was performed using a standard alkaline transfer method. The precut nylon membrane was wetted in distilled water, and was soaked in 0.4 M NaOH for 10-15 minutes. The gel was soaked 0.25 M HCl for 10 minutes, rinsed twice in distilled water, and soaked in 0.4 M NaOH for 5-15 minutes. The southern blot transfer was set up as follows: a Whatman paper bridge was assembled over a gel support and was suspended in 0.4 M NaOH; two pieces of gel-sized pieces of Whatman paper were presoaked in 0.4 M NaOH, and set upon the bridge; the gel was placed bottom side up onto the Whatman paper pieces and the nylon membrane was placed on top of the gel; two additional pieces of gel-sized Whatman paper were placed onto the membrane, and a stack of paper towels was piled onto the paper. Between each layer, a small amount of 0.4 M NaOH was added and all the bubbles were rolled out prior to the addition of the next layer. A glass plate was placed on top of this and a small weight (~200 g) was placed on the plate. The passive transfer was performed overnight at room temperature. The following day, the membrane was removed from the gel and cross-linked using a UV Stratalinker 1800 (Stratgene, La Jolla, CA) . A photograph was taken of the gel under UV light to confirm efficient transfer. The membrane was stored between 2 pieces of Whatman paper at room temperature until use.

2.L-2. Southern blot analysis. Hybridization of radioactively labeled PCR amplified inserts from individual clones or total cDNA populations was performed as described in section 2.H. Intensities of the bands observed on the autoradiograph were analyzed using the Kodak Digital Science DC120 Zoom Digital Camera and Kodak ID Image Analysis Software (Eastman Kodak Co., Rochester, NY).

2.M. NORTHERN BLOT ANALYSIS

2.M-1. Northern blot transfer. GeneScreen Plus membrane (NEN Life Science Products, Boston, MA) was presoaked in 2X SSC (20X=3M NaCl, 180 mM Na citrate; pH 7.0) for at least 15 minutes. The transfer of the RNA from the gel to the membrane was performed by passive transfer in 10X SSC in the following order: a Whatman bridge the width of the gel and extending into the 10X SSC; 2 pieces of Whatman paper cut to the exact dimensions of the gel; the gel (upside-down so that the flat face of the gel comes into contact with the membrane); the presoaked membrane; 2 pieces of Whatman paper of the same size of the gel; blotting paper/paper towels cut to the exact size of the gel (stack about 4 inches thick); and a glass plate and small weight (~200 g). Between each layer, a small amount of 10X SSC was added and all the bubbles were rolled out prior to the addition of the next layer. The passive transfer was left overnight at room temperature. The following day, the membrane was removed from the gel and the RNA was cross-linked onto the membrane using a UV Stratalinker 1800 (Stratagene, La Jolla, CA). A photograph was taken of the gel under UV light in order to confirm efficient transfer of the RNA out of the gel. The membrane was stored between 2 pieces of Whatman paper at room temperature until use.

2.M-2 Northern blot analysis. Hybridization of radioactively labeled PCR amplified inserts from individual clones was performed as described in section 2.H. For each analysis, the intensities of the bands observed on the autoradiograph were analyzed using the Kodak Digital Science DC120 Zoom Digital Camera and Kodak ID Image Analysis Software (Eastman Kodak Co., Rochester, NY). This in turn was normalized with the intensity of the 18S ribosomal RNA bands observed on the gel used in the Northern blot transfer. The 18S ribosomal RNA band was used as a loading and a transfer control for Northern blot analysis (Correa-Rotter *et al*, 1992). Dividing the hybridization intensity of the autoradiograph bands by the fluorescence intensity of the corresponding 18S bands resulted in a normalization of the band intensity to account for the loading difference between lanes.

2.N. WESTERN BLOT ANALYSIS

2.N-1. Western blot transfer. The polyacrylamide gel and the Transblot 0.2 µm transfer nitrocellulose membrane (BioRad, Hercules, CA) were soaked in Blot buffer (25 mM Tris-HCl pH 8.1-8.4, 190 mM glycine, 20% [v/v] methanol, water up to 2 liters) for 20 minutes prior to assembly of the Western blot transfer. The Western blot transfer was assembled in blotting buffer using the Mini-PROTEAN 3 Cell system (Biorad, Hercules, CA) as follows: absorbent pad, 1 piece of Whatman paper, polyacrylamide gel, nitrocellulose membrane, Whatman paper, and then the absorbent pad. Once assembled, the Western blot transfer was performed overnight (16 hours) at 100 mA. To determine the success of protein transfer, membranes were stained for 1 minute in Ponceau S stain (0.5% [w/v] Ponceau S, 1% glacial acetic acid), and rinsed in distilled water, and an image was obtained using a digital scanner. Gels were stained in Coomassie Blue stain (0.1% Coomassie R-250, 40% methanol, 10% acetic acid) for 15 minutes and de-stained in a solution of 40% methanol, and 10% acetic acid for 15 minutes. An image was obtained using a digital scanner.

2.N-2.Western blot analysis of proteins. Membranes were rinsed in 1X TBS pH 7.6 for 15 minutes at room temperature. Membranes were then incubated in blocking buffer (1X TBS pH 7.6 [10X TBS=0.28 M NaCl, 20 mM Tris-HCl pH 7.6], 0.1% Tween 20, 5% skim milk powder/ BSA/ pre-immune serum) for 1 hour at room temperature with gentle agitation. Membranes were then washed 3 times for 5 minutes in TBS/T (1X TBS pH 7.6, 0.1% Tween 20) with gentle agitation. Primary antibody was added to the membrane at the appropriate dilution in antibody buffer (1X TBS pH 7.6, 0.1% Tween 20, 5% skim milk powder/ BSA) and was allowed to incubate overnight at 4°C. Membranes were washed as before and horseradish peroxidase (HRP)-conjugated secondary antibody was added at the appropriate dilution in antibody buffer. The membranes were incubated with the secondary antibody for 1 hour at room temperature. Membranes were washed as before. The presence of the specific protein as indicated by antibody binding was visualized using ECL Western blotting detection reagents (Amersham Biotech, Piscataway, NJ) according to the manufacturer's protocols. Detection Reagents 1 and 2 were mixed in equal volumes, immediately added to membranes, and incubated for 1 minute. The solutions were then poured off and the membranes were wrapped in Saran Wrap and exposed to autoradiography film for times ranging from 5 seconds to 30 minutes depending on the intensity of the fluorescence obtained. Specific information regarding the antibodies used in Western blot analysis is provided in Table 2.3.

2.O. DNA SEQUENCING

2.O-1. Manual DNA Sequencing

2.O-1a. Preparation of samples. Manual sequencing of gel purified PCR products was performed using the ThermoSequenase Radio-labeled Terminator Cycle Sequencing Kit (USB Corporation, Cleveland, Oho). Four terminator mixtures were prepared on ice and consisted of 2 μl of nucleotide master mix (7.5 μM dATP, dCTP, dGTP, and dTTP), and 0.5 μl of α-^{32}P-ddNTP (G, A, T or C). The reaction mixture consisted of 2 μl of reaction buffer (260 mM Tris-HCl pH 9.5 and 65 mM $MgCl_2$), 500 ng of DNA, 2.5 pmol of template specific sequencing primer, 2 μl Thermo Sequenase polymerase (4 units/μl) and water to a final volume to 20 μl. 4.5 μl of the reaction mixture was added to 4 tubes, each

Primary Antibodies									
target protein	company	cat #	species	mono- vs. polyclonal	Immunogen	Coupled to	peptide detected	dilution - Western	dilution - immuno.
actin	Chemicon	MAB1501	mouse	monoclonal	N-terminus	n/a	42 kDa	1:1000	n/a
Apaf-1	Cedarlane Laboratories	sc-7232	goat	polyclonal	N-terminus	not KLH	130 kDa	1:100-1:1000	n/a
Bad	StressGen Biotechnologies	AAP-020	rabbit	polyclonal	KSDPGIRSLGSDAGGRR	KLH	23 kDa	2 ug/ml	n/a
Bax	StressGen Biotechnologies	AAS-040	rabbit	polyclonal	ELALDPVPQDASTKKLSEC	KLH	22 kDa	1:500	n/a
Bcl-2	StressGen Biotechnologies	AAP-071	rabbit	polyclonal	AGRTGYDNREIVMKYIHY	KLH	25 kDa	1:250	n/a
Bcl-w	StressGen Biotechnologies	AAP-050	rabbit	polyclonal	DFVGYKLRQKGYVC	KLH	20 kDa	4 ug/ml	n/a
caspase 1	Cedarlane Laboratories	sc-1597	goat	polyclonal	C-terminus	not KLH	45 kDa (UP), 20 kDa and 10 kDa (P)	1:100	1:100
caspase 2	Cedarlane Laboratories	sc-1217	goat	polyclonal	N-terminius	not KLH	46 kDa (UP)	1:100-1:1000	n/a
caspase 3	Cedarlane Laboratories	sc-1224	goat	polyclonal	N-terminus	not KLH	33 kDa (UP), 11 kDa (P)	1:100-1:1000	1:1000
caspase 3	Cell Signaling technology	#9661	rabbit	polyclonal	caspase 3 cleavage site	KLH	17-20 kDa (P)	1:50	1:1000
caspase 3	StressGen Biotechnologies	AAP-113	rabbit	polyclonal	full length human caspase 3	none	34 kDa (UP), 20 kDa and 18 kDa (P)	1:5000	1:1000
caspase 6	Cedarlane Laboratories	sc-1230	goat	polyclonal	C-terminus	not KLH	32-33 kDa (UP), 20 kDa (P)	1:100-1:1000	n/a
caspase 7	Cedarlane Laboratories	sc-6138	goat	polyclonal	C-terminus	not KLH	35 kDa (UP)	1:100-1:1000	n/a
caspase 8	StressGen Biotechnologies	AAP-108	rabbit	polyclonal	CEVSNKDDKKNMGKQ	KLH	55 and 53 kDA (UP)	4 ug/ml	n/a
caspase 8	StressGen Biotechnologies	AAP-118	rabbit	polyclonal	full length caspase 8	none	55/57 kDa (P), 42/44 kDa (P), 25 kDa and 10 kDa (P)	1:1000	1:1000
caspase 9	StressGen Biotechnologies	AAP-109	rabbit	polyclonal	CGGEQKDHGFEVASTSPEDE	KLH	46 kDa (UP), 36 kDa (P)	4 ug/ml	1:100
caspase 9	Cedarlane Laboratories	sc-7885	goat	polyclonal	N-terminus		45 kDa (UP), 10 kDa (P)	1:200-1:1000	1:500
caspase 9	Cell Signaling technology	#9507	rabbit	polyclonal	N-terminus	KLH	38 kDa (P) and 17 kDa (P)	1:100	1:1000
Fas	StressGen Biotechnologies	AAP-221	rabbit	polyclonal	ESLKRRRVHETDKNC	KLH	44 kDa	1:2000	n/a
Fas ligand	Oncogene Research Products	PC78	rabbit	polyclonal	QLSLINFEESKTFFGL	not KLH	35-43 kDa	5 ug/ml	n/a
GFAP	Calbiochem	345860	rat	monoclonal	full length protein	none	56 kDa	0.1-0.5 ug/ml	1:100
MRG-1/CITED2/p35	T. Shioda (MGH Cancer Center, Charleston, MA)	n/a	rabbit	polyclonal	NQYFNHHPYPHNHYM	n/a	23 kDa	1:1000	n/a
NFKB	StressGen Biotechnologies	KAP-TF112	rabbit	polyclonal	N-terminus	KLH	50 kDa	0.5 ug/ml	n/a
p53	Oncogene Research Products	PC35	sheep	polyclonal	recombinant bacterial expressed p53	n/a		1:2500	n/a
PARP	StressGen Biotechnologies	AAP-250	rabbit	polyclonal	GVDEVAKKKSKKEKD	KLH	113 kDa (UP), 85 kDa (P), 29 kDa (P)	1:250	1:10
PARP	Cell Signaling technology	#9542	rabbit	polyclonal			116 kDa (UP), 89 kDa (P) and 24 kDa (P)	1:50	1:1000
PARP	Cell Signaling technology	9545	rabbit	polyclonal	PARP cleavage [illegible]	KLH	89 kDa (P)	1:1000	1:100
cytochrome c	Dr. Larry Prochaska, Wright State University	n/a	rabbit	polyclonal	n/a	n/a	12 kDa	1:1000	n/a
Secondary Antibodies									
target protein	company	cat #	species	mono- vs. polyclonal	Immunogen	Coupled to	peptide detected	dilution - Western	dilution - immuno.
mouse IgG	StressGen Biotechnologies	SAB-100	goat	polyclonal	mouse IgG	n/a	mouse IgG	1:1000-1:10,000	n/a
rabbit IgG	StressGen Biotechnologies	SAB-300	goat	polyclonal	rabbit IgG	n/a	rabbit IgG	1:1000-1:10,000	n/a
rabbit IgG	Jackson ImmunoResearch	111-166-006	goat	polyclonal	rabbit IgG	n/a	rabbit IgG	n/a	1:100-1:800
rat IgG	Jackson ImmunoResearch	112-166-006	goat	polyclonal	rat IgG	n/a	rat IgG	n/a	1:100-1:800
rat IgG	StressGen Biotechnologies	SAB-200	rabbit	polyclonal	rat IgG	n/a	rat IgG	1:1000-10,000	n/a
sheep IgG	Calbiochem	402100	rabbit	polyclonal	sheep IgG	n/a	sheep IgG	1:10,000	n/a

Table 2.3. Specific information regarding antibodies used in the course of this study for immunohistochemistry and Western analysis. Antibodies used for immunohistochemistry were tested for specificity by Western analysis prior to use.

containing 2.5 µl of one of the four terminator mixtures. The contents were mixed well, and the reactions underwent 45 cycles at 95°C for 30 seconds, 55°C for 30 seconds, and 72°C for 120 seconds. Four µl of stop solution was added to each of the reactions, which were then stored on ice until use. Prior to loading the samples on a polyacrylamide sequencing gel (section 2.O-1b) the samples were heated to 70°C for 2 minutes to denature the DNA. Five µl of each sample was loaded per lane.

2.O-1b. Preparation of polyacrylamide sequencing gels. Fifty ml of polyacrylamide sequencing gel (8 M urea, 10% [v/v] 30% acrylamide-bis solution 19:1 [BioRad, Hercules, CA], 1X TBE [5X stock=0.45 M Tris-HCl, 2.75 M boric acid, 10 mM EDTA; pH 8.0]) was degassed using a standard vacuum line. APS and TEMED were added to a final concentration of 7.5% (v/v) and 0.05% (v/v), respectively, and the mixture was immediately poured between two siliconized glass plates (with 1 mm combs and spacers, held together with bull-dog clamps) and allowed to polymerize. The bottom spacer was removed and the gel was placed into a standard dual reservoir sequencing apparatus and both reservoirs were filled with 1X TBE. The gel was pre-run at 40W for 30 minutes. The wells were washed with 1X TBE and 5 µl of the sequencing reactions were loaded into the wells. The samples were resolved by electrophoresis at 40W until the lower blue dye reached the bottom of the gel. A second loading of the samples was performed in the remaining wells as before. The gel was run as before until the lower blue dye was 1 cm from the bottom of the gel. The gel was removed from the plates and placed on two pieces of Whatman paper, and covered with saran wrap. The gel was then dried in a gel dryer. The saran wrap was removed and the gel was exposed to autoradiography film at room temperature until an adequate exposure was obtained. The sequence was read from the autoradiographs and was entered into a word file for further analysis.

2.O-2. Automated DNA sequencing. Automated DNA sequencing was performed using the DYEnamic Cycle Sequencing kit (APBiotech, Piscataway, NJ). Four µl of sequencing reaction premix (APBiotech, Piscataway, NJ) was mixed with 0.1 pmol template DNA and 2.5 pmol of primer (final reaction volume of 10 µl). The sequencing program consisted of 25 cycles of 95°C for 20 seconds, 50°C for 30 seconds and 60°C for 1 minute. 1 µl of sodium acetate/EDTA buffer (1.5 M sodium acetate, 250 mM EDTA; pH 8.0) and 40 µl of cold absolute ethanol was added and the DNA was precipitated at -20°C overnight. The reactions were centrifuged at 13,000 rpm for 30 minutes at 4°C, and the supernatant was removed. Fourty µl of 70% ethanol was added and the reactions were centrifuged as before for 15 minutes. The supernatant was removed, and the pellet was dried. Sequence was obtained using a Beckman CEQ 2000 DNA Analysis system (Beckman Coulter Canada Ltd., Mississauga, ON) by Pat Murray and Lisa Ostafichuk (Molecular Biology Sequencing Unit, Department of Biological Sciences, University of Alberta). Sequence information was stored as a text file that was used for further analysis.

2.P. BIOINFORMATIC ANALYSIS

2.P-1. Key websites used for bioinformatic analysis. Sequenced clones were subjected to BLAST analysis to determine their putative identification. Based on their identification, the clones were further characterized using bioinformatic analysis. Table

2.4 lists the websites used for bioinformatic characterization of the differentially expressed clones isolated from the screening of the cDNA library.

2.P-2. Development of Sitefind program. In order to analyze known protein databases for the presence of specific consensus target sequences, specific caspase cut sites, a search program entitled "Sitefind" was developed. Sitefind was implemented in Perl 5.6.0 and most of the query utilities were written in Python 1.5.2 by Gerry Patterson (Edmonton, AB). Reports were generated into spreadsheet formats that were analyzed using MS Excel. Databases used in the analysis including NCBI Protein Entrez (http://www.ncbi.nlm.nih.gov.80/entrez/query.fcgi?db=Protein), and RetNet (http://www.sph.uth.tmc.edu/Retnet/home.htm). Human genes that were identified as having potential cut sites were divided into functional categories and compared to their respective rat and mouse orthologs to determine if there was a bias in the types of proteins potentially targeted by the caspase cascade, and if the potential cut sites were conserved. Statistical analysis, including Goodness of Fit test and Chi squared analysis, was performed using Microsoft Excel (Office 97).

2.Q. IMMUNOFLUORESCENCE

2.Q-1. Isolation of optic cups. Rats were euthanized in CO_2 saturated chambers. A mark was made onto the cornea with a permanent marker, indicating the superior portion of the eye, and the eye was then enucleated. A small fixative access slit was made in the superior cornea with a razor blade, at the point where the cornea and sclera meet.

Website Name	Website address
OMIM:	http://www.ncbi,nlm.nih.gov/entrez/query.fcgi?db=OMIM
Entrez:	http://www.ncbi.nlm.nih.gov/Entrez/
GenBank:	http://www.ncbi.nlm.nih.gov/GenBank
BLAST:	http://www.ncbi.nlm.nih.gov/BLAST/
Unigene:	http://www.ncbi.nlm.nih.gov/entrez/query.fcgi?db=unigene
ORF Finder:	http://www.ncbi.nlm.nih.gov/gorf/gorf.html
Clusters of Orthologous Groups:	http://www.ncbi.nlm.nih.gov/COG/
PubMed:	http://www.ncbi.nlm.nih.gov/entrez/query.fcgi?db=PubMed
Genome DataBase:	http://www.gdb.org
GeneCards:	http://bioinfomatics.weizmann.ac.il/cards/
Primer3:	http://www-genome.wi.mit.ed units/cgi-bin/primer/primer3_www.cgi
SwissProt:	http://www.ebi.ac.uk/swissprot/
ClustalW:	http://www2.ebi.ac.uk/genemark
GRAIL:	http://compbio,ornl.gov/Grail-1.3
Pedro's BioMolecular Research Tools:	http://www.public.iastate.ed units/~pedro/research _tools.html
Gene Mark:	http://www2.ebi.ac.uk.genemark
BCM Search Launcher:	http://searchlauncher.bcm.tmc.ed units/
Locus Link:	http://www.ncbi.nlm.nih.gov/LocusLink/
Sacchromyces Genome Database:	http://www.yeastgenome.org/
Kyoto Encyclopedia of Genes and Genomes:	http://www.genome.ad.jp/kegg/
RetNet:	http://www.sph.uth.tmc.edu/Retnet/home.htm
Canadian Bioinfomatic Resource	http://cbr-rbc.nrc.cnrc.gc.ca
ProtParam	http://us.expasy.org/cgi-bin/protparam
EMBL-EBI Gene Wise 2 gene analysis program	http://www.ebi.ac.uk/Wise2/index.html
BCM Promoter Prediction program	http://searchlauncher.bcm.tcm.edu/cgi-bin/seq-search/gene-search.pl
EMBOSS-CpG Plot program	http://www.ebi.ac.uk/emboss/ cpgplot/cpgplot.html
EMBL-EBI GeneMark gene prediction program	http://www.ebi.ac.uk/genemark/ index.html
Gene Regulation Match gene tool	http://www.gene-regulation.com/cgi-bin/pub/programs/match/bin/match.cgi?

Table 2.4. Web-sites used for the bioinformatic analysis of the isolated differentially expressed clones.

2.Q-2. Fixation. The eye was incubated in 10 ml of 4% paraformaldehyde in sodium phosphate buffer (pH 7.4) for 10 to 15 minutes. The eye was then removed from the solution and the cornea was cut around the optic cup, leaving a small corneal flap at the inferior edge to act as a reference point. The lens was removed, and the eye was incubated in fresh 4% paraformaldehyde for 4 hours at 4°C with gentle shaking. The left eyes were used for cryosectioning, while the right eye was used for paraffin sectioning.

The left eye was washed 3 times in phosphate buffered saline (PBS) for 2 minutes each. The optic cup was cyropreserved in 30% sucrose in phosphate buffer for 12 hours. The cornea flap was removed and the optic cup was frozen in OCT in a plastic sectioning holder on dry ice. A mark was made on the plastic holder to indicate the superior region of the eye. The blocks were stored at -80°C until use.

The right eye was washed 3 times in PBS for 2 minutes each. The optic cup was incubated through a dehydration series of 30%, 50% and 70% ethanol for 1 hour each at 4°C. The dehydrated optic cups were stored in fresh 70% ethanol at 4°C until use.

2.Q-3. Cryosectioning of the rat retina. 4 μm retinal sections were cut along the nasal-temporal axis of the rat optic cups using a Kryostat 1720 digital Leitz-mgw Lauda cryostat (Brinkman, Mississauga. ON), producing sections that ran parallel to the superior-inferior axis of the optic cup. Internal temperatures of the cryostat were as follows: the knife blade was at -29°C, the internal environment was at -30°C, and the sample platform was between -13°C and -19°C. Individual sections were placed onto Fisher Superfrost Plus slides (Fisher, Nepean, ON) and were stored, wrapped in foil at -

70°C until use. Sections were performed with the help of Dr. Laith Dabbagh at the Cross Cancer Institute.

2.Q-4. Immunohistochemisty on frozen sections. Frozen slides were thawed to room temperature and then incubated with TBS/T blocking buffer (50 mM Tris-HCl pH 7.4, 150 mM NaCl, 0.1% Trition X-100 and 5% [w/v] skim milk powder) for 1 hour. The blocking buffer was removed and 100 µl of primary antibody at the appropriate dilution in blocking buffer was added directly onto the tissue section. The slide was incubated at 4°C overnight in a humidifying chamber. The slide was washed 3 times in TBS/T (50 mM Tris-HCl pH 7.4, 150 mM NaCl, 0.1% Trition X-100) for 5 minutes each. The slide was then incubated with secondary antibody at the appropriate dilution in blocking buffer at room temperature for 1 hour. For fluorescent-tagged antibodies, the incubation and all subsequent steps were performed in the dark, using a safe light. The slide was washed as before and the coverslip was placed over the tissue and the tissue was observed under appropriate microscopic conditions. For fluorescent microscopy the Nikon-Confocal Laser Scanning Microscope MD-Multi-probe 2001 was used, along with the analysis program Image Space 2 (Molecular Dynamics/ AP Biotech, Piscataway, NJ), with the assistance of Dr. Rakesh Bhatnagar, Jack Scott, and Randy Mandryk (Department of Biological Sciences Microscopy Unit, University of Alberta). Specific information regarding the antibodies used for immunofluorescence is provided in table 2.3.

2.Q-5. Haematoxylin and acidified eosin staining of sections. Integrity of the sections used for immunofluorescence was determined by Haematoxylin and Acidified Eosin

Staining (modified from Harris, 1900). Slides were placed in two washes of toluene for 5 minutes each, followed by an alcohol dehydration series (consisting of two incubations in absolute ethanol for 2 minutes each, one incubation in 90% ethanol for 2 minutes, one incubation in 70% ethanol for 2 minutes, and one incubation in 50% ethanol for 2 minutes). The slides were rinsed in distilled water and then placed in Harris's haematoxylin solution for 3-10 minutes until the desired staining was obtained. Over-stained slides were washed with 0.1% HCl to de-stain, and the staining step was repeated. The slides were rinsed in running water for 5 minutes. The slides were incubated in 70% ethanol for 2 minutes, and then in acidified eosin for 1 minute. The slide was washed twice in absolute ethanol for 2 minutes each, and then twice in toluene for 2 minutes each. Mounting media was added to the slides and the stained sections were covered with a cover slip and were observed under the light microscope.

2.R. FUNCTIONAL ANALYSIS OF THE YEAST *DPH5* GENE

2.R-1. Oxidative stress assay on wild-type and mutant yeast cells. Yeast diphthamide methyltransferase deletion (orf:ylr172c, strain BY4741, MATa, his3delta1, leu2delta0, met15delta0, ura3delta0, yrl172c/dph5) and wild-type (BY4741, MATa, his3delta1, leu2delta0, met15delta0, ura3delta0) strains were purchased from ATCC (Manassas, VA). Strain identity was confirmed using PCR and sequence analysis using *DPH5* gene specific primers (yDPH EXT.1 = 5'-GCCAACAACATCTCCCAGTT-3', yDPH EXT.2 = TCCAGGATCGCTCTTGTTCT-3', yDPH INT.1 = 5'-GCCAACAACATCTCCCAGTT-3', and yDPH INT.2 = 5'-TCCAGGATCGCTCTTGTTCT-3') (Figure 2.6). Wild-type and dph5 mutant yeast cells

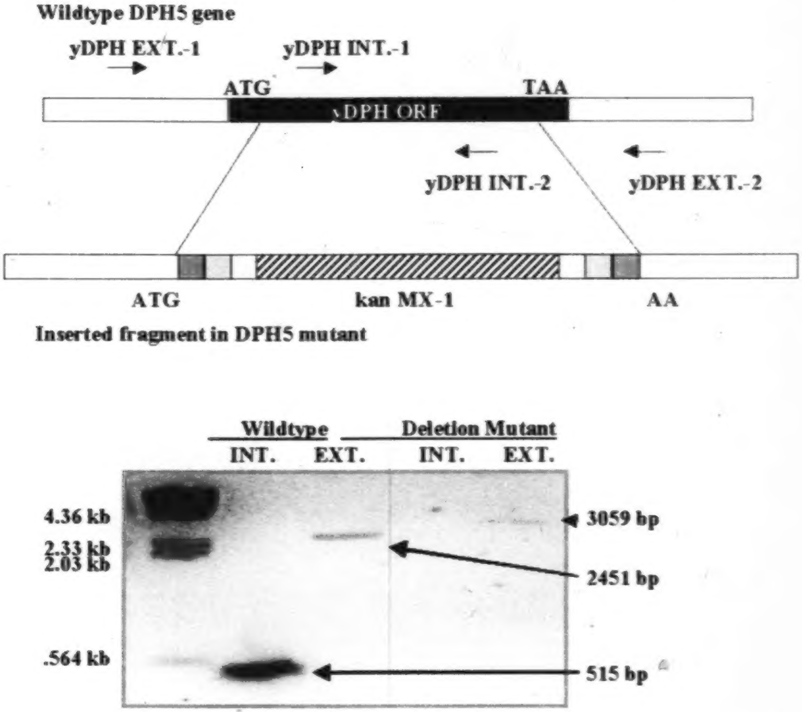
Wildtype DPH5 gene
yDPH EXT.-1
yDPH INT.-1
ATG
TAA
yDPH ORF
yDPH INT.-2
yDPH EXT.-2
ATG
kan MX-1
AA
Inserted fragment in DPH5 mutant
Wildtype
Deletion Mutant
INT.
EXT.
INT.
EXT.
4.36 kb
2.33 kb
2.03 kb
.564 kb
3059 bp
2451 bp
515 bp

Figure 2.6. Confirmation of genotype of *DPH5* deletion mutant and wildtype yeast strains. Genotypes of wildtype and *DPH5* deletion strains were confirmed using PCR and sequence analysis. Primers were designed to internal (yDPH INT.-1 and yDPH INT.-2) and external (yDPH EXT.-1 and yDPH EXT.-2) sequences of the yeast *DPH5* gene. Colony PCR was performed and PCR products were resolved by gel electrophoresis. Gel purified PCR products were sequenced and NCBI BLAST analysis was performed to confirm strain genotype.

were grown overnight in 100 ml of YEPD media (2% bacto-peptone, 1% yeast extract, 0.11 M dextrose, 1.5% agar; pH 5.8) at 28°C. Cells were harvested during the exponential phase, and resuspended in YEPD media (pH 3.0), to a cell density of 10^7 cells/ ml. Cells were treated with either 0, 20, 40, 80, 120, 160 or 200 mM of acetic acid, or 0, 1, 3, 5, 10, 15, or 180 mM H_2O_2. The cells were incubated, at 28°C for 200 minutes in a shaking water bath. The cells were plated on YEPD plates (pH 7), and incubated at 30°C for three days. Number of colonies was determined, and compared to untreated controls.

2.S. TRANSMISSION ELECTRON MICROSCOPY OF YEAST CELLS

2.S-1. Fixation of yeast cells. Cells used for electron microscopy were treated as described in section 2.R-2. Following 200 minute treatment with various concentrations of either H_2O_2 or acetic acid, cells were centrifuged at 2500 rpm and resuspended in 2.5% glutaraldehyde in phosphate/Mg++ buffer (40 mM K_2HPO_4, and 0.5 M $MgCl_2$; pH 6.5) and incubated overnight at 4°C. Cells were washed three times in sorbitol wash buffer (1.2 M sorbitol, 1 mM EDTA, 1 mM β-mercaptoethanol, 10 mM Tris-HCl; pH 7.5) and pelleted cells were resuspended in1 ml sorbitol wash buffer. 0.5 mg of zymolase (US Biological, Swampscott, MS) was added, and the cells were incubated with shaking at 25°C for 2 hours. The cells were washed three times in sorbitol wash buffer as before, and then resuspended in 0.5% osmium tetroxide in 1X PBS (10X PBS = 1.37 M NaCl, 26.8 mM KCl, 43 mM NaH_2PO_4, 14.7 mM KH_2PO_4) for 2 hours. The cells were washed twice in distilled water and then were incubated with 1% (w/v) uranyl acetate. The cells were carried through a dehydration series (consisting of 5 minutes in each of 50%

ethanol, 70% ethanol, 90% ethanol, 95% ethanol, and 4 washes in 100% ethanol). The cells were centrifuged at 2500 rpm and resuspended twice in propylene oxide, and then the pelleted cells were resuspended in propylene oxide:SPURS resin (1:1) and incubated overnight at room temperature. Fresh SPURS resin was added and the cells were incubated at 60°C for 24 hours to allow the resin to harden.

2.S-2. Sectioning for TEM. Silver-Gold Sections (70-90 nm) were cut using a Reichert-Jung Ultracut E microtome by Ron Koss, Department of Biological Sciences, University of Alberta. Sections were mounted on a 200 mesh copper grid and were stored at room temperature until use.

2.S-3. Visualization of sections. Sections were visualized using a Morgani FEI Transmission Electron Microscope with the assistance of Dr. Rakesh Bhatnagar, Jack Scott, and Randy Mandryk (Department of Biological Sciences Microscopy Unit, University of Alberta).

Chapter 3

Activation of members of the caspases cascade in the rod outer segments by intense green light-induced retinal degeneration.

Contributors:

Dr. Daniel Organisciak, Ruth Darrow, and Linda Barsalou: rat retinal tissues, gel electrophoresis of DNA fragmentation ladders, isolation of purified ROS

Laith Dabbagh: sectioning of rat retinae

Pat Murray, Lisa Ostafichuk (MBSU): automated sequencing

Randy Mandryk, Jack Scott, Dr. Rakesh Bhatnagar: technical assistance with immunofluorescence

Rhonda Kelln: opsin northern analysis

Ruby Grewal: arrestin northern analysis

Gerard Patterson: construction of Gene Browser program

3.A. INTRODUCTION

Apoptosis has been associated with several degenerative disorders such as Alzheimer disease, Huntington disease, and inherited retinal degenerations (Wilson, 1999; Portera-Cailliau *et al*, 1994; Chang *et al*, 1993; Lolley *et al*, 1994; Smith *et al*, 1995; Wong, 1994; Wong *et al*, 1994a, b; Tso *et al*, 1994; Papermaster, 1995; Li *et al*, 1985; Milam *et al*, 1995). With respect to retinal degeneration, the sequence of events that lead to photoreceptor cell loss are not well understood. Induction of retinal degeneration by intense green light in rats (LIRD) involves excessive bleaching of rhodopsin (Noell *et al*, 1966), oxidative stress, and DNA fragmentation (Organisciak *et al*, 1995), all of which are indicative of active cell death and photoreceptor cell loss (Organisciak *et al*, 1994; Hafezi *et al*, 1997a, b; Wenzel, 2000). Photoreceptor apoptosis also requires alteration and modification in gene and protein expression (Wong *et al*, 1994b; 2001; Hafezi *et al*, 1999a, b; Wenzel *et al*, 2000; Jomary *et al*, 1999; Organisciak *et al*, 1998). Another key event in many tissues undergoing active cell death is the activation of cysteine-dependent aspartate-specific proteases, known as caspases. Caspases are generally activated by proteolysis (MacFarlane *et al*, 1997), and once activated can trans-activate other inactive pro-caspase family members, leading to the induction of a cascade of events that result in the amplification of a death signal. The activated caspases also cleave many key structural, metabolic, and regulatory proteins, whose modification underlies the morphological appearance and biochemical changes associated with apoptosis (Wolf and Green, 1999; Slee *et al*, 1999; Cohen, 1997; Budihardjo *et al*, 1999).

A number of studies have analyzed the role of caspases in light-induced retinal degeneration in rodents using either white (Donovan *et al*, 2001, 2002; Grimm *et al*, 2000), or blue light (Wu *et al*, 2002). Both white and blue light can damage photoreceptors (PR) as well as the retinal pigment epithelium (RPE). The extent of the damage depends on the duration of light exposure. Brief exposures lead to primarily photoreceptor cell damage whereas long exposures lead to damage of photoreceptors and RPE (Ham *et al*, 1976; Sperling, 1980a, b; Sperling *et al*, 1980; Ham *et al*, 1982; Ruffolo *et al*, 1984). In the current study we use green light as the incident light because we are trying to mimic the conditions that are most like a "retinitis pigmentosa condition", which is defined by loss of rod photoreceptor cells. Green light (490-580 nm) overlaps the activation wavelength of rhodopsin, the primary chromophore in rod cells.

We have used a unique approach to study the levels of caspase transcripts and proteins over the course of green light-induced retinal degeneration in rats. Caspases cut target proteins at specific consensus sequences, typically following an aspartate residue (Henning *et al*, 2000). Standard caspase assays involve the incubation of cell extracts with a small synthetic peptide containing a particular consensus sequence. If any of the caspases in the extract are able to cleave this substrate, a chromogenic or fluorogenic product is produced. Though quite sensitive, several problems occur when using conventional caspase assays. First, most commonly used substrates are recognized by numerous different caspase family members, making it difficult to identify which caspase molecule(s) is (are) activated (Henning *et al*, 2000). As well, some non-caspase proteases may also cleave the synthetic substrate molecules, potentially giving false positive results. In a mixed population of cells, such as a tissue sample, it becomes impossible to determine which cell populations are responsible for the proteolytic activity acting on the substrates. In addition, cleavage of a specific peptide in an *in vitro* assay does not necessarily mean that the downstream apoptotic targets have been cleaved. Several studies have recently demonstrated low-level caspase activation in non-apoptotic environments. (Wellington *et al*, 2002; Alam *et al*, 1999, Cheng and Zochodne, 2003). Therefore, the presence of activated caspases may not necessarily be indicative of an activated pro-apoptotic caspase cascade. As a result of these potential short-comings of conventional caspase assays, we chose to perform Western blot analysis using antibodies that detect the proteolytic products of downstream caspase targets to study the sequential activation the caspase family of proteins. As well, immunohistochemistry was used to study the sub-cellular location of the caspases within the photoreceptor cells of the retina.

We have demonstrated for the first time that green light activates caspase 1, caspase 8 and caspase 9-mediated cascades that lead to the activation of caspase 3 and caspase 6 and the inactivation of poly(ADP-ribose) polymerase (PARP). As anticipated, these events precede the occurrence of maximum detectable DNA fragmentation and coincide with changes in normal photoreceptor gene expression. Moreover, we report for the first time that normal retina appears to have an abundant store of caspases in the outer segment of the photoreceptor cells and that during the course of retinal degeneration, caspases and their targets relocate into the cell bodies of those cells.

3.B. RESULTS

3.B-1. Defining the treatment profile

In the current study, rhodopsin and other photoreceptor cell-specific genes were used as markers for "normal" dark-reared photoreceptor cell function. Changes in the mRNA levels of these genes were used to define the treatment conditions that result in photoreceptor cell dysfunction (Figure 3.1A). The control mRNA levels (0 hours of light exposure) of each gene are shown in the first lane of each autoradiograph. Following 4 hours of light exposure, a marginal increase in the normal levels of opsin (all 4 isoforms), IRBP (both isoforms) and arrestin is detected. Following 8 hours of light exposure, the levels of opsin and arrestin decrease to approximately control levels. The levels of mRNAs for all 3 genes further decrease following 16 hours of light to below control levels. In contrast, the expression of recoverin mRNA shows a progressive decrease at all time points following light exposure. In all cases, a shift in mRNA levels for each gene examined occurred at some point within the first 4 hours of light exposure. In contrast, levels of DNA fragmentation were not noticeable until after 8 hours of light exposure with maximum levels apparent after 16 hours (Figure 3.1B). The detection of DNA fragmentation is an indication that a large number of cells within the tissue studied are undergoing the late stages of active cell death. With respect to the light exposure profile we have analyzed, changes in photoreceptor gene expression precede the light exposure period required to induce detectable DNA ladders.

3.C-2. Activation of initiator caspases

A number of branches of the caspase cascade can lead to the demise of a given cell (Figure 3.2). Central to caspase-mediated active cell death are the activation of initiator caspases, which define a specific cascade pathway, including caspase 1, 8 and 9.

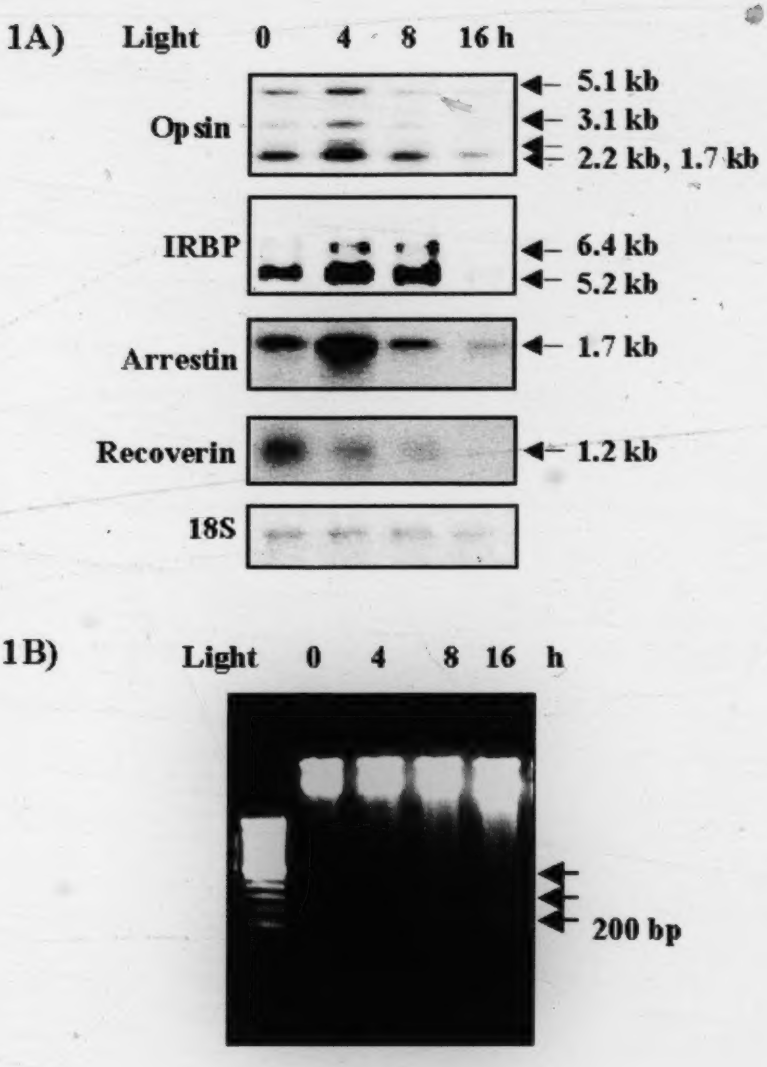
1A)
Light 0 4 8 16 h
Opsin
5.1 kb
3.1 kb
2.2 kb, 1.7 kb
IRBP
6.4 kb
5.2 kb
Arrestin
1.7 kb
Recoverin
1.2 kb
18S
1B)
Light 0 4 8 16 h
200 bp

Figure 3.1. Extent of photoreceptor dysfunction in the light-treated retina. (A) Changes in the expression patterns of photoreceptor-expressed genes following light treatment. Northern analysis of opsin, IRBP, arrestin, and recoverin was performed in duplicate on 10 µg of total RNA isolated from dark-reared rats exposed to 4, 8, or 16 hours of intense green light. In all cases representative Northern results are shown. (B) Extent of DNA fragmentation induced by light exposure. Rats were exposed to 0, 4, 8, or 16 hours of intense green light and the degree of DNA fragmentation was analyzed in duplicate by neutral agarose gel electrophoresis of 4 µg DNA per lane.

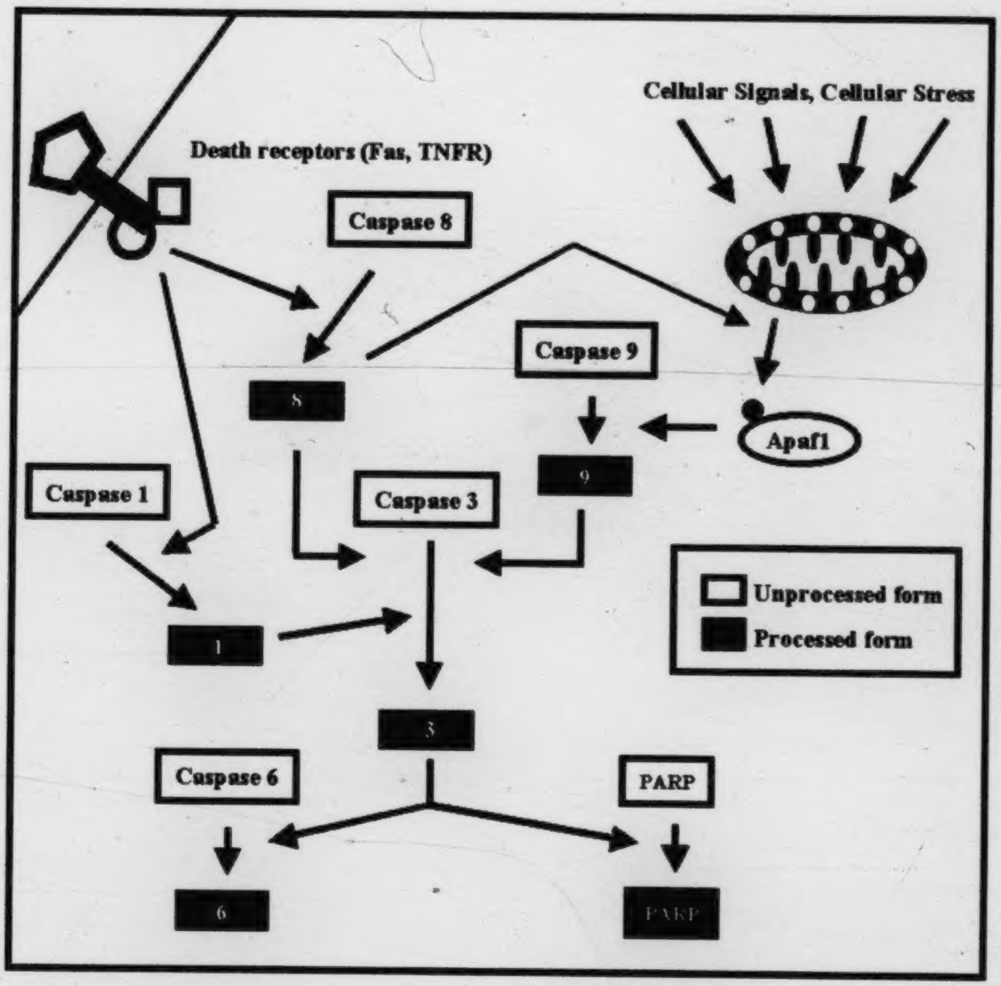
Cellular Signals, Cellular Stress
Death receptors (Fas, TNFR)
Caspase 8
8
Caspase 9
9
Apaf1
Caspase 1
Caspase 3
1
3
Unprocessed form
Processed form
Caspase 6
PARP
6
PARP

Figure 3.2. Cellular caspases can be activated through internal or external signaling mechanisms. External activation of caspases involves the activation of death receptors that leads to the aggregation of internal adapter molecules that facilitate the activation of caspase 1 and/or caspase 8. Signals acting at the level of the mitochondria, regulated by members of the Bcl-2 family, result in the release of cytochrome c. Cytochrome c interacts with the adapter molecule Apaf1, to facilitate the activation of caspase 9. The signals acting at the level of the mitochondria may originate within the cell itself, or can originate from receptor-mediated activation of caspase 8, through the adapter molecule Bid. The activation of caspase 1, 8 and 9 can lead to the activation of caspase 3, which will cleave downstream target molecules such as caspase 6 and PARP, leading to cellular dysfunction and apoptosis. For review see Slee et al, 1999.

Western analysis of caspase 8 identified the unprocessed 55 and 57 kDa protein, as well as the 44 kDa and 25 kDa-processed proteins (Figure 3.3A). The 55 and 57 kDa unprocessed proteins show similar patterns over the time course of degeneration, with increased levels after light exposure. The level of the 44 kDa processed caspase 8 protein was negligible in unexposed control animals. However, its level increased markedly after light exposure. The 25 kDa processed caspase 8 protein also mirrored this profile except the levels began to decrease after a 16 hours light exposure.

Western blot analysis of caspase 1 revealed the unprocessed 45 kDa protein, as well as the processed 20 kDa fragment (Figure 3.3B). There was a progressive decrease in the level of unprocessed caspase 1 following 4, 8, and 16 hours of light treatment. The 20 kDa processed form of caspase 1 was not detectable in the untreated retinae, but was observed following 4, 8 and 16 hours of light-treatment.

Western blot analysis of caspase 9 revealed the 45 kDa unprocessed form and the 10 kDa processed fragment. Although the 45 kDa protein was present in untreated animals, its levels increased after light exposure (Figure 3.3C). The 10 kDa fragment was absent in untreated animals and its levels increased progressively during the 4, 8 and 16 hours of light treatment.

3.C-3. Activation of caspase 3 and cleavage of downstream targets

All three of the activated initiator caspases, caspase 1, 8 and 9, converge at a common downstream point, specifically, the proteolytic activation of caspase 3. Western blot analysis demonstrated that the levels of the unprocessed form of caspase 3 increased after a 4 hour light exposure and remained elevated throughout the period of light exposure (Figure 3.4A). Levels of the 11, 17, and 19 kDa processed caspase 3 peptides,

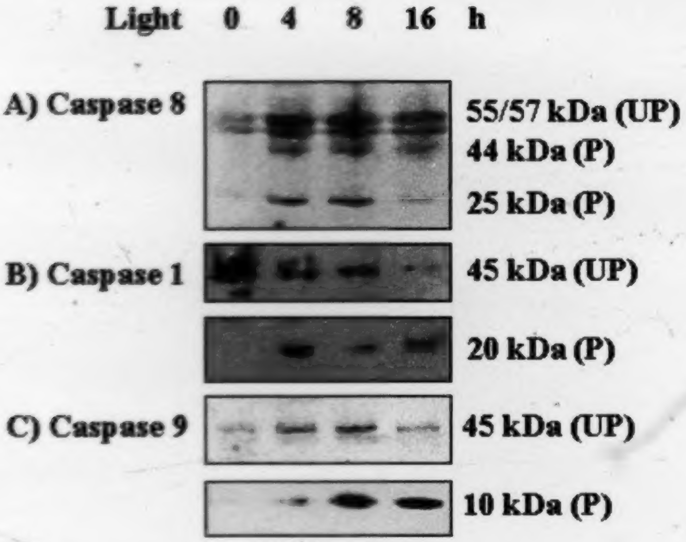
Light 0 4 8 16 h
A) Caspase 8
55/57 kDa (UP)
44 kDa (P)
25 kDa (P)
B) Caspase 1
45 kDa (UP)
20 kDa (P)
C) Caspase 9
45 kDa (UP)
10 kDa (P)

Figure 3.3. Activation of upstream caspases following exposure to green light. Western analysis of (A) caspase 8, (B) caspase 1 and (C) caspase 9 protein levels was performed in triplicate on 10 μg of protein lysates from light-treated and control retinae. In all cases, representative Westerns are shown (abbreviations: UP = unprocessed; P = processed). Specific information regarding the antibodies used is contained in Table 2.3.

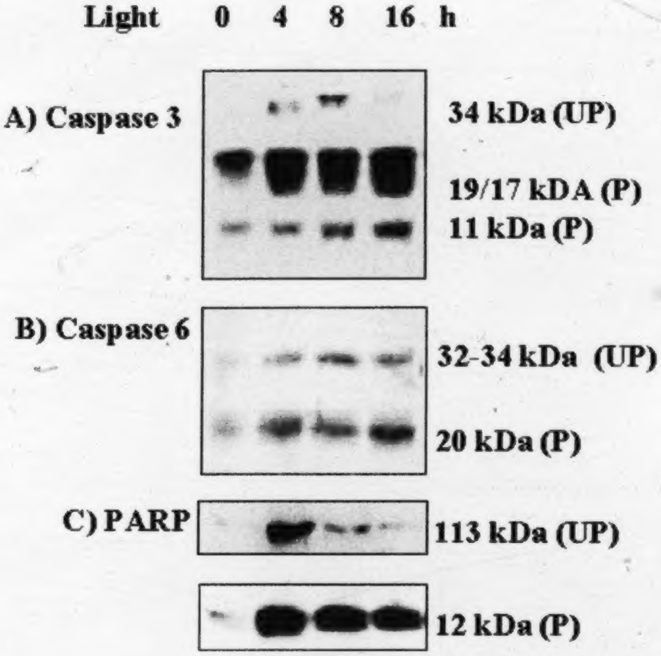
Light 0 4 8 16 h
A) Caspase 3
34 kDa (UP)
19/17 kDA (P)
11 kDa (P)
B) Caspase 6
32-34 kDa (UP)
20 kDa (P)
C) PARP
113 kDa (UP)
12 kDa (P)

Figure 3.4. Proteolytic processing of downstream targets. Western blot analysis of protein lysates from light-treated and control retinae (10 μg per lane) was performed in triplicate to detect the proteolytic processing of downstream targets including (A) caspase 3, (B) caspase 6 and (C) PARP. In all cases, representative Western blot results are shown (abbreviations: UP = unprocessed; P = processed). Specific information regarding the antibodies used is contained in Table 2.3.

indicative of proteolytic activation, also showed a progressive increase during LIRD.

Caspase 6 and PARP are downstream targets of activated caspase 3 and both are cleaved during LIRD (Figure 3.4B and C). The levels of both the unprocessed and processed (20 kDa) forms of caspase 6 increased after 4 hours of light exposure and remained elevated throughout the period of light exposure (Figure 3.4B). Caspase 3-mediated proteolysis of PARP, a protein involved in DNA repair (Althaus, 1992), leads to its inactivation, allowing DNA fragmentation to proceed. Levels of the unprocessed form of PARP showed an increase following 4 hours of light-exposure and then decreased following 8 and 16 hours of light exposure. Western blot analysis of the 12 kDa PARP cleavage product showed an increase in protein levels following 4, 8, and 16 hours of light treatment as compared to the control retinae (Figure 3.4C).

3.C-4. Localization of caspases and their targets in the normal and light-treated retina

As high levels of caspase activation were observed following 8 hours of light-exposure, immunofluorescence was performed on cryosections from control and 8-hour light-treated retinae. There was strong staining for caspases 1, 3, 8, 9, and PARP in the inner and outer segments in both dark-reared and light-treated retinae (Figure 3.5). This staining appears to be specific, as it was reproducible using several different antibodies from several different manufacturers (data not shown). In order to confirm that this was indeed the case, Western blot analysis of caspases 3, 8 and 9, as well as PARP was performed on protein lysates from purified outer segments (OS) isolated from cyclic-reared rats. These rats were used to determine if the OS localization occurred under

Figure 3.5. Localization of activated caspases in dark-reared and 8-hour light-treated retinae. (A) Haematoxylin and eosin staining was performed on representative 8-hour light-treated retinal section. (B) Toluidine blue staining was performed on representative 8-hour light-treated retinal section (C) Staining of a dark-reared-retina section in the absence of primary antibody (negative control) (D) Staining of a dark-reared retina section with anti-GFAP antibody. Dark-reared retinae are shown in E, G, I, K and M and 8 hour light-treated retinae are shown in F, H, J, L, and N. Immunohistochemistry was performed in triplicate using antibodies that recognize the processed and unprocessed forms of caspase 1 (E and F); the processed form of caspase 3 (G and H), the processed and unprocessed forms of caspase 8 (I and J); and the processed forms of caspase 9 (K and L), and PARP (M and N). (O) Average number of positively staining nuclei per mm^2 in the outer nuclear layer of dark-reared and 8 hour light-treated rat retinae. The number of positively staining nuclei was determined for caspases 3, 9 and PARP (processed forms), and caspases 1 and 8 (processed and unprocessed forms). On each of sections, the number of positively staining nuclei was counted and this number was divided by the area for each section as determined by pixel analysis using the Linux-based GIMP Image Analysis program. The results were averaged from a minimum of three sections for each antibody used. Specific information regarding the antibodies used is contained in Table 2.3. (Abbreviations used: UP = unprocessed; P = processed; magnification 40X). (Scale bar = 100 μm).

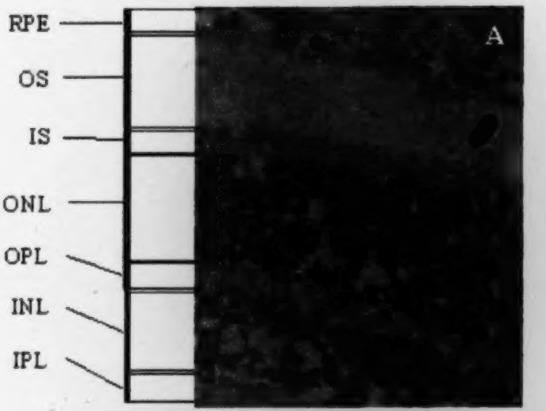
RPE
OS
IS
ONL
OPL
INL
IPL
A

H and E staining

Toluidine blue staining

No primary AB

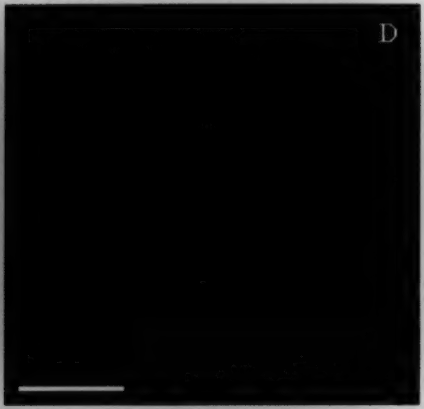

anti-GFAP

Dark-reared

8 hours light

anti-caspase 1

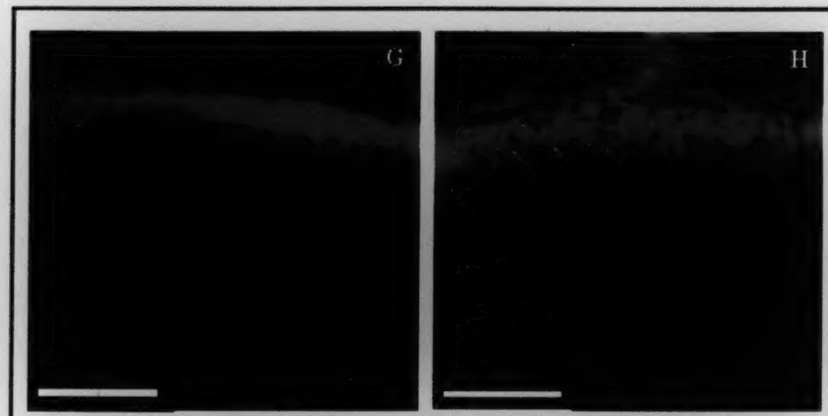

Dark-reared 8 hours light
anti-caspase 3

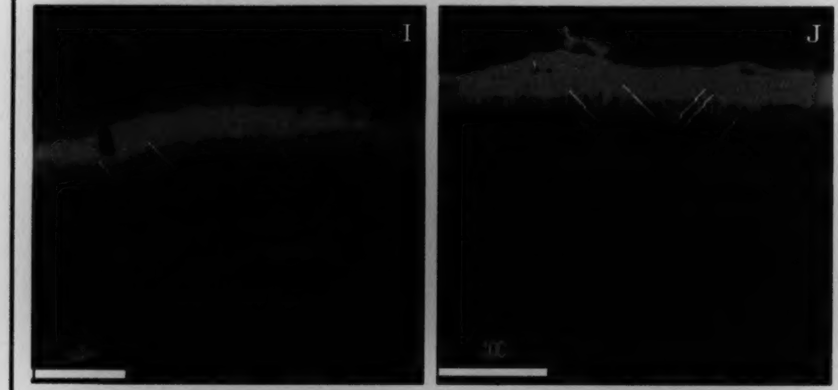

Dark-reared 8 hours light
anti-caspase 8

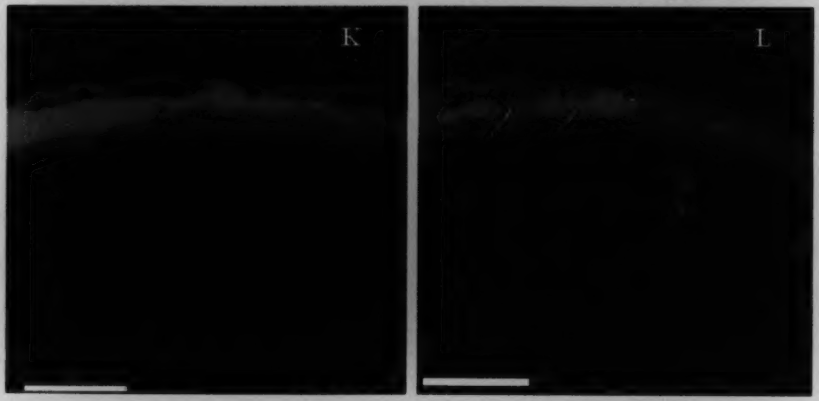

Dark-reared 8 hours light
anti-caspase 9

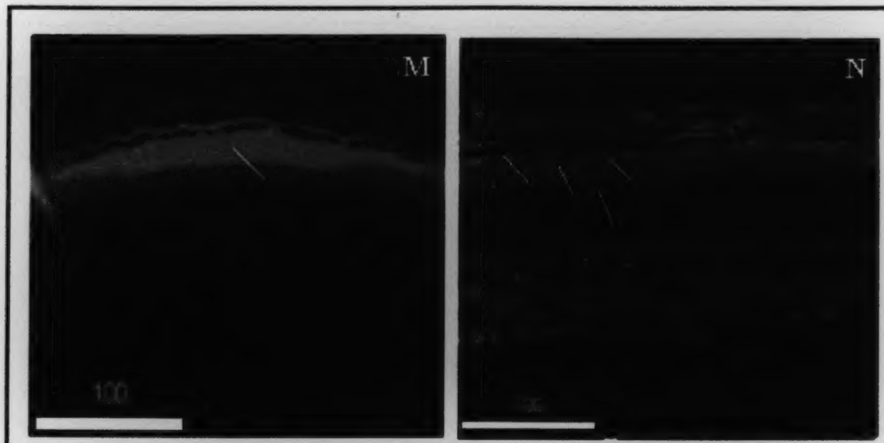

Dark-reared 8 hours light

anti-PARP

O)

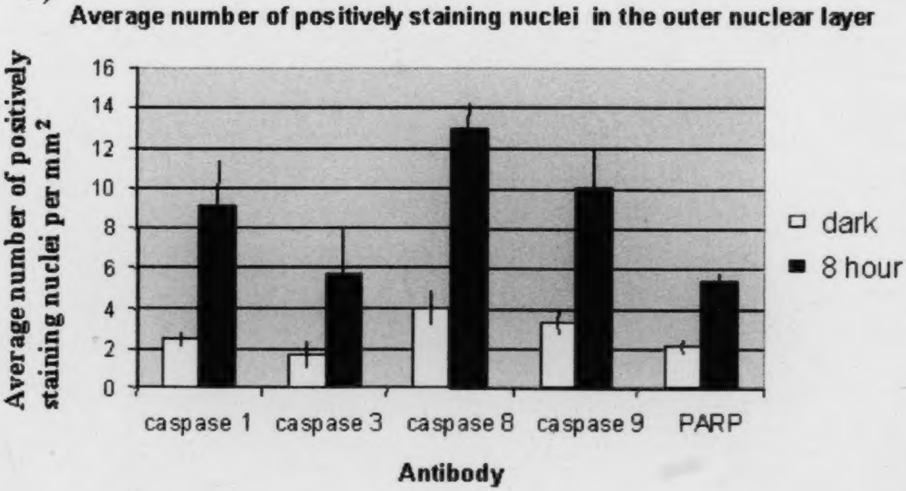

normal rearing conditions in the rat. The 45 kDa caspase 9 peptide, the 44 kDa caspase 8 peptide, and the 34 kDa caspase 3 peptide, were all present in the OS protein lysates (Figure 3.6). As well, the 12 kDa PARP was also visible in the OS lysates. These results were also confirmed using different antibodies from different manufacturers (data not shown).

Increased staining of caspases 1, 3, 8, 9, and PARP was localized to specific photoreceptor cell bodies in the outer nuclear layer (ONL) of the light-treated retina as compared to untreated controls. This suggests a translocation from the cytoplasm to the nucleus following light exposure (Figure 3.5). There was an increase in the number of positively staining photoreceptor cell nuclei per mm^2 in 8 hour light-treated retinae as compared to the dark-reared controls for caspase 1 (dark retina=2.5 +/-0.4, 8 hour=9.1 +/- 2.4), caspase 3 (dark=1.7 +/-0.7, 8 hour=5.7 +/-2.3), caspase 8 (dark=4.0+/-0.9, 8 hour=13 +/- 1.3), caspase 9 (dark=3.3+/-0.6, 8 hour=10.0+/-2.1) and PARP (dark=2.1+/- 0.4, 8 hour=5.4+/-0.4) (Figure 3.5O). In all cases, the differences in number of positively staining photoreceptor nuclei observed in control versus light-treated retinae are statistically significant as determined by t-test analysis ($p=0.05$). Immunofluorescence using antibodies to GFAP, a protein marker used to identify Muller glial cells, was used as a control to demonstrate specificity of staining.

3.D. DISCUSSION

Activation of caspases has been observed in several models of retinal degeneration, including the rd mouse, the RCS rat, lead, calcium and N-methyl-N-nitrosourea-induced photoreceptor cell death in rats, transgenic models of retinal

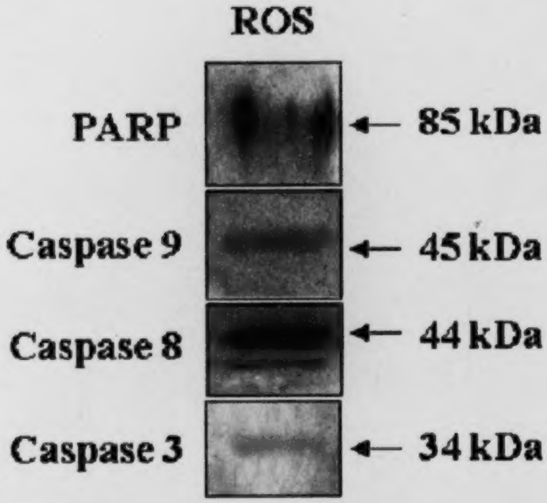

ROS
PARP
85 kDa
Caspase 9
45 kDa
Caspase 8
44 kDa
Caspase 3
34 kDa

Figure 3.6. Western blot analysis of purified outer segments performed to detect the presence of caspases and PARP. Outer segments were isolated from cyclic-reared rat retinae using gradient centrifugation. Protein lysates from the OS were analyzed in duplicate by Western blot analysis for the presence of the processed and unprocessed forms of caspases 3, 8, and 9, as well of for the presence of PARP. In each case, representative Western blots are shown. Specific information regarding the antibodies used is contained in Table 2.3.

degeneration, and oxidative- stress induced death of photoreceptor cells in culture (Lolley *et al*, 1994; Katai *et al*, 1999; He *et al*, 2000; Yoshizawa *et al*, 1999; Liu *et al*, 1999; Krishnamoorthy *et al*, 1999). In addition, over-expression of the anti-apoptotic Bcl-2 has been demonstrated to inhibit caspase activation by preventing cytochrome c release from the mitochondria (Adams *et al*, 1998), and has a protective effect in various animal models of retinal degeneration including LIRD in mice (Chen *et al*, 1996). However, oxidative stress-mediated retinal cellular apoptosis *in vitro* seems to occur through a caspase-independent pathway (Carmody and Cotter, 2000).

Activation of caspase 3 is integral in the death cascade since it leads to the inactivation of PARP, which turn allows low molecular weight DNA fragmentation to occur. Both caspase 1 and caspase 8 are activated by a receptor-mediated pathway that can be initiated by signals originating at the cell surface through the aggregation of Fas or tumor necrosis factors and their respective adapter molecules (Budihardjo *et al*, 1999; Suda and Nagata, 1994). With respect to caspase 9, an internal signal acts at the level of the mitochondria to regulate its activation. This event is mediated through interactions with cytochrome c, Apaf-1 and members of the Bcl-2 family. Whereas caspase 8 can act independently of caspase 9, the two pathways are not necessarily mutually exclusive as caspase 8 can indirectly activate caspase 9 via Bid (Slee *et al*, 1999). Caspase 1 on the other hand is activated independently of caspases 8 and 9. Therefore, even though caspases 8 and 9 could be acting through the same branch of the cascade, the activation of caspase 1 indicates that there are indeed multiple branches of the cascade being activated in LIRD.

The activation of multiple branches of the caspase cascade suggests that photoreceptor cell degeneration in LIRD is the result of multiple signaling events that converge on a common pathway. In addition, activation of receptor-mediated branches of the caspase cascade, via caspase 8 or caspase 1, suggest that apoptosis in LIRD is not just the result of an internal cellular dysfunction mediated by intense light exposure, but that it also involves possible "death signals" from neighboring cells.

Elevated levels of processed caspases 1, 3, 6, 8 and 9 were all observed in the retinae of light-treated rats. These proteolytically processed caspases are likely active since, in each case, we found evidence that known substrates of the caspase in question were also cleaved.

Our results also demonstrate that the levels of the unprocessed forms of caspases 3, 6, 7, 8 and 9, as well as PARP, are also increased after light exposure. Combined, our results suggest that both translational and proteolytic post-translational regulation, underlie the elevation in protein levels observed in the degenerating retina. The increase in levels of unprocessed caspases in the light-exposed retina suggests the retina enters a primed state to undergo further degeneration.

The presence of low levels of the cleaved forms of caspases 3, 6, 8, and 9 in untreated animals suggests that proteins may have a basal housekeeping function in addition to their roles in active cell death. There is a growing body of evidence to suggest that activation of the caspase cascade plays a role in proliferation, cell signaling, and differentiation in a variety of cell types (Schwerk and Schulze-Osthoff, 2003; Fischer *et al*, 2003, Los *et al*, 2001). Selective activation of caspases 3, 6, and 7, and cleavage of specific target molecules occurs as a physiological response in non-apoptotic activation of stimulated lymphocytes (Alam *et al*, 1999). Caspase-mediated cleavage of Huntington protein has been detected in the brains of unaffected human controls (Wellington *et al*, 2002). As well, the up-regulation and activation of caspase 3 in non-apoptotic diabetic rat dorsal root ganglia has also been reported (Cheng and Zochodne, 2003). It is likely that anti-apoptotic factors such as members of the Bcl-2 family, as well as known inhibitors of apoptosis proteins (IAPs) are present to prevent basal levels of activated caspases from driving the activation of the full cascade, and that multiple signals are required for a cell to proceed fully into the apoptosis process (Miller, 1999). This would provide a fail-safe mechanism that would serve to prevent full-scale activation of caspases in non-apoptotic tissues, while still allowing non-death related roles in these tissues.

Aside from the requirements for multiple "death-promoting" signals for the full-scale activation of the caspase cascade, several other regulatory mechanisms of caspases have also been suggested. For example, there may be a difference in cellular targets in non-apoptotic versus apoptotic cells (Fischer *et al*, 2003). In addition, the localization of activated caspases, or potential substrates within a cell may differ between apoptotic and non-apoptotic cells. For example, the localization of caspases to the outer segments of the normal retinae may provide a mechanism to help regulate the levels of key proteins involved in phototransduction. Bioinformatic sequence analysis of OS proteins involved in the phototransduction cascade suggests that several proteins involved in this process may be targeted by caspases, as rodent and human orthologs contain conserved potential caspase cleavage sites (data not shown). These include the rat, mouse and human orthologs for retinal G-coupled receptor opsin, alpha transducin, guanylate cyclase 2a, melanopsin, IRBP, rod phosphodiesterase (PDE) 6 alpha, beta and gamma, and cone PDE alpha and gamma. In addition, localization to the inner segment would provide a means to regulate proteins involved in cellular metabolism. This is supported by the finding that the caspase cascade plays a role in proliferation, cell signaling, and differentiation (Schwerk and Schulze-Osthoff, 2003; Fischer *et al*, 2003, Los *et al*, 2001) necessitating the cytoplasmic localization of these proteins.

The translocation of activated caspases 3 and 9, as well as caspases 1 and 8 (processed and unprocessed forms) to the ONL during LIRD may be a mechanism of switching the non-apoptotic function of the activated caspases to an apoptotic role. Translocation to the nucleus following the phototoxic signal would allow the activated caspases to target the DNA repair machinery, including PARP, leading to DNA fragmentation. The presence of DNA fragmentation in the green light-treated photoreceptor cell has been demonstrated previously through gel electrophoresis as well as TUNEL staining by other groups (Abler *et al*, 1996; Shahinfar *et al*, 1991).

Another mechanism through which the apoptotic decision could be mediated in LIRD would be through the regulation of gene expression. Translocation to the nucleus during LIRD would allow caspase-mediated proteolysis of transcription factors or other components of the transcriptional machinery, facilitating changes in gene expression. This appears to be occurring in LIRD as changes in photoreceptor gene expression (opsin, IRBP, arrestin and recoverin) coincide with the translocation of activated caspases to the ONL in the light-treated retina.

The significant increase in the number of photoreceptor cell nuclei in the ONL staining positively for the members of the caspase cascade, as well as cleaved PARP following light treatment suggests that their activation is important in mediating the transition from a normal to an apoptotic cell. This is supported by the recent findings in the blue light-treated retina where functionally active caspase 3 was localized to the ONL during LIRD (Wu *et al*, 2002). This group also demonstrated the same intense staining in the outer segments that we observed. Although this group attributed this to non-specific staining, the fact that this pattern was also observed in our study using different antibodies suggest that the staining may be specific. As the antibodies were raised against different target peptides [full length caspase molecules (caspase 8) and N terminal or C terminal peptide fragments (caspases 1, 3, 9 and PARP], it is unlikely that all antibodies would cross-react with non-specific epitope to give the same staining pattern. As different carrier molecules were used in the preparation of the antibodies, it is unlikely that the antibodies are reacting to a peptide found in the carriers. This and the fact that the same staining pattern was observed for all caspase antibodies, but not with the GFAP antibody, nor with the no primary and no secondary antibody controls, suggests that a cytoplasmic localization may be an intrinsic feature of activated caspases and may be of functional significance. In addition, the presence of caspases in purified OS lysates from cyclic-reared rats further supports the immunohistochemical localization of caspases to the OS. Further studies, including the use of pre-immune serum or blocking peptide controls during immunohistochemistry, or immuno-affinity columns to help identify potential outer segment targets would provide further evidence of specificity.

The nuclear staining of PARP to the ONL is expected in light of its role in DNA repair, transcriptional regulation and chromatin structure (Skaper, 2003). The localization of PARP outside of the nucleus, exemplified by the staining in the inner and outer segments shown in this study, though unexpected, is not without precedent. Recent studies have localized PARP to the neuronal nuclei, the cytoplasm, as well as the proximal neurons of diabetic rat neurons of the dorsal root ganglia (Cheng and Zochodne, 2003). The cytoplasmic staining of PARP can be attributed to a role for PARP in mitochondrial DNA repair in the mitochondria of rat fibroblasts and neuronal cell cultures (Du *et al*, 2003). Du *et al* demonstrated that low basal levels of activated PARP provides a survival role in the repair of nuclear and mitochondria DNA damage, while large scale activation of PARP in response to oxidative stress or excitotoxicity leads to NAD+ depletion, loss of mitochondrial transmembrane potential, and apoptosis due to energy deficiency. This group also demonstrated that the levels of PARP activity in the mitochondria were significantly higher than the levels in the nucleus. PARP also plays an important role in mitochondrial-mediated induction of apoptosis by facilitating the translocation of apoptosis inducing factor (AIF) from the mitochondria to the nucleus (Yu *et al*, 2002). More proximal cellular roles of PARP are also possible as other members of the poly(ADP-ribosylation) family have been linked to many cellular events, ranging from cell signaling and metabolism, regulation of the cytoskeleton, and protein:protein interactions (Corda and DiGirolamo, 2003). Poly(ADP) ribosylation is also an important regulator of vesicle transport and exocytosis (Gasman *et al* 2003; Stamnes, 2002), events which occur at high levels in the OS of the retina. In light of this, it is possible that the co-localization of PARP and the caspases to the ONL, IS and OS of the photoreceptor cells is partially due to the regulatory role of the caspases on PARP. In control retina, low levels of PARP in the mitochondria and nucleus, facilitating DNA repair, could be kept in check by the inactivation of PARP by low level caspase activation. Following light damage, upregulation of PARP in the mitochondria could lead to mitochondrial dysfunction and the induction of apoptosis. The subsequent activation of the caspases could then inactivate PARP, resulting in an inability to repair the increasing levels of DNA damage within the cell, facilitating DNA fragmentation and cell death.

Our findings of caspase activation in photoreceptor cell loss in LIRD contrast with those found by other groups reporting an absence of caspase 3 activation in the mouse light-treated retina. Grimm *et al* (2000) reported an upregulation of caspase 1 mRNA in both pigmented and albino mice, as well as in pigmented c-fos knockout mice, while finding no upregulation of caspase 3 mRNA. Although these results suggest that there is no transcriptional control of caspase 3 mRNA in the light-treated mouse retina, this study does not address changes in protein levels or the possibility of proteolytic activation of the caspases. Similarly, reports by Donovan *et al* (2001, 2002) failed to demonstrate the activation of caspase 3, or the cleavage of PARP in mice treated with intense white light for 2 hours followed by 0, 6, 14, or 24 hour dark recovery periods. It is likely that the use of extremely intense white light (5000 lux) induces retinal cell loss through a different mechanism than that induced by the moderate intensity light (1200 lux) used in the present study. Previous studies have found that the intensity of light differentially affects the rate and extent of photoreceptor cell loss (Noell *et al*, 1966). There may also be a species difference involved, as all studies published to date report caspase-dependent mechanisms underlying retinal cell death in the rat (Chen *et al*, 2001; Barber *et al*, 2001; Singh *et al*, 2001; Yoshizawa *et al*, 2000; He *et al*, 2000).

Therefore, in light of these findings and those recently described in the blue-light treated retina, we suggest that there may be a common step in the progression from a normal to a degenerate photoreceptor cell in LIRD in rats. Although different wavelengths of light are known to affect different targets within the retina (Noell *et al*, 1966), it is possible that either the blue or green light target may culminate in a common step, the functional activation of various members of the caspase cascade within the rat photoreceptor cell.

Chapter 4

Identification and bioinformatic characterization of differentially expressed LIRD genes.

Contributors:

Dr. Daniel Organisciak, Ruth Darrow, Linda Barsalou: rat retinal tissues

Pat Murray, Lisa Ostafichuk (MBSU): automated sequencing

Micah Chrenek: technical assistance for manual sequencing

Rhonda Kelln: opsin northern blot analysis

Ruby Grewal: arrestin northern blot analysis

4.A. INTRODUCTION

Retinitis pigmentosa and macular degeneration are the result of multi-factorial interactions involving both genetic and environmental factors (Wilson *et al*, 2002). This has also been shown to be the case in rodent models of photoreceptor cell loss. For example, the response to intense light exposure varies significantly between rat and mouse (La Vail *et al*, 1987; Keller *et al*, 2001), and between different mouse strains (LaVail *et al*, 1987; Wenzel *et al*, 2001a; 2003; Danciger *et al*, 2003). Even within a particular transgenic strain there is significant variability in phototoxic sensitivity between littermates (Hao *et al*, 2002; Vaughan *et al*, 2003). Therefore, rather than focusing on a single gene, it is important to understand the global profile of gene expression that determines the physiological state of a cell. Changes in the gene expression regime of a cell leads to changes in phenotype, cell identity, function and morphology, and in extreme cases, to cellular dysfunction, and disease. Changes in gene expression are also important in the progression of apoptotic cell death (Bursch *et al*, 1990). Global inhibition of transcription and/or translation can inhibit apoptotic cell death, due to the requirement for de novo mRNA and protein synthesis (Yonish-Rouach *et al*, 1995; Naora *et al*, 1995).

Although extensive research has been performed to study the molecular mechanisms involved in light-induced retinal degeneration (LIRD) in rats, a relatively small number of key players have been identified. Members of the phototransduction cascade such as rhodopsin, arrestin, rhodopsin kinase, and transducin have been shown to be differentially expressed during LIRD (Organisciak *et al*, 1991; Farber *et al*, 1991). Transcriptional regulators such as AP-1 and NFκB have also been linked to differential gene expression in light-treated retinae (for review see Remé *et al*, 1998). Work in our laboratory has demonstrated that members of the ribosomal binding protein family, involved in gene expression at the translational level, are differentially expressed during LIRD (Stepczynski, 2001; Grewal *et al*, 2004). In addition, our lab and others have shown that key stress response proteins, such as HO-1, SOD, the crystallin family of chaperones, and various heat shock proteins are also differentially expressed during LIRD (MacDonald, 2003; Kutty *et al*, 1995; Sakaguchi *et al*, 2003). Though individual proteins have been studied in detail, little is known about the overall global molecular environment.

The work described here represents a comparative approach to analyze the difference in molecular environments between a normal and light-treated apoptotic retina in wild-type rats. Construction and screening of a light-treated retinal cDNA library identified genes differentially expressed during the active execution phase of apoptotic cell death in LIRD. We hypothesize that the differential expression of these genes is important in mediating the abnormal physiological state that occurs in the light-treated retina. Extensive bioinformatic analysis provides insight into the identity, expression profiles, and functions of these genes. Our results suggest that the response to intense light exposure in LIRD involves global changes in the expression of many widely expressed genes. Therefore, photoreceptor cell loss in LIRD may result from global cellular dysfunction rather than a dysfunction involving photoreceptor or retinal cell-specific pathways.

4.B. RESULTS

4.B-1. Construction and preliminary characterization of the 8-hour execution phase cDNA library

Using poly(A+) RNA isolated from 8-hour light-treated retinae, a cDNA library was constructed that represented genes expressed during the execution phase of cell death in LIRD. This library was constructed from approximately 400 ng of high quality poly(A+) RNA (extracted from approximately 95 μg of total RNA). From this, approximately 150 ng of cDNA was produced using the Stratagene Lambda ZAP cDNA Synthesis System. Following size fractionation and packaging into a lambda UNI-ZAP XR vector, the titer of the resulting cDNA library was determined. The titer was calculated to be approximately 370 pfu/μl, suggesting that the library contained 1.85 million clones.

To ensure that the phage particles produced during the library synthesis step contained inserts of sufficient size to warrant further characterization of the library, 50 random plaques were isolated, and the inserts were amplified by PCR using vector specific T7 and T3 primers. The average insert size was determined to be approximately 2.2 kb.

4.B-2. Primary screening of the execution phase cDNA library

The execution phase cDNA library was plated to a density of approximately 400 pfu/plate on NZY media. Duplicate plaque lifts were hybridized with triple labeled (α-^{32}P-dCTP, -dATP, and -dGTP) total cDNA population probes produced from mRNA isolated from either dark-reared control retinae or 8-hour light treated retinae.

Approximately 2000 (6.7%) of the 30,000 plaques screened contained inserts that appeared to be differentially expressed. These were isolated and placed in SM buffer. A sample plate from the differential screen, is shown in Figure 4.1, with representative of control specific, control enriched, 8 hour specific, 8 hour enriched, and equally expressed clones. Specific clones represent those that show hybridization with only the control or 8 hour cDNA probes, while enriched clones show hybridization with both probes, but hybridize more strongly with one probe versus the other.

4.B-3. Secondary and tertiary screening of the putative differentially expressed clones

Inserts from phage containing putative differentially expressed cDNAs were amplified using vector-specific T7 and T3 primers, and products resolved in duplicate by gel electrophoresis. The DNA was transferred to nylon membranes by Southern blotting. Membranes were screened as indicated for the primary screen and differentially expressed cDNAs were identified. Approximately 1600 (5.3%) clones survived the secondary screen and were further analyzed. Examples of the secondary screening results are illustrated in Figure 4.2.

PCR amplification of the phage inserts from the secondary screen revealed several distinct products in many of the isolated plaques, indicating that the plaques were derived from several different phage particles. The plaques therefore underwent tertiary screening in order to isolate individual clones. Each original plaque was re-plated on individual plates, and 6 different plaques were isolated from each plate. The inserts were amplified by PCR, and the amplified products were resolved by duplicate gel

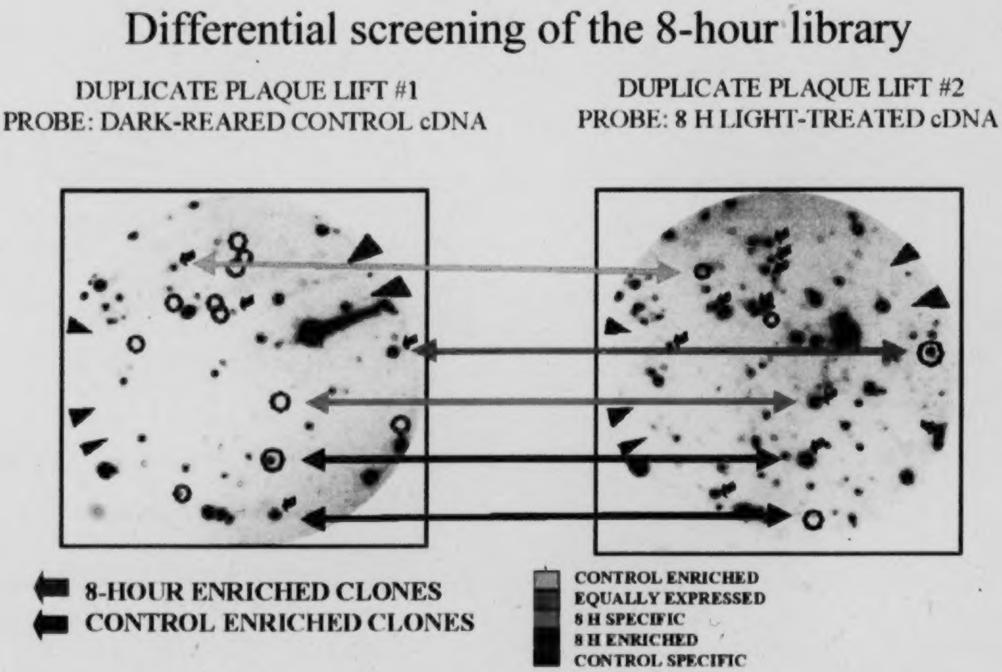
Differential screening of the 8-hour library
DUPLICATE PLAQUE LIFT #1
PROBE: DARK-REARED CONTROL cDNA
DUPLICATE PLAQUE LIFT #2
PROBE: 8 H LIGHT-TREATED cDNA
8-HOUR ENRICHED CLONES
CONTROL ENRICHED CLONES
CONTROL ENRICHED
EQUALLY EXPRESSED
8 H SPECIFIC
8 H ENRICHED
CONTROL SPECIFIC

Figure 4.1. Representative results from the screening of the 8-hour cDNA library. The 8-hour cDNA library was plated out to an approximate density of 400 pfu/plate. Duplicate plaque lifts were produced and screened with $\alpha^{32}P$-dATP, dGTP and dCTP- labeled total cDNA probe produced from 8-hour or control RNA. Clones identified as either dark or 8-hour enriched, or dark or 8-hour specific were isolated and further characterized (indicated by the green and black circles or single arrows). Examples of control enriched, control specific, 8-hours enriched, 8-hour specific or equally expressed phage are indicated by the colored double arrows.

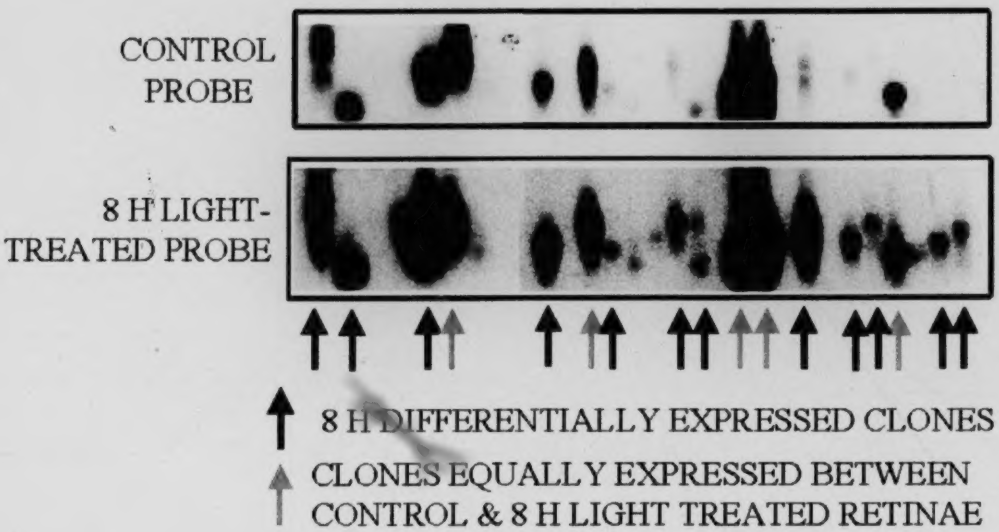
CONTROL PROBE
8 H LIGHT-TREATED PROBE
8 H DIFFERENTIALLY EXPRESSED CLONES
CLONES EQUALLY EXPRESSED BETWEEN CONTROL & 8 H LIGHT TREATED RETINAE

Figure 4.2. Representative results from the secondary screening of differentially expressed clones isolated from the 8-hour library. Differentially expressed clones isolated from the primary screen were amplified by PCR using vector specific primers and were resolved by duplicate gel electrophoresis. Duplicate Southern transfers were performed, and membranes were screened with α^{32}P-dATP, dGTP and dCTP-labeled total cDNA probe produced from 8-hour or control RNA. Clones representing differentially expressed transcripts were isolated, plaque purified and were used in the tertiary screen.

electrophoresis, transferred to membranes and screened as described above, except that total cDNA population probes were synthesized using standard cDNA synthesis protocols, and hence were not amplified. This change was made because of the increased availability of retinal tissue, as well as to ensure that the differential status of the clones was not an artifact of the PCR amplification process. A total of 151 individual clones (0.5% of the 30,000 clones screened initially) appeared to contain inserts derived from differentially expressed genes. The 109 clones that contained insert sizes of 300 bp or greater were selected for further characterization.

4.B-4. Confirmation of the differential status of isolated clones by Northern blot analysis

As the primary and secondary screenings of the library, were performed with PCR amplified total cDNA probes, there was a risk of false positive or negative results because of the possibility of differential amplification efficiencies between templates. Therefore, the expression patterns of several clones was confirmed by Northern blot analysis. Of 49 inserts initially selected, 39 gave usable Northern blot results. In all cases, mRNA levels were normalized to the 18S ribosomal RNA to account for loading differences between lanes. Our Northern blot analysis demonstrate that the majority of the clones isolated are indeed differentially expressed, validating our results from the library screen (Figure 4.3). The 10 clones that failed to produce usable data either generated no signal or generated an excessive background signal.

Figure 4.3. Northern analysis of differentially expressed clones. Northern blot analysis of a selection of differentially expressed clones was performed on total RNA isolated from control and 8-hour light treated rat retinae. Gel-purified PCR products corresponding to the isolated clones were used as probes. Hybridization signals (top dark bands) were compared to the intensity of the 18S rRNA band (bottom light bands) for normalization. Additional Northern blot analysis by Jadwiga Stepczynski (Stepczynski, 2001; Grewal *et al*, 2004), Benjamin MacDonald (MacDonald, 2003), and Chris Carlson (Biology 499 independent research project) confirmed the differential status of clones 107-4, 1307-4, 146-1, 146-4, 185-2, 8-2, and 155-3 (data not shown).

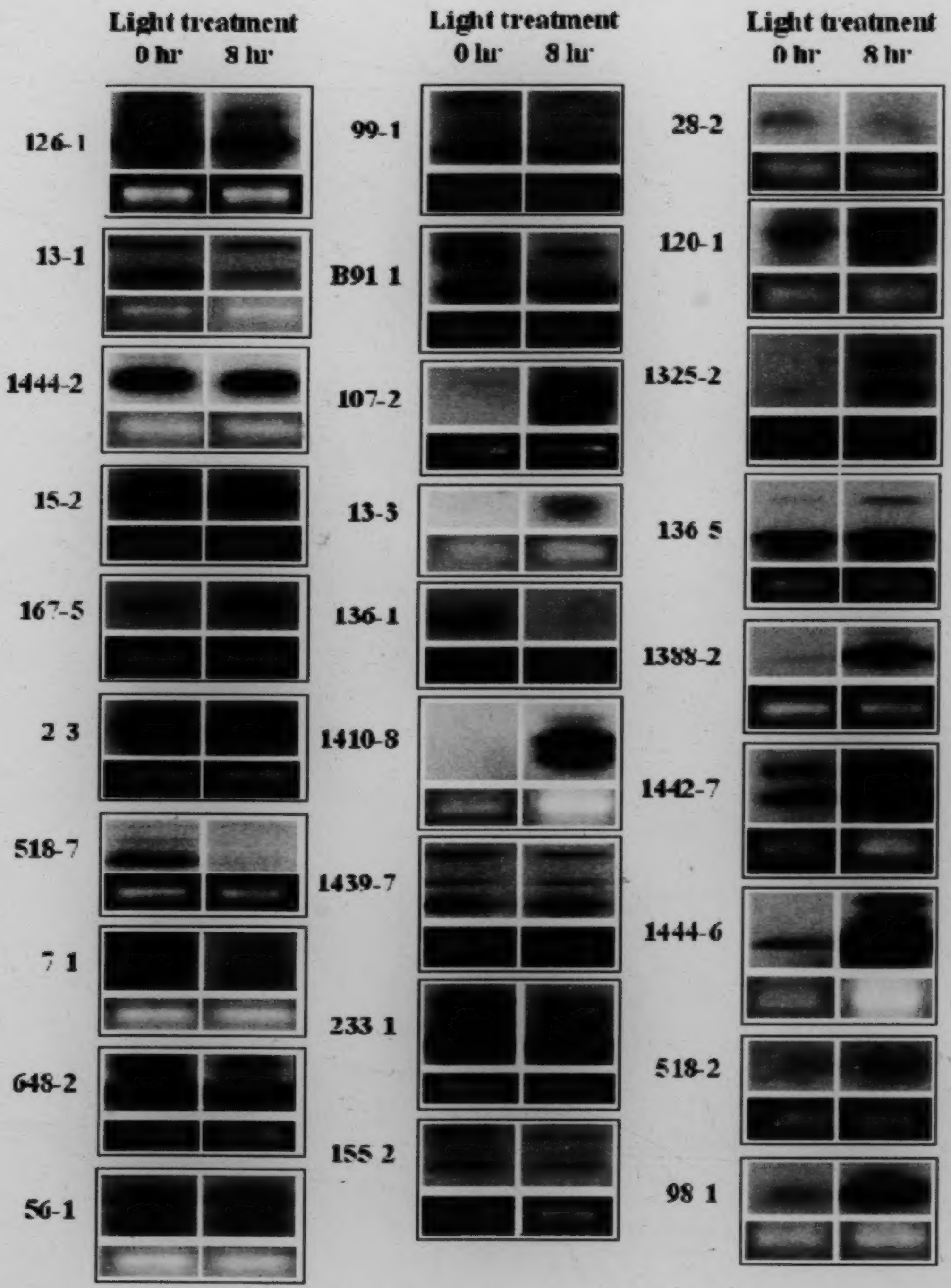
Light treatment
0 hr
8 hr
126-1
13-1
1444-2
15-2
167-5
2 3
518-7
7 1
648-2
56-1
Light treatment
0 hr
8 hr
99-1
B91 1
107-2
13-3
136-1
1410-8
1439-7
233 1
155 2
Light treatment
0 hr
8 hr
28-2
120-1
1325-2
136 5
1388-2
1442-7
1444-6
518-2
98 1

4.B-5. Sequence analysis of the differentially expressed clones isolated from the execution phase library

The identity of the differentially expressed clones was determined by sequence analysis. Of the 109 clones that were sequenced, 82 (75.2%) gave usable sequences. Sequences were determined to be usable if over 100 bp of clear sequence (lacking areas of significant repeats, and in which the nucleotide identity was easily determined, as opposed to denoted by an N [unknown]) was obtained. These sequences were then used for BLAST analysis and the putative clone identity was determined. In some instances the identity of the clone could not be determined because the percent identity was low or limited to short regions. This was due to the quality or limited amount of the sequence obtained for some of the clones, and the limited rat sequence data available at the time of the analysis. Therefore, the "best fit" or "most likely" gene identity was used for further bioinformatic analysis. The criteria used for determining gene identity were at least 75 bp of conserved nucleotide sequence between the available LIRD clone sequence and the sequence available in the NCBI Entrez nucleotide database, with a minimum of 80% identity, and a minimum e-value of 3E-15 (representing a 1/3 X 10^{15} chance that the alignments occurred by chance).

Sequence analysis suggested that 15.9% (13/82) of the sequences represented novel clones with less than 75 bp of sequence similarity to sequences available in the NCBI database. A total of 56.1% (46/82) of the sequences represented known rat sequences, while 28.0% (23/82) represented rat sequences with homology to sequences identified in other species. The results of the sequence analysis are summarized in Table 4.1. Five genes were identified more than once. These include clones B34-1 and B34-5

Table 4.1. Sequence analysis of clones differentially expressed between 8-hour retinae and dark-reared control. Sequencing of purified PCR products corresponding to the isolated differentially expressed clones was performed by either manual or automated sequencing. Sequences obtained were analyzed by BLAST analysis, and the putative gene identities were recorded. Clones with less than 75 bp of sequence similarity to sequences available in the NCBI database were considered unique.

Clone #	Identity	Score	GenBank Accession #	E-value	Identities		Date	Amt. Seq.	Northern confirmation?
107-2	rat similar to GS3955 protein	260	27717062	6.00E-64	133/134	M	Nov-98	230	Yes
	mouse TRB-2	234	20072067	4.00E-59	128/130				
107-4	rat ribosomal protein L5	149	gb M17419 RATRPL5	2.00E-34	149/163 91%	M	Nov-98	171	Yes (JS)
136-1	rat aldolase C	936	emb X06984 RNALDCR1	0	515/535 96%	A	Mar-99	600	Yes
136-5	unique (human KIAA0044)	86	dbj D26445 HUMORFY	3.00E-15	79/88 90%	M	Nov-98	207	Yes
155-2	mouse ubiquitin conjugating enzyme UBCM2	993	emb X92664 MMUBCM2	0	584/611 95%	A	Mar-99	700	Yes
	rat heterogeneous nuclear ribonucleoproteins methyltransferase-like 2 (Hrmt1l2)	926	13242254	0	509/523				
155-3	rat guanine nucleotide releasing protein (Mss4)	198	S29714	3.00E-49	100/100 100%	A	Mar-99	260	Yes
155-7	mouse EcDNA1 and EcDNA4 - RNA binding protein	587	gb L17076 MUSNOVEL	e-165	432/479 90%	A	Mar-99	500	Yes
	mouse Merc =RNA binding protein	571	gb S72641	e-161	430/479 89%				
165-8	rat similar to tousled-like kinase 2, serine/threonine kinase	257	27669660	4.00E-66	142/145	M	Mar-99	225	Yes?
	mouse tousled-like kinase (mtt1)	194	gb AF045253 AF045253	5.00E-48	136/146 93%				
186-2	rat ribosomal binding protein S16	975	emb X17665 RRRPS16	0	522/529 98%	A	Mar-99	550	Yes (JS)
233-1	mouse rhodopsin	295	gb M55171 MUSOPS	6.00E-79	252/258 97%	A	Mar-99	540	Yes (RR)
518-2	mouse angio-associated migratory protein	283	21594730	6.00E-74	228/247	M	Nov-98	269	Yes
	human angio-associated migratory cell protein (AAMP)	176	gb M95627 HUMAAMP1X	1.00E-42	113/121 93%				
518-7	rat 33-kDa phototransducing protein	823	gb M33530 RAT33DPPT	0	479/496 96%	A	Mar-99	700	Yes?
633-5	unique (mouse major histocompatibility complex region NG27, NADH oxidoreductase, NG29, KIFC1, Fas-binding protein, BING1, tapasin, RalGDS-like, KE2, BING4, beta 1,3-galactosyl transferase, and RPS18 genes	56	gb AF110520 MMHC425018	2.00E-05	44/47 93%	M	Nov-98	100	Yes
633-6	mouse RIKEN cDNA C530025K05 gene	337	26523349	1.00E-89	344/396	A	Mar-99	450	Yes
648-2	unique (human elongation factor-1 gamma	48	emb Z11531 HSEF1GMR	6.00E-04	39/44 88%	M	Nov-98		Yes
648-4	rat mitochondrial cytochrome c oxidase I	803	gb M27315 RATMTCYTOC	0	421/429 98%	A	Mar-99	450	No
			emb X14848.1 CAA32966						
648-6	rat NADH subunit 4L	825	emb X14848 MIRNXX	0	432/440 98%	A	Mar-99	450	Yes
703-1	rat X- chromosome linked phosphoglycerate kinase	1047	gb M31788 RATPGKXL	0	623/652 95%	A	Mar-99	700	Yes
709-3	mouse similar to DEAD/H box polypeptide 26	476	18088138	e-131	337/367 (91%)				No
902-4	rat ubiquitin and ribosomal protein S27a	460	emb X81839 RNUBIS27A	e-127	234/235 99%	A	Mar-99	600	No?
1307-4	rat ribosomal protein S10	944	emb X13549 RNRPS10R	0	532/546 97%	A	Mar-99	600	Yes (JS)
1325-2	mouse RIKEN cDNA 1210001E11 gene	759	15080581	0	461/486 (94%)	A	Mar-99	600	Yes
	human splicing factor SPp55-3	567	gb U30829 HSU30829	e-159	439/489 89%				
1325-3	human splicing factor SPp55-4	731	gb U30883 HSU30883	e-159	439/489 89%	A	Mar-99	500	No
1325-8	human splicing factor SPp55-5		gb U30883 HSU30884	e-159	439/489 89%	A	Mar-99	700	No
1388-2	rat 3-hydroxy-3-methylglutaryl CoA lyase	307	emb Y10054 RN3HGMCL	5.00E-82	161/163 98%	M	Nov-98	220	Yes
1410-8	rat Cbp/p300-interacting transactivator with Glu/Asp-rich carboxy-terminal domain 2 (Cited2) mRNA	607	16758611	e-171	306/306 (100%)	A	Mar-99	330	Yes
	mouse mrg-1	480	emb Y15163 MMY15163	e-133	289/302 95%				
1439-3	rat rhodopsin	761	emb Z46957 RNOPS	0	383/385	A	Mar-99	400	Yes
1439-7	rat rhodopsin	361	emb Z46957 RNOPS	4.00E-96	204/209 97%	M	Nov-98	210	Yes
1442-1	rat polyubiquitin (four repetitive ubiquitins in tandem)	896	djb D16554 RATPOLYU	0	464/475 97%	A	Mar-99	600	No
1442-7	rat polyubiquitin (four repetitive ubiquitins in tandem)	398	dbj D16554 RATPOLYU	e-109	210/212 99%	M	Nov-98	263	No
1442-8	Rat similar to coatomer protein complex, subunit gamma 1, coat protein gamma-cop mRNA	818	27712395	0.00E+00	467/486 (96%)	A	Mar-99	500	No
1444-2	mouse ATF4 (CREB, cAMP response element binding protein)	341	dbj AB012277 AB012277	3.00E-92	208/220 94%	M	Nov-98	300	Yes
1444-5	rat retinal protein (RRG4)	1033	gb U40999 RNU40999	0	673/695 97%	A	Mar-99	600	Yes

Clone #	Identity	Score	GenBank Accession #	E-value	Identities		Date	Amt. Seq.	Northern confirmation?
1497-3	rat ubiquitin ligase (Nedd4)	426	gb U60842 RNU60842	e-118	266/283 96%	M	Nov-98	322	Yes
1-2	human eukaryotic translation elongation factor 1 delta (EEF1D)	317	ref NM 001960.1 EEF1D	2.00E-84	382/458 83%	A	Dec-99	560	No
2-3	rat similar to chaperonin subunit 4 (delta), TCP-1 delta mRNA	706	27697896	0	399/417 (95%)	A	Dec-99	500	Yes
	Mouse CcTd (chaperonin containing TCP delta subunit	315	emb Z31554 MMCCTDE	9.00E-84	178/186 95%				
7-1	rat clone RP31-153J8 strain Brown Norway sequence	198	cc	5.00E-48	162/184 (88%)	A	Dec-99	350	Yes
8-2	rat B2 crystallin	884	emb X16072 RNCRYBB2	0	551/586 94%	A	Dec-99	600	Yes [illegible]
11-1	mouse unconventional myosin 15	95.6	gb AF144093.1 AF144093	2.00E-17	95/111 85%	A	Dec-99	600	No
13-1	rat clone BB1.4.1 unknown Glu-Pro dipeptide repeat protein mRNA	145	gb U40628 RNU40628	1.00E-32	73/73 100%	A	Dec-99	500	Yes
13-3	Rat mitochondrial adenine nulcotide translocator 2	496	gi 399694 dbj D12771.1 RATANT2	e-136	252/253 99%	A	Dec-99	320	Yes
16-2	rat protein-arginine methyltransferase	850	gb U60882 RNU60882	0	471/486 97%	A	Dec-99	600	Yes
20-2	mouse RIKEN clone, weakly similar to PUTATIVE DIPHTHINE SYNTHASE, 2410012M04 cDNA	517	NM_027193.2	0	499/522 93%	A	Dec-99	600	Yes
	human CGI-30 protein		gb AF132964.1 AF132964	e-144	364/400 91%				
32-1	rat synuclein, gamma	868	emb X86789 RNSDSYNGE	0	433/460m92 %	A	Dec-99	700	No
39-6	rat beta prime COP	669	gb AF002705 AF002705	e-166	358/380 94%	A	Dec-99	700	No
49-1	rat cytochrome oxidase VIa	442	emb X72757 RNCOX6A	e-122	223/223 100%	A	Dec-99	300	No
56-1	mouse retinol dehydrogenase II mRNA	188	17390608	1.00E-44	154/174 (88%)	A	Dec-99	200	No
	rat LOC299161	327	27688187	2.00E-86	165/165 (100%)				
63-6	mouse rhoC (ras homolog gene family, member C, ras homolog 9	690	emb X80638 MMRHOCR	0	516/573 90%	A	Dec-99	650	No
66-2	rat LOC299696	932	27717826	0	623/643 (96%)	A	Dec-99	700	No
98-1	rat guanylate cyclase activating protein 1 (GCAP1)	746	27681846	0	397/402 (98%)	A	Dec-99	420	Yes
99-1	mouse Psme3 gene for PA28 gamma subunit - proteosome subunit	238	dbj AB007139 AB007139	7.00E-61	207/237 87%			330	Yes
99-2	rat similar to TATA box binding protein -like protein (TATA box binding protein related factor 2, STUD protein)	900	27729632	0	499/517 (96%)	A	Dec-99	700	No
102-3	unique					A	Dec-99	310	No
117-1	rat similar to Tubulin-specific chaperone B (Tubulin folding cofactor B, Cytoskeleton-associated protein CKAP1)	575	27731049	e-161	309/316 (97%)	A	Dec-99	330	No
120-1	rat delta-4-3-ketosteroid 5-beta-reductase	172	dbj D17309 RATK95BR	6.00E-41	112/121 92%	A	Dec-99	400	Yes
126-1	rat brain hexokinase	229	gb J04526 RATHEXOKIN	7.00E-58	146/156 93%	A	Dec-99	170	No
130-2	rat erythrocyte protein band 4.1-like 1 (Epb4.1l1) transcript variant 1	326	25742684	7.00E-86	172/176 (97%)	A	Dec-99	300	No
146-1	rat ribosomal protein L4	1043	emb X82180 RNL4	0	591/612 96%	A	Dec-99	670	Yes (JS)
146-4	rat ribosomal protein L4	916	emb X82180 RNL6	0	605/619 97%	A	Dec-99	600	Yes (JS)
703-6	mouse MAP1B protein	464	gb AF115776.1 AF115776	e-129	331/361 91%	A	Dec-99	440	No
B7-4	rat GRIFFIN	777	gb AF082160.1 AF082160	0	406/411 98%	A	Dec-99	600	No
B29-1	mouse RIKEN clone, suppressor of bimD6 homolog	56	12836166	8.00E-06	42/48 (87%)	A	Dec-99	620	No
B33-1	rat MYR1 mRNA for myosin I heavy chain	950	emb X68199 RNMYR1A	0	518/531 97%	A	Dec-99	680	No
B33-2	rat triosephosphate isomerase	1046	gb L36250 RATTRIS	0	578/594 96%	A	Dec-99	600	No
B91-1	rat similar to poly glutamine tract binding protein	1090	27731048	e-161	308/316 (97%)	A	Dec-99	590	Yes
B11-7	mouse RIKEN clone 5830418K08	168	26892608	9.00E-39	216/264 (81%)	A	Dec-99	600	No
B26-3	mouse RIKEN cDNA 2610034F16	281	29166790	4.00E-73	199/215 (92%)	A	Dec-99	270	No
102-4	unique					A	Dec-99	300	No
102-6	similar to NADH:ubiquinone oxidoreductase B15 subunit	441	XM_213819	6.00 E-16	92/136	A	Dec-99	300	No
119-6	unique	44.1	gi 10636814 AF204176.2	0.078	22/22 100%	A	Sep-00	480	No
123-3	Mouse upregulated during skeletal muscle growth 4 (Usmg4)	323	gi 14010868 NM_031401.1	6.00E-86	292/316 92%	A	Sep-00	650	No
126-4	Mus musculus adult male brain cDNA, RIKEN	234	gi 12852209 dbj AK014391.1	2.00E-59	189/212 (89%)	A	Sep-00	270	No
136-2	unique					A	Sep-00	471	No
147-1	Very AT rich unique?					A	Sep-00	620	No
22-3	unique					A	Sep-00	770	No
B33-3	unique					A	Sep-00	820	No
B34-6	Homo sapiens putative integral membrane transporter (LC27)	105	gi13643960 XM_011642.2	4.00E-20	160/199 80%	A	Sep-00	600	No
B34-1	Homo sapiens putative integral membrane transporter (LC27)	212	gi13643960 XM_011642.3	3.00E-52	199/225 88%	A	Sep-00	700	No
63-2	unique							480	No

Clone #	Identity	Score	GenBank Accession #	E-value	Identities		Date	Amt. Seq.	Northern confirmation?
120-5	Rattus norvegicus platelet-activating factor acetylhydrolase alpha 1 subunit (PAF-AH alpha 1)	712	gi 2501886 gb AF016047.1	0	373/379 98%	A	Dec-99	400	No
129-5	Mus musculus integrin alpha V, mRNA	127	gi|29179564 gb BC048857.	3.00E-26	82/88 (93%)	A	Dec-99	480	No
52-1	unique					A	Dec-99	675	No

(representing LOC315047, similar to lysosomal-associated transmembrane protein 4; denoted by B34-1 in further analysis); clones 1439-3, 1439-7 and 233-1 (encoding rhodopsin; denoted by 233-1); clones 146-1 and 146-4 (encoding Rpl4, ribosomal binding protein L4; denoted by 146-1); clones 1325-2, 1325-3 and 1325-8 (representing LOC311612, similar to Sfrs6, splicing factor arginine/serine-rich 6; denoted by 1325-2); and clones 1442-1 and 1442-7 (encoding poly-ubiquitin; denoted by 1442-1). Therefore, of the 82 clones isolated from the library screen, a total of 62 different genes were identified as differentially expressed during LIRD (henceforth denoted as LIRD genes) and were used for further analysis. The remaining 13 clones represented novel genes, with no significant similarity to sequences in the database.

Of the identified, only rhodopsin had been previously shown to be differentially expressed during LIRD (Noell *et al*, 1971a, b; Organisciak *et al*, 1977). The identification of this gene from our library lends some credibility to our results and suggests that the screening process was successful in identifying differentially expressed genes.

4.B-6. Identification of mouse and human orthologs of rat LIRD clones

The full-length nucleotide and protein sequences were determined for the rat LIRD genes using bioinformatic analysis. For further bioinformatic analysis, the full-length rat sequences (designated LIRD genes or proteins) were used, rather than the partial LIRD clone sequences. Genes that were represented by more than one clone from the library screening were treated as one gene for further analysis, and the 13 novel genes that showed no similarity to sequences in the database were not used for further bioinformatic analysis.

Once the full-length rat sequences were established, the NCBI HomoloGene database was analyzed to determine the ortholog identity (including accession numbers), and percent identity between the rat, mouse and human orthologous nucleotide and protein sequences. Gene and protein sequences were available for 59 of the 62 genes identified as LIRD genes. Gene and protein sequences were unavailable for clones 102-5, 129-5 and 7-1. As illustrated in Figure 4.4, rat LIRD genes showed significant homology with their mouse and human orthologs. On average, the rat LIRD genes shared 93.5% identity with their corresponding mouse orthologs at the nucleotide level, and 95.9% identity at the amino acid level. The percent identity between rat and human sequences was lower, with 88.2% identity at the nucleotide level, and 93.4% identity at the amino acid level. Similar results were obtained when comparing mouse and human sequences, with 88.5% identity at the nucleotide level and 93.4% identity at the protein level. Therefore, there is strong sequence conservation between the rat and mouse orthologs, as well as between the rodent and human orthologs. This strong evolutionary conservation between these diverse species suggests that their functions are conserved as well.

4.B-7. Comparison of chromosomal locations of human LIRD gene orthologs to those of known retinal disease genes

As our primary interest was to identify genes potentially involved in photoreceptor cell loss in LIRD, we were interested to see if any of the LIRD genes isolated corresponded to genes known to be associated with human retinal disease. In addition, as genes belonging to common functional groups often cluster within a

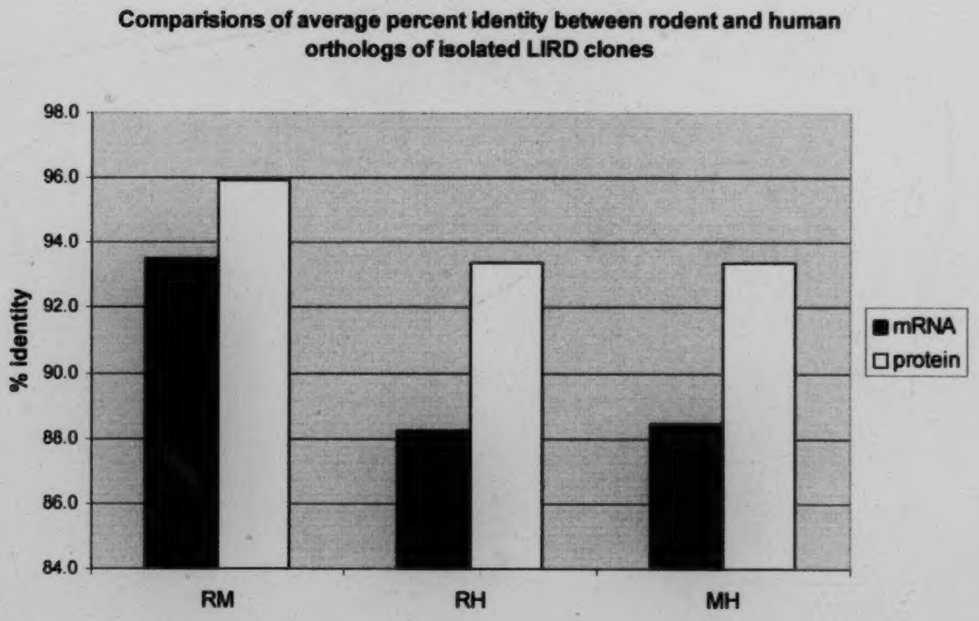

Figure 4.4. Degree of identity between rodent and human orthologs of the isolated LIRD clones. Using the NCBI HomologGene database as well as sequence analysis programs such as NCBI Blast and Clustal W, the percent identity at the nucleotide and protein levels was determined for the LIRD orthologs. Comparisons were made between rat and mouse (RM), rat and human (RH), and human and mouse (MH) nucleotide and protein sequences, and the averages for each category was determined.

particular chromosomal segment (Strachan and Read, 1999; Piatigorsky and Wistow, 1989), we wanted to see if there was any clustering of the LIRD genes on particular chromosomes or chromosomal segments and to determine whether these regions were known to contain human retinal disease genes. (The term retinal disease gene is used here to denote genes in which mutations are known to lead to retinal degeneration in humans).

Using the NCBI Map Viewer and LocusLink databases, the chromosomal locations of the human orthologs of the LIRD genes was determined. Of the 62 LIRD genes analyzed, 54 could be located to a specific chromosomal region. For comparison, we determined the chromosomal locations of the 152 known human retinal disease genes listed in the RetNet database. (The 152 RetNet retinal disease genes include both disease genes with known map locations and gene identities [101/152], as well as those with mapped critical regions where the disease gene has not yet been identified but the approximate chromosomal location is known).

The human X chromosome has the highest number of known retinal disease genes, with 13.2% of the known retinal disease genes mapping to it (Figure 4.5A). 1.7% of all the genes on the X chromosome represent retinal disease genes, as are 1.2% of the genes on chromosome 4, and 0.88% of the genes on chromosomes 6 and 10 (Figure 4.5B). In comparison, 17.1 % of mitochondrial-encoded genes are retinal disease genes.

To determine whether there was any overlap between the positions of known retinal disease genes and the human orthologs of the LIRD genes, we compared the map locations of these two classes of genes. Interestingly, there was a strong correlation between the chromosomal locations of the retinal disease genes and the LIRD homologs (Table 4.2). We found that 85.2% of LIRD orthologs were located in a chromosomal

A)

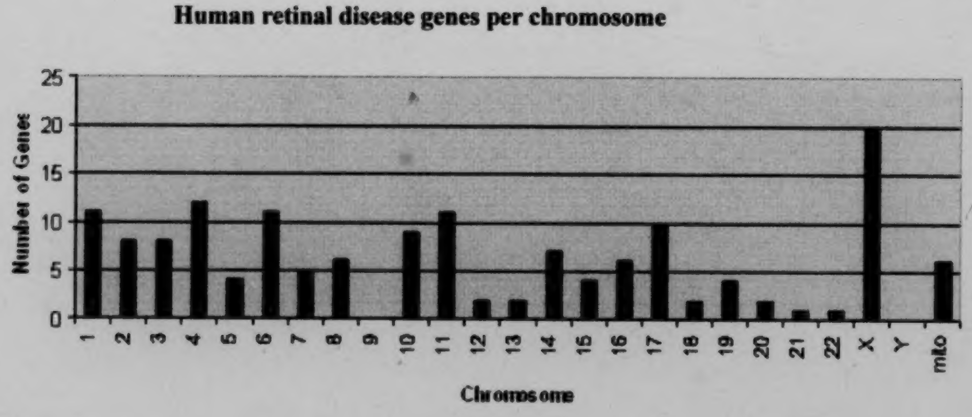

B)

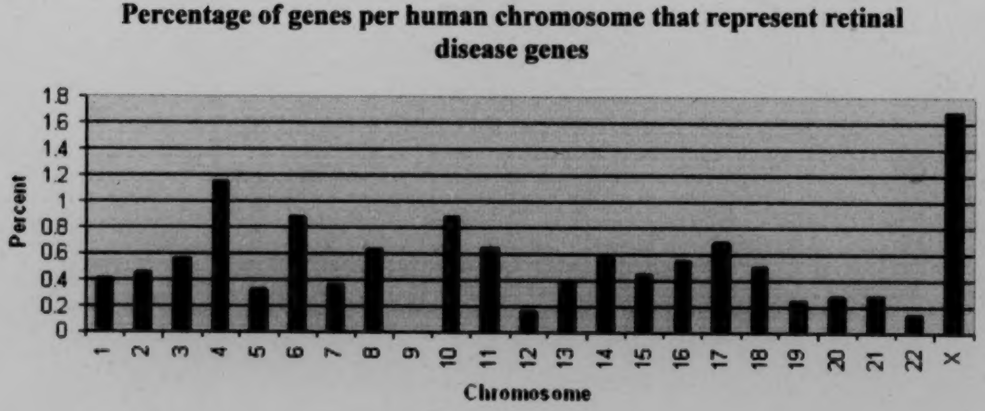

Figure 4.5. Percentage of genes on each human chromosome that represent a retinal disease associated gene. The identities of genes known to cause human retinal disease were determined using the RetNet database. (A) The chromosomal locations of these genes was determined using the NCBI MapViewer and LocusLink databases. (B) The percentage of the genes on each chromosome that represent known retinal disease genes was determined. Because of scaling constraints, the values for the mitochondrial chromosome were not included on the graph. For the gene on the human mitochondrial chromosome, 17.1% represent known retinal disease genes.

Table 4.2. Comparison of the human chromosomal locations of known retinal disease genes with human orthologs of the LIRD genes. Known retinal disease genes were identified using the RetNet database. Chromosomal locations of these genes, and the human LIRD orthologs were determined using the NCBI LocusLink and MapViewer databases. Chromosomal positions were aligned and comparisons were made to determine degree of chromosomal clustering between these two groups of genes. LIRD genes that correspond to known retinal disease genes are indicated in the grey boxes.

Known retinal disease gene	Disease gene map location	LIRD ortholog map location	LIRD clone #	LIRD ortholog
GNAT2	1p13.3	1p13.1	63-6	ARHC: ras homolog gene family, member C, ARH9, RHOC, RHOH9, RhoC, Aplysia ras-related homolog 9, Aplysia RAS-related homolog 9
COL11A1	1p21.1	1p21.2	28-2	CGI-30: CGI-30 protein
ABCA4	1p22.1	1p22.1	107-4	Rpl5 ribosomal protein L5
RPE65	1p31.2			
LCA9	1p36	1p36.1-p35	1388-2	HMGCL: 3-hydroxymethyl-3-methylglutaryl-Coenzyme A lyase (hydroxymethylglutaricaciduria)
CORD8	1q12-q24			
HPRP3	1q21.2			
ARMD1	1q25.3-q31.1	1q25.2	518-7	phosducin, 33kDA phototransducing protein, PHD, MEKA, PhLP, PhLOP
CRB1	1q31.3	1q32-q41	155-3	RABIF: RAB interacting factor, also MSS4, RASGFR3, RASGRF3
AXPC1	1q31-q32			
USH2A	1q41			
ALMS1	2p13.1	2p15	2-3	CCT4: chaperonin containing TCP1, subunit 4 (delta), SRB, Cctd, chaperonin containing t-complex polypeptide 1, delta subunit
EFEMP1	2p16.1	2p16	902-4	RPS27A: ribosomal protein S27a; CEP80, UBA80, UBCEP1, HUBCEP80
RP28	2p16-p11			
		2p25.1	107-2	TRB2 tribbles homolog 2
CNGA3	2q11.2	2q12-q34	B33-1	MYO1B: myosin IB, myr1, myosin-I alpha
MERTK	2q13			
BBS5	2q31	2q32.1	155-2	UBE2E3 ubiquitin-conjugating enzyme E2E 3
CERKL	2q31.2-q32.3	2q35	518-2	AAMP: angio-associated, migratory cell protein
SAG	2q37.1			
SCA7	3p14.1			
GNAT1	3p21.31			
CRV	3p21.3-p21.1			
USH2B	3p24.2-p23			
ARL6	3q11.2	3q21.3	1442-8	Copg1: coatomer protein complex, subunit gamma
RHO	3q22.1	3q21-q24	233-1	RHO: rhodopsin (opsin 2, rod pigment) (retinitis pigmentosa 4, autosomal dominant), RP4, OPN2)
USH3A	3q25.1	3q23	39-5	COPB2: coatomer protein complex, subunit beta 2 (beta prime)
OPA1	3q29			
STGD4	4p			
CNCG	4p12			
PROML1	4p15.32			
WFS1	4p16.1			
PDE6B	4p16.3			
MCDR2	4p16.3-p15.2			
WFS2	4q22-q24			
MTP	4q23			
BBS7	4q27			
LRAT	4q32.1			
RP29	4q32-q34			
CYP4V2	4q35.2			
MCDR3	5p15.33-p13.1	5q13	708-3	MAP1B: microtubule-associated protein 1B,MAP5, FUTSCH
WGN1	5q13-q14			
MASS1	5q14.3			
PDE6A	5q33.1			
BCMAD	6p12.3-q16			
GUCA1A	6p21.1	6p21.1	[illegible]	GUCA1A: guanylate cyclase activator 1A (retina), GCAP, GUCA, GCAP1, GUCA1
RDS	6p21.2	6p21.31	1307-4	(RAT: Rps10: ribosomal protein S10)(MOUSE: 2210402A09Rik: RIKEN cDNA 2210402A09 gene)(HUMAN: RPS10: ribosomal protein S10)
TULP1	6p21.31	12q24.2/ 6p21	48-1	COX6A1: cytochrome c oxidase subunit VIa polypeptide 1, COX6A, COX6AL
LCA5	6q11-q16			
RIMS1	6q13			
ELOVL4	6q14.1			
MCDR1	6q14-q16.2			
RP25	6cen-q15			
PEX7	6q23.3	6q22.1-q22.3	99-2	TBPL1: TBP-like 1,TLF, TLP, STUD, TRF2, MGC:8389, MGC:9620, second TBP of unique DNA, TATA box binding protein-related facter 2

Known retinal disease gene	Disease gene map location	LIRD ortholog map location	LIRD clone #	LIRD ortholog
RCD1	6q25-q26	6q23.3	1410-8	CITED2: Cbp/p300-interacting transactivator, with Glu/Asp-rich carboxy-terminal domain, 2; MRG1, P35SRJ
RP9	7p14.3			
MDDC	7p21-p15			
PEX1	7q21.2			
IMPDH1	7q32.1	7q32-q33	120-1	AKR1D1: aldo-keto reductase family 1, member D1 (delta 4-3-ketosteroid-5-beta-reductase), SRD5B1, 3o5bred, steroid 5-beta-reductase, beta polypeptide 1 (3-oxo-5 beta-steroid delta 4-dehydrogenase beta 1)
OPN1SW	7q32.1	7q34	633-6	DKFZP586F2423: hypothetical protein
CORD9	8p11			
RP1	8q12.1			
TTPA	8q12.3			
PXMP3	8q21.13	8q24.3	1-2	EEF1D: eukaryotic translation elongation factor 1 delta (guanine nucleotide exchange protein, EF-1D
CNGB3	8q21.3			
ROA1	8q21-q22			
PHYH	10p13			
RNANC	10q21	10q22	126-1	HK1: hexokinase 1.
PCDH15	10q21.1	10q23.2-q23.3	32-1	SNCG: synuclein, gamma (breast cancer-specific protein 1), SR, BCSG1, persyn, synoretin
CDH23	10q22.1	10q26	B25-3	PEGASUS: zinc finger protein, subfamily 1A, 5 (Pegasus), ZNFN1A5, zinc finger transcription factor Pegasus
RGR	10q23.1			
RBP4	10q23.33			
PAX2	10q24.31			
OAT	10q26.13			
EVR3	11p13-p12			
USH1C	11p15.1			
TEAD1	11p15.3			
ROM1	11q12.3			
VMD2	11q12.3			
BBS1	11q13			
VRNI	11q13			
LRP5	11q13.2			
MYO7A	11q13.5			
FZD4	11q14.2			
C1QTNF5	11q23.3	11q21	B11-7	LOC283262: hypothetical gene supported by AL833615
		12p13	B33-2	TPI1: triosephosphate isomerase 1, TPI
COL2A1	12q13.11			
		12q24.2/ 6p21	48-1	COX6A1: cytochrome c oxidase subunit VIa polypeptide 1, COX6A, COX6AL
RB1	13q14.2	13q14.12-q14.2	708-3	DDX26: DEAD/H (Asp-Glu-Ala-Asp/His) box polypeptide 26; HDB, DBI-1, DICE1, Notchl2, RNA helicase HDB
RHOK	13q34			
ACHM1	14			
MCDR4	14q			
NRL	14q11.2			
RPGRIP1	14q11.2			
LCA3	14q24	14q24.1	56-1	RDH11: retinol dehydrogenase 11 (all-trans and 9-cis), MDT1, PSDR1, RALR1, ARSDR1, CGI-82, HCBP12, FLJ32633, CGI-82 protein, HCV core-binding protein, prostate short-chain, dehydrogenase reductase 1, androgen-regulated short-chain dehydrogenase/reductase 1
RDH12	14q24.1			
USH1A	14q32	14q32	136-5	PPP2R5C: protein phosphatase 2, regulatory subunit B (B56), gamma isoform,
TTC8	14q32.11			
		15q	1497-3	NEDD4: neural precursor cell expressed, developmentally down-regulated 4

Known retinal disease gene	Disease gene map location	LIRD ortholog map location	LIRD clone #	LIRD ortholog
NR2E3	15q23	15q22	146-1	RPL4: ribosomal protein L4, HRPL4, 60S ribosomal protein L4, homologue of Xenopus ribosomal protein L1
MRST	15q24			
BBS4	15q24.1			
RLBP1	15q26.1			
CLN3	16p11.2			
RP22	16p12.3-p12.1			
ABCC6	16p13.11			
BBS2	16q12.2			
CNGB1	16q13			
CDH3	16q22.1			
CACD	17p13			
GUCY2D	17p13.1			
AIPL1	17p13.2			
PRPF8	17p13.3			
CORD4	17q			
		17p11.2	11-1	MYO15A: myosin XVA, DFNB3, MYO15, unconventional myosin-15
		17p12-p11.2	1442-1	UBB: ubiquitin B, polyubiquitin B
UNC119	17q11.2	17q11.2	1444-6	unc-119 homolog (C. elegans), HRG4, retinal protein 4
		17cen-q12	136-1	aldolase C, fructose-bisphosphate
CA4	17q23.2	17q21	99-1	PSME3: proteasome (prosome, macropain) activator subunit 3 (PA28 gamma; Ki), Ki, 11S regulator complex gamma subunit, activator of multicatalytic protease subunit 3
RGS9	17q24.1	17q23	165-8	Tlk2: tousled-like kinase 2)(HUMAN: TLK2: tousled-like kinase 2
SANS	17q24-q25			
FSCN2	17q25.3			
OPA4	18q12.2-q12.3			
CORD1	18q21.1-q21.3			
R9AP	19q13.12	19q13.1	185-2	(RAT: Rps16: ribosomal protein S16)(MOUSE: similar to ribosomal protein S16)(HUMAN: RPS16: ribosomal protein S16)
CRX	19q13.32	19q13.1	120-5	PAFAH1B3: platelet-activating factor acetylhydrolase, isoform Ib, gamma subunit 29kDa
OPA3	19q13.32	19q13.11-q13.12	117-1	CKAP1: cytoskeleton-associated protein 1, CG22, TBCB
PRP31	19q13.42	19q13.3	15-2	HRMT1L2: HMT1 hnRNP methyltransferase-like 2 (S. cerevisiae), ANM1, HCP1, IR1B4, PRMT1
JAG1	20p12.2			
MKKS	20p12.2			
		20q11.21-q11.23	165-7	RALY RNA binding protein (autoantigenic, hnRNP-associated with lethal yellow)
		20q11.2-q12	130-2	EPB41L1: erythrocyte membrane protein band 4.1 like 1, 4.1N, neuronal protein 4.1
		20q12-q13.1	1325-2	SFRS6: splicing factor, arginine/serine-rich 6; B52, SRP55
USH1E	21q21			
TIMP3	22q12.3	22q11.23	8-2	CRYBB2: crystallin, beta B2, CCA2, CRYB2, CRYB2A
		22q13.1	1444-2	ATF4: activating transcription factor 4 (tax-responsive enhancer element B67, CREB2, TXREB, CREB-2, TAXREB67
CACNA1F	Xp11.23			
RP2	Xp11.23			
NDP	Xp11.3			
PRD	Xp11.3-p11.23			
NYX	Xp11.4			
RPGR	Xp11.4			
OPA2	Xp11.4-p11.2			
COD4	Xp11.4-q13.1			
AIED	Xp11.4-q21			
DMD	Xp21.2-p21.1			
RP6	Xp21.3-p21.2			
RP23	Xp22			
RS1	Xp22.13			

Known retinal disease gene	Disease gene map location	LIRD ortholog map location	LIRD clone #	LIRD ortholog
PGK1	Xq21.1	Xq13	783-1	PGK1: phosphoglycerate kinase 1; PGKA
CHM	Xq21.2	Xp11.23	B91-1	PQBP1: polyglutamine binding protein 1, NPW38, nuclear protein containing WW domain 38 kD
TIMM8A	Xq22.1			
RP24	Xq26-q27	Xq24-q26	13-3	SLC25A5: solute carrier family 25 (mitochondrial carrier; adenine nucleotide translocator), member 5, T2, T3, ANT2, 2F1 adenine nucleotide translocator 2 (fibroblast)
COD2	Xq27			
OPN1LW	Xq28			
OPN1MW	Xq28			
KSS	mitochondrion	mito	648-4	MTCO1: cytochrome c oxidase I;COI
LHON	mitochondrion	mito	648-6	MTND4L: NADH dehydrogenase 4L
MTATP6	mitochondrion			
MTTH	mitochondrion			
MTTL1	mitochondrion			
MTTS2	mitochondrion			

band that had at least one retinal disease gene. It is also interesting to note that only 4 of the 54 human LIRD orthologs with known chromosomal locations (7.4%), represent known retinal disease genes. These include rhodopsin (*RHO*, clone 233-1), mutations in which cause 40% of autosomal dominant retinitis pigmentosa (Dryja *et al*, 1991, RetNet database, September 2004) and phosphoglycerate kinase (*PKG1*, clone 703-1), which is linked to a single case of retinitis pigmentosa (Tonin *et al*, 1993). The other two LIRD orthologs, specifically guanylate cyclase activator 1A (*GUCA1A*, clone 98-1, Downs *et al*, 2001), and the unc-119 homolog HRG4 (*RRG4*, clone 1444-6; Kobayashi, *et al*, 2000), are known to cause autosomal dominant cone-rod dystrophy.

4.B-8. Analysis of LIRD gene expression

Using the NCBI Unigene database, the specific tissue expression patterns were determined for the rat LIRD genes, as well as for the corresponding mouse and human orthologs. Analysis was performed for a variety of neuronal and ocular tissues, as well as non-neuronal, fetal and cancer tissues. These results are shown in Table 4.3.

Though 62 different genes were identified as LIRD genes from the library screen, rat expression data were only available for 46 of these. Analysis of the available expression profiles of these genes shows widespread expression in both neuronal and non-neuronal tissues. Analysis of ocular tissues showed that the highest numbers of genes were expressed in the retinal ganglion cells (38.3%). Only 2 (4.3%) genes demonstrated retina-specific expression: rhodopsin (clone 233-1) and phosducin (clone 518-7). A total of 42.6% of the rat LIRD genes showed expression in the fetal brain, and 53.2% demonstrated expression in the placenta. In addition, 38.3% were identified in rat cancer

Table 4.3. Percentages of clones/orthologs expressed in specific tissues. The specific tissue expression was determined for rat, mouse and human LIRD orthologs. The specific tissue expression in each species was combined to indicate the cross-species specific tissue expression. Expression information derived from the NCBI Unigene database.

Tissue Expression

OCULAR	combined	rat	mouse	human
cornea	18.2	14.9		3.9
eye	89.1	4.3	83.9	39.2
anterior segment	14.5			15.7
iris	36.4			39.2
lens	54.5			50.8
optic nerve	40.0			43.1
retina	94.5	10.6	91.1	82.4
fovea & maculer	49.1			52.9
RGC	38.2	38.3		
RPE and choroid	83.6		46.4	88.4
trabecular meshwork	23.6			25.5
NEURONAL	combined	rat	mouse	human
brain	92.7	55.3	92.7	84.3
cerebellar cortex	16.4			17.6
cerebellum	78.9	10.6	63.6	77.5
corpora quadrigemina	36.4	2.1	36.4	
corpus striatum	12.7	2.1	12.7	
cortex	43.6	19.1	34.5	
dorsal root ganglia	63.6	57.4		33.3
frontal cortex	43.6			47.1
hippocampus	65.5	2.1	34.5	60.8
medulla	60.0	2.1	25.1	43.1
olfactory epithelium	54.5	2.1	50.9	7.8
otic epithelium	63.6	2.1	60.0	39.2
PNS	20.0			21.6
pineal gland	45.5	21.3		39.2
sciatic nerve	29.1			31.4
spinal cord	63.6	4.3	56.4	25.5
sympathetic trunk	50.9	2.1	25.5	41.2
visual cortex	72.7	2.1	72.7	
white matter	32.7			35.3
SKIN, FAT, BONE. MUSCLE	combined	rat	mouse	human
adipose	61.8	27.7	20.0	50.0
bone	56.4	2.1	14.5	52.9
bone marrow	74.5	2.1	54.5	64.7
cartilage	61.8	40.4	1.8	39.2
epidermis	76.4	2.1	61.8	68.6
gingiva	18.9			11.8
larynx	7.3			7.8
melanocyte	56.4			60.8
muscle	63.6	23.4	23.6	60.8
senescent fibroblast	34.5			37.3
synovial membrane	45.5		43.6	17.6
tongue	36.4		29.1	15.7
LYMPHATOC	combined	rat	mouse	human
B-cells	80.0	2.1	40.0	80.4
hematopoietic cells	34.5		34.5	
leukocyte	39.2			41.2
lymph	45.5			49.0
lymph node	80.0		45.5	41.2
lymphocyte	25.5			27.5
macrophage	65.5		34.5	56.9
natural killer cells	41.8		9.1	41.2
spleen	81.8	34.0	60.1	39.2
T cells	43.6		38.2	21.6
RESPIRATORY AND CIRCULATORY	combined	rat	mouse	human
aorta	56.4	2.1	25.5	45.1
blood	40.0		18.9	41.2
blood vessels	29.1			31.4
diaphragm	18.2		18.2	
heart	87.3	44.7	78.2	78.4
lung	87.3	40.9	80.1	90.2
[illegible]	combined	rat	mouse	human
adrenal gland	58.2	2.1	3.6	60.8
breast	89.1	2.1	83.6	82.4
hypothalamus	74.5	31.9	23.6	78.6
lacrimal gland	20.8		5.5	17.6
maxillary gland	40.0		32.7	15.7
pancreas	60.1	6.4	67.3	39.2
pancreatic islet	63.6	6.4		64.7
pituitary gland	72.7	40.9	56.4	60.8
prostate	80.0	59.6		80.4
salivary gland	47.3		47.3	
thymus	83.6	2.1	81.8	39.2
thyroid	56.4	4.3	40.1	35.3
[illegible]	combined	rat	mouse	human
bladder	34.5	2.1	34.5	3.9
bowel	21.8		21.8	
cecum	21.8		21.8	
colon	78.2		52.7	80.4
gall bladder	21.8		3.6	19.6
kidney	87.3	55.3	80.0	80.4
liver	87.3	8.5	67.3	90.2
small intestine	34.5		30.9	7.8
stomach	76.4	2.1	50.9	74.5

Tissue Expression

[illegible]	combined	rat	mouse	human
cervix	56.4			60.8
endometrium	27.3			29.4
epididymis	25.5		16.4	11.8
ovary	80.0	38.3	41.6	64.7
testis	87.3	34.0	81.8	80.4
uterus	80.0	2.1	41.8	76.5
[illegible]	combined	rat	mouse	human
amnion	63.6		40.0	43.1
blastocyst	40.1		40.1	
branchial arches	43.6		43.6	
colon epithelia progenitor cells	25.5		25.5	
cord blood	34.5			37.3
craniofacial tissues	16.4		16.4	
decidual tissue	12.7		12.7	
diencephalon	23.6		23.6	
dissected endoderm	21.8		21.8	
ectoplacental cone	25.5		25.5	
egg	30.9		30.9	
embryo	47.3	21.3	40.1	43.1
body below diaphragm	7.3		7.3	
between diaphragm and neck	47.3		47.3	
limb, maxilla and mandible	38.2		38.2	
embryonic stem cell	85.5		40.1	84.3
embryonic trophoblasts	23.6		60.0	25.5
fetal brain	54.5	47.6		43.1
fetal eye	60.1			74.5
fetal intestines	25.5	25.5		
fetal liver	32.7		16.4	23.5
fetal pancreas	32.7			35.3
fetal spleen	20.0			21.6
fetus	40.1		40.1	
forelimb	18.2		18.2	
gastric epithelial progenitor	14.5		14.5	
gonad	18.9		20.0	
granulocyte-macrophage progenitors	1.8		1.8	
male genital ridge/mesonephros	20.0		20.0	
mesenchymal stem cell	21.8		21.8	
hematopoietic progenitor cells	1.8		1.8	
myeloid progenitors	1.8		1.8	
neuroepithelial cells	52.7			56.9
optic vesicle and lens placode	16.4		16.4	
osteoblast	29.1		29.1	
parthenogenote	21.8		21.8	
pharyngeal arch	5.5			5.9
placenta	83.6	53.2	61.8	76.5
primitive streak	5.5		5.5	
small intestinal epithelial progenitors	30.9		30.9	
Trophoblast	60.0		60.0	
undifferentiated limb	47.3		47.3	
urogenital ridge	12.7		12.7	
umbilical vein	1.8			2.8
[illegible]	combined	rat	mouse	human
embryonal tumor	54.5			50.0
unspecified	78.9	38.3	82.1	
Adrenocarcinoma	81.8			90.2
Carcinoma	81.8			90.2
Hematocarinoma	67.3			72.5
Sarcoma	81.8			90.2
Glailblast	76.4			82.4
Neruoblastoma	76.4			82.4
Retinoblastoma	61.8			66.7

Legend:

▨	0-10%
▨	10-29%
▨	30-49%
▨	50-59%
▨	60-69%
▨	70-79%
▨	80-89%
▨	90-100%

tissues. Therefore, the majority of rat LIRD clones are widely expressed in both adult and fetal tissues, as well as in cancer cells lines and tissues.

To compensate for the limited expression data currently available in the rat, bioinformatic analysis of specific tissue expression was performed in mice. As expected, widespread tissue expression was also observed for the majority of the 55 mouse LIRD orthologs for which expression information was available. Similar to rat, the LIRD genes were expressed in both neuronal and non-neuronal tissues. In ocular tissues, the majority were expressed in the whole eye (83.9%), and the isolated retina (91.1%). Only 1 (1.8%) mouse ortholog was specifically expressed in the retina: rhodopsin (233-1). Crystallin β-b2 (clone 8-2) appeared to be eye-specific, while the phosducin gene (clone 518-7), which was retina-specific in the rat, showed expression in the brain as well as the retina.

As the mouse is a common model system to study developmental processes, more extensive information regarding mouse fetal tissue expression was available than was for the rat. Many of mouse orthologs were expressed in isolated blastocysts (49.1%), pooled fetal tissue (49.1%), embryonic stem (ES) cells (49.1%), and undifferentiated limb (47.3%). There was also a significant number of orthologs expressed in extra-embryonic tissues including the trophoblast (60.0%) and placenta (61.8%). In addition, 82.1% of the mouse orthologs showed expression in cancer tissues, a proportion significantly higher than that observed in rats.

Similar analysis of the 51 human orthologs for which human tissue expression was available demonstrated that 82.4% of the human orthologs were expressed in the retina, 80.4% were expressed in the RPE/choroid, 58.8% were expressed in the lens, and 52.9% were expressed in the fovea/macula. Only 2 (3.9%) of the human orthologs showed ocular specific expression, including rhodopsin (233-2) and phosducin (518-7). Again, human orthologs of the LIRD genes were widely expressed in both neuronal and non-neuronal tissues. In fetal tissues, most orthologs were expressed in the fetal eye (74.5%), ES cells (84.3%) and placenta (76.5%).

The expression of genes in cancer cells has been extensively studied in human cells, significantly more so than in mice and rats. Therefore, a large body of cancer expression information was available for the human orthologs of the rat LIRD clones. A total of 88.2% of the human LIRD orthologs were expressed in adenocarcinoma (cancers of the glands, including the breast and testis) and carcinoma (cancers of the skin and epithelial tissues) tissues. Hematocarcinomas (cancer of the blood and immune system), and sarcomas (cancers of cells/tissues of mesodermal origins in muscle, bone, cartilage, connective tissue, bladder, kidney, lung, liver, and spleen), showed expression of 72.5% and 88.2% of the LIRD orthologs, respectively. Cancers of the sympathetic neurvous system (neuroblastomas) and glial cells (glioblastomas) both showed expression of 82.4% of the LIRD orthologs. A total of 66.7% of the LIRD orthologs were expressed in retinoblastoma (cancer of the retina and eye) tumors and cell lines.

Informative analysis of the expression data is confounded by the limited information available for some tissues and for some organisms. Rats tend to show lower levels of expression than mouse tissues, though this is likely due to the fact that fewer genes have been studied in rats and more limited specific tissue expression analysis has been performed. To try to overcome this problem, expression data were compiled from rat, mouse and humans. In ocular tissues, 89.1 % of the LIRD genes showed expression in the eye, with 94.5% showing expression within the retina, 49.1% in the fovea/macula, and 83.6% in the RPE/choroid. A total of 92.7% of LIRD genes were expressed in the brains of rat, mouse or human, with the highest expression in the cerebellum (70.9%) and the visual cortex (72.7%). In non-neuronal tissues, the highest LIRD gene expressing tissues were the heart (87.3%), lung (87.3%), breast (89.1%), thymus (83.6 %), kidney (87.3%), liver (87.3%), testis (87.3%), and prostate (80.0%). In regards to fetal tissues, the fetal eye (69.1%), ES cells (85.5%) and placenta (83.6%), showed the highest percentage of LIRD genes expressed in rat, mouse or human tissues. Analysis of cancer tissues in rat, mouse or human, showed that all but 3 LIRD genes, rhodopsin, phosducin, and crystallin β-b2, were expressed in cancer tissues in at least one species. It is interesting to note that these are also the genes that demonstrate the strongest enriichment in retinal or neuronal tissues in rat, mouse and humans.

In general, the LIRD genes appear to be widely expressed gene in all three species analyzed. Therefore, these results suggest that the cell loss in LIRD may be due to a more global cellular dysfunction rather than a photoreceptor cell-specific response.

4.B-9. Analysis of LIRD gene function

To determine whether particular pathways are predominantly affected during LIRD, LIRD genes were separated into functional categories. To achieve this, the NCBI Conserved Domain database, LocusLink, OMIM (Online Mendelian Inheritance in Man) and PubMed databases, as well the KEGG (Kyoto Encyclopedia of Genes and Genomes) pathway database were mined for information pertaining to the function of the identified LIRD genes. Based on the information obtained, the LIRD genes were divided into functional categories. Table 4.4 summarizes these results. As shown in Figure 4.6, the

Table 4.4. Functional analysis of the LIRD genes. Using the NCBI Pubmed and Conserved Domain Databases, as well as the KEGG biochemical database, the putative functions of the identified LIRD genes was determined. Using this information the genes were divided into functional categories. Multiple clones that corresponded to the same gene were only counted as one gene. Duplicate clones are shown in grey and were not included in this analysis.

CLONES SHOWING 75 BP OR MORE OF SEQUENCE SHOWING AT LEAST 80% HOMOLOGY.

Clone	Function	Rat Alias	Mouse Alias	Human Alias	Domains
2-3	chaperones and heat shock proteins	Cct4: chaperonin subunit 4 delta	Cct4: chaperonin subunit 4 delta, A45, Cctd, A45, Cctd	CCT4: chaperonin containing TCP1, subunit 4 delta, SRB, Cctd, chaperonin containing t-complex polypeptide 1, delta subunit	TCP-1/cpn60 chaperonin family. This family includes members from the HSP60 chaperone family and the TCP-1 (T-complex protein) family
32-1	chaperones and heat shock proteins	Sncg: synuclein, gamma	Sncg: synuclein, gamma, persyn	SNCG: synuclein, gamma breast cancer-specific protein 1, SR, BCSG1, persyn, synoretin	Synuclein
8-2	chaperones and heat shock proteins	Crybb2: crystallin, beta B2, CRYBB2	Crybb2: crystallin, beta B2, Aey2, Phil, Cryb-2, Philly cataract betaB2-crystallin	CRYBB2: crystallin, beta B2, CCA2, CRYB2, CRYB2A, D22S665	Beta/Gamma crystallin
B7-4	chaperones and heat shock proteins	Grifin: galectin-related inter-fiber protein	Grifin: galectin-related inter-fiber protein, E130101O17Rik	n/a	Galectin, Galactoside-binding lectin
11-1	cytoskeleton	LOC303191: similar to unconventional myosin 15 - mouse fragment	Myo15: myosin XV, sh2, sh-2, Myo15a, shaker 2 myosin XVA	MYO15A: myosin XVA, DFNB3, MYO15, unconventional myosin-15	Myosin head,Myosin. Large ATPases, Myosin heavy chain
117-1	cytoskeleton	LOC292777: similar to Tubulin-specific chaperone B Tubulin folding cofactor B Cytoskeleton-associated protein CKAPI	Ckap1: cytoskeleton-associated protein 1, CG22, TBCB, CKAPI, 2410007D12Rik	CKAP1: cytoskeleton-associated protein 1, CG22, TBCB, CKAPI	CAP-Gly domain. CAP stands for cytoskeleton-associated proteins, COG5244, NIP100, Dynactin complex subunit involved in mitotic spindle partitioning in anaphase B
120-5	cytoskeleton	LOC296456, similar to integrin alpha v subunit.	Mus musculus integrin alpha V, mRNA cDNA clone IMAGE:5362798, partial cds	ITGAV, integrin, alpha V (vitronectin receptor, alpha polypeptide, antigen CD51).	Integrin alpha (beta-propellor repeats)
130-2	cytoskeleton	Epb4.1l1: erythrocyte protein band 4.1-like 1	Epb4.1l1: erythrocyte protein band 4.1-like 1, 4.1N, NBL1	EPB41L1: erythrocyte membrane protein band 4.1-like 1, 4.1N, KIAA0338, MGC11072, neuronal protein 4.1, neuron-type nonerythroid protein 4.1	FERM domain (Band 4.1 family). This domain has been renamed the FERM domain, which stands for F for 4.1, E for Ezrin, R for radixin and M for moesin
518-2	cytoskeleton	similar to hypothetical protein MGC30680	Aamp: angio-associated migratory protein	AAMP: angio-associated, migratory cell protein	FOG: WD40 repeat
703-8	cytoskeleton	LOC294684: similar to microtubule-associated protein MAP 1B - rat fragment	Mtap1b: microtubule-associated protein 1 B, LC1, MAP5, MAP1B, Mtap5, Mtap-5, A230055D22, microtubule associated protein 5	MAP1B: microtubule-associated protein 1B,MAP5, FUTSCH	Presenilin
B33-1	cytoskeleton	Myo1b: myosin Ib, Myr1	Myo1b: myosin IB, myosin Ib	MYO1B: myosin IB, myr1, myosin-I alpha	Myosin. Large ATPases. ATPase
102-5	energy metabolism	similar to NADH:ubiquinone oxidoreductase B15	NDUFB4, NADH dehydrogenase (ubiquinone) 1 beta subcomplex, 4	NDUFB4, NADH dehydrogenase (ubiquinone) 1 beta subcomplex, 4, 15kDa.	NADH-ubiquinone oxidoreductase B15 subunit (NDUFB4)
126-1	energy metabolism	Hk1: Hexokinase 1, HEXOKIN, RATHEXOKIN	Hk1: hexokinase 1, dea, Hk-1, downeast anemia	HK1: hexokinase 1, HKI, HXK1	Hexokinase
13-3	energy metabolism	Slc25a5: solute carrier family 25 mitochondrial carrier; adenine nucleotide translocator, member 5, Ant2, adenine nucleotide translocator 2, fibroblast isoform ATP-ADP carrier protein	Slc25a5: solute carrier family 25 mitochondrial carrier; adenine nucleotide translocator, member 5, Ant2, adenine nucleotide translocase adenine nucleotide translocator 2, fibroblast	SLC25A5: solute carrier family 25 mitochondrial carrier; adenine nucleotide translocator, member 5, T2, T3, ANT2, 2F1 adenine nucleotide translocator 2 fibroblast	Mitochondrial carrier protein

Clone	Function	Rat Alias	Mouse Alias	Human Alias	Domains
136-1	energy metabolism	Aldoc aldolase C, fructose-biphosphate	Aldo3 aldolase 3, C isoform	ALDOC aldolase C, fructose-bisphosphate	Fructose-bisphosphate aldolase class-I
48-1	energy metabolism	Cox6a1: cytochrome c oxidase, subunit VIa, polypeptide 1, COX6AL	Cox6a1: cytochrome c oxidase, subunit VI a, polypeptide 1, VIaL, subunit VIaL liver-type	COX6A1: cytochrome c oxidase subunit VIa polypeptide 1, COX6A, COX6AL	Cytochrome c oxidase subunit VIa
648-4	energy metabolism	mt-Co1: cytochrome c oxidase subunit 1, Co1, Cox1, mt_Co1	mt-Co1: cytochrome c oxidase I, mitochondrial; COI, CoxI	MTCO1: cytochrome c oxidase I;COI	Cytochrome C and Quinol oxidase polypeptide I
648-6	energy metabolism	mt-Nd4l: NADH dehydrogenase 4L, mitochondrial	mt-Nd4l: NADH dehydrogenase 4L, mitochondrial; URF4L	MTND4L: NADH dehydrogenase 4L	NADH dehydrogenase (ubiquinone) activity, mitochondrial electron transport, NADH to ubiquinone, oxidoreductase activity
703-1	energy metabolism	Pgk1: phosphoglycerate kinase 1; Pgk	Pgk1: phosphoglycerate kinase 1	PGK1: phosphoglycerate kinase 1; PGKA	Phosphoglycerate kinase
B33-2	energy metabolism	Tpi1: triosephosphate isomerase 1, Tpi, Triosephosphate isomerase 1	Tpi: triosephosphate isomerase,Tpi-1	TPI1: triosephosphate isomerase 1, TPI	Triosephosphate isomerase
B34-1	intra-cellular transport	LOC316047, similar to lysosomal-associated transmembrane protein 4 beta.	Laptm4b, lysosomal-associated protein transmembrane 4B.	LAPTM4B, lysosomal associated protein transmembrane 4 beta.	Golgi 4-transmembrane spanning transporter
B34-5	intra-cellular transport	LOC316047, similar to lysosomal-associated transmembrane protein 4 beta.	Laptm4b, lysosomal-associated protein transmembrane 4B.	LAPTM4B, lysosomal associated protein transmembrane 4 beta.	Golgi 4-transmembrane spanning transporter
63-6	kinases and phosphatases	LOC295342: similar to Transforming protein RhoC H9	Arhc: ras homolog gene family, member C, Arh9, RhoC, ras homolog 9 RhoC, aplysia ras-related homolog 9 RhoC	ARHC: ras homolog gene family, member C, ARH9, RHOC, RHOH9, RhoC, Aplysia ras-related homolog 9, Aplysia RAS-related homolog 9 oncogene RHO H9, RAS homolog gene family, member C oncogene RHO H9	Rho (Ras homology) subfamily of Ras-like small GTPases, Ras family. Includes sub-families Ras, Rab, Rac, Ral, Ran, Rap Ypt1
107-2	kinases and phosphatases	similar to GS3955 protein	expressed sequence AW319517	TRB2 tribbles homolog 2	protein kinase
136-5	kinases and phosphatases	LOC298329: similar to protein phosphatase 2A Balpha3 regulatory subunit	Ppp2r5c: protein phosphatase 2, regulatory subunit B B56, gamma isoform, Band 8A protein phosphatase 2, regulatory subunit	phosphatase 2, regulatory subunit B B56, gamma isoform, B56G, MGC23064,Serine/threonine protein phosphatase 2A, 56 kDa regulatory subunit,	regulatory B subunit (B56 family). Protein phosphatase 2A (PP2A) is a major intracellular protein phosphatase that regulates multiple aspects of cell growth and metabolism
165-8	kinases and phosphatases	similar to tousled-like kinase 2; serine/threonine kinase; tousled-like kinase	Tlk2: tousled-like kinase 2	TLK2: tousled-like kinase 2	Serine/Threonine protein kinases, catalytic domain
120-1	lipid, CHO and amine acid metabolism	Akr1d1: aldo-keto reductase family 1, member D1 delta 4-3-ketosteroid-5-beta-reductase	Akr1d1: aldo-keto reductase family 1, member D1, MGC25614	AKR1D1: aldo-keto reductase family 1, member D1 delta 4-3-ketosteroid-5-beta-reductase, SRD5B1, 3o5bred, steroid 5-beta-reductase, steroid-5-beta-reductase, beta polypeptide 1 3-oxo-5 beta-steroid delta 4-dehydrogenase beta 1	Aldo/keto reductase family. This family includes a number of K+ ion channel beta chain regulatory domains - these are reported to have oxidoreductase activity

Clone	Function	Rat Alias	Mouse Alias	Human Alias	Domains
120-5	lipid, CHO and amino acid metabolism	Pafah1b3: platelet-activating factor acetylhydrolase, isoform 1b, alpha1 subunit	Pafah1b3: platelet-activating factor acetylhydrolase, isoform 1b, alpha1 subunit, Pafahg, mus[g]	PAFAH1B3: platelet-activating factor acetylhydrolase, isoform Ib, gamma subunit 29kDa, Platelet-activating factor acetylhydrolase, isoform Ib, gamma subunit platelet-activating factor acetylhydrolase, isoform Ib, gamma subunit 29kD	Platelet activating factor acetylhydrolase. Platelet activating factor acetylhydrolase (PAF-AH) is a subfamily of phospholipases A2, responsible for inactivation of platelet-activating factor through cleavage of an acetyl group.
1388-2	lipid, CHO and amino acid metabolism	Hmgcl: 3-hydroxy-3-methylglutaryl CoA lyase	Hmgcl: 3-hydroxy-3-methylglutaryl-Coenzyme A lyase	HMGCL: 3-hydroxymethyl-3-methylglutaryl-Coenzyme A lyase hydroxymethylglutaricaci	HMGL-like
15-2	lipid, CHO and amino acid metabolism	Hrmt1l2: heterogeneous nuclear ribonucleoproteins methyltransferase-like 2 S. cerevisiae	Hrmt1l2: heterogeneous nuclear ribonucleoproteins methyltransferase-like 2 S. cerevisiae, Mrmt1, Prmt1, 6720434D09Rik, arginine N-methyltransferase 1	HRMT1L2: HMT1 hnRNP methyltransferase-like 2 S. cerevisiae, ANM1, HCP1, IR1B4, PRMT1	Predicted RNA methylase
1439-5	phototransduction	Rhodopsin retinitis pigmentosa 4, autosomal dominant	Rho: rhodopsin; Ops, RP4, Opn2, [illegible], [illegible]; L opsin opsin 2, LWS opsin, Rod Opsin, Red Opsin, Long Wavelength Sensitive opsin	RHO: rhodopsin opsin 2, rod pigment retinitis pigmentosa 4, autosomal dominant; RP4, OPN2	G-protein coupled photoreceptor activity, 7 transmembrane receptor (rhodopsin family)
1439-7	phototransduction	Rhodopsin retinitis pigmentosa 4, autosomal dominant	Rho: rhodopsin; Ops, RP4, Opn2, [illegible], [illegible]; L opsin opsin 2, LWS opsin, Rod Opsin, Red Opsin, Long Wavelength Sensitive opsin	RHO: rhodopsin opsin 2, rod pigment retinitis pigmentosa 4, autosomal dominant; RP4, OPN2	G-protein coupled photoreceptor activity, 7 transmembrane receptor (rhodopsin family)
233-1	phototransduction	Rho: Rhodopsin	Rho: rhodopsin	RHO: rhodopsin opsin 2, rod pigment retinitis pigmentosa 4, autosomal dominant, RP4, OPN2	7 transmembrane receptor (rhodopsin family)
518-7	phototransduction	Pdc: phosducin; Rpr1, 33DPTP	Pdc, Rpr1, Rpr-1, photoreceptor 1	phosducin, 33kDA phototransducing protein, PHD, MEKA, PhLP, PhLOP	Phosducin
98-1	phototransduction	LOC301233: similar to Guanylyl cyclase activating protein 1 GCAP 1 Guanylate cyclase activator 1A	Guca1a: guanylate cyclase activator 1a retina, GC-A, Gcap1, Guca1	GUCA1A: guanylate cyclase activator 1A retina, GCAP, GUCA, GCAP1, GUCA1	COG5126, FRQ1, Ca2+-binding protein (EF-Hand superfamily)
B91-1	protein:protein interactions	LOC302557: similar to polyglutamine binding protein 1	Pqbp1: polyglutamine binding protein 1, Sfc2, scurfy candidate 2	PQBP1: polyglutamine binding protein 1, NPW38, nuclear protein containing WW domain 38 kD	Domain with 2 conserved Trp (W) residues, WW domain. The WW domain is a protein module with two highly conserved tryptophans that binds proline-rich peptide motifs in vitro

Clone	Function	Rat Alias	Mouse Alias	Human Alias	Domains
56-1	retinol metabolism	LOC296161	Rdh11: retinol dehydrogenase 11, Mdt1, Psdr1, SCALD, Arsdr1, CGI-82, HCBP12, M42C60, 2610319N22Rik, all-trans and 9-cis short-chain aldehyde dehydrogenase, short-chain dehydrogenase/reductase 1, cell line MC/9.IL4 derived transcript 1, androgen-regulated short-chain dehydrogenase/reductase 1	RDH11: retinol dehydrogenase 11 all-trans and 9-cis, MDT1, PSDR1, RALR1, ARSDR1, CGI-82, HCBP12, FLJ32633, CGI-82 protein, HCV core-binding protein, retinol dehydrogenase 11, prostate short-chain, dehydrogenase reductase 1, androgen-regulated short-chain dehydrogenase/reductase 1	short chain dehydrogenase
107-4	RNA and ribosomal binding protein translation	Rpl5 ribosomal protein L5	Rpl5 ribosomal protein L5	RPL5 ribosomal protein L5	Ribosomal L18p/L5e family
1-2	RNA and ribosomal binding protein translation	similar to Elongation factor 1-delta EF-1-delta Antigen NY-CO-4	Eef1d: eukaryotic translation elongation factor 1 delta guanine nucleotide exchange protein, 5730529A16Rik	EEF1D: eukaryotic translation elongation factor 1 delta guanine nucleotide exchange protein, EF-1D, FLJ20897, guanine nucleotide exchange protein eukaryotic translation elongation	Elongation factor 1B conserved domain
1307-4	RNA and ribosomal binding protein translation	RPS10: ribosomal protein S10	RPS10: ribosomal protein S10	RPS10: ribosomal protein S10	Plectin/S10 domain
146-1	RNA and ribosomal binding protein translation	Rpl4: ribosomal protein L4	Rpl4: ribosomal protein L4, 2010004J23Rik: RIKEN cDNA 2010004J23 gene	RPL4: ribosomal protein L4, HRPL4, 60S ribosomal protein L4, homologue of Xenopus ribosomal protein L1	Ribosomal protein L4/L1 family.
146-6	RNA and ribosomal binding protein translation	Rpl4: ribosomal protein L4	Rpl4: ribosomal protein L4, 2010004J23Rik: RIKEN cDNA 2010004J23 gene	RPL4: ribosomal protein L4, HRPL4, 60S ribosomal protein L4, homologue of Xenopus ribosomal protein L1	Ribosomal protein L4/L1 family.
165-7	RNA and ribosomal binding protein translation	Raly, similar to hnRNP-associated with lethal yellow	Raly, similar to hnRNP-associated with lethal yellow	RALY RNA binding protein autoantigenic, hnRNP-associated with lethal yellow	RNA recognition motif, RNA-binding proteins (RRM domain)
185-2	RNA and ribosomal binding protein translation	Rps16: ribosomal protein S16	similar to ribosomal protein S16	RPS16: ribosomal protein S16	Ribosomal protein S9/S16.
902-4	RNA and ribosomal binding protein translation	LOC294081: similar to fusion protein: ubiquitin bases 43_513; ribosomal protein S27a bases 217_532	Rps27a: ribosomal protein S27a; 0610006J14Rik	RPS27A: ribosomal protein S27a; CEP80, UBA80, UBCEP1, HUBCEP80	Ubiquitin homologues, Ribosomal protein S27AE
28-2	RNA and ribosomal binding protein translation	LOC295394: similar to RIKEN cDNA 2410012M04	2410012M04Rik: RIKEN cDNA 2410012M04 gene	CGI-30: CGI-30 protein	Diphthamide biosynthesis methyltransferase
1325-2	RNA splicing	LOC311612: similar to RIKEN cDNA 1210001E11	Sfrs6: splicing factor, arginine/serine-rich 6; 1210001E11Rik	SFRS6: splicing factor, arginine/serine-rich 6; B52, SRP55	RNA recognition motif
1325-3	RNA splicing	LOC311612: similar to RIKEN cDNA 1210001E11	Sfrs6: splicing factor, arginine/serine-rich 6; 1210001E11Rik	SFRS6: splicing factor, arginine/serine-rich 6; B52, SRP55	RNA recognition motif
1325-4	RNA splicing	LOC311612: similar to RIKEN cDNA 1210001E11	Sfrs6: splicing factor, arginine/serine-rich 6; 1210001E11Rik	SFRS6: splicing factor, arginine/serine-rich 6; B52, SRP55	RNA recognition motif
1410-8	transcription factor	Cited2: Cbp/p300-interacting transactivator, with Glu/Asp-rich carboxy-terminal domain, 2, mrg-1	Cited2: Cbp/p300-interacting transactivator, with Glu/Asp-rich carboxy-terminal domain, 2; Mrg1, Msg2, p35srj, ER164-like	CITED2: Cbp/p300-interacting transactivator, with Glu/Asp-rich carboxy-terminal domain, 2: MRG1, P35SRJ	transcription factor activity, regulation of transcription from Pol II promoter
1444-2	transcription factor	Atf4: activating transcription factor ATF-4	Atf4: activating transcription factor 4, Atf-4, C/ATF, CREB2, TAXREB67	ATF4: activating transcription factor 4 tax-responsive enhancer element B67, CREB2, TXREB, CREB-2, TAXREB67	bZIP transcription factor, basic region leucin zipper

Clone	Function	Rat Alias	Mouse Alias	Human Alias	Domains
633-6	transcription factor	similar to OASIS protein; BBF-2 (drosophila) homolog.	RIKEN cDNA C530025K05 gene	CREB3L2, cAMP responsive element binding protein 3-like 2, DKFZP586F2423: hypothetical protein	basic region leucin zipper
99-2	transcription factor	LOC292173: similar to TATA box binding protein-like protein 1 TBP-like protein 1 TATA box binding protein-related factor 2 TBP-related factor 2 STUD protein 21-kDa TBP-like protein	Tbpl1: TATA box binding protein-like, STD, TLF, TRP, Tlp, TRF2, 4732475G08, TBP-like factor, TBP-like protein, TBP-related factor 2, TATA box binding protein-like protein, TATA box binding	TBPL1: TBP-like 1,TLF, TLP, STUD, TRF2, MGC:8389, MGC:9620, TBP-like protein, TBP-related factor 2, 21-kDA TBP-like protein, second TBP of unique DNA	Transcription factor TFIID (or TATA-binding protein, TBP), TATA-box binding protein (TBP), component of TFIID and TFIIIB
B25-3	transcription factor	LOC309031: similar to zinc finger protein, subfamily 1A, 5; zinc finger transcription factor Pegasus	mouse RIKEN cDNA 2610034F18	PEGASUS: zinc finger protein, subfamily 1A, 5 Pegasus, ZNFN1A5, zinc finger transcription factor Pegasus	KOG3623: Homeobox transcription factor SIP1 [Transcription]
1442-1	ubiquitinylation	Loc192255: polyubiquitin	Ubb: ubiquitin B, Ubb2	UBB: ubiquitin B, MGC8385, polyubiquitin B	Ubiquitin family
1442-7	ubiquitinylation	Loc192255: polyubiquitin	Ubb: ubiquitin B, Ubb2	UBB: ubiquitin B, MGC8385, polyubiquitin B	Ubiquitin family
1497-3	ubiquitinylation	Nedd4a: neural precursor cell expressed, developmentally down-regulated gene 4A, Neural precursor cell expressed, developmentally down-regulated gene 4, Nedd4	Nedd4: neural precursor cell expressed, developmentally down-regulted gene 4, Nedd4, Nedd4a, Nedd4-1, E430025J12Rik, neural precursor cell expressed, developmentally down-regulated gene 4	NEDD4: neural precursor cell expressed, developmentally down-regulated 4, KIAA0093	C2 domain, Domain with 2 conserved Trp (W) residues, Protein kinase C conserved region 2 (CalB), COG5021, HUL4, Ubiquitin-protein ligase, HECT-domain (ubiquitin-transferase). The name HECT comes from Homologous to the E6-AP Carboxyl Terminus, WW domain.
155-2	ubiquitinylation	similar to Ubiquitin-conjugating enzyme E2-23 kDa Ubiquitin-protein ligase Ubiquitin carrier protein	Ube2e3: ubiquitin-conjugating enzyme E2E 3, UBC4/5 homolog	UBE2E3 ubiquitin-conjugating enzyme E2E 3	Ubiquitin-conjugating enzyme E2, catalytic domain
99-1	ubiquitinylation	LOC287716: similar to proteaseome prosome, macropain 28 subunit, 3	Psme3: proteaseome prosome, macropain 28 subunit, 3, Ki	PSME3: proteasome prosome, macropain activator subunit 3 PA28 gamma; Ki, Ki, PA28G, REG-GAMMA, PA28-gamma, Ki antigen, Ki nuclear autoantigen, proteasome activator 28-gamma, 11S regulator complex gamma subunit, activator of multicatalytic protease subunit 3	Proteasome activator pa28 beta subunit. PA28 activator complex
1442-8	vessicle transport	LOC297428: similar to coatomer protein complex, subunit gamma 1; coat protein gamma-cop	Copg1: coatomer protein complex, subunit gamma , D6Wsu16e, D6Ertd71e	COPG: coatomer protein complex, subunit gamma, COPG, coat protein gamma-cop, coatomer protein complex, subunit gamma 1	COG5240, SEC21, Vesicle coat complex COPI, gamma subunit [Intracellular trafficking and secretion]
1444-6	vessicle transport	Unc119: UNC-119 homolog C. elegans	Unc119h: unc119 homolog C. elegans, HRG4, UNC119	UNC119: unc-119 homolog C. elegans, HRG4, retinal protein 4, unc119 C.elegans homolog	KOG4037: Photoreceptor synaptic vesicle protein HRG4/UNC-119 [Intracellular trafficking, secretion, and vesicular transport, Signal transduction mechanisms]
155-3	vessicle transport	similar to Mss4 protein	RIKEN cDNA E130318E12 gene	RABIF: RAB interacting factor, also MSS4, RASGFR3, RASGRF3	Nucleotide exchange factor for Rab-like small GTPases (RabGEF), Mss4 type

Clone	Function	Rat Alias	Mouse Alias	Human Alias	Domains
39-5	vessicle transport	Copb2: beta prime COP	Copb2: coatomer protein complex, subunit beta 2 beta prime	COPB2: coatomer protein complex, subunit beta 2 beta prime, beta'-COP, betaprime-COP,	Coatomer WD associated domain
66-2	unknown	RAT: LOC299696			n/a
123-3	unknown	n/a	Mus musculus upregulated during skeletal muscle growth 4 Usmg4,	n/a	n/a
126-4	unknown	n/a	RIKEN cDNA 3526402H21	n/a	n/a
708-3	unknown	similar to DEAD/H (Asp-Glu-Ala-Asp/His) box polypeptide 26; RNA helicase HDB; deleted in cancer 1; RNA helicase HDB/DICE1; DEAD box protein.	Ddx26: DEAD/H Asp-Glu-Ala-Asp/His box polypeptide 26; HDB, DICE1, Notch2l	DDX26: DEAD/H Asp-Glu-Ala-Asp/His box polypeptide 26; HDB, DBI-1, DICE1, Notchl2, DKFZP434B105, DEAD box protein, RNA helicase HDB; deleted in cancer 1; RNA helicase	Calcium-binding EGF-like domain, nucleic acid binding
7-1	unknown	Rattus norvegicus 14 BAC CH230-13H11 Children's Hospital Oakland Research Institute complete sequence	n/a	n/a	n/a
B11-7	unknown	similar to KIAA1731 protein, LOC363018	5830418K08Rik: RIKEN cDNA 5830418K08 gene	LOC283262: hypothetical gene supported by AL833615	n/a
CLONES SHOWING LESS THAN 75 BP OF SEQUENCE SHOWING AT LEAST 80% HOMOLOGY.					
13-1	unique(weakly similar)	nucleolar protein 3 (apoptosis repressor with CARD domain); ARC: apoptosis repressor with CARD, unknown Glu-Pro dipeptide repeat protein	nucleolar protein 3 (apoptosis repressor with CARD domain); ARC: apoptosis repressor with CARD, unknown Glu-Pro dipeptide repeat protein	nucleolar protein 3 (apoptosis repressor with CARD domain); ARC: apoptosis repressor with CARD, unknown Glu-Pro dipeptide repeat protein	Down-regulation of ARC (apoptosis repressor with caspase recruitment domain) contributes to vulnerability of hippocampal neurons to ischemia/hypoxia.(PMID: 12753927)
648-2	unique (weakly similar)	LOC293725: similar to Elongation factor 1-gamma EF-1-gamma eEF-1B gamma	eukaryotic translation elongation factor 1 gamma.	EEF1G: eukaryotic translation elongation factor 1 gamma, pancreatic tumor-related protein	Elongation factor 1 gamma, conserved domain, Glutathione S-transferase
B28-1	unique (weakly similar)	similar to sudD, suppres	Riok3: RIO kinase 3 yeast, Sudd, 1200013N13Rik, sudD, suppressor of bimD6 homolog Aspergillus nidulans	RIOK3: RIO kinase 3 yeast, SUDD, sudD suppressor of bimD6 homolog A. nidulans, homolog of the Aspergillus nidulans sudD gene product, sudD suppressor of	RIO-like kinase
633-5	unique (weakly similar)	unique	mouse major histocompatibility complex region NG27, NADH oxidoreductase, NG29, KIFC1, Fas-binding protein, BING1, tapasin, RalGDS-like, KE2, BING4, beta 1,3-galactosyl transferase, and RPS18 genes	n/a	n/a
102-4	unique (no hits)				
102-3	unique (no hits)				
119-5	unique (no hits)				
135-2	unique (no hits)				
147-1	unique (no hits)				
22-3	unique (no hits)				
52-1	unique (no hits)				
63-2	unique (no hits)				
B33-3	unique (no hits)				

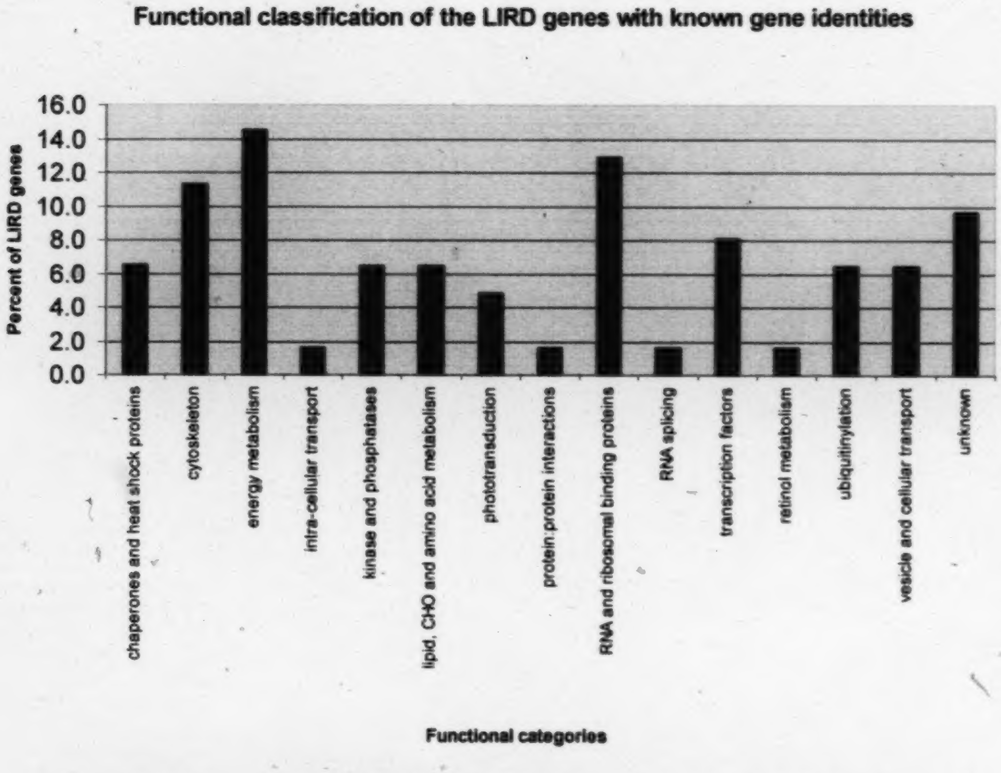

Figure 4.6. Functional analysis of the LIRD genes. Using the NCBI Pubmed and Conserved Domain Databases, as well as the KEGG biochemical database, the putative functions of the identified LIRD genes was determined. Using this information the genes were divided into functional categories.

majority of the 62 LIRD genes identified from the library screen fell into the categories of energy metabolism (14.5%), RNA and ribosomal binding protein (12.9%), and cytoskeleton (11.3%). A total of 6.5% of the LIRD genes were classified as either chaperones and heat shock proteins; kinases and phosphatases; genes involved in lipid, carbohydrate and amino acid metabolism; ubiquitinylation; or vesicle transport proteins. Transcription factors accounted for 8.1% of the LIRD genes, while 1.6% of the LIRD were associated with intra-cellular transport, protein:protein interactions, retinol metabolism, or RNA splicing. Finally, 9.7% of the LIRD genes represented known genes with unknown function.

4.B-10. Analysis of ubiquitinylation and phototransduction associated genes

To determine whether LIRD genes that fell into a particular functional category demonstrated similar patterns of expression to each other, Northern blot analysis was performed on clones associated with ubiquitinylation and phototransduction. Of the clones involved in the phototransduction cascade, clone 518-7 (phosducin) and clone 98-1 (*GCAP*) were analyzed for expression levels over the progression of LIRD. In addition, Northern blot analysis was performed using rhodopsin and arrestin clones isolated by Rhonda Kelln and Ruby Grewal in our laboratory, an *IRBP* clone generously provided by Dr. Diane Borst (Borst *et al*, 1988) and a recoverin clone purchased from Research Genetics. These results are shown in Figure 4.7. The phosducin transcript demonstrated high expression in dark-reared control animals. This level decreased significantly following 4 hours of light exposure, and was reduced to almost undetectable levels after 8 or 16 hours of light exposure. *GCAP* on the other hand, was expressed at low levels in

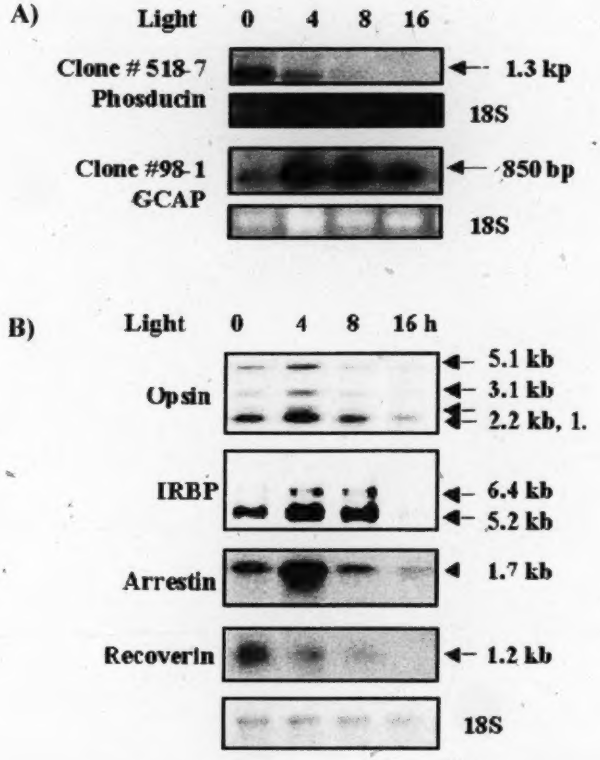
A)
Light
0
4
8
16
Clone # 518-7
Phosducin
1.3 kp
18S
Clone #98-1
GCAP
850 bp
18S
B)
Light
0
4
8
16 h
Opsin
5.1 kb
3.1 kb
2.2 kb, 1.
IRBP
6.4 kb
5.2 kb
Arrestin
1.7 kb
Recoverin
1.2 kb
18S

Figure 4.7. Northern blot analysis of phototransduction-related LIRD genes. Changes in the expression patterns of photoreceptor-expressed LIRD genes following light treatment. (A) Northern blot analysis of phosducin and *GCAP* was performed using 10 μg of total RNA isolated from dark-reared rats exposed to 0, 4, 8, or 16 hours of intense green light. (B) Northern blot analysis of additional phototransduction specific genes including rhodopsin, *IRBP*, arrestin, and recoverin were performed as above, though probes were obtained from additional sources.

control animals, and was significantly induced following 4 and 8 hours of light treatment. This level dropped following 16 hours of light exposure. Rhodopsin, *IRBP* and arrestin were all induced following 4 hours of light exposure, and the level of expression was reduced following 8 and 16 hours of light exposure. In regards to arrestin and rhodopsin, the transcript levels returned to control levels following 8 hours of light exposure, and were reduced even further following 16 hours. The two *IRBP* transcripts observed on the Northern blots remained at elevated levels after 8 hours of light treatment, however, they were barely undetectable following 16 hours of light exposure. Recoverin expression was not induced following light exposure, but showed a progressive decrease in transcripts levels with increasing light exposures. Based on these results, coordinate expression patterns are not apparent.

The opposite was true for the various members of the ubiquitinylation cascade identified from the library screen. As illustrated in Figure 4.8, all of the analyzed transcripts associated with ubiquitinylation were induced following 4 hours of light exposure and decreased to varying degrees with increasing light exposure. Clone 1442-7, representing poly-ubiquitin, was strongly induced following 4 hours of light exposure, and though the level decreased following 8 and 16 hours of treatment, the transcript was maintained at higher levels than seen in the control retinae. Clones 1497-3, and 155-2, representing *NEDD4* and *UBCM2*, respectively, showed a reduction in transcript levels following 8 and 16 hours of light exposure, to levels significantly below those seen in untreated retinae. Northern blot analysis was also performed using the human *PGP9.5* ubiquitin carboxyl terminal hydroxylase as a probe (obtained from Dr. Steven Bernstein, unpublished probe). The expected rat ortholog of *PGP9.5*, ubiquitin carboxy-terminal

Figure 4.8. Northern blot analysis of genes associated with ubiquitinylation. (A) Overview of the ubiquitinylation cascade. Ubiquitinylation is the process by which a variety of proteins are targeted for degradation by a multi-protein proteosome complex. In this ATP-dependent process the carboxyl group of a small monomer protein known as ubiquitin (Ub) is conjugated via a thioester bond to a ubiquitin activating enzyme (E1) (reviewed by Yamao, 1999). The now activated Ub molecule is transferred to one of numerous Ub-conjugating enzymes (E2), again via a thiol ester linkage. The Ub molecule can then be ligated to a target protein directly, or the Ub molecule is next transferred to the thiol group of a Ub ligase enzyme (E3). The E3 enzyme will then transfer the activated UB from E2 to a lysine ε-amino group of a previously Ub-bound target protein, forming an isopeptide bond. In the presence of specialized Ub conjugating factor (E4), long chains of Ub are added in conjunction with the activities of E1, E2 and E3. This Ub-target protein complex can then be degraded by the 26S proteosome, releasing peptide fragments and the multi-chain Ub complex. Ub isopeptidase enzymes then break down this complex of Ub molecules, and free Ub proteins are recycled for the next round of ubiquitinylation. Ub molecules can also be removed from the target proteins through the actions of Ub-carboxyl terminal hydroxylases (PGP9.5), hence preventing degradation. (B) Changes in the expression patterns of ubiquitinylation-specific LIRD genes following light treatment. Northern analysis was performed on 10 μg of total RNA isolated from dark-reared rats exposed to 0, 4, 8, or 16 hours of intense green light. Probes used for the hybridization were either PCR products produced from amplification of LIRD clones, as was the case for poly-Ub, Nedd4 and UbcM2, or were obtained from additional sources, as was the case for PGP9.5.

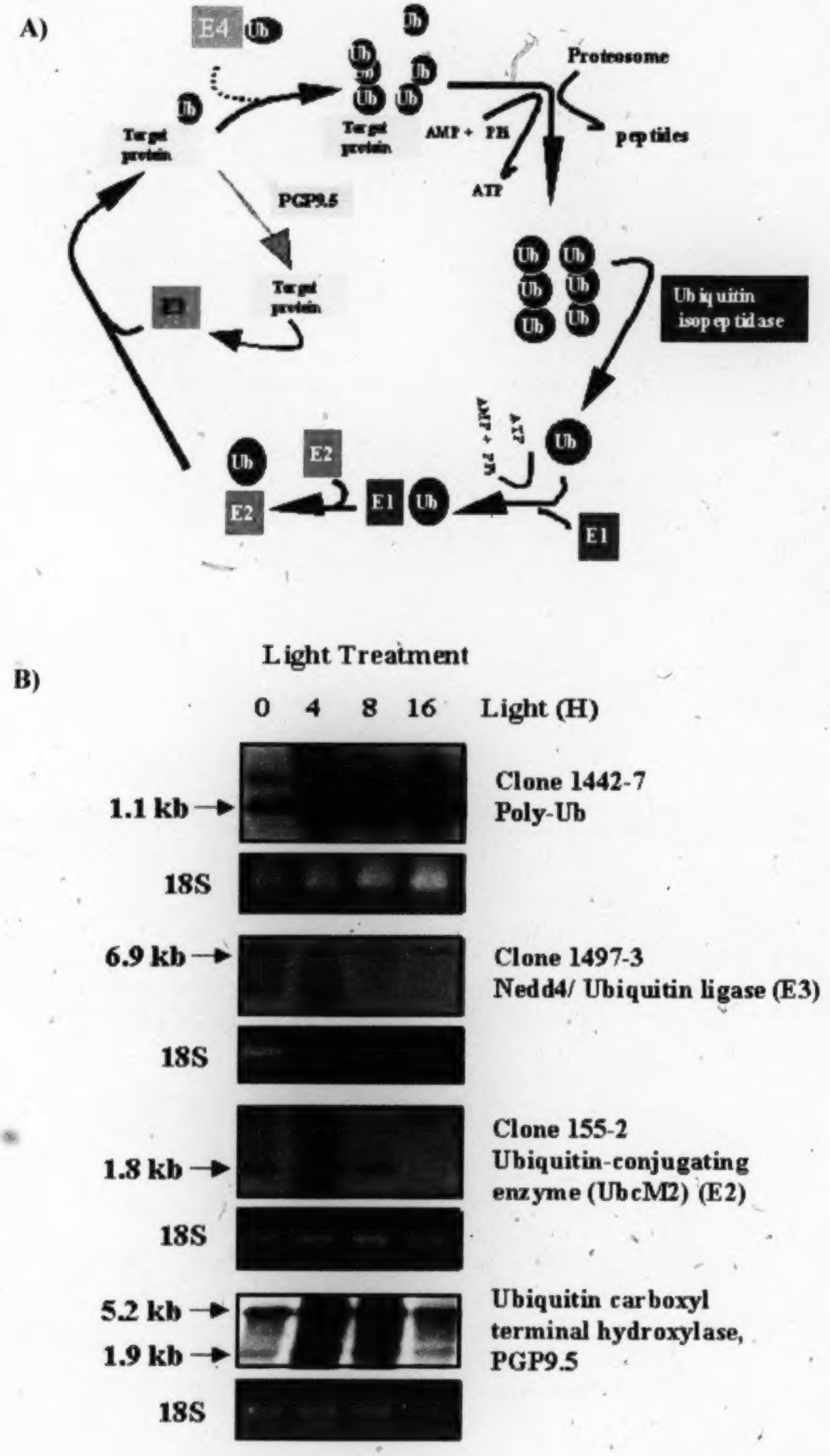
A)
E4
Ub
Target protein
PGP9.5
Target protein
E3
Proteosome
AMP + PPi
ATP
peptides
Ubiquitin isopeptidase
AMP + PPi
ATP
E1
E2
B)
Light Treatment
0
4
8
16
Light (H)
1.1 kb
Clone 1442-7
Poly-Ub
18S
6.9 kb
Clone 1497-3
Nedd4/ Ubiquitin ligase (E3)
18S
1.8 kb
Clone 155-2
Ubiquitin-conjugating enzyme (UbcM2) (E2)
18S
5.2 kb
1.9 kb
Ubiquitin carboxyl terminal hydroxylase, PGP9.5
18S

hydroxylase L1 (*UCHL1*), is 1.1 kb, and is 88% identical at the nucleotide level. Interestingly, neither of the two transcripts observed on Northern blots corresponded to the expected size of the rat transcript. Both transcripts were induced following 4 and 8 hours of light exposure, and returned to control levels following 16 hours of light-exposure. Therefore, in the case of LIRD genes associated with ubiquitinylation, there appears to be an early induction, followed by a decrease in these levels with increasing light exposure.

4.C. DISCUSSION

4.C-1. Differential gene expression during LIRD

Differential gene expression is a major factor influencing not only tissue identity, but also the physiological events that occur within the cells of a particular tissue. Apoptosis is an active event within a cell, requiring de novo mRNA and protein synthesis (Yonish-Rouach *et al*, 1995; Naora *et al*, 1995). We propose that the progression from a normal to an apoptotic retina requires change in the expression patterns of many types of genes, including those required for normal cell function, and those that promote the cell death pathway. By understanding the molecular events that differ between a normal and apoptotic retina, we hope to be able to provide insight into some of the critical players of the apoptotic pathway in LIRD.

The average eukaryotic gene spans 16.6 kb, contains 7 exons and encodes a transcript of 2.4 kb which contains 1.2 kb of coding sequence, 750 bp of 5' UTR (untranslated region) and 450 bp of 3' UTR (Lewin, 1994). Size analysis of the cDNA inserts isolated from the execution phase library indicated that the average insert size was

2.2 kb, suggesting a high likelihood of isolating full length clones. This, and the relatively high frequency of unique clones isolated from the differential screen, suggests that this library is an important tool for the identification of novel retinal gene. Identification of novel gene sequences, or novel splice variants is a benefit of this technique that is not possible with other techniques such as microarray screening (Green *et al*, 2001). In addition, the high rate of confirmation of the differential status of the clones by Northern blot analysis, suggests that the level of false positives is quite low, a feature that gives this technique an advantage over others such as differential display, which is known to be associated with a high rate of false positives (Green *et al*, 2001; Martin and Pardee, 2000).

Another important feature to consider when analyzing the feasibility of a particular transcription profiling technique is the ability of the system to achieve complete representation of the expressed sequences within a cell. A typical cell contains approximately 360,000 mRNA transcripts, representing 12,000-37,000 different mRNA species (Alberts *et al*, 1994; Williams, 1981). Highly abundant transcripts are present at 12,000 copies per cell, and moderately abundant transcripts are present at 300 copies per cell (Alberts *et al*, 1984). Transcripts present at 15 copies or less per cell, which are considered rare, account for approximately 45% of the total mRNA, and 90-95% of the different transcript species within a cell (Bonaldo *et al*, 1996; Alberts *et al*, 1984). As approximately 10,000 different unique transcripts species are present in any given cell, including the retina (Lewin, 1994), at least $4.6 \times 10^4 - 1.7 \times 10^5$ clones must be present in a cDNA library to represent all low, middle and high abundant transcripts (Wong, 1991). Since the titer of the execution phase library described here is at least 10 times this number, there is a high probability that it contains a majority (if not all) of the expressed transcripts from the 8 hour light-treated retinae. As only 30,000 clones were screened here, it is unlikely that all potential transcripts are represented in our initial screenings, and so many rare transcripts are likely to have been missed. More extensive screening attempts will be needed to identify rare retinally-expressed transcripts.

Of the initial 30,000 clones screened, 2000 were identified as being differentially expressed in the primary screen. Of these, 1600 survived the secondary screen, while only 109 survived the tertiary screen. There are several reasons for this drastic reduction in the number of differentially expressed clones. First, the phage were plated out at a density of approximately 400 pfu per plate. This resulted in the plaques being located in very close proximity to each other, making it difficult to isolate only one pure plaque. Second, if several plaques were clustered very close together, it was difficult to determine with certainty, which one represented the differentially expressed clone identified during the primary screen. Therefore, all plaques in the immediate vicinity were pooled to ensure that the correct plaque was isolated. Third, over time the phage particles will diffuse through the medium, potentially contaminating nearby plaques, and resulting in multiple phage within a single isolated plaque. Fourth, during the purification process, clones that produced PCR products of less than 300 bp were discarded to maximize the isolation of full length clones. In addition, the total cDNA population probes used in the primary and secondary screens were PCR amplified prior to use due to limitations in tissue availability, while the probes utilized in the tertiary screen were not amplified. Results in our lab by Micah Chrenek (unpublished observations) suggest that there may be differences in amplification efficiencies of the various template populations within a mixed probe. This is further supported by our observation that clone 28-2, identified as a highly expressed dark-enriched clone, also showed strong expression with the 8 hour probe (Figure 5.2, Chapter 5). This contrasted with the results of Northern blot analysis which showed relatively low expression of clone 28-2 in the dark-reared retinae, and significantly lower expression in the 8-hour treated retinae (Figure 5.3, Chapter 5). Though there is a similar trend in expression patterns between the primary, secondary and tertiary screens and the Northern blot analysis, the relative expression levels observed in the library screenings do not appear particularly accurate. These results also suggest that differentially expressed transcripts that were amplified less efficiently during the probe preparation process may have been missed during the screening steps. Therefore, caution must be taken in interpreting the differences in expression levels of clones as observed during the screening steps. The same caution should be applied to all PCR-based transcription profiling techniques such as differential display, SAGE (serial analysis of gene expression), and related techniques (Green *et al*, 2001).

Determining the chromosomal locations of the LIRD genes and their respective orthologs demonstrated that some chromosomes contain a higher frequency of LIRD genes than others. In all three species analyzed, the mitochondrial genome had a higher proportion of LIRD gene orthologs than any nuclear chromosome. This finding may be significant due to the fact that over 150 disease-causing mutations have been identified in mitochondrially-encoded genes, affecting everything from cancer and diabetes to neurodegeneration and aging (Wittenhagen and Kelley, 2003; Ohta, 2003). It is also important to note that more than half of the disease causing mutations identified in the mitochondrial genome, occur within the genes encoding tRNAs (Wittenhagen and Kelly, 2003). tRNA gene mutations have been identified as a causative agent in a number of human retinal diseases including macular pattern dystrophy type II (Bonte *et al*, 1997; Harrison *et al*, 1997; Massin *et al*, 1995; van den Ouweland *et al*, 1992), pigmentary retinopathy with sensorineural hearing loss (Crimi *et al*, 2003) and RP with progressive sensorineural hearing loss (Mansergh *et al*, 1999). Therefore, considering the significant role of mutations in tRNA genes in human disease one could speculate that there is a role for differential tRNA expression during the progression of LIRD. Unfortunately, the methods utilized for cDNA synthesis, did not make it possible to assess the differential status of the mitochondrial tRNA genes following light exposure, and further analysis is required.

Comparisons of the chromosomal locations of the human LIRD orthologs with those listed in the RetNet retinal disease gene database, demonstrated that the majority of human LIRD orthologs (85.2%) cluster in regions containing known retinal disease genes. In addition, genes known to be associated with human retinal disease were also shown to cluster on particular regions of the genome. The close association between the LIRD orthologs and human retinal disease genes suggest the possibility that the LIRD genes identified in the execution phase cDNA library may represent as of yet unidentified retinal disease genes. The fact that several LIRD orthologs are known retinal disease genes, including rhodopsin, guanylate cyclase activator 1A, the unc-119 homolog *HRG4*, and phosphoglycerate kinase 1 (RetNet databases and corresponding references therein), supports this hypothesis.

When expression profiles were analyzed in rodent and human orthologs, it became evident that the majority of the LIRD genes and orthologs were widely or ubiquitiously expressed throughout the body. Though this analysis is hampered by the limited expression analysis in rats, it appears that the majority of LIRD genes are expressed in the brain, heart, lung, prostate, pituitary gland and kidney in all three species analyzed. In addition, the majority of LIRD genes were expressed in the placenta, and cancer tissues in all three species. When the expression of all three species was pooled together to obtain a more complete picture, it became evident that 94.9% of the LIRD genes are expressed in the retina. The remaining 5.1% of genes represented transcripts not previously shown to be expressed in the retina. As well, almost half of the human LIRD orthologs were expressed within the cone-rich fovea and macular regions of the human retina. This is interesting, as rodents do not contain a fovea or macula. Therefore, the screening of the execution phase cDNA library is a valuable tool for identifying retinally-expressed genes, as well as orthologs of potential macular-expressed genes.

All but three of the genes identified from the execution phase cDNA library were widely expressed in both adult and fetal tissues. Only rhodopsin, phosducin, and crystallin β-b2 demonstrated retinal or neuronal specific expression. This suggests that during the progression of LIRD, global housekeeping and common cell function genes are differentially expressed rather than retinal cell-specific genes. This would lead to a general cellular dysfunction involving many global systems. This further suggests that the molecular mechanisms underlying tissue degeneration in LIRD may be common to degeneration in other tissues as well.

It is also interesting to consider the fact that the genes that demonstrated retinal-specific expression were the only genes that did not show expression in cancer cells. Considering the features of both cancer and apoptotic cells, this is not entirely unexpected. Apoptosis requires differential gene expression affecting numerous cellular pathways (Bursch *et al*, 1990), and is associated with condensation and cleavage of the DNA, a breakdown of cell:cell and cell:extracellular matrix (ECM) remodeling (Kerr and Harmon, 1991). In addition, there are alterations and disruptions of the cytoskeleton and membrane chemical composition, blebbing of the cell membrane, and the formation of apoptotic bodies. Many of these events are not unique to apoptosis, and are evident in the morphology of cancer cells as well. Cancer cells show changes in a cell's ability to undergo apoptotic cell death, alterations in chromosome and DNA integrity, alterations in chemical reactions as a result of differential gene expression, breakdown of cell:cell and cell:ECM adhesions, and modification of membrane components (Phillis and Goodwin, 2003). Therefore, the cellular pathways altered in apoptosis, likely show significant overlap with those involved in cellular transformation. As a result, changes in the expression profiles of common genes would be expected in both cell states. As the progression of cellular transformation is often associated with a "de-differentiation" of cells, changes in more global pathways rather than in cell-specific ones would be expected. This and the similarities of gene expression régimes between cancer and apoptotic cells further supports the hypothesis that apoptosis in LIRD is due to changes in global rather than specific cellular processes.

The global response to LIRD is also suggested by the "*in silico*" functional analysis of the LIRD genes. The functional groups identified are those that occur in the majority of the cells in the body, rather than representing photoreceptor- or retinal-specific pathways. This further suggests that LIRD results in a global cellular response, rather than one limited to only photoreceptor-specific pathways or even to known apoptotic regulators such as the caspases or Bcl-2 family. Though these apoptotic regulators were not identified in the library screen, our analysis of caspases in LIRD demonstrate that these pro-apoptotic factors are involved (Chapter 3). As these factors are generally regulated at the post-translational level it not surprising that they were not identified as differentially expressed clones.

4.C-2. *In silico* functional analysis of LIRD clones

In silico functional analysis of LIRD genes, and searches of the relevant literature suggested that many of the LIRD genes are known to play a role in apoptosis and/or oxidative stress. As well, analysis of their functions shed some light on their potential role in LIRD as discussed below.

4.C-2a. Kinases, phosphatases and their regulators

Cell:cell communication between the numerous cell types within the retina is critical for normal retinal function (Cohen, 1992; Hart, 1992; Nicholls *et al*, 1992). Alterations in signaling molecules such as kinases, phosphatases and their respective regulatory factors, as well as cross-talk between signaling cascades, can affect many functional pathways, potentially leading to a global cellular response. As well, changes or dysfunction in one cell type can lead to alterations within neighboring cell types. This is especially evident in many cases of retinal disease, where defects in one cell type are manifested by the loss of a different cell type (Alkimets *et al*, 1997; Lagali *et al*, 2000; Zhang *et al*, 2003; Mandel *et al*, 2004).

Signal transduction and alterations in the levels of cellular phosphorylation levels are likely important mediators in the progression of LIRD. Cross-talk between signaling pathways also provides potential means to link various cellular events into a global cellular response. For example, clone 63-6 belongs to the Rho family of Ras-like GTPases. These membrane-associated molecules link signals originating at the plasma membrane to the internal cellular signal transduction cascade, regulating development (Wahl *et al*, 2000; Habas *et al*, 2003), the cell cycle and proliferation (Lacal, 1997), and the cytoskeleton (Maekawa *et al*, 1999). Rho proteins are also important regulators of apoptosis and cancer (Coleman and Olson, 2002; Lacal, 1997; Aznar *et al*, 2004). There is also evidence that reactive oxygen species mediate their apoptotic effects through Rho GTPases (Fiorentini *et al*, 2003; Gregg *et al*, 2004; Chiarugi, 2003). Therefore, this gene represents a mechanism by which the induction of the oxidative stress environment associated with LIRD would be able to lead to differential expression of genes affecting numerous cellular pathways. Similarly, members of the tribbles family, as represented by clone 107-2, TRB2 (tribbles homolog 2), are known to regulate the downstream kinases AKT/PKB (Du *et al*, 2003) and MAPK (Kiss-Toth *et al*, 2004), subsequently regulating proliferation (Seher and Leptin, 2000), development (Grosshans and Wieschaus, 2000) and apoptosis in response to neurotrophin deprivation (Mayumi-Matsuda *et al*, 1999).

Phosphatases act in opposition to kinases to regulate protein function. Clone 136-5 represents the serine/threonine phosphatase subunit, Ppp2r5c, an important regulatory component of the protein phosphatase 2A. Protein phosphatase 2A is a key regulator of DNA replication and gene expression, exocytosis (Sim *et al*, 2003), development (Viallet *et al*, 2003), signal transduction and metabolism (Vazquez-Prado *et al*, 2003), cancer

(Van Hoof and Goris, 2004; Deichmann *et al*, 2001; Ito *et al*, 2003) and apoptosis (Garcia *et al*, 2003; Van Hoof and Goris, 2003). PP2A also appears to regulate the level of phosphorylation of opsin and phosducin following exposure to light (Brown *et al*, 2002). Considering that one of the triggers of LIRD is believed to be the large scale bleaching of rhodopsin following intense light exposure, Ppp2r5c and the subsequent activities of protein phosphatase 2A would provide a downstream mechanism in which the bleached rhodopsin could activate the apoptotic cascade.

4.D-2b. Cytoskeleton components

Apoptosis is characterized by key morphological changes facilitated by changes in the cytoskeleton and extracellular matrix (Bursch *et al*, 1990; Kerr and Harmon, 1991). LIRD genes such the tubulin specific cytoskeleton associated protein (*CKAP1*, clone 117-1), and the microtubule associated protein *MAP1B* (clone 703-8) regulate microtubule formation (Tian *et al*, 1997). Defects in the other microtubule associated proteins, such as Tau, are known to lead to cell dysfunction and death due to defects in cellular transport and unstable tubulin proteins (Guise *et al*, 1999; Fath *et al*, 2002; Elyaman *et al*, 2002). The role of *CKAP1* during apoptosis is unknown, while *MAP1B* has a critical role in neuron outgrowth and axon formation, as knock-out mice were not viable and heterozygotes showed neuronal and vision defects (Edelmann *et al*, 1996; Gonzalez-Billault *et al*, 2004; Tucker, 1990). In addition, *MAP1B* is regulated downstream of the activation of Rho GTPases (Salinas, 1999). Therefore, *MAP1B* may provide a link between the induction of oxidative stress in LIRD, and the apoptotic alterations in the cytoskeleton, through the activities of the Rho GTPases.

Cellular transport is also important for normal photoreceptor cell function, and defects in this process are known to be associated with retinal degeneration in human disease. The well studied molecular motor myosin VIIa, the product of the Usher syndrome 1B gene, is associated with deafness and photoreceptor cell loss leading to blindness (Joensuu *et al*, 2003). Mutations in this protein result in defective rhodopsin translocation from the inner segment to the outer segments of rod photoreceptor cells, and subsequent photoreceptor dysfunction (Wolfrun and Schmitt, 2000). Two differentially expressed LIRD genes, myosin 15 (clone 11-1) and myosin 1B (clone B33-1) are functionally related to myosin V11a. Though the specific target molecules for myosin 15 and myosin 1B are not known, they may also play an important role in transport of additional cellular molecules within the photoreceptor cell.

Aside from regulating cell structure and transport, components of the cytoskeleton are also important mediators of cell signaling. Clone 129-5 is similar to the integrin alpha V subunit previously identified in humans. Integrins are important receptors for a variety of different ECM factors, and regulate changes in cell adhesion and structural components of the actin cytoskeleton (Blystone, 2004; Sastry and Horwitz 1993, Hynes, 1992). In addition, by acting as membrane bound receptors, integrins are able to transform external signals to intracellular signaling response, leading to proliferation (Ross, 2004; Lee and Juliano, 2004), differentiation, changes in gene expression and death of the cell (Lee and Juliano, 2004; Damsky and Werb, 1992). Integrin signaling has also been shown to regulate the development of reactive oxygen species, in addition to being itself regulated by reactive oxygen species. This complex relationship between integrins and oxidative stress is able to regulate integrin binding and signaling pathways

(Gregg *et al*, 2004). The oxidative stress-mediated activation of integrins leads to the activation of NFκB, and Rho-GTPases, both of which are associated with apoptosis in many systems, including LIRD (Coleman and Olson, 2002; Lacal, 1997; Wu *et al*, 2002). Integrin alpha V is highly expressed throughout retinal development and is believed to play an important role in the phagocytosis of outer segments shed by the photoreceptor cells (Clegg *et al*, 2000). As well, integrins have been shown to regulate angiogensis during development (Bader *et al*, 1998) and in cancer progression (Westlin, 2001). Blocking integrin alpha V expression in a murine model of oxygen-induced ischemic retinopathy prevented neovascularization (Luna *et al*, 1996), an important event in the progression of macular disease (Liu and Regillo, 2004; Zarbin, 2004).

4.C-2c. Energy metabolism

Alterations in levels of metabolic proteins and changes to the levels of ATP production would have profound effects on the overall function of metabolically active tissues such as the retina. Several clones identified as differentially expressed LIRD genes are known to be involved in energy metabolism of the cell, specifically, as enzymes catalyzing glycolysis and ATP production through the electron transport chain.

Glycolysis is the process of converting one molecule of glucose into two molecules of pyruvate (Horton *et al*, 1993). Several enzymes involved in this pathway were identified as LIRD genes including hexokinase (*HK1*, clone 126-1), aldolase C (*ALDOC*, clone 136-1), phosphoglycerate kinase (*PGK1*, clone 703-1) and triosephosphate isomerase (*TPI*, clone B33-2). Aside from their role in glycolysis, several of these genes play important roles in apoptosis and/or retinal disease. For example, *HK1* has been shown to be repressed following the induction of apoptosis in response to growth factor withdrawal (Vander Heiden *et al*, 2001), and over-expression of *HK1* is able to prevent apoptosis in rat fibroblast cell lines (Gottlob *et al*, 2001; Bryson *et al*, 2002).

HK1 regulates the opening of the mitochondrial voltage dependent anion channel (VDAC), [also known as the permeability transition pore (PTP)] (Beutner *et al*, 1998), in conjunction with members of the Bcl-2 family (Adams and Cory, 1998; Yang *et al*, 1995). The opening of the VDAC leads to cytochrome c release (Pastorino *et al*, 2002), changes in mitochrondrial membrane potential, and the downstream activation of the caspase cascade (Slee *et al*, 1999). In apoptotic cells, homo-dimers of Bax bind to the VDAC, resulting in its opening, and the induction of apoptosis. HK1 is able to prevent Bax binding to the VDAC, hence preventing the induction of apoptosis (Pastorinon *et al*, 2002). The protein kinase Alt/protein kinase B, has been shown to regulate the interaction of HK1 and Bax in a glucose dependent manner (Majewski *et al*, 2004). Similarly, the levels of glucose regulate the levels of phosphorylated BAD, a promoter of apoptosis, which also regulates hexokinase activity (Danial *et al*, 2003). Therefore, HK1 represents an important link between metabolism and the induction of apoptosis (Pastorino and Hoek, 2003). Interestingly, HK1 has also been shown to play an important anti-oxidant role, preventing the production of reactant oxygen species, another known inducer of cellular dysfunction and apoptosis (Da-Silva *et al*, 2004), and an important trigger in LIRD.

Inhibition of triosephosphate isomerase (clone B33-2) results in increased neuronal cell death of cultured mouse cortical cells (Sheline and Choi, 1998). Mutations in *TPI* are linked to chronic haemolytic anemia and neurodegeneration associated with triosephosphate isomerase deficiency (Olah *et al*, 2002). The mutant form of TPI is structurally unstable and becomes predisposed to form aggregates with microtubules, similar to those seen in patients with Alzheimer disease. In Alzheimer disease, the link between defects in ATP production and aberrant protein folding and localization is evident, as alterations in the levels of glucose and ATP regulate the proper insertion of the β-amyloid precursor protein (βAPP) into the synaptic membranes (Meier-Ruge *et al*, 1997, Olah *et al*, 2002). Misfolded βAPP binds to and inhibits metabolic enzymes, an event that further reduces glycolysis and oxidative phosphorylation. Therefore, studies involving *TPI* demonstrate a link not only between cellular metabolism and apoptosis, but a novel link between cellular metabolism and protein folding.

Defects in phosphoglycerate kinase (PGK-1, clone 703-1) are associated with retinitis pigmentosa with myopathy (Tonin *et al*, 1993). PGK1 has also been shown to be secreted by cancer cell lines, where it acts as a disulfide reductase, regulating the cells' response to oxidative stress (Lay *et al*, 2000). In this role, PKG-1 cleaves a disulfide bond in the protein plasmin, which plays a role in angiogenesis (Hogg *et al*, 2002). PGK-1 has also been shown to be induced following apoptotic cell death in retinal cell cultures in response to both hypoxia and serum withdrawal (Xu *et al*, 1999). Additional roles for PKG-1 in the nucleus as a DNA binding protein have also been suggested, suggesting a role in transcription, DNA replication or chromatin structure (Ronai, 1993).

Several LIRD genes encode enzymes involved in oxidative phosphorylation. These include a rat gene similar to NADH ubiquinone dehydrogenase (clone 102-5), cytochrome oxidase 6A (clone 48-1), cytochrome oxidase 1 (clone 648-4) and NADH dehydrogenase 4L (clone 648-6), and adenine nucleotide translocator 2 (clone 13-3). The LIRD genes NADH dehydrogenase 4L (*ND4L*) and NADH ubiquinone dehydrogenase (*NDUFB4*) are both members of the NADH-ubiquinone oxidoreductase complex of the electron transport chain. The complex as a whole has been well-studied, although less is known about the individual subunits that make up this complex. Several subunits have been associated with apoptosis and neurodegenerative disease, specifically Parkinson disease, Alzheimer disease and Down syndrome (Fearnley *et al*, 2001; Kim *et al*, 2001; Swerdlow *et al*, 1996). Little information is available regarding *ND4L* and *NDUFB4*, though several studies have demonstrated mutations in *ND4L* as the genetic basis of several cases of Leber optic atrophy (LHON) (Brown *et al*, 1995; 2002a; 2002b, 2002c).

The LIRD genes, cytochrome c oxidase 1 (cox1) and cytochrome oxidase 6a1 (Cox6a1), represent two of the thirteen members of complex IV of the electron transport chain. Though the specific role of these genes in not known during apoptosis, the activity of Complex IV is known to be repressed in cardiomyocytes cells treated with H2O2, providing a link between oxidative stress and disruption of energy metabolism (Long *et al*, 2004). In addition, the levels of cytochrome c oxidase III, as well as several additional oxidative phosphorylation associated genes including NADH dehydrogenase subunit 3 (ND-3), and ATPase 6, are known to be modulated in response to light levels, providing a direct link between light exposures and ATP synthesis (Haung *et al*, 2004).

Adenine nucleotide translocator 2 (ANT2, clone 13-3) regulates the exchange of matrix ATP for cytosolic ADP across the inner mitochondrial membrane during oxidative phosphorylation (Brown and Wallace, 1994; Graham *et al*, 1997). The level of ADP in mitochondria plays a critical role in the regulation of cellular metabolism, making ANT2 an important regulator of a cells metabolic output. In addition, ANT2 has been shown to be a component of the VDAC, and has been shown to play a regulatory role in apoptosis (Marzo *et al*, 1998). In apoptotic cells, ANT2 interacts with the pro-apoptotic Bax and the VDAC, facilitating the release of cytochrome c (Brenner *et al*, 2000). This ANT2-Bax interaction is regulated by the anti-apoptotic properties of the Bcl-2 protein. Oxidation of a critical thiol residue on ANT2 prevents association with Bcl-2 and promotes interactions with Bax and the induction of apoptosis (Constantini *et al*, 2000). Therefore, like numerous other energy metabolism associated LIRD genes, ANT-2 represents a possible mechanism linking ATP synthesis levels, oxidative stress and the activation of caspases and apoptosis.

4.C-2d. Transcriptional Regulators

Apoptosis is mediated by changes in gene expression (Bursch *et al*, 1990), and inhibition of transcription and/or translation is able to prevent the induction of apoptosis (Naora, 1995; Yonish-Rouach, 1995). Several of the clones identified as LIRD genes represent known transcription factors, including activator of transcription 4 (ATF4/CREB2), Cited2/Mrg-1 (Cbp/p3000-interacting transactivator with Glu/Asp-rich carboxyl terminal domain), TATA box binding protein related factor 2 (TBPL2), the rat orthologs of the mouse cAMP responsive element binding protein 3-like 2 (CREB3L2) and zinc finger protein, subfamily 1A, 5 (Zfpn1a5).

Basal transcription is mediated through the interactions of RNA polymerase II with a complex of TF (transcription factor) IIA, B, D, E and F (Alberts *et al*, 1994; Walker *et al* 2004). Though TFIID itself is generally comprised of a TATA binding protein (TBP) and various TATA box binding protein related factors, TBP can be replaced by one of several TATA binding protein like proteins (TBPL) that regulate the basal transcription of a subset of genes in a temporal and spatial manner (Walter *et al*, 2004; Rabenstein *et al*, 1999). The LIRD clone TBPL2 represents one such protein that could replace TBP in the transcriptional initiation complex, regulating the expression of genes containing TATA-less promoters (Shimada *et al*, 2003). Interestingly, TBPL2 is normally sequestered in the cytoplasm, but is translocated into the nucleus in response to cell stress, where it regulates the induction of apoptosis. Therefore, TBPL2 may regulate the differential expression of a specific subset of genes in response to oxidative stress during LIRD.

CITED2, also known as MRG-1, acts as a transcriptional regulator by binding to the co-activators CBP and p300, and has been shown to be important in controlling cell growth, apoptosis, transformation and embryonic development. (Shikama *et al*, 1997; Goodman and Smolik, 2000; Giordano and Avantaggiati *et al*, 1999). CITED2 is shown activated by cytokine signaling, specifically IL-9, and has been shown to compete with the transcriptional activator HIF-1 for CBP/p300 binding (Sun *et al*, 1998). The HIF-1/p300/CBP complex is able to activate VEGF, which leads to neovascularization in several systems, including the retina (Grimm *et al*, 2002). CITED2 regulates two known pro-apoptotic mediators of LIRD, including AP-1, where CITED 2 regulates AP-1 activity by functioning as a co-activator (Fox *et al*, 2004) and p53, where Cited2 regulates the activity of p53 by controlling the ubiquitin-mediated proteolysis of p53 (Matt *et al*, 2004). As well, CITED2 has been shown to bind to the TATA-binding protein transcriptional activator, modulating its activity as well. Therefore, CITED2 may regulate the activity of more ubiquitiously expressed transcriptional activators by controlling which interactions are able to form under certain conditions, potentially leading to the induction of apoptosis.

A common event in the progression of apoptosis is repression of translation; and re-activation of protein synthesis in a cell promotes survival (for review see Pachen, 2003; Ron, 2002; Clemens *et al*, 2000). Though most proteins are not translated during apoptotic repression of protein synthesis, several transcripts are known to be preferentially translated. One such transcript encodes ATF4/CREB2 (Blais *et al*, 2004). The endoplasmic reticulum kinase PERK, known to regulate the repression of translation (for review see Pachen, 2003; Ron, 2002; Clemens *et al*, 2000), is also known to induce the translation of ATF4 in response to hypoxia (Blais *et al*, 2004). ATF4 then activates the protein phosphatase 1 regulatory subunit GADD34, which leads to the dephosphorylation of eIF2alpha. Therefore, the activation of ATF4 may be an important step in the reactivation of protein synthesis in cells subjected to hypoxia and oxidative stress (Blais *et al*, 2004; Harding *et al*, 2003; Novoa *et al*, 2003). ATF4 is also known to regulate *VEGF* (Roybal *et al*, 2004) and *HO-1* (He *et al*, 2001), both of which have been identified as potential mediators of LIRD (Grimm *et al*, 2002; Kutty *et al*, 1995; Organisciak *et al*, 1998; Wong *et al*, 2001). During murine lens development, a lack of ATF4 results in large scale apoptosis of lens-precursor cells, leading to failure in lens formation (Hettmann *et al*, 2000). In addition, over-expression of *ATF4* in the mammary glands of transgenic mice leads to premature mammary gland involution (Bagheri-Yarmand *et al*, 2003), a process known to involve apoptosis (Furth *et al*, 1997). Interestingly, an additional member of the ATF4/CREB2 family of transcription factors, the putative rat ortholog of CREB3L2 (clone 633-6), was also identified as a LIRD gene, though the role of this gene in apoptosis is unknown.

4.C-2e. Ribosomal binding proteins, splicing factors and translational regulators

Like transcription, translation is essential to the progression of apoptosis (Noara, 1995; Yonish-Rouach, 1995). Inhibition of translation, through agents such as cycloheximide, results in inhibition of apoptosis, including that induced by phototoxic injury in rats (Shahinfar *et al*, 1991). Work in our laboratory has demonstrated that ribosomal binding proteins, known regulators of translation, are important players in the progression of LIRD (Stepczynski 2001; Grewal and Stepczynski *et al*, 2004). To date there are over 80 different ribosomal binding proteins known to associate with the ribosome (Kenmochi *et al*, 1998). By altering the makeup of ribosomal binding proteins associated with the ribosome, translation and possibly transcript preferences can be regulated (Grewal and Stepczynski *et al*, 2004). As well, aside from their role in translation, ribosomal binding proteins play roles in many cellular processes including apoptosis, differentiation, development, proliferation, repair of DNA damage, and disease progression (Wool *et al*, 1995; Naora *et al*, 1998; Chiao *et al*, 1992; Deutsch *et al*, 1997; Frigerio *et al*, 1995; Pogue-Geile *et al*, 1991; Neumann and Krawinkel, 1997; Horino *et al*, 1998; Seshadri *et al*, 1993; Watson *et al*, 1992; Goldstone *et al*, 1993; Wool, 1996; Naora and Naora, 1999; Zhang *et al*, 2002; Kim *et al*, 1995).

The LIRD gene *DPH5*, which encodes a diphthamide methyltransferase, is a potential regulator of translation elongation. The role of this gene in apoptosis is discussed in detail in chapter 5. Interestingly, another LIRD gene, encoding eukaryotic translation elongation factor 1 delta (eEF-1δ), also regulates translational elongation. Though eEF-1δ has not been linked to apoptosis, it has been shown to be induced in cancer cells (Joseph *et al*, 2002). Several other translation elongation factors have also been linked to the progression of cancer, degenerative disease and apoptosis in various systems (for review see Thorton *et al*, 2003; Abbott and Proud, 2004; Kaufman, 2004).

Two LIRD genes identified are known to play a role in RNA splicing, including RALY (similar to hnRNP-associated with lethal yellow gene product), and the rat *SFRS6* (splicing factor arginine/serine rich 6). RALY is a member of the class of heterogeneous nuclear riboproteins that interact with immature hnRNA molecules in the nucleus and function in their translocation to the cytoplasm and splicing into mature mRNA (Pinol-Roma, 1997). SFRS6 is involved in RNA splicing and regulates the selection of splice sites (Lai *et al*, 2003). Though the role of these genes in apoptosis is unknown, differential alternative splicing is known to be involved in the regulation of the AMPA (alpha-amino-3-hydroxy-5-methyl-4-isoxazole propionate) receptor GluR1 (glutamate receptor 1) during LIRD (Harada *et al*, 1998)

4.C-2f. Chaperone and heat shock proteins

The induction of apoptosis in LIRD involves the production of high levels of oxidative stress (Yamashita *et al*, 1992; Organisciak *et al*, 1992b), likely produced in response to rhodopsin bleaching by intense light exposure (Demontis *et al*, 2002;

Delmelle *et al*, 1977). Oxidative stress leads to damage to cellular proteins, lipids and DNA, and the subsequent induction of heat shock proteins and chaperones, as the cell attempts to deal with the accumulating misfolded proteins (for review see Pachen, 2003; Ron, 2002; Clemens *et al*, 2000). Failure to induce such stress proteins would lead to an inability to repair cellular damage leading to an accumulation of misfolded proteins, disruption of cellular pathways, and eventual cell death. Work in our lab by Benjamin MacDonald involved analysis of the expression of heat shock proteins and crystallins, including the LIRD gene B2-crystallin (Crybb2), during LIRD. Though originally identified as the major structural protein of the lens (Sergeev *et al*, 2004), crystallins have more recently been demonstrated to function as heat shock proteins in other tissues (Magabo *et al*, 2000), and are believed to play a protective role in the retina in response to light exposure (Jones *et al*, 1999; Sakaguchi *et al*,2003). Results in our laboratory determined that there are two waves of stress protein induction, an early response, likely representing the cell's attempt to deal with the increasing levels of oxidative damage, and a late response, representing the attempt of the surviving cells to deal with the stresses incurred by being in an apoptotic environment (MacDonald, 2002).

Cct4 (chaperonin subunit 4) is a component of a multi-peptide complex responsible for mediating the correct folding of newly translated cellular proteins including actin, tubulin and alpha transducin (Yokota *et al*, 2001; Farr *et al*, 1997; McCallum *et al*, 2000). The levels of intact transducin help regulate the phototransduction cascade, and are altered following light exposure. Mice lacking alpha transducin show reduced sensitivity to LIRD under certain conditions (Hao *et al*, 2002; Grimm *et al*, 2000). Though the exact role of Cct4 during apoptosis has not been determined, mutations in Cct4 are linked to neuronal degeneration in the mutilated-foot rat, which loses sensory neurons in the limbs and skin (Hsu *et al*, 2004).

Synuclein proteins are also members of multi-protein chaperone complexes. Alpha synuclein, has been well studied and is known to be a major protein involved in the progression of Parkinson disease (PD), Alzheimer disease and other neurodegenerative disorders where protein aggregates are involved (for review see Bertoli-Avella *et al*, 2004; Spliiantini *et al*, 1997; Takeda *et al*, 1998). In PD, defective alpha synuclein is a major component in Lewy body aggregates. Though the LIRD gene gamma synuclein (*SNCG*) has not been associated with degenerative disorders, studies in breast cancer lines have demonstrated that SNCG is a component of a multi-protein chaperone complex in the endoplasmic reticulum, in conjunction with numerous heat shock proteins including HSP70 and HSP90 (Jiang *et al*, 2004). Here SNCG helps regulate the formation of membrane bound steroid receptors destined to be expressed on the cell surface, thereby potentially helping to regulate signaling by these molecules.

4.C-2g. Vesicle transport

During normal photoreceptor cell function, there is extensive shedding of the ROS, requiring high levels of proteins and fatty acid synthesis to replace the lost outer membranes. Membrane associated proteins or secreted proteins are synthesized predominantly in the rough endoplasmic reticulum, are then carried through the Golgi apparatus, and then to the membrane via vesicle transport. One of the major groups of proteins involved in vesicle transport are the coatamer protein coated vesicles. The coatamer protein is a complex of seven subunits including the α, β, β', δ, ε, γ, and ζ COP subunits (reviewed in Wegmann *et al*, 2004). Two of these subunits, the gamma and beta prime complex were identified as LIRD genes in this study. Following assembly into vesicles, molecules move to their destination in a manner regulated by Rab GTP binding proteins. The LIRD gene, *MSS4*, encodes a GTP-GDP exchange protein that associates with the Rab proteins and modulates their function (M□ller-Pillasch *et al*, 1997). An additional LIRD gene, *RRG4*, is believed to be associated with vesicle transport, though its exact role in this process is still speculative (Kubota *et al*. (2002). Mutations in the human ortholog of this gene, *HRG4*, are associated with photoreceptor cell loss and the development of cone-rod dystrophy (Kobayashi *et al*, 2000). Though these genes have not been directly associated with apoptosis, it is possible that alterations in the expression levels of these genes during LIRD could disrupt cellular transport and localization of membrane bound or secreted proteins leading to cellular dysfunction and the induction of apoptosis.

4.C-2h. Ubiquitinylation

Several of the differentially expressed LIRD clones are known components of the ubiquitinylation pathway. These include the ubiquitinylation conjugating enzyme *UBCM2* (clone 155-2), poly-ubiquitin (clone 1442-1) and the ubiquitin ligase *NEDD4* (clone 1497-3). Ubiquitinylation plays a key role in protein trafficking (Dunn *et al*, 2004; Marmor and Yaaarden, 2004), regulation of the cell cycle, cytokine-induced gene expression, differentiation, cell death and stress response (Obin *et al*, 1998). Ubiquitinylation is also a critical mechanism for the removal of stress-damaged or conformationally altered proteins via degradation by the 26S proteosome (Ciechanover and Schwartz, 1994; Wilkinson, 1995), and is known to play an important role in mediating Parkinson disease, Alzheimer disease (Kajimoto *et al*, 1992) and LIRD (Yamashita *et al*, 1992).

NEDD4 (Neuronal precursor cell expressed, developmentally down-regulated) is a ubiquitin (Ub) ligase involved in calcium-mediated ubiquitinylation of membrane associated ion channels, receptors and transport proteins (Kumar *et al*, 1997; Harvey and Kumar, 1999; Dinudom *et al*, 1998; Fotia *et al*, 2004; Dieter *et al*, 2004; Henke *et al*, 2004). The ubiquitin conjugating enzyme UBE2E3, isolated from the execution phase cDNA library screen, also plays a role in the ubiquitinylation of Na+ channels (Debonneville and Staub, 2004).

NEDD4 has also been shown to promote the degradation of the anti-apoptotic Bcl-10, resulting in the repression of NFκB (Scharschmidt *et al*, 2004), an important pro-apoptotic factor in LIRD (reviewed by Remé *et al*, 1998). In addition, though Bcl-10 itself has not been studied in retinal apoptosis, members of the Bcl-2 family of apoptotic regulators have also been linked to photoreceptor cell loss in LIRD (Takahashi *et al*, 2004; Wu *et al*, 2003; Shinoda *et al*, 2001; Crawford *et al*, 2001). NEDD4 is also a target of the activated caspase cascade, specifically of caspases 3, 6 and 7, following the induction of apoptosis (Harvey *et al*, 1998). This may result in defects within the ubiquitinylation pathway of the cell, possibly resulting in the accumulation of pro-apoptotic proteins, which are normally cleared by ubiquitinylation. Alternatively, a defective ubiquitinylation system would likely not be able to keep up with the accumulating damaged proteins induced by excessive light or oxidative stress, and hence these defective proteins would build up and lead to cellular dysfunction and death. This hypothesis is supported by the observation that photoreceptor apoptosis and degeneration in RP is induced by chronic expression of aberrant photoreceptor proteins (Dryja *et al*, 1991; Papermaster and Windle, 1995).

NEDD4 also regulates the ubiquitinylation of the angiogenesis associated VEGF receptor 2 levels (Murdaca *et al*, 2004), and the glutamate transporter EAAT1 (Boehmer *et al*, 2003). Glutamate is the key neurotransmitter released by resting photoreceptor cells. Therefore, NEDD4 may play a role in the regulation of the level of neuronal excitation within the retina. Ubiquitinylation is also believed to regulate the phototransduction cascade. Both rhodopsin and transducin are conjugated to ubiquitin following light exposure (Obin *et al*, 1996).

Northern blot analysis of LIRD genes associated with ubiquitinylation showed that all of the genes studied showed an initial induction following 4 hours of light treatment, with a subsequent decrease in expression levels after 8 and 16 hours of light exposure. This suggests an early attempt by the cell to deal with the light-induced accumulation of damaged proteins by increasing the levels of proteins associated with ubiquitin-mediated proteolysis. As LIRD progresses, a reduction in the levels of these proteins may contribute to global cellular dysfunction, promoting cell death, due to a reduced ability to clear damaged and misfolded proteins resulting from the oxidative stress and apoptotic environment. The similar expression patterns of all of the ubiquitinylation genes analyzed is not unexpected, in light of the fact that ubiquitinylation itself is a multi-step process involving the actions of numerous proteins for completion. Therefore, in order to increase the levels of ubiquitinylation and ubiquitinylation-mediated proteolysis within the cell, the induction of several genes is required. As well, since ubiquitinylation is a mechanism used to regulate levels of key target proteins within a cell, the induction of genes such as PGP9.5, which can reverse the ubiquitinylation of these proteins, would also be expected to play a role in the regulation of the enzymes that are actively ubiquitinylating proteins in the cell.

4.C-2i. Phototransduction

Only a small number of phototransduction or photoreceptor specific genes were found to be differentially expressed during the progression of LIRD. Indeed, of the 4 different genes identified, only rhodopsin and phosducin were limited to or highly enriched in photoreceptor cells. Rhodopsin, one of the major protein constituents of the rod outer segments, consists of an opsin protein and a chromophore 11-cis-retinaldehyde, constituting the primary photopigment within the rod cells. The identification of rhodopsin as a LIRD gene is important in light of its significant role in retinal disease, oxidative stress and lights phototoxic effects. Mutations in rhodopsin account for over 15% of known cases of retinitis pigmentosa (NCBI OMIM website, entry 180380, rhodopsin, July 2004). Over 70 different disease-causing mutations are known to occur in rhodopsin, and many of these lead to an inability to respond to light and initiate the phototransduction cascade, leading to cellular dysfunction, death of the photoreceptor cells and subsequent blindness. Rhodopsin is also a key factor in the etiology of photoreceptor cell death in response to light. In rodent models of retinal cell loss, mice lacking rhodopsin are resistant to light-induced photoreceptor cell loss (Grimm *et al*, 2000b), and the levels of rhodopsin per eye are an important indicator of retina cell sensitivity to phototoxic stress (Noell *et al*, 1971a, b; Organisciak *et al*, 1977;

Organisciak *et al*, 1991; Katz *et al*, 1993). In addition, it is the light-induced bleaching of rhodopsin that is believed to be one of the key triggers of cell death in LIRD.

In addition to the over stimulation of the phototransduction cascade, the bleaching of rhodopsin may lead to increases in the levels of oxidative stress in a cell, as the bleached form of rhodopsin is known to induce oxidative free radical formation (Delmelle *et al*, 1977) and lipid peroxidation (Demontis *et al*, 2002), known mediators of cell death in LIRD. Therefore, the initial induction of rhodopsin following 4 hours of light treatment may represent the cell's initial attempt to increase the levels of available unbleached rhodopsin as the retina struggles to regenerate the large population of rhodopsin bleached by intense light exposure. Though initially a survival attempt, this increase in rhodopsin eventually proves to be a disadvantage to the photoreceptor cell, as it too becomes bleached leading to an increase in oxidative stress, overloading the already overtaxed regeneration systems. This would lead to cell dysfunction and the induction of the apoptotic cascade.

An inability to regenerate the bleached rhodopsin has been shown to protect against LIRD (Wenzel *et al*, 2001a). Knock-out mice lacking RPE65, a RPE-expressed gene that plays a role in rhodopsin regeneration, are resistant to LIRD (Redmond *et al*, 1998; Grimm *et al*, 2000b; Grimm *et al*, 2001). In addition, the LIRD gene retinol dehydrogenase 11 (RDH11), which is also localized to the RPE, is involved in the conversion of all-trans retinal into 11-cis retinal, facilitating the regeneration of unbleached rhodopsin (Haeseleer *et al*, 2002). Therefore, by altering the ability of the retina to regenerate the high levels of bleached rhodopsin incurred by light exposure, the sensitivity to light exposure can be controlled. Specifically, inhibiting or reducing the regeneration of rhodopsin following large-scale bleaching, prevents continuous over-activation of the phototransduction cascade, protecting against cell death.

The induction of the LIRD gene guanylate cyclase activator 1a (*GUCA1A*) following 4 and 8 hours of light exposure would likely also represent an initial response to the over-stimulation of the phototransduction cascade in response to light. Guanylate cyclase helps to control the level of polarization, and hence neurotransmitter release by the photoreceptor cell, by regulating the levels of GTP that is converted to cGMP. In an unstimulated cell, cGMP interacts with cellular calcium gated channels, keeping them open and resulting in a continuous depolarization of the cell, and glutamate release to the bipolar cells. In a light stimulated cell, the levels of cGMP drop, the ion channels close, the cell becomes hyperpolarized, and glutamate release stops. This leads to changes in the bipolar cells that facilitate the transduction of the visual signal through the retina to the brain. By regulating the levels of guanylate cyclase and hence cellular cGMP levels, guanylate cyclase activator protein 1a would help to prevent over stimulation of the retina by keeping levels of cGMP high, subsequently keeping the ion channels open and the photoreceptor cell in a depolarized state. This may represent a survival tactic to help counteract the effect of the light signal and return the photoreceptor to a normal state. This in essence could also help to keep the effect of the toxic light levels limited to the photoreceptor cell rather than spreading it to the other cells of the retina, which are known to survive following toxic light exposures (Noell *et al*, 1966). GUCA1A function is critical for the survival of the photoreceptor cells, as mutations in this gene are known to cause photoreceptor cell loss in humans and transgenic mice (Olshevskaya *et al*, 2004; Wilkie *et al*, 2001; Downes *et al*, 2001; Payne *et al*, 1998).

Phosducin helps to control phototransduction by competing with α-transducin for binding to β- and γ-transducin in a light-dependent manner (Thulin *et al*, 2001; Xu *et al*, 1995; M□ller *et al*, 1996; Savage *et al*, 2000; Lee *et al*, 1984). When the β- and γ-subunits are bound to phosducin, they are unable to bind to α-transducin, and the downstream phototransduction cascade can not be activated. Therefore, the repression of phosducin following light exposure would be expected to result in an increase in β- and γ-subunits available for binding by α-transducin, facilitating the large-scale activation of the phototransduction cascade. Alternatively, the repression of phosducin may have a different function within the photoreceptor. Normally phosducin is localized to the inner segment of the photoreceptor cell, and is translocated to the outer segment following light treatment (Thulin *et al*, 1999). Therefore, it is possible that aside from its role in modulating phototransduction in the outer segment, phosducin regulates G-protein signaling in the inner segment as well. Interestingly, phosducin-like proteins have been shown to negatively regulate the activities of the chaperonin complex (McLaughlin *et al*, 2002), a component of which, Cct4, was identified as a LIRD gene. Therefore, the repression of phosducin during LIRD may lead to the activation of numerous cellular processes dependent on G-protein signaling in addition to potential effects on the phototransduction cascade.

Northern blot analysis of several genes associated with the phototransduction cascade demonstrated that, unlike the genes involved in the ubiquitinylation pathway, there was no evidence of coordinate expression seen with the genes involved in phototransduction. This is not unexpected as phototransduction is a cyclic process and involves both positive and negative regulation of protein functions for its completion.

The observed induction of opsin and IRBP at the onset of intense light exposures would be expected to promote the activation of the phototransduction cascade by increasing the amount of photo-pigment available to absorb the increased light. The repression of recoverin and phosducin following light exposure would also increase the activity of the phototransduction cascade. Recoverin is able to inhibit opsin phosphorylation by rhodopsin kinase, thereby terminating the activation of the phototransduction cascade (Chen, 2002). Phosducin in its role in the regulation of transducin, would also the regulate the activation of the phototransduction cascade (Thulin *et al*, 2001; Xu *et al*, 1995; M□ller *et al*, 1996; Savage *et al*, 2000; Lee *et al*, 1984). Repression of both of these proteins would result in a decreased termination of the light-induced signaling induced by bleached rhodopsin. In contrast, the induction of arrestin, and GCAP, would be expected to shut down the phototransduction cascade in response to intense light. Increases in the levels of guanylate cyclase would open ion channels, returning the photoreceptor to its depolarized state (Sarri *et al*, 1992). Arrestin binds to phosphorylated opsin, limiting its activation of transducin, and therefore terminating the activation of the phototransduction cascade. The termination of the phototransduction cascade allows for all of the key players to return to a resting state, where they can be reactivated to again reinitiate the active phototransduction cascade.

Therefore, alterations in the level of any of the genes involved in phototransduction would result in an imbalance in the phototransduction cascade, subsequent photoreceptor cell dysfunction and potential cell death.

4.C-3. Summary

The work described here represents the first step in the characterization of the global molecular events associated with the progression of LIRD. Our results suggest that apoptosis in LIRD is largely mediated by global cellular dysfunction, in conjunction with a small number of photoreceptor cell- or retinal cell-specific changes. These changes appear to be mediated by the differential expression of genes showing widespread tissue expression, rather than retinal- or photoreceptor-specific genes.

It is important to keep in mind, when considering any mRNA profiling technique, that regulation at the level of transcription is only one step in the complex regulatory circuits controlling gene expression. One must keep in mind that other mechanisms will be involved in the regulation of gene expression, including transcript targeting to the ribosome by ribosomal binding proteins, regulation of translation efficiency of the ribosome, alternate splicing, post-translational modifications, and protein-protein interactions. Our approach only detects changes at the transcriptional level. Therefore, when interpreting the results of this study, one must remember that changes in protein expression may not always be correlated with changes in transcript levels (Gygi *et al*, 1999; Madi *et al*, 2003). For example, microarray analysis of light-induced gene expression by Choi *et al* (2001) failed to demonstrate changes in the expression levels of several pro-apoptotic genes, including the members of the caspase cascade. In regards to the caspases, which are largely regulated at the post-translational level, this may explain why this category of genes was not identified in our screen.

Indeed, those LIRD genes that have been shown to be associated with apoptosis are known to act through the disruption or alteration of global events rather than by direct activation or repression of apoptosis-specific events. As the majority of apoptosis-associated LIRD genes identified were dark-enriched, this suggests a repression of normal cell function, rather than the specific activation of apoptotic events. In addition, many of the LIRD genes, though acting predominantly in a particular cellular pathway, were able to affect numerous distinct pathways as well, further suggesting a global rather than a specific response.

One should also keep in mind that it is not possible to determine from this analysis any cause or effect relationship between the differential expression of a gene and the progression of LIRD. One is also not able to determine the identity of the cells in which the differential expression of a particular gene is occurring, or even if the cells are surviving or dying during LIRD. In addition, the differential expression patterns observed is representative of the combined expression of a particular gene within the numerous cell types of the retina. For example, the induction of a gene in one cell type could be masked by a similar level of repression of the same gene in other cells. Keeping these shortfalls in mind, analysis of differential gene expression still provides a good starting point to identify potentially important genes for further characterization. To be truly informative, our data will need to be linked with detailed bioinformatic analysis, functional analysis, and protein analysis.

The results of this study stresses the importance of focusing on the entire cellular and tissue environment when studying a particular physiological process rather than on one particular gene or protein, or even one cell type. It is likely a combination of events, and shifts within cellular and tissue dynamics that underlie most cellular change, including apoptosis.

Chapter 5

Identification of a novel rat diphthamide methyltransferase, which plays a role in oxidative stress-induced cell death.

Contributors:

Dr. Jack vonBorstel: technical support for yeast assays

Dr. Daniel Organisciak, Ruth Darrow, and Linda Barsalou: rat retinal tissues

Pat Murray, Lisa Ostafichuk (MBSU): automated sequencing

Ron Koss: yeast sections for TEM

Randy Mandryk, Jack Scott, and Dr. Rakesh Bhatnagar: technical assistance with TEM

5.A. INTRODUCTION

Light-induced retinal degeneration in rats (LIRD) is a well-studied model of human retinal dystrophy (Wong *et al*, 2001, Noell *et al*, 1966; Organisciak and Winkler, 1994; Remé *et al*, 2003). Photoreceptor cell loss following exposure to intense green light is believed to occur as a result of the large scale bleaching of the photo-pigment rhodopsin (Noell *et al*, 1971a, b), and apoptotic cell death (Organisciak *et al*, 1994; Hafezi *et al*, 1999a; Wenzel, 2000) as indicated by the presence of DNA fragmentation and TUNEL positive nuclei (Organisciak *et al*, 1995, Abler *et al*, 1996; Shahinfar *et al*, 1991). In addition, the development of an oxidative stress environment is an important event in light-induced cell death (Demontis *et al*, 2002; Carmody *et al*, 1999; Organisciak *et al*, 1984, Tso *et al*, 1984; and Demontis *et al*, 2002). Pretreatment of rats with anti-oxidants such as ascorbic acid, dimethylthiourea (DMTU), or exogenous thioredoxin protects against light-induced photoreceptor cell loss in rodent models (Li *et al*, 1985; Organisciak *et al*, 1984; Organisciak *et al*, 1992b; and Tanito *et al*, 2002a, b).

As the molecular mechanisms involved in LIRD are not well understood it was our goal to identify genes that were differentially expressed following exposure to intense green light. As such, we constructed a rat retinal cDNA library from retinae treated with 8 hours of intense green light, a treatment believed to represent an execution phase of active cell death (Wong *et al*, 2001). Differential cross screening of this cDNA library was performed using total cDNA populations derived from control dark-reared rat retinae or from 8-hour light-treated retinae. This resulted in the identification of a large number of differentially expressed cDNA clones. One such clone was found to represent a previously uncharacterized rat gene with significant homology to the yeast *DPH5* gene, which encodes a diphthamide methyltransferase.

In yeast, *DPH5* is known to encode a AdoMet-dependent methyltransferase which, in the presence of S-adenosyl-L-methionine, catalyzes the modification of EF (elongation factor)-2 2-[3-carboxyamido-3-(methylammonio)-propyl]-L-histidine into EF-2 diphthine, a precursor of the final product EF-2 diphthamide (Figure 5.1; Mattheakis *et al*, 1992; Moehring *et al*, 1984; Chen and Bodley, 1988; Chen *et al*, 1985). This single histidine residue on EF-2 is the only known amino acid in the cell to be modified by DPH5. Although the functional significance of this modification in a normal cell is unknown, the formation of EF-2 diphthamide is known to convey sensitivity to exogenous ADP ribosylation factors such as diphtheria toxin and *Pseudomonas* toxin A (Moehring *et al*, 1980; Foley *et al*, 1995). Such exogenous toxins transfer an ADP ribose group from NAD+ to the imidazole ring of EF-2 diphthamide (Moehring *et al*, 1980; Moehring *et al*, 1984; Van Ness *et al*, 1980a, b; Morimoto and Bonavida, 1992). This results in an inactivation of EF-2, a subsequent block in translation, and apoptotic cell death (Morimoto and Bonavida, 1992; Kurita *et al*, 2003). This inhibition is very efficient, as only a single diphtheria toxin molecule is sufficient to kill a mammalian or yeast cell (Yamaizumi *et al*, 1978; Chen *et al*, 1985; Murakami *et al*, 1982). Cells mutant for *DPH5* or other members of the diphthamide biochemical pathway show normal protein synthesis, but are resistant to the effects of diphtheria toxin and *Pseudomonas* toxin A (Moehring *et al*, 1980; Phan *et al*, 1983; Foley *et al*, 1995; Mattheakis *et al*, 1992; Chen *et al*, 1985).

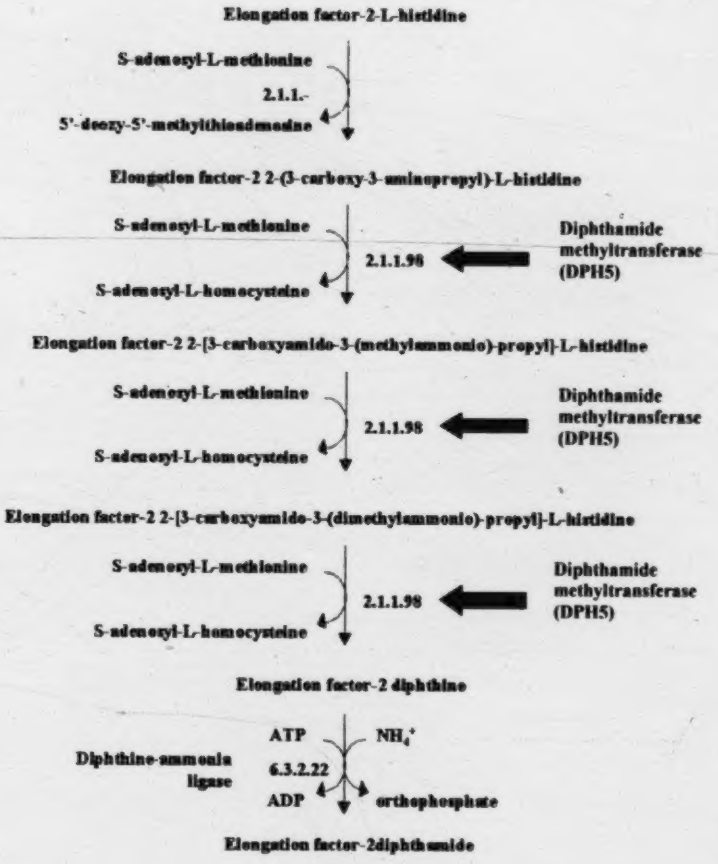
Elongation factor-2-L-histidine
S-adenosyl-L-methionine
2.1.1.-
5'-deoxy-5'-methylthioadenosine
Elongation factor-2 2-(3-carboxy-3-aminopropyl)-L-histidine
S-adenosyl-L-methionine
2.1.1.98
S-adenosyl-L-homocysteine
Diphthamide methyltransferase (DPH5)
Elongation factor-2 2-[3-carboxyamido-3-(methylammonio)-propyl]-L-histidine
S-adenosyl-L-methionine
2.1.1.98
S-adenosyl-L-homocysteine
Diphthamide methyltransferase (DPH5)
Elongation factor-2 2-[3-carboxyamido-3-(dimethylammonio)-propyl]-L-histidine
S-adenosyl-L-methionine
2.1.1.98
S-adenosyl-L-homocysteine
Diphthamide methyltransferase (DPH5)
Elongation factor-2 diphthine
ATP
NH$_4^+$
Diphthine-ammonia ligase
6.3.2.22
ADP
orthophosphate
Elongation factor-2diphthamide

Figure 5.1. Formation of EF-2 diphthamide. (A) Modification of EF-2 by DPH5, with the reaction catalyzed by known DPH5 orthologs indicated by the arrow. Image adopted from the WIT/EMP/MPW biochemical pathway database (http://mips.gsf.de/genre/proj/ yeast/searchEntryActiondo?text=).

This work represents the first report of the isolation and characterization of a novel rat gene believed to encode a diphthamide methyltransferase. This gene is repressed following treatments of intense green light that are believed to represent the execution and oxidative stress phase of LIRD. As well, using an oxidative-stress sensitivity assay in yeast we demonstrated that yeast DPH5 loss-of-function mutant cells were more sensitive to oxidative stress-mediated cell death than wild-type cells. Analysis of the wild-type and mutant yeast cells using transmission electron microscopy (TEM) demonstrated morphological features characteristic of apoptotic cell death following the induction of oxidative stress. This suggests that the repression of rat DPH5 during LIRD may increase the sensitivity of retinal cells to oxidative stress and the apoptotic events that develop following light treatment. Considering the function of the yeast DPH5, it is also possible that this increased sensitivity could be mediated at the level of translation elongation.

5.B. RESULTS

5.B-1. Isolation of the putative rat diphthamide methyltransferase gene

Of the 151 clones that survived the PCR-based secondary and tertiary screening, one clone, designated clone 28-2, was chosen for further characterization (Figure 5.2). Clone 28-2 contained an approximately 1260 bp insert. Northern analysis using the PCR-amplified insert of clone 28-2 as a probe further confirmed the differential status of this clone, and identified a single transcript of approximately 1400 nt (Figure 5.3). This transcript was expressed at low levels in dark-reared and 4 hour light-treated animals, and demonstrated a progressive decrease in expression levels following 8 and 16 hours of

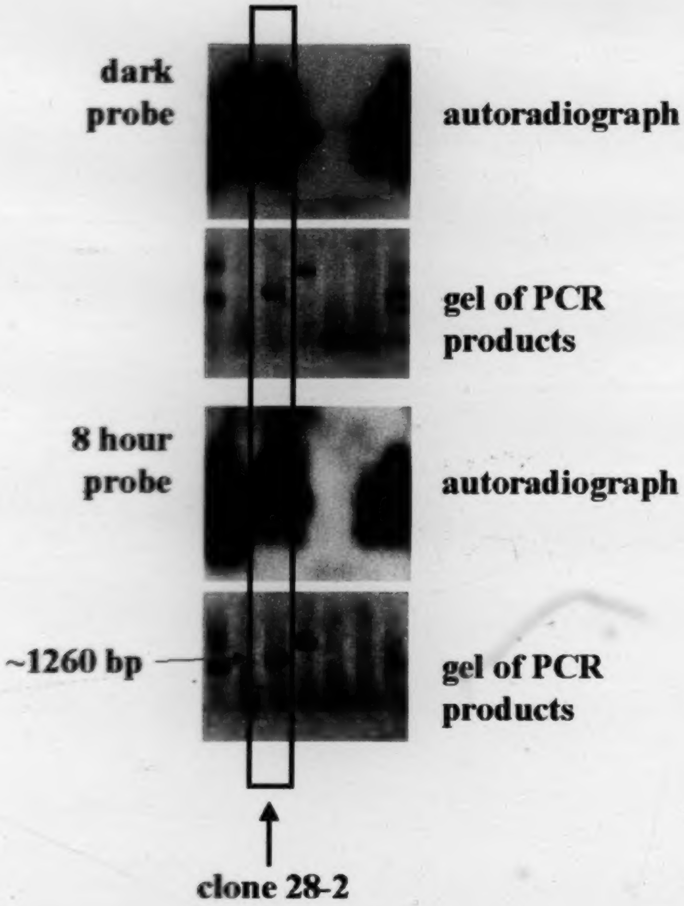

dark probe
autoradiograph
gel of PCR products
8 hour probe
autoradiograph
~1260 bp
gel of PCR products
clone 28-2

Figure 5.2. Identification of clone 28-2 as a dark-enriched EST using a PCR-based secondary and tertiary screen. Differentially-expressed clones isolated from differential cross screening of an 8 hour cDNA library were amplified by PCR using T7 and T3 vector specific primers. PCR products were resolved in duplicate by gel electrophoresis and DNA was transferred to duplicate membranes by Southern transfer. Membranes were hybridized with radioactively labeled total cDNA populations from either 8 hour light-treated retinae or dark-reared control retinae. Clones representing differentially expressed transcripts in the secondary screen were purified by plaque purification and re-screened as described for the secondary screen. The box shows results of the secondary screen of clone 28-2 and these results mimic those observed for the tertiary screen. Bands outside of the box represent additional clones analyzed in the secondary screen.

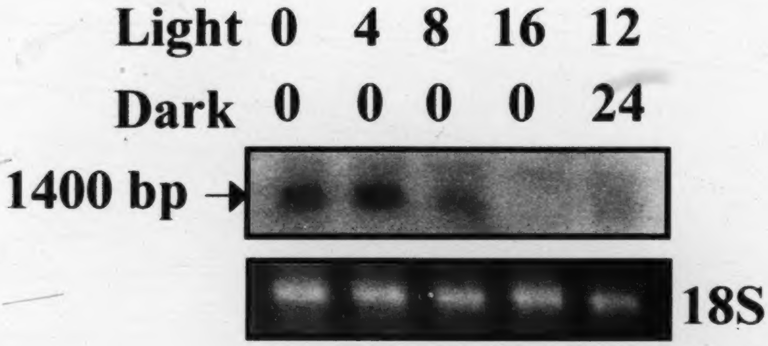

Figure 5.3. Northern blot analysis of expression levels of the rat *DPH5* gene over the course of LIRD. Northern analysis of the rat *DPH5* gene expression was performed using 10 μg of total RNA isolated from control retinae and from retinae treated with intense green light for various periods of time. The gel purified PCR product of clone 28-2 was used as a probe. Northern analysis was performed in triplicate and a representative gel and autoradiograph are shown.

light treatment as well as with a treatment of 12 hours of light followed by a 24 hour dark recovery period.

Initial sequence analysis of the PCR-amplified insert was performed using automated DNA sequencing followed by BLAST analysis of the obtained sequence. This resulted in the identification of clone 28-2 as a previously unidentified rat clone with sequence similarity to a mouse RIKEN 2410012M04 cDNA (NM_027193.2, Expect value = 0.0, 489/522 bp., 93% identity), as well as to an uncharacterized cDNA encoding a human protein designated CGI-30 (AF_132964.1, Expect value = e-144, 364/400 bp., 91% identity).

When clone 28-2 was initially isolated, rat genomic sequences or expressed sequence tag (EST) sequences corresponding to this gene were not available in the database. Therefore, comparisons were made between the human CGI-30 cDNA sequence, the mouse RIKEN cDNA sequence, and the sequence obtained for clone 28-2. Putative open reading frames (ORFs) were determined for the rat, mouse and human cDNA sequences using NCBI's ORF finder to identify possible proteins encoded by these sequences. The mouse sequence (12845948) contained an open reading frame of 846 bp, suggesting a protein of 281 amino acids. The human sequence (17440830) contained an open reading frame of 858 bp, encoding a protein of 285 amino acids. Pair-wise BLAST analysis of the mouse and human sequences indicated 85% identical residues over a total of 865 base pairs, while the homology between the putative mouse and human proteins was found to be 90% identical residues (258/285), or 96% similar residues (274/285). BLAST protein analysis was performed on the putative mouse protein sequence. The result of this analysis demonstrated that the putative mouse protein has significant homology with proteins identified in *D. melanogaster* (NP_524452.4, 63% identity, 77% similarity), *C. elegans* (NP_496427.1, 62% identity, 77% similarity) and *S. cerevisiae* (NP_013273.59% identity, 74% similarity) (data not shown). There was also strong similarity in protein size, with the proteins of mouse, human, *D. melanogaster*, *C. elegans*, and *S. cerevisiae* containing 281, 285, 271, 270, and 300 amino acids, respectively.

Because of the strong similarity between the mouse and human sequences, as well as between these and other evolutionarily distant orthologs, primers potentially corresponding to the 5' (28-2 up = ATGCTTTACTTGATCGGCTTGGGCC) and 3' (28-2 down = CGGAATCCCAGAGTACTGATGGACTCTGA) ends of the rat ORF were designed. PCR on total dark-reared retinal cDNA was performed in an attempt to isolate the rat ORF. An 884 bp PCR fragment was generated, and sequence comparison to the mouse and human sequences confirmed that it contained a putative rat ORF. The rat ORF contained 846 bp, potentially encoding a protein of 281 amino acids with a predicted molecular mass of 31.2 kDa (determined using the ProtParam protein analysis tool).

5.B-2. Bioinformatic analysis of the putative rat ORF and putative protein

The sequence for the putative rat ORF was used for BLAST analysis to determine the degree of homology with previously identified orthologs. The rat ORF shows the highest identity with the mouse RIKEN clone [NM_027193; 810/846 (95%)], the human CGI-30 clone [BC053857; 708/794 (89%)], and a newly submitted rat cDNA sequence [XM_215691; 587/587 (100%) and 260/260 (100%)] generated using gene prediction analysis. Several human and mouse EST sequences also showed significant similarity to the rat ORF, although this similarity occurred over more limited regions. These results are summarized in Figure 5.4, which shows the percent similarity and alignment of known sequences showing 50% or greater identity with the rat ORF.

The protein sequence encoded by the rat ORF was used for protein BLAST analysis and was aligned with sequences of previously identified orthologs (Figure 5.5). The rat protein sequence appears to be highly conserved, with homologies ranging from 98% identity to the protein predicted by the mouse RIKEN clone 2410012M04, 90% identity to the human CGI-30 protein, to 57% identity (73% similarity) to DPH5 in *Saccharomyces cerevisiae*. Of all the identified orthologs of the rat gene, only the yeast DPH5, which encodes a diphthamide methyltransferase, has been characterized to any extent. Analysis of the putative rat protein for conserved domains using the NCBI Conserved Domain Search tool also identified a diphthamide methyltransferase domain. The rat diphthamide methyltransferase domain has 96.9% alignment (252/260 amino acid residues) with the yeast DPH5 domain, with an E (expect) value of $2e^{-79}$.

5.B-3. Determining the rat gene structure

With advances in the sequencing of the rat genome, the rat chromosome sequence corresponding to the rat ORF subsequently became available in the NBCI genome database. The putative rat ORF was aligned to the rat chromosome 2 super contig (NW_043548.1) using BLAST analysis. Comparison of the ORF sequence, clone 28-2 sequence, and genomic sequence suggested that the rat gene contains 7 exons, and spans a region of at least 33,800 bp. The intron-exon boundaries were identified using the

Figure 5.4. Alignment of the rat *DPH5* mRNA sequence with known orthologs. Alignment of the nucleotide sequence of the rat *DPH5* mRNA and ORF with available DNA sequences (ESTs and transcripts) of known orthologs showing 50% or greater identity was performed using NCBI BLAST analysis. A) Summary of alignment of the rat mRNA with sequences available for various orthologs. The putative 5' and 3' UTRs of the rat mRNA are shown by black bars, while the rat exons are illustrated by white bars. The hatched bars illustrate regions of homology to the putative rat transcript. The start and end sites of the regions of homology for the rat mRNA are noted above the bar, while the start and end sites for the ortholog sequence are below, as is the percent identity between the rat and ortholog sequence. The sizes of the various ESTs are noted at the end of each line. B) Nucleotide alignment of the putative rat ORF with those of known orthologs. Conserved nucleotides in regions of homology between the rat ORF and the various orthologs are underlined.

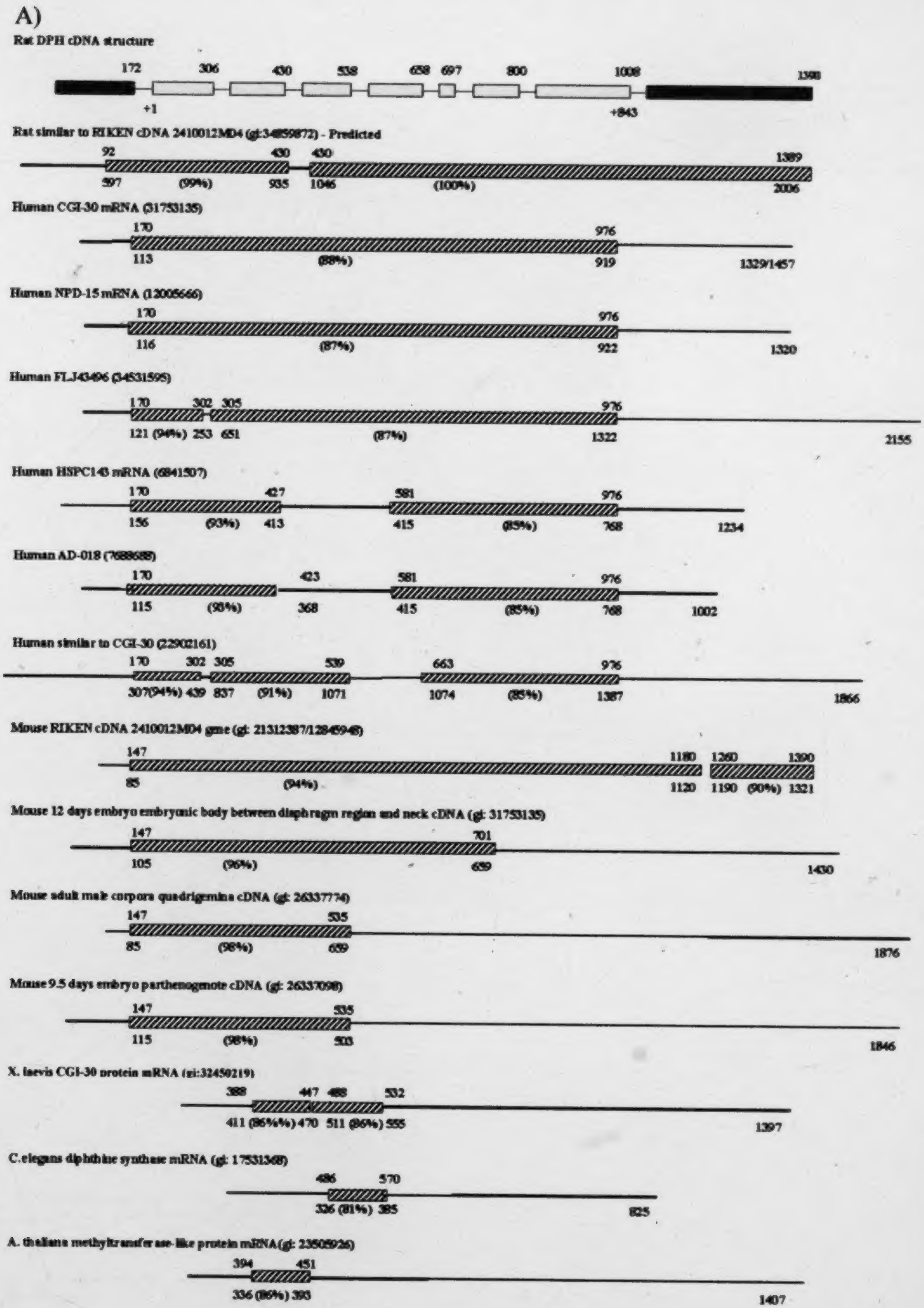
A)
Rat DPH cDNA structure
172 306 430 538 658 697 800 1008 1398
+1 +843
Rat similar to RIKEN cDNA 2410012MD4 (gi:34859872) - Predicted
92 430 430 1389
597 (99%) 935 1046 (100%) 2006
Human CGI-30 mRNA (31753135)
170 976
113 (88%) 919 1329/1457
Human NPD-15 mRNA (12005666)
170 976
116 (87%) 922 1320
Human FLJ43496 (34531595)
170 302 305 976
121 (94%) 253 651 (87%) 1322 2155
Human HSPC143 mRNA (6841507)
170 427 581 976
156 (93%) 413 415 (85%) 768 1234
Human AD-018 (7688688)
170 423 581 976
115 (93%) 368 415 (85%) 768 1002
Human similar to CGI-30 (22902161)
170 302 305 539 663 976
307(94%) 439 837 (91%) 1071 1074 (85%) 1387 1866
Mouse RIKEN cDNA 2410012M04 gene (gi: 21312387/12845948)
147 1180 1260 1390
85 (94%) 1120 1190 (90%) 1321
Mouse 12 days embryo embryonic body between diaphragm region and neck cDNA (gi: 31753135)
147 701
105 (96%) 659 1430
Mouse adult male corpora quadrigemina cDNA (gi: 26337774)
147 535
85 (98%) 659 1876
Mouse 9.5 days embryo parthenogenote cDNA (gi: 26337098)
147 535
115 (98%) 503 1846
X. laevis CGI-30 protein mRNA (gi:32450219)
388 447 488 532
411 (86%%) 470 511 (86%) 555 1397
C.elegans diphthine synthase mRNA (gi: 17531368)
486 570
326 (81%) 385 825
A. thaliana methyltransferase-like protein mRNA(gi: 23505926)
394 451
336 (86%) 393 1407

B)

```
1     atgctttacttgatcggcttgggcctgggagatgccaaggacatcacagtcaagggcctg 60        RDPH CLONE SEQUENCE
109   atgctttacttgatcggcttgggcctgggagatgccaaggacatcaaagtcaagggcctg 168       Mouse RIKEN cDNA 2410012H04 gene
676   atgctttacttgatcggcttgggcctgggagatgccaaggacatcacagtcaagggcctg 735       Rat similar to RIKEN cDNA 2410012H04
      ............................................................
      .........126 atcgggttgggcctgggagatgccaaggacatcacagtcaagggcctg 173       Human CGI-30 protein, mRNA
      .........129 atcgggttgggcctgggagatgccaaggacatcacagtcaagggcctg 176       Human HPD015 mRNA
      .........134 atcgggttgggcctgggagatgccaaggacatcacagtcaagggcctg 181       Human cDNA FLJ43496 fis
      ............................................................
      .........169 atcgggttgggcctgggagatgccaaggacatcacagtcaagggcctg 216       Human HSPC143 mRNA
      .........128 atcgggttgggcctgggagatgccaaggacatcacagtcaagggcctg 175       Human AD-018 protein mRNA
      .........320 atcgggttgggcctgggagatgccaaggacatcacagtcaagggcctg 367       Human similar to CGI-30 protein
      ............................................................
      ............................................................       X. laevis cDNA clone MGC:64452
      ............................................................       A. thaliana methyltransferase-like
      ............................................................       C.elegans diphthine synthase (2L641)


61    gaagttgtgagacgctgcagtcgcgtgtatctggaagcctacacctcagtcctgactgta 120       RDPH CLONE SEQUENCE
169   gaagttgtgagacgatgcagtcgcgtgtatctggaagcctacacctcagtcctgactgta 228       Mouse RIKEN cDNA 2410012H04 gene
736   gaagttgtgagacgctgcagtcgcgtgtatctggaagcctacacctcagtcctgactgta 795       Rat similar to RIKEN cDNA 2410012H04
      ............................................................
174   gaagttgttagacgctgcagtcgagtgtatctggaagcctacacctcagtcctaactgta 233       Human CGI-30 protein, mRNA
177   gaagttgttagacgctgcagtcgagtgtatctggaagcctacacctcagtcctaactgta 236       Human HPD015 mRNA
182   gaagttgttagacgctgcagtcgagtgtatctggaagcctacacctcagtcctaactgta 241       Human cDNA FLJ43496 fis
      ............................................................
217   gaagttgttagacgctgcagtcgagtgtatctggaagcctacacctcagtcctaactgta 276       Human HSPC143 mRNA
176   gaagttgttagacgctgcagtcgagtgtatctggaagcctacacctcagtcctaactgta 235       Human AD-018 protein mRNA
368   gaagttgttagacgctgcagtcgagtgtatctggaagcctacacctcagtcctaactgta 427       Human similar to CGI-30 protein
      ............................................................
      ............................................................       X. laevis cDNA clone MGC:64452
      ............................................................       A. thaliana methyltransferase-like
      ............................................................       C.elegans diphthine synthase (2L641)


121   gggaaggaagccctggaagaattttatggaagaaaattgattcttgctgacagagaagaa 180       RDPH CLONE SEQUENCE
229   gggaaggaagccctggaagagttttatggaagaaaattgattcttgctgacagagaagaa 288       Mouse RIKEN cDNA 2410012H04 gene
796   gggaaggaagccctggaagaattttatggaagaaaattgattcttgctgacagagaagaa 855       Rat similar to RIKEN cDNA 2410012H04
      ............................................................
234   gggaaggaagccttggaagagttttatggaagaaaattggttgttgctgatagagaagaa 293       Human CGI-30 protein, mRNA
237   gggaaggaagccttggaagagttttatggaagaaaattggttgttgctgatagagaagaa 296       Human HPD015 mRNA
242   gggaaggaagcc 253 ............................................       Human cDNA FLJ43496 fis
      ..........651 -ggaagagttttatggaagaaaattggttgttgctgatagagaagaa 696
277   gggaaggaagccttggaagagttttatggaagaaaattggttgttgctgatagagaagaa 336       Human HSPC143 mRNA
236   gggaaggaagccttggaagagttttatggaagaaaattggttgttgctgatagagaagaa 295       Human AD-018 protein mRNA
428   gggaaggaagcc 439 ............................................       Human similar to CGI-30 protein
      .....440/837  ggaagagttttatggaagaaaattggttgttgctgatagagaagaa 488/882
      ............................................................       X. laevis cDNA clone MGC:64452
      ............................................................       A. thaliana methyltransferase-like
      ............................................................       C.elegans diphthine synthase (2L641)


181   gtagaacaagaagcagataatatttttaaggatgcagatgtcagtgatgttgcattcctc 240       RDPH CLONE SEQUENCE
289   gtagaacaagaagcagataatatttttaaggatgcagatgtcagtgatgttgcgttcctt 348      M ouse RIKEN cDNA 2410012H04 gene
856   gtagaacaagaagcagataatatttttaaggatgcagatgtcagtgatgttgcattcctc 915       Rat similar to RIKEN cDNA 2410012H04
      ............................................................
294   gtggaacaagaagcagataatattttaaaggatgctgatatcagtgatgttgcattcctt 353       Human CGI-30 protein, mRNA
297   gtggaacaagaagcagataatattttaaaggatgctgatatcagtgatgttgcattcctt 356       Human HPD015 mRNA
      ............................................................       Human cDNA FLJ43496 fis
697   gtggaacaagaagcagataatattttaaaggatgctgatatcagtgatgttgcattcctt 756       Human HSPC143 mRNA
337   gtggaacaagaagcagataatattttaaaggatgctgatatcagtgatgttgcattcctt 396       Human AD-018 protein mRNA
296   gtggaacaagaagcagataatattttaaaggatgctgatatcagtgatgttgcattcctt 355       Human similar to CGI-30 protein
      ............................................................
489   gtggaacaagaagcagataatattttaaaggatgctgatatcagtgatgttgcattcctt 545/942   X. laevis cDNA clone MGC:64452
      ..................................411 tgtcagtgatgtagcacttctt 432      A . thaliana methyltransferase-like
      ........................................336 tgatgtcgcttttctc 351       C.elegans diphthine synthase (2L641)
      ............................................................


241   gtggttggtgatccattcggggctacaacacacagtgatcttattctgagagcaacgaag 300       RDPH CLONE SEQUENCE
349   gtggttggtgatccatttggggctacaacacacagtgatcttattctgagagcaacaaag 408        ouse RIKEN cDNA 2410012H04 gene
916   gtggttggtgatccattcgg 935.....................................       Rat similar to RIKEN cDNA 2410012H04
                1046 gggctacaacacacagtgatcttattctgagagcaacgaag 1086
354   gtggttggtgatccatttggggccacaacacacagtgatcttgttctaagagcaacaaag 413       Human CGI-30 protein, mRNA
357   gtggttggtgatccatttggggccacaacacacagtgatcttgttctaagagcaacaaag 416       Human HPD015 mRNA
      ............................................................       Human cDNA FLJ43496 fis
757   gtggttggtgatccatttggggccacaacacacagtgatcttgttctaagagcaacaaag 816       Human HSPC143 mRNA
397   gtggttggtgatccatt 413 .......................................       Human AD-018 protein mRNA
356   gtggttggtgatc 368 ...........................................       Human similar to CGI-30 protein
      ............................................................
546   gtggttggtgatccatttggggccacaacacacagtgatcttgttctaagagcaacaaag 605/1002  X. laevis cDNA clone MGC:64452
433   gtggttggtgatcctttggggctacaacccatagtga 470 ...................      A . thaliana methyltransferase-like
352   gttgttggtgatcctttcggagctacaacgcatagtgatctt 393 ..............       C.elegans diphthine synthase (2L641)
      ............................................................
```

```
301  ttgggcatcccttatcaagttattcacaatgcctccataatgaacgctgtaggctgctgt 360        RDPH CLONE SEQUENCE
409  ttgggcatcccttatcaagttattcacaatgcctccataatgaacgctgtaggctgctgt 468        Mouse RIKEN cDNA 2410012H04 gene
     ............................................................            Rat similar to RIKEN cDNA 2410012H04
1087 ttgggcatcccttatcaagttattcacaatgcctccataatgaacgctgtaggctgctgt 1146
414  ctgggaattccttatagagttattcacaatgcctccataatgaatgctgtaggctgctgt 473        Human CGI-30 protein, mRNA
417  ctgggaattccttatagaggtattcacaatgcctccataatgaatgctg-aagctgctgg 476        Human NPD015 mRNA
     ............................................................            Human cDNA FLJ43496 fis
817  ctgggaattccttatagagttattcacaatgcctccataatgaatgctgtaggctgctgt 876
     ............................................................            Human HSPC143 mRNA
     ............................................................            Human AD-018 protein mRNA
     ............................................................            Human similar to CGI-30 protein
606  ctgggaattccttatagagttattcacaatgcctccataatgaatgctgtaggctgctgt 665/1062
     ..............511 gttattcacaatgcttccatcatgactgctgtgggctgttgt 552        X. laevis cDNA clone MGC:64452
     ............................................................            A. thaliana methyltransferase-like
     ............326 aagtgattcacaatgcttccatcatgaatgcagttggctgttgt 369          C.elegans diphthine synthase (2L641)


361  ggtttacagttgtacaggtttggagaaacagtttctattgtttttggacggacacttgg 420         RDPH CLONE SEQUENCE
469  ggtttgcagttgtacaggtttggagaaacagtttctattgtgttttggacggacacttgg 528        Mouse RIKEN cDNA 2410012H04 gene
     ............................................................            Rat similar to RIKEN cDNA 2410012H04
1147 ggtttacagttgtacaggtttggagaaacagtttctattgtttttggacggacacttgg 1206
474  ggtttacagttatataagtttggagagacagtttctattgtttttggacagacacttgg 533         Human CGI-30 protein, mRNA
477  gggttacaggtatataagtttggagagacaggttctattggtttttggacagacacttgg 536        Human NPD015 mRNA
     ............................................................            Human cDNA FLJ43496 fis
817  ggtttacagttatataagtttggagagacagtttctattgtttttggacagacacttgg 936
     ..................................................415 ggacacttgg 424       Human HSPC143 mRNA
     ..................................................373 ggacacttgg 382       Human AD-018 protein mRNA
     ............................................................            Human similar to CGI-30 protein
666  ggtttacag 674/1071 .........................................
553  ggt 555 ....................................................            X. laevis cDNA clone MGC:64452
     ............................................................            A. thaliana methyltransferase-like
370  ggactacaactctacaatttcggagaaacagtttcaattgt 410 ..............            C.elegans diphthine synthase (2L641)


421  agaccagagagcttctttgacaaggtgaagaagaaccgagaaaatggcatgcacactttg 480        RDPH CLONE SEQUENCE
529  cgaccagagagcttctttgacaaggtgaagaggaaccgggccaatggcatgcacacgctg 588        Mouse RIKEN cDNA 2410012H04 gene
     ............................................................            Rat similar to RIKEN cDNA 2410012H04
1207 agaccagagagcttctttgacaaggtgaagaagaaccgagaaaatggcatgcacactttg 1266
534  agaccagaaagcttctttgacaaagtgaagaagaacagacaaaatggcatgcacacatta 593        Human CGI-30 protein, mRNA
537  ggaccagaaagcttctttgacaaagtgaagaagaacagacaaaatggcatgcacacatta 596        Human NPD015 mRNA
     ............................................................            Human cDNA FLJ43496 fis
937  agaccagaaagcttctttgacaaagtgaagaagaacagacaaaatggcatgcacacatta 996
425  agaccaga-agcttctttgacaaagtgaagaagaacagacaaaatggcatgcacacatta 484        Human HSPC143 mRNA
383  agaccagaaagcttctttgacaaagtgaagaagaacagacaaaatggcatgcacacatta 442        Human AD-018 protein mRNA
     ............................................................            Human similar to CGI-30 protein
     ............................................................
     ............................................................            X. laevis cDNA clone MGC:64452
     ............................................................            A. thaliana methyltransferase-like
     ............................................................            C.elegans diphthine synthase (2L641)


481  tgcttacttgatatcaaggtgaaggagcagtctctggagaacctcatcaggggaaggaag 540        RDPH CLONE SEQUENCE
589  tgcttactcgatatcaaagtgaaggagcagtctctggagaacctcatcagaggaagaaag 648        Mouse RIKEN cDNA 2410012H04 gene
     ............................................................            Rat similar to RIKEN cDNA 2410012H04
1267 tgcttacttgatatcaaggtgaaggagcagtctctggagaacctcatcaggggaaggaag 1326
594  tgtttactagacatcaaagtaaaggagcagtctttggaaaatctaatcaagggaaggaag 653        Human CGI-30 protein, mRNA
597  tgtttactagacatcaaagtaaaggagcagtctttggaaaatctaatcaagggaaggaag 656        Human NPD015 mRNA
     ............................................................            Human cDNA FLJ43496 fis
997  tgtttactagacatcaaagtaaaggagcagtctttggaaaatctaatcaagggaaggaag 1056
485  tgtttactagacatcaaagtaaaggagcagtctttggaaaatctaatcaagggaaggaag 544        Human HSPC143 mRNA
443  tgtttactagacatcaaagtaaaggagcagtctttggaaaatctaatcaagggaaggaag 502        Human AD-018 protein mRNA
     ...... 1074 atcaaagtaaaggagcagtctttggaaaatctaatcaagggaaggaag 1121       Human similar to CGI-30 protein
     ............................................................
     ............................................................            X. laevis cDNA clone MGC:64452
     ............................................................            A. thaliana methyltransferase-like
     ............................................................            C.elegans diphthine synthase (2L641)


541  atctatgaacctcctcgttacatgagtgtgaaccaggcagcacagcagctcctagaaatt 600        RDPH CLONE SEQUENCE
649  atctatgaacccccctcggtacatgagtgtgaaccaggcggcccagcagcttctagagatt 708       Mouse RIKEN cDNA 2410012H04 gene
     ............................................................            Rat similar to RIKEN cDNA 2410012H04
1327 atctatgaacctcctcgttacatgagtgtgaaccaggcagcacagcagctcctagaaatt 1386
654  atctatgaacctccacggtatatgagtgtaaaccaagcagcccagcagcttctggagatt 713        Human CGI-30 protein, mRNA
657  atctatgaacctccacggtatatgagtgtaaaccaagcagcccagcagcttctggagatt 716        Human NPD015 mRNA
     ............................................................            Human cDNA FLJ43496 fis
1057 atctatgaacctccacggtatatgagtgtaaaccaagcagcccagcagcttctggagatt 1116
545  atctatgaacctccacggtatatgagtgtaaaccaagcagcccagcagcttctggagatt 604        Human HSPC143 mRNA
503  atctatgaacctccacggtatatgagtgtaaaccaagcagcccagcagcttctggagatt 562        Human AD-018 protein mRNA
1122 atctatgaacctccacggtatatgagtgtaaaccaagcagcccagcagcttctggagatt 1181       Human similar to CGI-30 protein
     ............................................................
     ............................................................            X. laevis cDNA clone MGC:64452
     ............................................................            A. thaliana methyltransferase-like
     ............................................................            C.elegans diphthine synthase (2L641)
```

```
601  gttcaaaatcacagagcacgtggggaggcaccagcaatcactgaggagacactctgtgtc 660
709  gttcagaatcacagagcacgcggggaggaaccagcaatcactgaggagacactctgtgtc 768
     ............................................................
1387 gttcaaaatcacagagcacgtggggaggcaccagcaatcactgaggagacactctgtgtc 1446
714  gttcaaaatcaaagaatacgaggagaagaaccagcagttaccgaggagacactttgtgtt 773
717  gttcaaaatcaaagaatacgaggagaagaaccagcagttaccgaggagacactttgtgtt 776
     ............................................................
1117 gttcaaaatcaaagaatacgaggagaagaaccagcagttaccgaggagacactttgtgtt 1176
605  gttcaaaatcaaagaatacgaggagaagaaccagcagttaccgaggagacactttgtgtt 664
563  gttcaaaatcaaagaatacgaggagaagaaccagcagttaccgaggagacactttgtgtt 622
1182 gttcaaaatcaaagaatacgaggagaagaaccagcagttaccgaggagacactttgtgtt 1241
     ............................................................
     ............................................................
     ............................................................
     ............................................................
```

RDPH CLONE SEQUENCE
Mouse RIKEN cDNA 2410012M04 gene
Rat similar to RIKEN cDNA 2410012M04

Human CGI-30 protein, mRNA
Human NPD015 mRNA
Human cDNA FLJ43496 fis

Human HSPC143 mRNA
Human AD-018 protein mRNA
Human similar to CGI-30 protein

X. laevis cDNA clone MGC:64452
A. thaliana methyltransferase-like
C.elegans diphthine synthase (2L641)

```
661  ggcttagccagagttggagcggaagaccagaaaattgcagcaggcactttacagcaaatg 720
769  ggcttagccagagtgggagctgaagatcagaaaattgcagcaggcacgttacagcagatg 828
     ............................................................
1447 ggcttagccagagttggagcggaagaccagaaaattgcagcaggcactttacagcaaatg 1506
774  ggcttagccagggttggagccgacgaccagaaaattgcagcaggcactttaaggcaaatg 833
777  ggcttagccagggttggagccgacgaccagaaaattgcagcaggcactttaaggcaaatg 836
     ............................................................
1177 ggcttagccagggttggagccgacgaccagaaaattgcagcaggcactttaaggcaaatg 1236
665  ggcttagccagggttggagccgacgaccagaaaattgcagcaggcactttaaggcaaatg 724
623  ggcttagccagggttggagccgacgaccagaaaattgcagcaggcactttaaggcaaatg 682
1242 ggcttagccagggttggagccgacgaccagaaaattgcagcaggcactttaaggcaaatg 1301
     ............................................................
     ............................................................
     ............................................................
     ............................................................
```

RDPH CLONE SEQUENCE
Mouse RIKEN cDNA 2410012M04 gene
Rat similar to RIKEN cDNA 2410012M04

Human CGI-30 protein, mRNA
Human NPD015 mRNA
Human cDNA FLJ43496 fis

Human HSPC143 mRNA
Human AD-018 protein mRNA
Human similar to CGI-30 protein

X. laevis cDNA clone MGC:64452
A. thaliana methyltransferase-like
C.elegans diphthine synthase (2L641)

```
721  tgtacagtgagcttgggagaaccattgcattctttggtcattacaggggggcaacctgcac 780
829  tgcacagtgagcttgggagaaccactgcattctttggtcattacaggggggcaacctgcac 888
     ............................................................
1507 tgtacagtgagcttgggagaaccattgcattctttggtcattacaggggggcaacctgcac 1566
834  tgcactgtggacttgggagaaccattgcattccttgatcatcacaggaggcagcatacat 893
837  tgcactgtggacttgggagaaccattgcattccttgatcatcacaggaggcagcatacat 986
     ............................................................
1237 tgcactgtggacttgggagaaccattgcattccttgatcatcacaggaggcagcatacat 1296
725  tgcactgtggacttgggagaaccattgcattccttgatcatcacaggaggcagcatacat 784
683  tgcactgtggacttgggagaaccattgcattccttgatcatcacaggaggcagcatacat 742
1302 tgcactgtggacttgggagaaccattgcattccttgatcatcacaggaggcagcatacat 1361
     ............................................................
     ............................................................
     ............................................................
     ............................................................
```

RDPH CLONE SEQUENCE
Mouse RIKEN cDNA 2410012M04 gene
Rat similar to RIKEN cDNA 2410012M04

Human CGI-30 protein, mRNA
Human NPD015 mRNA
Human cDNA FLJ43496 fis

Human HSPC143 mRNA
Human AD-018 protein mRNA
Human similar to CGI-30 protein

X. laevis cDNA clone MGC:64452
A. thaliana methyltransferase-like
C.elegans diphthine synthase (2L641)

```
781  ccactggagatggaaatgctaagtctcttctctataccggaatcccagagtactgatgga 840
889  ccactggagatggagatgctaagtctcttctctataccggaatcccagagtactgatgga 948
     ............................................................
1567 ccactggagatggaaatgctaagtctcttctctataccggaatcccagagtactgatgga 1626
894  ccaatggagatggagatgctaagtct 919 ..............................
897  ccaatggagatggagatgctaagtct 922 ..............................
     ............................................................
1297 ccaatggagatggagatgctaagtct 1322 .............................
785  ccaatggagatggagatgctaagtct 809 ..............................
743  ccaatggagatggagatgctaagtct 768 ..............................
     ccaatggagatggagatgctaagtct 1387 .............................
     ............................................................
     ............................................................
     ............................................................
     ............................................................
```

RDPH CLONE SEQUENCE
Mouse RIKEN cDNA 2410012M04 gene
Rat similar to RIKEN cDNA 2410012M04

Human CGI-30 protein, mRNA
Human NPD015 mRNA
Human cDNA FLJ43496 fis

Human HSPC143 mRNA
Human AD-018 protein mRNA
Human similar to CGI-30 protein

X. laevis cDNA clone MGC:64452
A. thaliana methyltransferase-like
C.elegans diphthine synthase (2L641)

```
841  ctctga 846 ..................................................
949  ctctga 954 ..................................................
     ............................................................
1627 ctctga 1632 .................................................
     ............................................................
     ............................................................
     ............................................................
     ............................................................
     ............................................................
     ............................................................
     ............................................................
     ............................................................
     ............................................................
     ............................................................
```

RDPH CLONE SEQUENCE
Mouse RIKEN cDNA 2410012M04 gene
Rat similar to RIKEN cDNA 2410012M04

Human CGI-30 protein, mRNA
Human NPD015 mRNA
Human cDNA FLJ43496 fis

Human HSPC143 mRNA
Human AD-018 protein mRNA
Human similar to CGI-30 protein
X. laevis cDNA clone MGC:64452
A. thaliana methyltransferase-like
C.elegans diphthine synthase (2L641)

Figure 5.5. Alignment of the putative rat DPH5 protein sequence with that of known orthologs. A) The putative protein sequence encoded by the identified rat ORF was determined using the NCBI ORF Finder program. This proposed protein sequence was then aligned with the sequences of known protein orthologs using NCBI Protein BLAST. Residues conserved among all orthologs are indicated. B) The percent identity and homology between the rat protein sequence and the various ortholog protein sequences analyzed including mouse RIKEN clone 2410012M04 (NP_081469), human unknown protein (AAH53857.1), human CGI-30 protein (NP_057042.1), human NPD015 protein (AAG44563.1), human AD-018 protein (AAF67485.1), human HSPC143 protein (AAF29107.1), *Drosophila melanogaster* Diphthamide methyltransferase CG31289-PA (NP_524452.4), *Caenorhabditis elegans* methyltransferase like protein (NP_496427.1), *Arabidopsis thaliana* methyltransferase like protein (NP_194907.1), *Dictyostelium discoideum* methyltransferase like protein (AAO51996), *Neurospora crassa* hypothetical protein (XP_327552.1), *Xenopus laevis* unknown protein (AAH54245.1), and *Saccharomyces cerevisiae* DPH5 protein (NP_013273.1).

A)

```
Rat DPH:                                         1  MLYLIGLGLGDAKDITVKGLEVVRRCSRVYLEAYTSVLTVGKEALEEFYGRKLILADREE 60
RIKEN cDNA 2410012M04 [M. musculus]              1  MLYLIGLGLGDAKDIKVKGLEVVRRCSRVYLEAYTSVLTVGKEALEEFYGRKLILADREE 60
Unknown protein [H.sapiens]                      1  MLYLIGLGLGDAKDITVKGLEVVRRCSRVYLEAYTSVLTVGKEALEEFYGRKLVVADREE 60
CGI-30 protein [H.sapiens]                       1  MLYLIGLGLGDAKDITVKGLEVVRRCSRVYLEAYTSVLTVGKEALEEFYGRKLVVADREE 60
NPD015 [H.sapiens]                               1  MLYLIGLGLGDAKDITVKGLEVVRRCSRVYLEAYTSVLTVGKEALEEFYGRKLVVADREE 60
AD-018 protein [H.sapiens]                       1  MLYLIGLGLGDAKDITVKGLEVVRRCSRVYLEAYTSVLTVGKEALEEFYGRKLVVADREE 60
HSPC143 [H.sapiens]                              1  MLYLIGLGLGDAKDITVKGLEVVRRCSRVYLEAYTSVLTVGKEALEEFYGRKLVVADREE 60
Diphthamide methyltransferase [D.melanogaster]   1  MFYLIGLGLGDLKDITVKGLEIVKQCSRVYLEMYTSILGCSLEDMQEFYGRPLLLADRDL 60
Methyltransferase like protein [C.elegans]       2  VFYLIGLGLGDVEDITVKGLNIVKNCARVHLEAYTSILCYGLDKTNLEKFYGREIIEADR 61
Methyltransferase like protein [A.thaliana       1  MLYIIGLGLGDEKDITLRGLEAVKKSQKVYMEAYTSILSFGLSADGLSNLEKFYGKPIIL 60
Methyltransferase like protein [D.discoideum]    2  VLYIIGLGLGDEKDVTIKGFEAIKKSSKIYLEAYTSILGGSTSIEALEKFYEKKIIIADR 61
Hypothetical protein[N.crassa]                   1  MLYLVGLGLSDETDITVKGLEVVKKAERVYLEAYTSILLVDQATLESYYGRPIVVADREM 60
hypothetical protein[X.laevis]                   1  MLYLIGLGLGDEKDVTLKGLEVIRSCARVYLEAYTSILTVRKETLEEFYGRELILADRET 60
Dph5 [S.cerevisiae]                              1  MLYLIGLGLSYKSDITVRGLEAIKKCSRVYLEHYTSILMAASQEELESYYGKEIILADRE 60

61  VEQEADNIFKDADVSDVAFLVVGDPFGATTHSDLILRATKLGIPYQVIHNASIMNAVGCCGLQLYRFGETVSIVFWTDTWRPESFFDKVKKNRENGMHTLCLLDIKVKEQSLENLIRGRK 180
61  VEQEADNIFKDADVSDVAFLVVGDPFGATTHSDLILRATKLGIPYQVIHNASIMNAVGCCGLQLYRFGETVSIVFWTDTWRPESFFDKVKRNRANGMHTLCLLDIKVKEQSLENLIRGRK 180
61  VEQEADNILKDADISDVAFLVVGDPFGATTHSDLVLRATKLGIPYRVIHNASIMNAVGCCGLQLYKFGETVSIVFWTDTWRPESFFDKVKKNRQNGMHTLCLLDIKVKEQSLENLIKGRK 180
61  VEQEADNILKDADISDVAFLVVGDPFGATTHSDLVLRATKLGIPYRVIHNASIMNAVGCCGLQLYKFGETVSIMLISVMLHSLWLVIHLDTWRPESFFDKVKKNRQNGMHTLCLLDIKVK 180
61  VEQEADNILKDADISDVAFLVVGDPFGATTHSDLVLRATKLGIPYRGIHNASIMNAEAAGGYRYISLERQVLLVFGQTLGGPESFFDKVKKNRQNGMHTLCLLDIKVKEQSLENLIKGRK 180
61  VEQEADNILKDADISDVAFLVVGDHL---------------------------------------------------DTWRPESFFDKVKKNRQNGMHTLCLLDIKVKEQSLENLIKGRK 129
61  VEQEADNILKDADISDVAFLVVGDPFGHL--------------------------------------ETRS-------------FFDKVKKNRQNGMHTLCLLDIKVKEQSLENLIKGRK 129
61  VEQGADEILAGAGESDVALLVVGDPFGATTHTDFILRAKEKNIPYKVIHNASIMNAVGCCGLQLYKFGETVSIPYWDETWKPDSFYDKIKLNRLHNMHTLCLLDIKVKEPTPESLMRKRK 180
62  TVVEQESDAILNGADKEDVALLVVGDPFGATTHADLVLRAKQQNIPVKVIHNASIMNAVGCCGLQLYNFGETVSIVMWTDEWQPESYYDKIALNRKRGMHTLCLLDIKTKEQTVENMMRG 181
61  ADREMVEEKAGDMIDEAIDNDVAFLVVGDPFGATTHSDLVVRAKTLGVKVEVVHNASVMNAVGICGLQLYHYGETVSIPFFTETWRPDSFYEKIKKNRSLGLHTLCLLDIRVKEPTFESL 180
62  EMVESGCEEMLKESTENDVSFLVVGDPFGATTHTDLVIRAKELSIPVKVIHNASIMNAIGCCGLQLYSYGQTISMVFFTETTKPDSWYDRVKINRVNGMHTLCLLDIKVKEQSIENMCRG 181
61  VESNSDEILRDADKVDVAFCVVGDPFGATTHTDLVLRARELGIQVRTVPNASIMSGIGAAGLQLYNFGQTVSMVFFLDNWRPASFYDRIKENRSIGLHTLVLLDIKVKEQSLENMARGRK 180
61  VEQEADEILRDAAVSDVALLVVGDPFGATTHSDLVLRAAKAGIQHHVIHNASIMTAVGCCGLQLYNFGETVSIVFWTDMWKPESFYDKIRRNRLSGMHTLCLLDIKVKEQSIENLM 176
61  LVETGSKQILNNADKEDVAFLVVGDPFGATTHTDLVLRAKREAIPVEIIHNASVMNAVGACGLQLYNFGQTVSMVFFTDNWRPDSWYDKIWENRKIGLHTLVLLDIKVKEQSIENMARGR 180

181 IYEPPRYMSVNQAAQQLLEIVQNHRARGEAPAITEETLCVGLARVGAEDQKIAAGTLQQMCTVSLGEPLHSLVITGGNLHPLEMEMLSLFSIPESQSTDGL 28
181 IYEPPRYMSVNQAAQQLLEIVQNHRARGEEPAITEETLCVGLARVGAEDQKIAAGTLQQMCTVSLGEPLHSLVITGGNLHPLEMEMLSLFSIPESQSTDGL 281
181 IYEPPRYMSVNQAAQQLLEIVQNQRIRGEEPAVTEETLCVGLARVGADDQKIAAGTLRQMCTVDLGEPLHSLIITGGSIHPMEMEMLSLFSIPENSSESQSINGL 285
181 EQSLEHLIKGRKIYEPPRYMSVNQAAQQLLEIVQNQRIRGEEPAVTEETLCVGLARVGADDQKIAAGTLRQMCTVDLGEPLHSLIITGGSIHPMEMEMLSLFSIPENSSESQSINGL 29
181 IYEPPRYMSVNQAAQQLLEIVQNQRIRGEEPAVTEETLCVGLARVGADDQKIAAGTLRQMCTVDLGEPLHSLIITGGSIHPMEMEMLSLFSIPENSSESQSINGL 285
130 IYEPPRYMSVNQAAQQLLEIVQNQRIRGEEPAVTEETLCVGLARVGADDQKIAAGTLRQMCTVDLGEPLHSLIITGGSIHPMEMEMLSLFSIPENSS 226
130 IYEPPRYMSVNQAAQQLLEIVQNQRIRGEEPAVTEETLCVGLARVGADDQKIAAGTLRQMCTVDLGEPLHSLIITGGSIHPMEMEMLSLFSIPENSSESQSINGL 234
181 EYMPPRFMTVAEAAHQLLSIVERKDSLEKNTVLNEQSLCVGLARVGQESQQIAVGTLLEMRSTDLGGPLHSLIIPAKEMHPLEVEFLQQYA 271
182 RKIFEPARYQKCSEAARQLLTIYERRKAKGEECAYDENTMVVGLARVGWDNQKIVYASMKDMSEMEMGEPLHSLIIP-GETHPLEVDMLETF 272
181 CRGGKKQYEPPRYMSVNTAIEQLLEVEQKH---GDS-VYGEDTQCVGFARLGSEDQTIVAGTMKQLESVDFGAPLHCLVIV-GETHPVEEEMLEFY 271
182 RLIYEPPRFMTVNQCIEQLLEIEEIRKEK----VYDQDTLCIGLSRVGQDDQQIISGTMKELLDVDFGAPLHSFIIC-GDMHFIEKEYFETFRVHKN 273
181 IYEPPRYMTVGTCAQQMLEIEEEKQEGVYGP----ESLAIGCARVGGKTEKFVSGTLKELCDADDLLGPPLHSLILLGRRTHELEHDFVREFAV 270
-------------------------------------------------------------------------------------------------
181 LIYEPPRYMSIAQCCEQLLEIEEK---RG-TKAYTPDTPAVAISRLGSSSQSFKSGTISELANYDSGEPLHSLVILGRQCH 257
```

B)

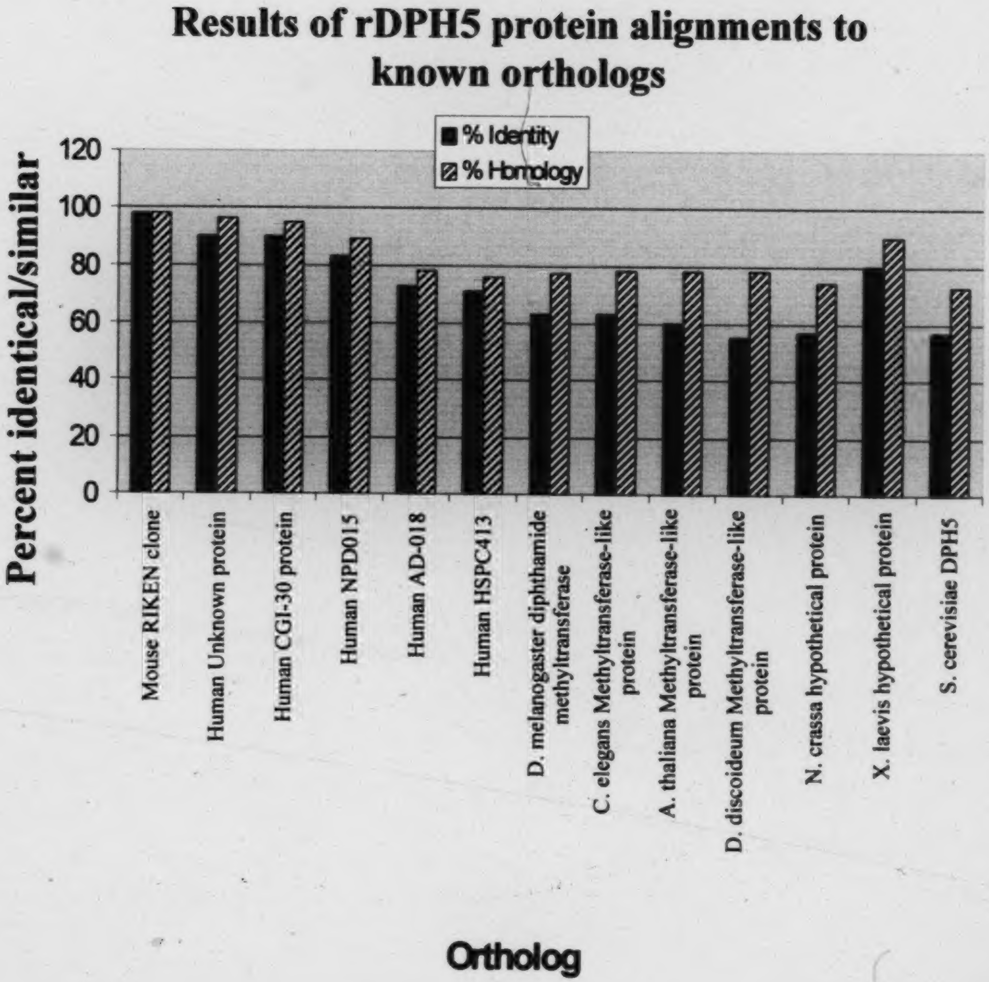
Results of rDPH5 protein alignments to known orthologs
% Identity
% Homology
Percent identical/similar
120
100
80
60
40
20
0
Mouse RIKEN clone
Human Unknown protein
Human CGI-30 protein
Human NPD015
Human AD-018
Human HSPC413
D. melanogaster diphthamide methyltransferase
C. elegans Methyltransferase-like protein
A. thaliana Methyltransferase-like protein
D. discoideum Methyltransferase-like protein
N. crassa hypothetical protein
X. laevis hypothetical protein
S. cerevisiae DPH5
Ortholog

EMBL-EBI Gene Wise 2 gene analysis program (Figure 5.6). The splice sites correspond to those suggested by mRNA and genomic alignments. Similar results are obtained by comparing the rat ORF to the mouse chromosome 3 super contig (NT_039240.1) (data not shown).

5.B-4. Analysis of the rat promoter and UTR sequence

Promoter analysis was performed using the BCM Promoter Prediction program, and the EMBOSS-CpG Plot program. CpG islands define the 5' end of many genes (Pedersen *et al*, 1999). A CpG Plot was performed using 10 kb of genomic sequence upstream of the rat ORF. A 228 bp CpG island was identified 169-397 bp upstream of the ATG translation start site (Figure 5.7). To determine whether this was a valid CpG island, similar analysis was performed using the corresponding regions of the mouse and human genomes (data not shown). A strong CpG island was identified in the human promoter in a conserved position to the rat CpG island. Interestingly, no CpG island was found in the 10 kb upstream of the translation start site of the mouse *DPH5* gene. Promoter prediction using the BCM Promoter Prediction program identified several potential core promoter sequences upstream of the rat transcription start site. Three of these, located at –5383, -3835 and –837 bases pairs upstream of the rat transcription start site, were conserved in position and sequence in the promoters between mouse and rat. A highly conserved TATA box was located at 160-210 bp upstream of the ATG start site, producing a potential 5' untranslated region (UTR) of 172 bp. This 5' UTR is of similar size to the 113 bp 5' UTR observed in the human CGI-30 cDNA, and the 85-115 bp 5' UTR observed in the mouse cDNA molecules (Figure 5.4).

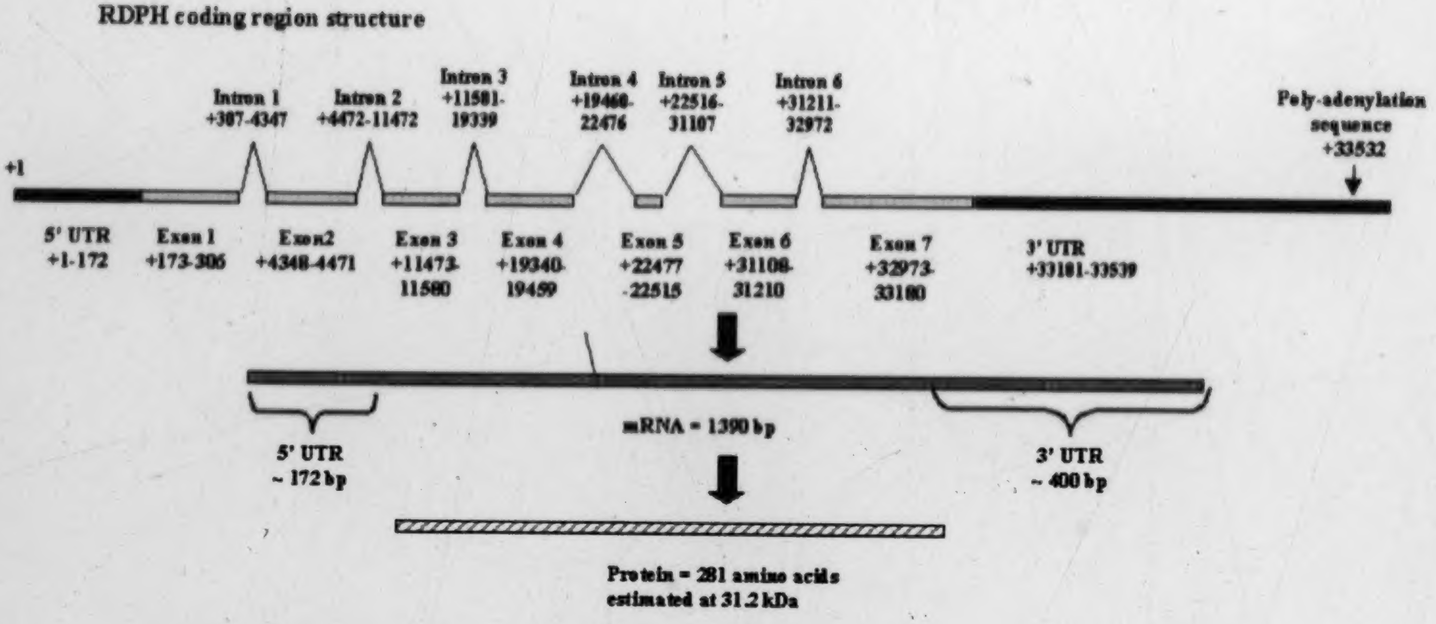
RDPH coding region structure
+1
Intron 1
+307-4347
Intron 2
+4472-11472
Intron 3
+11581-
19339
Intron 4
+19460-
22476
Intron 5
+22516-
31107
Intron 6
+31211-
32972
Poly-adenylation
sequence
+33532
5' UTR
+1-172
Exon 1
+173-306
Exon2
+4348-4471
Exon 3
+11473-
11580
Exon 4
+19340-
19459
Exon 5
+22477
-22515
Exon 6
+31108-
31210
Exon 7
+32973-
33180
3' UTR
+33181-33539
mRNA = 1390 bp
5' UTR
~ 172 bp
3' UTR
~ 400 bp
Protein = 281 amino acids
estimated at 31.2 kDa

Figure 5. 6. Summary of the rat *DPH5* gene structure. Rat *DPH5* gene structure was determined by aligning the isolated rat *DPH5* cDNA sequence, the putative rat ORF, the rat genomic sequence, and the NCBI rat partial 5' and 3' EST sequences using BLAST analysis. The EMBL-EBI Gene Wise 2 program was used to determine the intron-exon boundaries, which were confirmed by ORF and genomic DNA alignments. 5' and 3' UTRs are shown in black, and the exons are illustrated in light grey. The locations of the intron-exon boundaries, and the 5' and 3' UTRs are noted under the UTR/intron/exon labels. The transcript is shown in dark grey, and the hatch bar illustrates the protein.

Figure 5.7. Alignment of rat, mouse and human promoter sequences. 10 kb of genomic sequence lying upstream of the putative rat (chromosome 2, NW_043548.1), mouse (chromosome 3, NT_039240), and human (chromosome 1, gi:37546771) +1 transcriptional start site were aligned using NCBI pairwise match and CLUSTALW alignment programs. Promoter analysis, using the Gene Regulation-Match program, identified potential transcription factor binding sites. (A) The rat sequence is illustrated in grey with 500 bp intervals indicated. Regions of homology between the rat and mouse sequence are illustrated with the black lines, while regions of homology between rat and human are indicated with hatched bars. The start and end sites of the regions of homology for the rat genomic sequence are noted above the bar, as is the percent identity between the rat and ortholog sequence, while the start and end sites for the ortholog sequence are indicated below. Transcription factors conserved between the rat and mouse and/or human sequences are indicated. Positions of putative core promoter sequences (as identified using the EMBL-EBI GeneMark program) that are conserved between rat and mouse are illustrated by black boxes. There were no significant core promoter sequences conserved between rat and human promoter sequences. The patterned white box illustrates a putative CpG island, conserved in position between rat and human. B) The table notes the position, sequence and strand of transcription factors conserved between rat, mouse and human.

A)

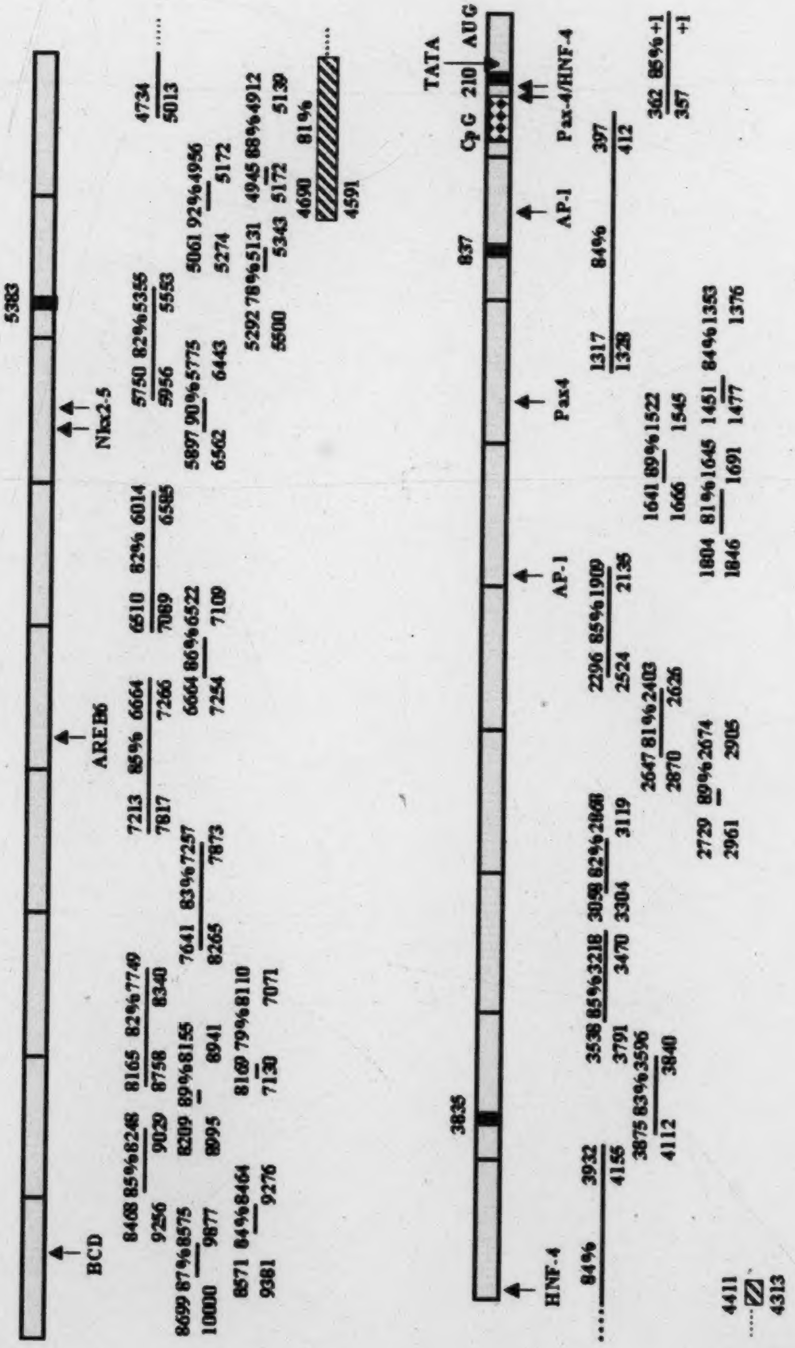

BCD
AREB6
Nkx2-5
5383
3835
837
HNF-4
AP-1
Pax4
AP-1
CpG
210
TATA
AUG
Pax-4/HNF-4
8468 85% 8248
9256 9029
8165 82% 7749
8758 8340
7213 85% 6664
7817 7266
6510 82% 6014
7089 6585
5750 82% 5355
5956 5553
4734
5013
8699 87% 8575
10000 9877
8209 89% 8155
8995 8941
7641 83% 7257
8265 7873
6664 86% 6522
7254 7109
5897 90% 5775
6562 6443
5061 92% 4956
5274 5172
8571 84% 8464
9381 9276
8169 79% 8110
7130 7071
5292 78% 5131
5500 5343
4945 88% 4912
5172 5139
4690 81%
4591
84%
3932
4155
3538 85% 3218
3791 3470
3058 82% 2868
3304 3119
2296 85% 1909
2524 2135
1317 84%
1328
397
412
3875 83% 3596
4112 3840
2647 81% 2403
2870 2626
1641 89% 1522
1666 1545
362 85% +1
357 +1
2729 89% 2674
2961 2905
1804 81% 1645
1846 1691
1451 84% 1353
1477 1376
4411
4313

B)

Transcription Factor	Rat Position/Strand	Rat Sequence	Mouse Position/Strand	Mouse Sequence	Human Position/Strand	Human Sequence
BCD	8679 (+)	ggGATTAa	9835 (+)	ggGATTAa		
AREB6	6893 (+)	tccttACCTGtgt	7667 (+)	tccttACCTGtgt		
Nkx-2-5	5909 (-)	CACTTga	6648 (-)	CACTTga		
Nkx2-5	5868 (+)	tcAAGTG	6608 (+)	tcAAGTG		
HNF-4	4466 (+)	gtaggttAAAAGgccagtg	4860 (+)	gtaggttAAAAGgccagtg	5462 (+)	gtaggttAAAAGgccagct
AP-1	1952 (+)	ggTGACTaaca	2348 (+)	ggTGACTaata		
Pax-4	1459 (+)	ggaggTCAGGggagaatcctg	1654 (+)	ggtggTCAGGggagacctctg		
AP-1	633 (+)	ggTGACTaagg	824 (+)	ggTGACTaagg		
Pax-4	276 (-)	cattcctgaccCTTGAcccct	461 (-)	cattcctgaccCTTGAcctct		
HNF-4	273 (-)	tcctgacCCTTGacccctg	458 (-)	tcctgacCCTTGacccctg		

To define the 5' boundary of the rat promoter sequence, 10 kb of upstream rat and mouse genomic sequences were analyzed for the presence of ORFs, which may represent upstream genes. Using the EMBL-EBI GeneMark gene prediction program, no potential open reading frames were identified in the 10 kb upstream of the transcription start site in mouse or rat promoter sequences. As no significant open reading frames were found within this area (using a threshold value of > 60%), the entire 10 kb region was analyzed for the presence of transcription factor binding sites using the Gene Regulation Match gene tool. Overall, of 45 potential binding sites, 9 are conserved between mouse and rat, including an AREB6 site, two Nkx-2-5 sites, two HNF-4 sites, two AP-1 sites, and a Pax-4 site (Figure 5.7). Of the conserved transcription factor binding sites, only one HNF-4 site is conserved in position, strand and identity in rat, mouse and human.

The 3' UTR was defined by determining the location of the AATAAA poly-adenylation sequence, which was located 352 bp downstream of the stop codon. The poly-adenylation sequence potentially results in the addition of a poly(A+) tail to a UG rich sequence, located 52 bp downstream of the poly-adenylation sequence. This would result in a 3' UTR of approximately 421 bp. This is similar to the 410-538 bp 3' UTR of the human CGI-30 clone which appears to be, and the 367 bp 3'UTR of the mouse RIKEN clone.

5.B-5. Potential for alternate splicing of the rat gene

Though only one transcript was observed by Northern analysis (Figure 5.3), comparisons of the human and mouse homologous sequences, as well the predicted rat sequence in the NCBI database, suggested the possibility of alternate splicing of the rat transcript. Several human ESTs appear in the database that have significant homology to the rat ORF (Figure 5.4). These include the human CGI-30 cDNA (gi:31753135), NPD-15 cDNA, FLJ43496 cDNA (gi:34531595), HSPC143 cDNA (gi:6841517), AD-018 (gi:7688688), and cDNA similar to CGI-30 (gi:22902161). Of these, only CGI-30 has a defined map location to chromosome 1p21.2, and no information is available in LocusLink or Unigene for the other human EST sequences. BLAST analysis using the human CGI-30 sequence showed that this sequence is 99 to 100% identical to the other human sequences in the databases, though the regions of identity vary with the different EST sequences. In addition, BLAST analysis of the human genome using the human EST sequences all showed identity to the same region on the chromosome 1 supercontig as the CGI-30 sequence. This suggests that alternate splicing of the human CGI-30 gene is likely responsible for the multiple different human EST sequences, rather than the presence of several distinct, related genes. This seems to be the case in the mouse as well. Analysis of the various mouse cDNA sequences, including the RIKEN cDNA 2410012M04 (gi: 21312387/12845948), and clones isolated from the embryonic diaphragm and neck (gi: 317531355), the embryonic parthenogenote (gi:26337098), and the adult corpora quadregemina (gi:26337774), demonstrated 99% identity between the different sequences. BLAST analysis of the mouse genome showed that only one locus, located at position G1 of chromosome 3, showed identity with the mouse ESTs.

Only one full-length rat mRNA sequence for the *DPH5* gene is currently available in the database (gi:34859872). This NCBI rat sequence is a predicted cDNA sequence and therefore has not been confirmed by isolation of a corresponding cDNA molecule. Comparison to the rat ORF sequence demonstrated 99 and 100% identity over the regions of homology, although two significant regions of the rat NCBI predicted cDNA sequence are lacking in the rat ORF proposed here (nucleotides 1-597 and 935-1046 of the NBCI predicted rat cDNA). These regions do not show similarity to any of the mouse or human EST sequences in the database. As well, the size of the NCBI predicted rat cDNA molecule exceeds that of the observed transcript identified by Northern analysis. In addition, the rat ORF proposed here, as well as those of mouse and human, contain 7 exons, while the NCBI predicted rat cDNA sequence would suggest 12 exons encoding a protein of 543 amino acids. BLAST analysis using the rat ORF presented here, shows identity with only one region in the rat genome, chromosome 2q41, ruling out again the possibility of multiple members of a gene family.

In addition to the NCBI-predicted rat cDNA sequence, several partial rat ESTs have recently appeared in the Unigene database. These include the following accession numbers: AA996583.1, AI 411817.1, AI411829.1, AW917269.1, BF557909.1, BI275276.1, BM386608.1, BQ202734.1, BQ781096.1, BQ782700.1, CB718378.1, CB731008.1 AND BC761633.1. Comparison of these to the rat transcript identified in this study, to the NCBI predicted rat DNA sequence, and to the rat genomic sequence, demonstrated that these ESTs all align with the rat sequence identified in this study. Interestingly, the regions within the NCBI predicted cDNA sequence that do not show similarity to the rat ORF, also do not show homology with any of the partial EST sequences suggesting that perhaps there are errors in the NCBI-predicted transcript. In addition, the failure to identify regions within the various partial ESTs that do not align with the rat ORF but still align with the rat chromosome 2 supercontig means that there is to date no evidence of alternate splicing of the rat transcript.

Comparison of the partial rat ESTs available in the database with the rat 3' UTR described here supports our sequence data and the proposed 3' UTR structure. Unfortunately, the available 5' EST sequences were not sufficient to compare to the 5'UTR proposed here.

The alignments of the ESTs and cDNA molecules described above are shown in Figure 5.4.

5.B-6. Determining the role of diphthamide methyltransferase during oxidative stress induced cell death

Analysis of the Northern blot data demonstrated a decrease in the levels of the rat transcript following light exposure. We attempted to determine the effect of this down-regulation in LIRD, using an oxidative stress sensitivity assay in yeast wild-type and DPH5 deletion strains. Exposure to hydrogen peroxide (H_2O_2) or acetic acid, and the subsequent induction of an oxidative stress environment, have been demonstrated to induce morphological changes commonly associated with apoptotic cell death in wild-type yeast cells (Madeo *et al*, 1999; and Ludovico *et al*, 2001).

Using the methods described by Ludovico *et al* (2001), exponential phase wild-type and DPH5 mutant yeast cells were treated with 0, 20, 40, 80, 120, 160 or 200 mM of acetic acid for 200 minutes. Cells were plated on YEPD media, and after 2-3 days, the number of colonies was determined. Acetic acid is known to induce apoptosis through cytoplasmic acidification, which leads to anion accumulation, inhibition of fermentation and cellular respiration, and cytochrome c release from the mitochondria (Leao and van Uden, 1986; Cassio *et al*, 1987; Pampulha and Loureiro, 1989), an event that is a known activator of the apoptosome in eukaryotic cells (Slee *et al*, 1999). As shown in Figure 5.8, the percent survival for both DPH5 mutant and wild-type cells decreased with increasing acetic acid concentration in a dose-dependent manner. In addition, the DPH5 mutant cells were more sensitive to oxidative stress-induced cell death by 40-160 mM acetic acid than their wild-type counterparts. These differences were significant for treatments of 40 mM and 160 mM as determined by t-test analysis (p=0.05). Treatments of 200 mM acetic acid, a treatment representing necrotic cell death, show little difference between the survival rates between wild-type and DPH5 mutant cells.

Using the methods described by Madeo *et al* (1999), we attempted to determine if the differential sensitivity of the mutant and wild-type yeast cells to acetic acid represented a generalized response to an oxidative stress environment. As such, the cells were treated with 0, 1, 3, 5, 10, 15, or 180 mM H_2O_2. H_2O_2 is known to induce apoptosis by increasing the superoxide and hydroxide concentrations within a cell, causing an acidification and reduction of cellular components including lipids, proteins and DNA (Clement *et al*, 1998; Ueda *et al*, 1992). This also induces the release of cytochrome c from the mitochondria, calcium mobilization, and changes in states of protein phosphorylation and gene expression (Neill *et al*, 2002; Maxwell *et al*, 2002; Kovtun *et al*, 2000). As was seen with acetic acid treatment, DPH5 mutant cells were more sensitive to oxidative stress-induced cell death than wild-type cells, though only for treatments of 10 and 15 mM H_2O_2 (Figure 5.9). The difference between DPH5 and wild-type cells treated with 15 mM H_2O_2 was significant as determined by t-test analysis (p=0.05). In addition, the percent survival for both cell types showed a decrease with increasing H_2O_2 concentrations.

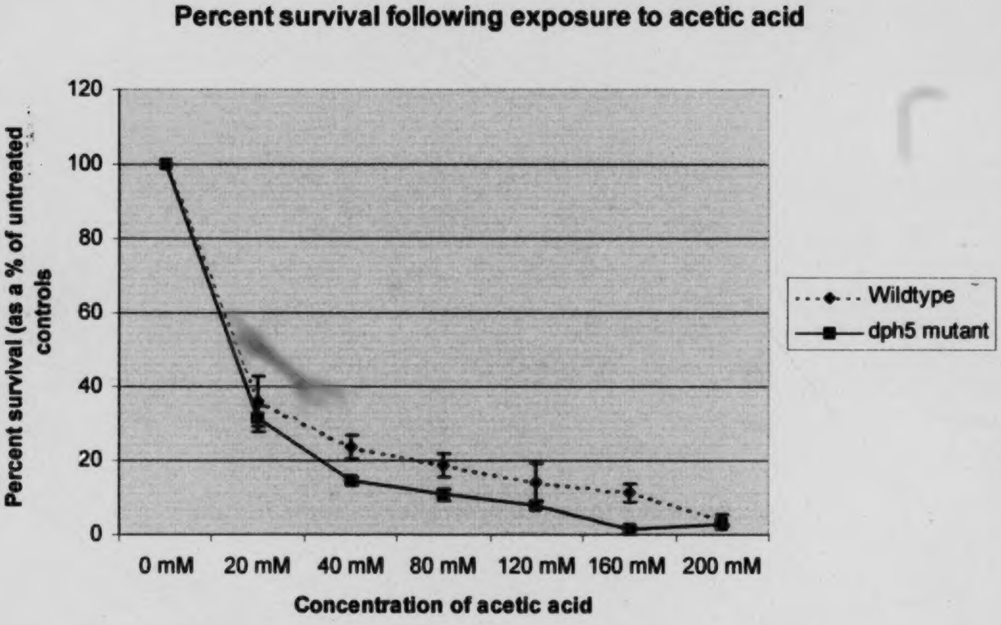

Figure 5.8. Percent survival of wild-type and DPH5 mutant yeast cells treated with varying concentrations of acetic acid. Wild-type and dph5 mutant cells were treated in triplicate with 20, 40, 80, 120, 160 and 200 mM acetic acid and percent survival as compared to untreated controls was determined.

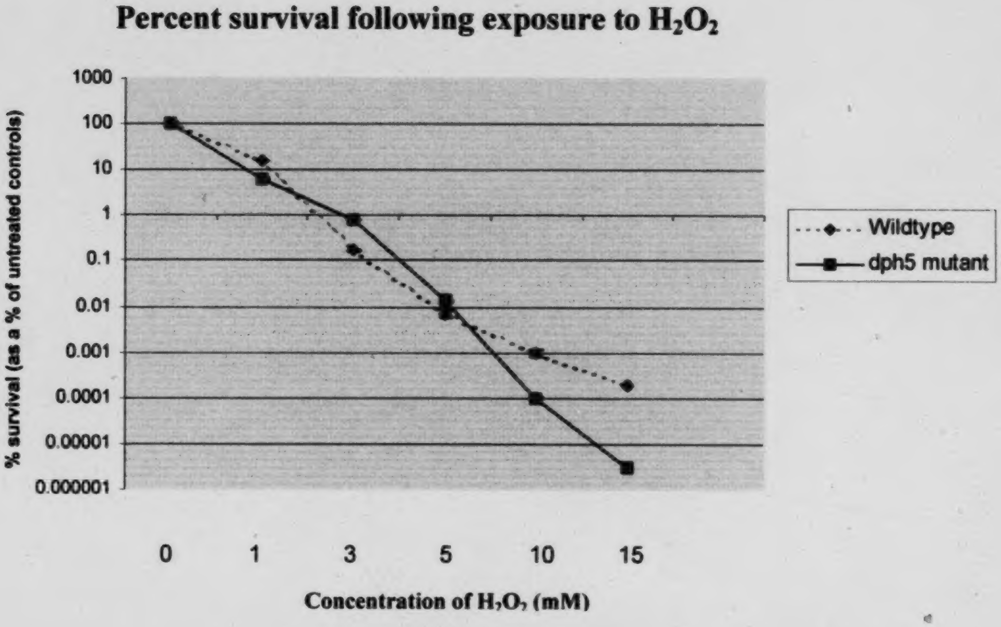

Figure 5.9. Percent survival of wild-type and DPH5 mutant yeast following treatment with varying concentrations of H_2O_2. Wild-type and dph5 mutant cells were treated in triplicate with 1, 3, 5, 10, 15 and 180 mM H_2O_2 and percent survival as compared to untreated controls was determined. There was a 0% survival for both wild-type and dph5 mutant cells for treatments of 180 mM H2O2. (As the above graph is logarithmic error bars are not indicated on the graph but are included in the results section of the text).

5.B-7. Transmission Electron Microscopy of yeast cells undergoing oxidative stress-induced cell death

To determine whether the yeast cells undergoing oxidative stress-induced cell death demonstrated the characteristic morphological features of apoptosis, rather than necrotic cell death, transmission electron microscopy (TEM) was performed. Cells were treated with 0, 3, 15 or 180 mM H_2O_2, or 0, 40, or 120 mM acetic acid for 200 minutes as before, and were analyzed using TEM. Treatment with 120 mM acetic acid resulted in signs of nuclear and cytoplasmic condensation, while treatment with 40 mM acetic acid has a much less pronounced effect on cellular morphology (Figure 5.10). Similarly, extensive chromatin and cytoplasmic condensation was observed with as little as 3 mM H_2O_2 in both wild-type and DPH5 cells, as was membrane blebbing (Figure 5.11 and 5.12). Treatment with 180 mM H_2O_2, on the other hand, resulted in morphology characteristic of necrotic cell death. For both treatments involving acetic acid and H_2O_2, no significant morphological differences were observed between wild-type and DPH5 mutant cells.

5.C. DISCUSSION

The results presented here represent the first identification and characterization of a rat gene believed to encode a putative diphthamide methyltransferase. This is also the first characterization of this gene in higher eukaryotic organisms. Our results suggest that this gene may play a role in mediating sensitivity to oxidative stress-mediated cell death.

Initial analysis of the rat DPH5 gene and protein sequence shows high identity

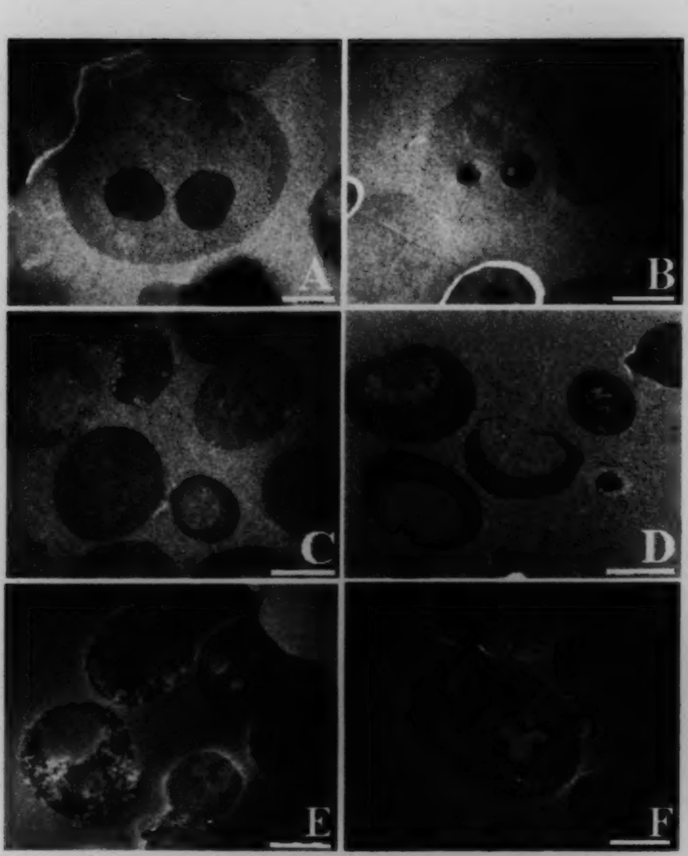

Figure 5.10. Transmission Electron Microscopy of wild-type and dph5 mutant cells treated with acetic acid. Wild-type (A, C, and E) and dph5 mutant (B, D, and F) yeast cells were treated with 0 mM (A, B), 40 mM (C, D), and 120 mM (E, F) acetic acid and were analyzed by TEM for characteristic features of apoptosis. Scale marker = 2000 nm.

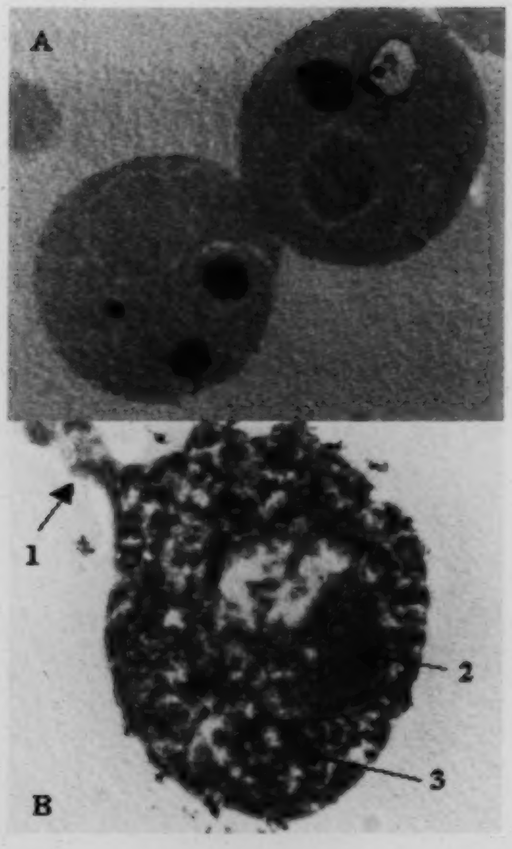

Figure 5.11. Analysis of dph5 mutant yeast cells treated with 10 mM H_2O_2 for characteristic signs of apoptosis. To confirm that the death of yeast cells was the result of apoptosis, dph5 mutant cells were treated with (A) 0 mM or (B) 10 mM H_20_2 and the cells were analyzed by Transmission Electron Microscopy for characteristic signs of apoptotic cell death including (1) membrane blebbing, (2) chromatin condensation, and (3) and cytoplasmic condensation. (Scale bar = 1000 nm)

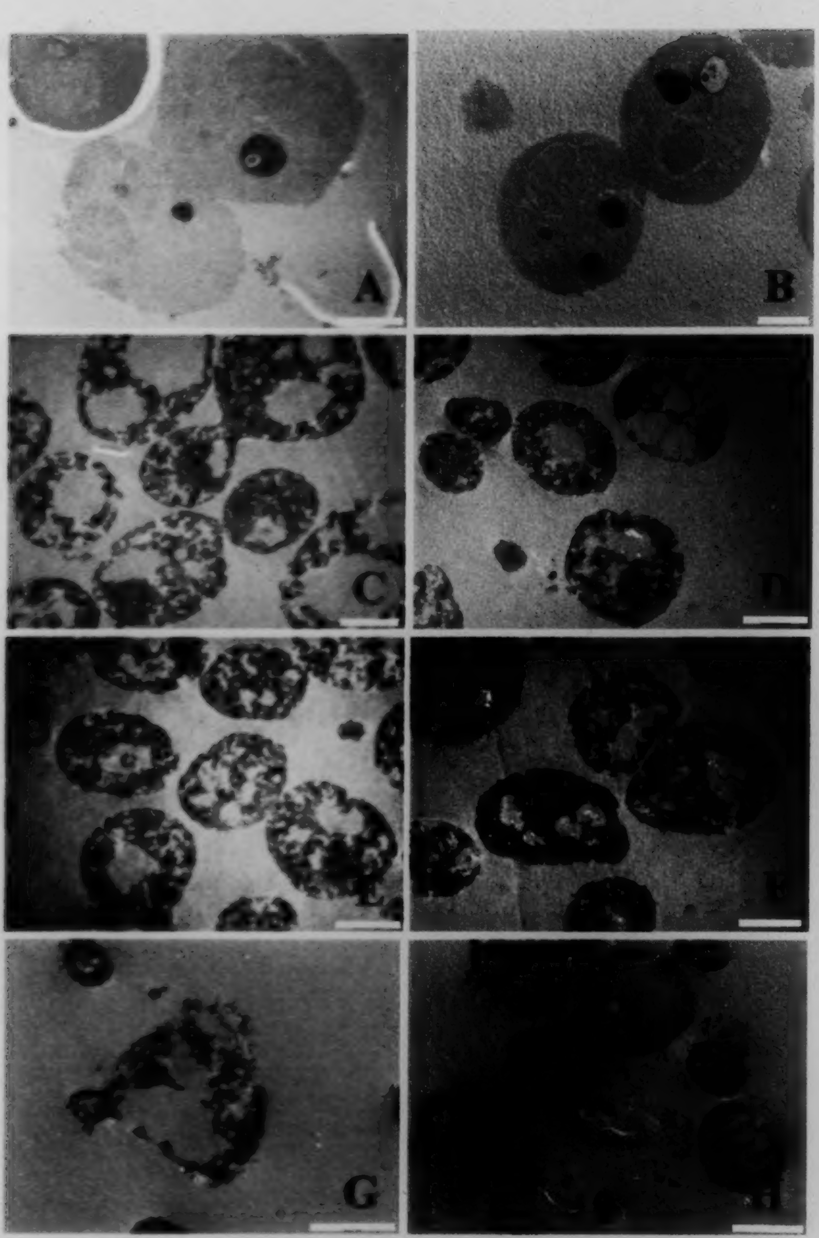

Figure 5.12. Transmission Electron Microscopy of wild-type and dph5 mutant cells treated with H_2O_2. Wild-type (A, C, E and G) and dph5 mutant (B, D, F, and H) yeast cells were treated with 0 mM (A, B), 3 mM (C, D), 15 mM (E, F) and 180 mM (G, H) H2O2 and were analyzed by TEM for characteristic features of apoptosis. Treatment of 180 mM was used to illustrate necrotic cell death where extensive membrane damage and leakage of cytoplasmic components is evident. (Scale bars for A and B = 1000 nM, and scale bars for C to H = 2000 nM).

and strong homology to many evolutionary diverse orthologous DNA sequences. This is expected in light of the findings of Pappenheimer (1983) which demonstrated the presence of diphthamide and mono-ADP ribosylation of EF-2 in cellular extracts from several members of the kingdom Archaebacteria, single-cell eukaryotes such as *Saccharomyces cerevisiae,* and human HeLa cell line. In addition, the target sequence within EF-2, containing the critical histidine residue modified by diphthamide methyltransferase enzymes, is also highly conserved throughout evolution, with the corresponding sequence in yeast being identical to that of humans (Perentesis *et al*, 1992; Brown and Bodley, 1979). The strong sequence conservation in both DPH5 and its target, EF-2, is very interesting given the fact that modification of EF-2 is not required for EF-2 function during translation, nor is a lack of DPH5 lethal in mutant cells (Phan *et al*, 1993; Mattheakis *et al*, 1992).

Analysis of 10 kb of upstream promoter sequence from rat, mouse and human showed high level of similarity between the rat and mouse promoters, but rather limited similarity between the rat and human sequences. Between the rat, mouse and human promoters, only one 278 bp region showed a high level of similarity between all three species. Within this region was one HNF-4 transcription factor binding site that was conserved between all 3 promoter sequences. HNF-4 expression has not previously been described in the retina of rat, mouse or human. HNF-4 has been shown to be repressed following hypoxia, a condition associated with the production of an oxidative stress environment (Mazure *et al*, 2001). Of the transcription factors conserved between the rat and mouse promoters, AREB-6, NKX2-5, AP-1 and Pax4 are known to be expressed in the retina according to the NCBI Unigene database. Of these, NKX2-5 has been suggested to play a role in cell survival (Tanaka *et al*, 2001), while AP-1 has been identified as a pro-apoptotic factor in many systems including the light-damaged mouse retina (Wenzel *et al*, 2000; Remé *et al*, 2003). In addition, AP-1 has been shown to be regulated by the induction of an oxidative stress environment by H_20_2 treatment (Feng *et al*, 2002; Scortegagna *et al*, 1999; Savolainen *et al*, 1998; and Iwata *et al*, 1997). Though further analysis is needed, the presence of several oxidative stress-regulated transcription factor-binding sites suggests that the repression of the rat *DPH5* gene in LIRD may occur in response to the induction of an oxidative stress environment. This is supported by Northern analysis of the rat *DPH5* transcript, that demonstrates a progressive decrease in expression levels following 8 and 16 hours of light exposure, which represent the execution phase and oxidative stress phase of apoptosis, respectively (Wong *et al*, 2001). The repression of DPH5 in response to oxidative stress has also been observed in yeast. Using microarray analysis in wild-type yeast cells, Gasch *et al* (2000) showed the *DPH5* transcript to be repressed following exposure to 0.3 mM H_2O_2 (Gasch *et al*, 2000).

For both yeast wild-type and DPH5 mutant cells, exposure to increasing levels of oxidative stress resulted in a decrease in cell survival. When the level of cell survival of the acetic acid or H_2O_2-treated wild-type cells was compared to the results described by Ludovico *et al* (2001) and Madeo *et al* (1999) the involvement of a cell's genetic background became apparent. The BY4741 strain of yeast used here was less sensitive to acetic acid than the W303-1A wild-type strain used by Ludovico *et al* (2001), while the former was more sensitive to H_2O_2 treatment than the KFY417 wild-type strains used by Madeo *et al* (1999). Differences in cell survival due to differences in genetic backgrounds are not unexpected as the cellular response to oxidative stress is very complex and involves many physiological processes within a cell.

Like the TEM studies performed by Ludovico *et al* (2001) and Madeo *et al* (1999), our results demonstrate that treatments with low levels of acetic acid (20 mM – 120 mM) or H_2O_2 (0.3 mM – 15 mM) result in nuclear and chromosomal condensation and membrane blebbing. These morphological characteristics are associated with apoptosis in other systems (Kerr and Harmon, 1991; Bursch *et al*, 1990), leading us to conclude that the observed cell death is occurring through apoptosis or an apoptotic-like mechanism. The notion that apoptosis occurs in single cell organisms is a controversial one. Supporters of this theory suggest that when a single cell within a population of genetically identical cells becomes damaged, it will make the autonomous decision to undergo programmed cell death. The making of this decision in an old or damaged progenitor cell would promote the survival of healthy progeny, as nutrients and space would no longer be wasted on the damaged cell. Skeptics of the occurrence of apoptosis in single cell organisms state that this would merely be the result of "survival of the fittest" or population selection by environmental factors, and not true apoptosis. Recent findings suggest that apoptosis may indeed by an evolutionarily conserved event. Though yeast contain few of the known inducers of apoptosis identified in mammalian systems, they do show the characteristic morphological features of apoptosis when expressing exogenous mammalian death genes (Madeo *et al*, 1997; Ligr, 1998; Greenhalf *et al*, 1996; Kang *et al*, 1999; Janes *et al*, 1997; Ink *et al*, 1997). As well, a caspase-like protease has been identified in yeast that mimics the activity of mammalian caspases, and is believed to form an apoptosome in a fashion similar to that involved in the activation of mammalian caspase 9 (Madeo *et al*, 2002). Similar apoptosis-inducing proteases have also been identified in other very ancient organisms such as the dinoflagellate *Peridinium gatunenase* (Vardi *et al*, 1999). Both the yeast and dinoflagellate caspase-like molecules are induced during oxidative stress-mediated apoptosis. Though these findings suggest that apoptosis is occurring in single cell organisms, further studies are required to definitively prove that this is true apoptotic cell death and not merely apoptosis-like in appearance.

The results of the oxidative stress-sensitivity assays performed in this study suggest that the lack of DPH5 in yeast loss-of-function mutant cells renders these cells significantly more sensitive to the oxidative stress than their wild-type counterparts. The role of DPH5 in oxidative stress-induced apoptotic cell death is unknown. In light of the role of its only known target, EF-2, in translation elongation, we can postulate that DPH5 may help regulate EF-2 function in this process. The modified form of EF-2 (EF-2 diphthamide) is not only sensitive to exogenous ribosylation factors, such as diphtheria toxin, but would likely also be sensitive to endogenous mono-ADP ribosylation factors. Mono-ADP ribosylation factors have been identified in a variety of eukaryotic cells (Bredehorst *et al*, 1978; Bredehorst *et al*, 1981; Hilz *et al*, 1982; Moss and Vaughn, 1978). Modification of EF-2 by DPH5 would allow EF-2 to be targeted and hence, inactivated by these cellular ribosylation factors. The identification of an ADP-ribosyl-transferase inhibitory factor in hamster kidney cells suggests that factors may also be present that help regulate the activity of the ADP-ribosyl-transferases (Lee and Iglewski, 1984). As the half-life of ADP-ribosyl-EF-2 is quite short (Siegmund and Klink, 1992), a balance between the activity of DPH5, ADP-ribosyl-transferases, and various inhibitory factors may facilitate the regulation of protein elongation during translation.

The regulation of translation is especially important in an apoptotic environment such as that observed in LIRD. Inhibition of translation during apoptosis is known to occur at the level of initiation of protein synthesis (for review see Clemens *et al*, 2000). A global shut down of protein synthesis occurs in response to a death signal, or to significant levels of cellular stress (for review see Pachen, 2003; Ron, 2002; Clemens *et al*, 2000). This is believed to act as both a survival and a death-inducing response. Increased stresses within the cell (oxidative stress or cellular damage for example) result in errors in protein folding and stress to the endoplasmic reticulum (ER). As the level of misfolded proteins increases, toxic aggregates tend to form, prompting the cell to induce a stress response which involves the activation of heat shock proteins and chaperones, as well as the shut-down of protein synthesis. By shutting off protein synthesis, the cell attempts to give the ER an opportunity to re-form or remove (via ubiquitin-mediated proteolysis) damaged proteins by reducing the overall level of client proteins accumulating in the ER. If the cell is able to deal with its damage in this way, it will restart translation, and activate survival-related pathways. An inability to deal with the damage would lead to the subsequent activation of death-inducing proteins and the induction of apoptosis. Therefore, the ability to restart translation following this global shut down separates cells that will survive and cells that will succumb to the apoptotic cascade (Paschen, 2003; Bodsch *et al*, 1985; Thilmann *et al*, 1986).

A decrease in diphthamide biosynthesis during apoptosis could possibly promote the reactivation of protein synthesis and survival of the cell. Alternatively, the reactivation of translation as a result of DPH5 repression may facilitate the *de novo* production of pro-apoptotic proteins, and the entry into a cell death pathway. This seems to be the more likely scenario as we have demonstrated, at least in yeast cells, that a lack of DPH5 expression results in an increased sensitivity to oxidative stress leading to apoptosis (or apoptosis-like cell death). Interestingly, DPH2L, another member of the diphthamide biosynthesis pathway, has also been shown to be repressed during the induction of apoptosis in several retinoid sensitive cancer cell lines (Liu *et al*, 2000). Blocking the elongation step of translation through inhibition of the elongation factor EF-1α (Chen, 2000), or using cyclohexamide, a known inhibitor of elongation (Alberts *et al*, 1994), is able to block apoptosis. Therefore, translational elongation is vital to the progression of apoptosis.

The regulation of protein synthesis at the elongation step may help to preferentially target specific transcripts for translation over others. During apoptosis, activated caspases target a variety of translation initiation factors including eIF4G, eIF4B, eIF3, eIF2 and the eIF4E binding protein 4E-BP1 (as reviewed by Clemens *et al*, 2000). This effectively prevents the initiation of translation by conventional means, which usually rely on the presence of a 5'CAP on mRNA molecules. A small number of mRNA molecules contain an internal ribosome entry site (IRES), and hence undergo CAP-independent initiation. Because these mRNA molecules do not rely on the same mechanisms of translation initiation as standard mRNA molecules, the translation of these mRNAs is resistant to the global repression of protein synthesis in apoptotic cells. Several mRNA molecules known to play a role in apoptosis, such as XIAP, c-myc, p97, DAP5, and Apaf-1, are translated in this IRES-mediated manner. Therefore, in apoptotic cells, which do not reactivate translation to normal levels (Paschen, 2003; Bodsch *et al*, 1985; Thilmann *et al*, 1986), elongation must be able to occur, while conventional initiation of translation does not. Therefore, regulation of translation at the level of elongation, possibly through DPH5, may be important in facilitating the translation of pro-apoptotic mRNAs during oxidative stress-induced apoptotic cell death.

In summary, DPH5 and the modification of EF-2 appear to be a common theme in oxidative stress-mediated apoptotic cell death in the light-damaged retina, and H_20_2- and acetic acid- treated yeast cells. We propose that the lack of DPH5 expression, through repression in the light-treated retinae or mutation in DPH5 mutant yeast cells , results in an increase in the levels of translation elongation which may facilitate the production of pro-apoptotic signals leading to cell death. Though further studies are needed, this work emphasizes that regulation of translation at the level of elongation may be an important event in the regulation of apoptosis.

Chapter 6

Summary

6.A. Defining the molecular phenotype in LIRD

Light-induced retinal degeneration in rats is a well-established model system of apoptosis-mediated photoreceptor cell loss. The photoreceptor cell death, the involvement of oxidative stress, and the involvement of light and rhodopsin, factors often shared between LIRD (Sanyal and Hawkins, 1986; Wang *et al*, 1997; Chen J *et al*, 1999; Chen CK *et al*, 1999; LaVail *et al*, 1999; Organisciak *et al*, 1999a, b) and human retinal dystrophies such as retinitis pigmentosa and macular degeneration (Beatrice *et al*, 2003; Taylor *et al*, 1990, Cruickshanks *et al*, 1993; Simons *et al*, 1993; Cideciyan *et al*, 1998, Cruickshanks *et al*, 2001), make LIRD a viable model of human retinal disease. Though several factors that play a role in the progression of apoptosis in this system have been identified, our understanding of the underlying events is still limited. It is our belief that the progression of apoptotic cell death in the light-treated retinae involves changes in the molecular phenotype of the cells within the retina. We propose that this change in the molecular environment of the apoptotic retinae is the result of differential gene expression in not only the dying cell populations, but also in the surviving cells as well. As such, it was the goal of this project to define the molecular changes that are occurring in the retinae during the active execution phase of cell death to increase our understanding of the molecular mechanisms involved in the degeneration process. The work presented here represents novel findings that further advance our understanding of the mechanisms associated with LIRD, and which provide a framework for further study in this field.

6.B. Mechanisms of gene regulation

Regulation of gene expression within eukaryotic cells is a complex multi-faceted process (for review see Alberts *et al*, 1994; van Driel *et al*, 2004; Remenyi *et al*, 2004; Custoidio and Carmo-Fonseca, 2001; Day and Tuite, 1998; Morey and Avner, 2004). Regulation of transcription is one of the first steps in the gene regulation cascade. The underlying factor of this process is the ability of the RNA polymerase protein complex to bind to the promoter of a given gene. This is mediated, and or inhibited by, a complex array of basal and specialized trans-acting factors and co-factors that act in combinations to regulate transcriptional initiation and elongation in positive or negative manners. In addition, cis-acting elements such as silencers, enhancers and promoters provide targets for these trans-acting factors and such interactions further mediate transcriptional regulation. Chromatin structure and the heterochromatin or euchromatin state of the DNA, regulate the interactions between cis- and trans-acting factors by altering the accessibility of binding and recognition sites within the DNA.

Transcription, if successful, is followed by regulation of the mRNA itself. Post-transcriptional modifications of the newly transcribed mRNA, such as the addition of the 5'CAP and 3' poly (A+) tail, all affect not only the stability and targeting of an mRNA molecule to and within the cytoplasm, but also the efficiency of translation initiation. As well, differential alternate splicing influences the identity of the final protein produced. Sequences in the untranslated regions of the mRNA, as well as the levels of key transport proteins in the nucleus and cytoplasm, regulate gene expression by controlling the transport of the mRNA from the nucleus into the cytoplasm. These factors also help regulate the final cytoplasmic destination (i.e. to cytoplasmic ribosomes, or ribosomes contained on the rough endoplasmic reticulum) and stability of the mRNA.

Next is the regulation at the level of translation (for review see Abbott and Proud, 2004; Alberts *et al*, 1994; Horton *et al*, 1992; Kaufmann, 2004; Ron, 2002; Thorton *et al*, 2003; Clemens *et al*, 2000; Calkhoven *et al*, 2002). Again cis- and trans-acting factors determine the efficiency of initiation and elongation of translation by the ribosomes. Molecules such as ribosomal binding proteins, initiation, elongation and termination factors, and numerous non-coding RNA molecules play a combined effect in determining if, when and to what extent a particular mRNA is translated. Once translation is complete, numerous chaperones and accessory molecules regulate the final folding of the peptide chain into a functional 3-dimensional protein. This protein itself is also regulated, by numerous events such as phosphorylation, protein:protein interactions, cellular targeting and sequestering, post-translational modifications, as well as proteolysis and degradation. This profoundly complex hierarchy of gene regulation allows the cell to regulate the expression of genes spatially, temporally, quantitatively and cell-autonomously. As well, due to the intricate interactions and the combinatory nature of the numerous factors involved in the various levels of gene regulation, subtle changes in a small number of factors can have a global effect on the molecular environment within a cell.

6.C. Degeneration in LIRD is the result of a global response

This project focused initially on transcriptional changes in gene expression. Differential cross screening of the 8 hour light-treated retinal cDNA library demonstrated changes in gene expression at the transcriptional level were evident during the active execution phase of apoptosis in LIRD. Bioinformatic analysis of the genes identified as differentially expressed during LIRD demonstrated that the majority of these were not retinal-specific, but rather were widely expressed in many tissues including adult and fetal tissues, as well as cancer cell lines and tumor tissues. In addition, *in silico* functional analysis of these genes illustrated that a wide diversity of cellular processes were represented by the differentially expressed transcripts. These results suggest that the majority of functional changes associated with LIRD do not occur in pathways that are photoreceptor cell-specific, or apoptotic-specific, but rather pathways that are involved in normal cell metabolism and function.

Several of the LIRD genes identified in this study are known to play a role in regulation of gene expression at the mRNA level. Numerous transcription factors and factors involved in RNA splicing and transport were isolated from the library screen, suggesting that regulation of gene expression at the mRNA level and RNA modification are required during the execution phase of cell death in this system. The differential expression of such genes would lead to differential expression and splicing of numerous downstream target genes, possibly providing a means of facilitating the global response occurring in LIRD.

Therefore, our results demonstrate for the first time that the changes in molecular phenotype associated with LIRD represent a global response, involving differential expression of genes related to diverse cellular processes rather than photoreceptor- or retinal cell-specific functions. It is the combined effect of these changes in gene expression that determines the outcome within the light-treated retinae, including cell death or cell survival.

6.D. Changes in gene expression at the translational level in LIRD

In addition to transcriptional control of gene expression during the active execution phase of LIRD, we also found evidence for translational regulatory mechanisms. Several of the differentially expressed genes are known to be associated with a more global regulation of translation. For example, several ribosomal binding proteins were identified in the screenings of the 8-hour execution phase cDNA library, and the 4-hour commitment phase cDNA library (constructed as part of this project, characterized by Jadwiga Stepczynski, Ben MacDonald and Rhonda Kelln in our lab). Further characterization of these ribosomal protein encoding genes by Jadwiga Stepczynski and Ruby Grewal has demonstrated that the ribosomal binding proteins function as important players in the progression of LIRD (Stepczynski 2001, Grewal and Stepczynski *et al*, 2004). Analysis of the expression patterns of genes encoding ribosomal binding proteins has suggested that the expression of various members of this family of proteins may be coordinately regulated during the progression of LIRD. As changes in the combinations of ribosomal binding proteins associated with a ribosome can alter transcript preferences during translation, the alteration of these proteins during LIRD may mediate changes in the expression of many genes at the translational level.

An example of a gene possibly involved in the regulation of translation that may act at a more global level is the protein encoded by the rat *DPH5* gene. Our analysis of the rat *DPH5* diphthamide methyltransferase represents the first identification and characterization of this gene in higher eukaryotes. Characterization of gene structure and Northern blot analysis suggests that this gene is repressed in response to oxidative stress following light-exposure. In addition, our analysis of the role of DPH5 in a yeast oxidative-stress sensitivity assay suggests that the lack of DPH5 promotes apoptotic (or apoptotic-like) cell death in response to oxidative stress.

The yeast DPH5 protein has been well characterized, and is known to modify a specific histidine residue on EF-2, into a specialized and highly conserved molecule known as diphthamide (Pappenheimer *et al,* 1983; Perentesis *et al,* 1988; Chen *et al,* 1985; Mattheakis *et al,* 1992). Ribosylation of the yeast EF-2 diphthamide by exogenous, and possibly endogenous ADP-ribosylation factors, results in the inhibition of EF-2 and subsequent inhibition of the elongation step of translation (Van Ness *et al,* 1980a, b). Within the LIRD retina, differential expression of the rat *DPH5* gene may result in alterations in the levels of EF-2 diphthamide production, providing a mechanism to alter the level of translation in conjunction with endogenous ADP-ribosylation enzymes. This would likely have significant effects on translation of the global population of mRNA molecules within the light-treated retina. As a global repression of protein synthesis is known to be associated with the progression of apoptosis, and one of the main indicators as to whether a cell will live or die relates to its ability to reverse this repression (Clemens *et al,* 2003), changes in the levels of rDPH5 could represent a trigger that could help regulate this decision. Therefore, these results are the first to suggest the importance of regulation of translational elongation during the progression of apoptosis in LIRD.

6.E. Changes in gene expression at the level of protein function

Our results suggest that differential gene expression during LIRD is regulated at the mRNA and protein levels. In addition, we have also demonstrated regulation at the level of protein function as well. Our results suggest that modulation of protein function through kinase and phosphatase activity may play an important role in LIRD due to the significant number of such enzymes identified during the library screen. The regulation of protein function through proteolysis and degradation appears to play an important role as well, as numerous genes whose protein products are involved in ubiquitinylation and proteolysis were identified as LIRD genes. The observed induction of LIRD proteins associated with ubiquitinylation (Figure 4.8, Chapter 4) likely represents the retina's attempt to deal with the accumulation of oxidative-stress damaged proteins following phototoxic light exposure (Naash *et al*, 1977, Obin *et al*, 1998, Obin *et al*, 1996). Therefore, as increasing oxidative stress within the retina likely causes damage to many cellular proteins, the induction of the ubiquitinylation pathway in an attempt to deal with this damage, would provide a mechanism of gene regulation of a large population of gene products.

Caspases, cysteine-dependent proteases known to cleave key cellular targets at aspartate containing consensus sequences, also appear to be involved in the regulation of protein activity during LIRD. Activated caspases are known to cleave a variety of cellular target proteins including key structural, metabolic, and regulatory proteins. Modification of these subsets of proteins leads to cellular dysfunction, and is associated with the morphological and biochemical changes associated with apoptosis (Budihardjo *et al*, 1999; Coehn, 1997; and Wolf and Green, 1999). Our results demonstrated for the first time, the potential involvement of the caspases during the apoptotic cell death following exposure to intense green light. Our results suggest that at least two branches of the caspase cascade are activated in the green light-treated retina, and that these activated caspases are localized to the photoreceptor cell during LIRD. As well, the detection of activated caspases coincides with the onset of photoreceptor cell dysfunction, as indicated by changes in photoreceptor cell gene expression, and precedes the onset of apoptotic cell death, as indicated by the detection of DNA fragmentation. Therefore, activation of the caspase cascade during LIRD would provide a mechanism to induce global morphological and cellular changes in the photoreceptor cell following phototoxic treatments.

6.F. Conclusion

The results of this study have demonstrated for the first time that the molecular and morphological features associated with apoptotic cell death in LIRD represent the combined effects of a series of events. Changes in gene expression involving several levels of regulation facilitate a global response within the cells of the retina.

Though expression studies such as ours do not allow one to determine in which cells the altered gene expression is occurring, or whether the altered gene expression leads to death or survival of the cell, they do stress the importance of considering the global molecular environment within a tissue when studying apoptosis and retinal degeneration. Focusing extensively on a single gene within a complex array of molecular changes may not be informative in explaining the underlying mechanism associated with a particular physiological event. As well, attempts to develop new therapies or replace damaged genes by gene therapy should be approached with caution as it is not currently possible to understand the global cellular implications of altering one factor within the intricate cellular environment.

6.G Future directions

This work represents a starting point in the study of apoptotic cell death in LIRD. Though the results discussed here are novel and illustrate the global nature of the photoreceptor response to phototoxic exposures, additional research is required to further substantiate these findings and to demonstrate the relevance of these findings to other models of apoptosis, photoreceptor cell loss and human retinal dystrophies.

6.G-1. Analysis of the role of caspases in LIRD. Further work in the analysis of caspases during photoreceptor cell death in LIRD would involve independent confirmation of the immunohisthochemistry results obtained in this study. The strong staining seen in the OS is suspect because of its intensity, consistency between control and experimental animals and consistency with all caspase antibodies used. Though preliminary control experiments, including the use of secondary antibodies only (negative control), anti-GFAP staining to demonstrate specificity of antibody binding using the described protocol, and Western blot analysis of purified OS suggest the validity of this staining, further evidence is needed. Preliminary work using blocking peptides during Western blot analysis and immunohistochemistry have supported our initial findings, as intensity of staining decreased or was abolished in the presence the peptides to which the antibodies were raised (data not shown). This work needs to be replicated to confirm the observed results. The use of pre-immune serum during immunohistochemistry should also be performed to demonstrate antibody specificity to the caspase eiptopes to which they were raised. In addition, immunohistochemistry using antibodies raised against proteins known to localize to the RPE, OS, and ONL (for example RPE65, rhodopsin, and CRX, respectively) would help to support the validity of the staining patterns observed in our study. Immuno-precipitation studies, followed by protein sequencing should be performed to confirm the identity of the peptides detected during Western blot analysis of purified OS proteins. In addition, performing assays using known caspase inhibitors on lysates from green light-treated retinae, may help to confirm the activation of the caspases in this system.

6.G-2. Analysis of differential gene expression during LIRD. The next step in the analysis of the differentially expressed genes identified in this study would be to perform *in situ* analysis to determine the localization of LIRD gene transcripts within the normal and light-treated retinae. Raising antibodies to the LIRD proteins would allow for analysis of gene expression at the protein level following Western blot analysis, and determine the localization of the LIRD proteins following immunohistochemistry. This could be performed in conjunction with TUNEL staining to determine if the cells expressing a given protein are undergoing apoptosis. Gene-specific functional analysis would be needed to assess the role of the LIRD genes in photoreceptor cell loss in this system.

6.G-3. Characterization of DPH5 in photoreceptor cell loss. Further work in the characterization of DPH5 in photoreceptor cells would involve *in situ* analysis to localize the *DPH5* transcript to the normal and light-treated retina. Antibodies could be produced against the DPH5 protein to allow for analysis of protein levels following light-exposure, and localization of the DPH5 protein to the retinae. *In vitro* promoter analysis, including gel-motility shift assays, and reporter assays using constructs containing various *DPH5* promoter mutants could help to confirm the identity of the factors involved in the oxidative-stress mediated repression of *DPH5* during LIRD.

Further functional analysis of DPH5 could involve the analysis of translational elongation during oxidative stress-induced cell death in yeast. Using ^{35}S-methionine incorporation during translation, the rate of protein synthesis could be assessed in DPH5 and wild-type yeast cell in response to oxidative stress. This work could also be carried out in photoreceptor cell cultures in which the levels of *DPH5* have been reduced by siRNA. SDS-Polyacrylamide gel electrophoresis could be used to determine if there is a difference in the proteins translated during cell death in *DPH5* knockdown and wild-type cells. If differentially expressed proteins were identified, protein isolation and sequencing could confirm the identities of the proteins, and may determine if DPH5 regulates the translation of internal ribosome entry site (IRES)-containing transcripts as proposed in chapter 5.

If money were not an issue, *DPH5* knock-out mice could be constructed and treated as in LIRD experiments used in this study. The rate and extent of cell death following light-exposure could be assessed in these animals and compared to the results in wild-type animals obtained in the current study. In addition, due to our limited knowledge of DPH5 function and regulation, it would be interesting to look at the role of DPH5 in other systems involving apoptosis or tissue degeneration, to determine if DPH5 plays a role in apoptosis in general.

BIBLIOGRAPHY

7 Abbott CM, Proud CG. Translation factors: in sickness and in health. *Trends Biochem Sci.* 2004; 29(1):25-31

Abler AS, Chang CJ, Ful J, Tso MO, Lam TT. Photic injury triggers apoptosis of phtoreceptor cells. *Res Commun Mol Pathol Pharmacol.* 1996; 92:177-89

Adams JM, and Cory S. The Bcl-2 family: Arbiters of cell survival. *Science.* 1998; 281:1322-1326

Alam A, Cohen LY, Aouad S, Sekaly R-P. Early activation of caspases during lymphocyte stimulation results in selective substrate cleavage in nonapoptotic cells. *J Exp Med.* 1999; 190:1879-1890

Alberts B, Bray D, Lewis J, Raff M, Roberts K, Watson JD. *Molecular Biology of the Cell, Third Edition.* Garland Publishing Inc. New York, NY, 1994

Allen DM, Hallows TE. Solar pruning of retinal rods in albino rainbow trout. *Vis Neurosci.* 1997; 14: 589-600

Allen DM, Pipes C, Deramus K Hallows TE. A comparison of light-induced rod degeneration in two teleost models. In *Retinal Degenerative Diseases and Experimental Therapy.* Plenum Publishers, New York, NY. 1999

Allikmets R, Singh N, Sun H, Shroyer NF, Hutchinson A, Chidambaram A, Gerrard B, Kaird L, Stauffer D, Peiffer A, Rattner A, Smallwood P, Li Y, Anderson KL, Lewis RA, Nathans J, Leppert M, Dean M, and Lupski JR. A photoreceptor cell-specific ATP-binding transporter gene (ABCR) is mutated in recessive Stargardt macular dystrophy. *Nat Genet.* 1997; 15:236-246

Althaus FR. Poly ADP-ribosylation: a histone shuttle mechanism in DNA excision repair. *J Cell Sci.* 1992; 102:663-70

Ambati J, Anand A, Fernandez S, Sakurai E, Lynn BC, Kuziel WA, Rollins BJ, Ambati BK. An animal model of age-related macular degeneration in senescent Ccl-2- or Ccr-2-deficient mice. *Nat Med.* 2003; 9(11):1390-7

Anderson RE, Maude MB, and Nielson JC. Effect of lipid peroxidation on rhodopsin regeneration. *Current Eye Res.* 1985; 4 (1):65-71

Aznar S, Fernandez-Valeron P, Espina C, Lacal JC. Rho GTPases: potential candidates for anticancer therapy. *Cancer Lett.* 2004; 206(2):181-91

Bader BL, Rayburn H, Crowley D, Hynes RO. Extensive vasculogenesis, angiogenesis, and organogenesis precede lethality in mice lacking all alpha-V integrins. *Cell*. 1998; 95: 507-519

Bagheri-Yarmand R, Vadlamudi RK, Kumar R. Activating transcription factor 4 overexpression inhibits proliferation and differentiation of mammary epithelium resulting in impaired lactation and accelerated involution. *J Biol Chem*. 2003; 278(19):17421-9

Barber AJ, Nakamura M, Wolpert EB, Reiter CE, Seigel GM, Antonetti DA, Gardner TW. Insulin rescues retinal neurons from apoptosis by a phosphatidylinositol 3-kinase/Akt-mediated mechanism that reduces the activation of caspase-3. *J Biol Chem*. 2001; 276:32814-21

Beatrice J, Wenzel A, Remé CE, Grimm C. Increased light damage susceptibility at night does not correlate with RPE65 levels and rhodopsin regeneration in rats. *Exp Eye Res*. 2003; 76(6):695-700

Berg JM, Tymoczko JL, Styer L. Biochemistry, fifth edition. WH Freeman and Co., New York, NY. 2002

Bertoli-Avella AM, Oostra BA, Heutink P. Chasing genes in Alzheimer's and Parkinson's disease. *Hum Genet*. 2004; 114(5):413-38

Beutner G, Ruck A, Riede B, Brdiczka D. Complexes between porin, hexokinase, mitochondrial creatine kinase and adenylate translocator display properties of the permeability transition pore. Implication for regulation of permeability transition by the kinases. *Biochim Biophys Acta*. 1998; 1368(1):7-18

Bicknell IR, Darrow R, Barsalou L, Fliesler SJ, Organisciak DT. Alterations in retinal rod outer segment fatty acids and light-damage susceptibility in P23H rats. *Mol Vis*. 2002; 8:333-40

Birch DG, and Jacobs GH. Light-induced damage to photopic and scotopic mechanisms in the rat depends on rearing conditions. *Exp. Neurology*. 1980; 68:269-283

Blais JD, Filipenko V, Bi M, Harding HP, Ron D, Koumenis C, Wouters BG, Bell JC. Activating transcription factor 4 is translationally regulated by hypoxic stress. *Mol Cell Biol*. 2004; 24(17):7469-82

Blystone SD. Integrating an integrin: a direct route to actin. *Biochim Biophys Acta*. 2004; 1692(2-3):47-54

Bodsch W, Takahashi K, Barbier A, Ophoff BG, Hossmann KA. Cerebral protein synthesis and ischemia. *Prog Brain Res*. 1985; 63:197-210

Boehmer C, Henke G, Schniepp R, Palmada M, Rothstein JD, Broer S, Lang F. Regulation of the glutamate transporter EAAT1 by the ubiquitin ligase Nedd4-2 and the serum and glucocorticoid-inducible kinase isoforms SGK1/3 and protein kinase B. *J Neurochem*. 2003; 86(5):1181-8

Bonaldo MF, Lennon G, Soares MB. Normalization and subtraction: two approaches to facilitate gene discovery. Genome Res. 1996; 6(9):791-806

Bonte CA, Matthijs GL, Cassiman JJ, Leys AM. Macular pattern dystrophy in patients with deafness and diabetes. *Retina*. 1997; 17(3):216-21

Borst DE, Nickerson JM. The isolation of a gene encoding interphotoreceptor retinoid-binding protein. *Exp Eye Res.* 1988; 47(6):825-38

Bradford MM. A rapid and sensitive method for the quantitation of microgram quantities of protein utilizing the principle of protein dye binding. *Anal Biochem*. 1976; 72:248-254

Bredehorst R, Wielckens K, Gartemann A, Lengyel H, Klapproth K, Hilz H. Two different types of bonds linking single ADP-ribose residues covalently to proteins. Quantification in eukaryotic cells. *Eur J Biochem*. 1978; 92(1):129-35

Bredehorst R, Wielckens K, Adamietz P, Steinhagen-Thiessen E, Hilz H. Mono(ADP-ribosyl)ation and poly(ADP-ribosyl)ation of proteins in developing liver and in hepatomas: relation of conjugate subfractions to metabolic competence and proliferation rates. *Eur J Biochem*. 1981; 120(2):267-74

Brenner C, Cadiou H, Vieira HL, Zamzami N, Marzo I, Xie Z, Leber B, Andrews D, Duclohier H, Reed JC, Kroemer G. Bcl-2 and Bax regulate the channel activity of the mitochondrial adenine nucleotide translocator. *Oncogene*. 2000; 19(3):329-36

Brown BA, Bodley JW. Primary structure at the site in beef and wheat Elongation factor 2 of ADP-ribosylation by diphtheria toxin. *FEBS Lett*. 1979; 103(2):253-5

Brown BM, Carlson BL, Zhu X, Lolley RN, Craft CM. Light-driven translocation of the protein phosphatase 2A complex regulates light/dark dephosphorylation of phosducin and rhodopsin. *Biochemistry*. 2002a; 41(46):13526-38

Brown MD, Wallace DC. Molecular basis of mitochondrial DNA disease. *J Bioenerg Biomembr*. 1994; 26(3):273-89

Brown MD, Torroni A, Reckord CL, Wallace DC. Phylogenetic analysis of Leber's hereditary optic neuropathy mitochondrial DNA's indicates multiple independent occurrences of the common mutations. *Hum Mutat*. 1995; 6(4):311-25

Brown MD, Starikovskaya E, Derbeneva O, Hosseini S, Allen JC, Mikhailovskaya IE, Sukernik RI, Wallace DC. The role of mtDNA background in disease expression: a new primary LHON mutation associated with Western Eurasian haplogroup. *J Hum Genet.* 2002b; 110(2):130-8

Bryson JM, Coy PE, Gottlob K, Hay N, Robey RB. Increased hexokinase activity, of either ectopic or endogenous origin, protects renal epithelial cells against acute oxidant-induced cell death. *J Biol Chem.* 2002; 277(13):11392-400

Budihardjo I, Oliver H, Lutter M, Luo X, Wang X. Biochemical pathways of caspase activation during apoptosis. *Annu Rev Cell Dev Biol.* 1999; 15:269-90

Bursch W, Kleine L, and Tenniswood M. The biochemistry of cell death by apoptosis. *Biochem Cell Biol.* 1990; 68: 1071-1074

Bush RA, Remé CE, and Malnoe A. Light Damage in the Rat Retina: The Effect of Dietary Deprivation of N-3 Fatty Acids on Acute Structural Alterations. *Exp Eye Res.* 1991; 53:741-752

Calkhoven CF, Muller C, Leutz A. Translational control of gene expression and disease. *Trends Mol Med.* 2002; 8(12):577-83

Canadian National Institute for the Blind website, http://www.cnib.ca/ July 1998

Carmody RJ, McGowan AJ, Cotter TG. Reactive oxygen species as mediators of photoreceptor apoptosis in vitro. *Exp Cell Res.* 1999; 248(2):520-30

Carmody RJ, Cotter TG. Oxidative stress induces caspase-independent retinal apoptosis in vitro. *Cell Death Differ.* 2000; 7:282-91

Cassio F, Leao C, van Uden N. Transport of lactate and other short-chain monocarboxylates in the yeast Saccharomyces cerevisiae. *Appl Environ Microbiol.* 1987; 53:509-513

Chang B, Hawes NL, Hurd RE, Davisson MT, Nusinowitz S, Heckenlively JR. Retinal degeneration mutants in the mouse. *Vision Res.* 2002; 42(4):517-25

Chang GQ, Hao Y, Wong F. Apoptosis: final common pathway of photoreceptor death in rd, rds, and rhodopsin mutant mice. *Neuron.* 1993; 11:595-605

Chen CK. Recovering and rhodopsin kinase. *Adv Exp Med Biol.* 2002; 514:101-7

Chen CK, Burns ME, Spencer M, Niemi GA, Chen J, Hurley JB, Baylor DA, Simon MI. Abnormal photoresponses and light-induced apoptosis in rods lacking rhodopsin kinase. *Proc Natl Acad Sci U S A.* 1999b; 96(7):3718-22

Chen E, Proestou G, Bourbeau D, Wang E. Rapid up-regulation of peptide Elongation factor EF-1α protein levels is an immediate early event during oxidative stress-induced apoptosis. *Exp Cell Res*. 2000; 259:140-148.

Chen J, Flannery JG, LaVail MM, Steinberg RH, Xu J, Simon MI. bcl-2 overexpression reduces apoptotic photoreceptor cell death in three different retinal degenerations. *Proc Natl Acad Sci USA*. 1996; 93:7042-7

Chen J, Simon MI, Matthes MT, Yasumura D, LaVail MM. Increased susceptibility to light damage in an arrestin knockout mouse model of Oguchi disease (stationary night blindness). *Invest Ophthalmol Vis Sci*. 1999a; 40(12):2978-82

Chen J-YC, Bodley JW, Livingston DM. Diphtheria toxin-resistant mutants of Saccharomyces cerevisiae. *Mol Cell Biol*. 1985; 5(12):3357-3360

Chen J-YC, Bodley JW. Biosynthesis of diphthamide in Saccharomyces cerevisiae: Partial purification and characterization of a specific S-adenosylmethionine:Elongation factor 2 methyltransferase. *J Biol Chem*. 1988; 263(24):11692-11696

Chen TA, Yang F, Cole GM, Chan SO. Inhibition of caspase-3-like activity reduces glutamate induced cell death in adult rat retina. *Brain Res*. 2001; 904:177-88

Cheng C and Zochodne DW. Sensory neurons with activated caspase-3 survive long-term, experimental diabetes. *Diabetes*. 2003; 52:2353-2371

Chiao PJ, Shin DM, Sacks PG, Hong WK, Tainsky MA. Elevated expression of the ribosomal protein S2 gene in human tumors. *Mol Carcino*. 1992; 5: 219-231

Chiarugi P. Reactive oxygen species as mediators of cell adhesion. *Ital J Biochem*. 2003; 52(1):28-32

Choi S, Hao W, Chen CK, Simon MI. Gene expression profiles of light-induced apoptosis in arrestin/rhodopsin kinase-deficient mouse retinas. *Proc Natl Acad Sci U S A*. 2001; 98(23):13096-101

Cicerone CM. Cones survive rods in the light-damaged eye of the albina rat. *Science*. 1976; 194:1183-1185

Cideciyan AV, Hood DC, Huang Y, Banin E, Li Z-Y, Stone EM, Milam AH, Jacobson SG. Disease sequence from mutant rhdopsin allele to rod and cone photoreceptor degeneration in man. *Proc Nat Acad Sci USA*. 1998; 95:7103-7108

Ciechanover A, Schwartz AL. The ubiquitin-mediated proteolytic pathway: mechanisms of recognition of the proteolytic substrate and involvement in the degradation of native cellular proteins. *FASEB J*. 1994; 8(2):182-91

Clegg DO, Mullick LH, Wingerd KL, Lin H, Atienza JW, Bradshaw AD, Gervin DB, Cann GM. Adhesive events in retinal development and function: the role of integrin receptors. *Results Probl Cell Differ.* 2000; 31:141-56

Clemens MJ, Bushell M, Jeffrey IW, Pain VM, Morley SJ. Translation inhibition factor modifications and the regulation of protein synthesis in apoptotic cells. *Cell Death and Differ*. 2000; 7:603-615

Clement MV, Ponton A, Pervaiz S. Apoptosis induced by hydrogen peroxide is mediated by decreased superoxide anion concentration and reduction of intracellular milieu. *FEBS Lett.* 1998 Nov 27;440(1-2):13-8

Cohen AI. The Retina. *Adlers Physiology of the Eye, 9th Edition*. Mosby Year Book, St. Louis, MI, 1992

Cohen GM. Caspases: the executioners of apoptosis. *Biochem J.* 1997; 326:1-16

Coleman ML, Olson MF. Rho GTPase signalling pathways in the morphological changes associated with apoptosis. *Cell Death Differ*. 2002; 9(5):493-504

Collier RJ, Zigman S. Comparison of retinal photochemical lesions after exposure to near-UV or short-wavelength visible radiation. In: *Inherited and Environmentally Induced Retinal Degenerations*. New York, NY. 1989

Corda D, and Di Girolamo M. Functional aspects of protein mono-ADP ribosylation. *EMBO J.* 2003; 22(9):1953-8

Correa-Rotter R, Mariash C, and Rosenberg ME. Loading and transfer control for Northern hybridization. *BioTechniques*. 1992; 12: 154-158

Cortina MS, Gordon WC, Lukiw WJ, Bazan NG. Light-induced photoreceptor damage triggers DNA repair: differential fate of rods and cones. *Adv Exp Med Biol*. 2003; 533:229-40

Costantini P, Belzacq AS, Vieira HL, Larochette N, de Pablo MA, Zamzami N, Susin SA, Brenner C, Kroemer G. Oxidation of a critical thiol residue of the adenine nucleotide translocator enforces Bcl-2-independent permeability transition pore opening and apoptosis. *Oncogene*. 2000; 19(2):307-14

Cousins SW, Espinosa-Heidmann DG, Alexandridou A, Sall J, Dubovy S, Csaky K. The role of aging, high fat diet and blue light exposure in an experimental mouse model for basal laminar deposit formation. *Exp Eye Res*. 2002; 75(5):543-53

Crawford MJ, Krishnamoorthy RR, Rudick VL, Collier RJ, Kapin M, Aggarwal BB, Al-Ubaidi MR, Agarwal N. Bcl-2 overexpression protects photooxidative stress-induced apoptosis of photoreceptor cells via NF-kappaB preservation. *Biochem Biophys Res Commun*. 2001; 281(5):1304-12

Crimi M, Galbiati S, Perini MP, Bordoni A, Malferrari G, Sciacco M, Biunno I, Strazzer S, Moggio M, Bresolin N, Comi GP. A mitochondrial tRNA(His) gene mutation causing pigmentary retinopathy and neurosensorial deafness. *Neurology*. 2003; 60(7):1200-3

Cruickshanks KL, Klein R, Klein BE. Sunlight and age-related macular degeneration. The beaver dam eye study. *Arch Ophthalmol*. 1993; 111:514-518

Crickshanks KJ, Klein R, Klein BE, Nondahl DM. Sunlight and the 5-year incidence of early age-related maculopathy: the beaver dam eye study. *Arch Ophthalmol*. 2001; 119:246-250

Custodio N, Carmo-Fonseca M. Quality control of gene expression in the nucleus. *J Cell Mol Med*. 2001; 5(3):267-75

Damsky CH, Werb Z. Signal transduction by integrin receptors for extracellular matrix: cooperative processing of extracellular information. *Curr Opin Cell Biol*. 1992; 4(5):772-81

Danciger M, Lyon J, Worrill D, LaVail MM, Yang H. A strong and highly significant QTL on chromosome 6 that protects the mouse from age-related retinal degeneration. *Invest Ophthalmol Vis Sci*. 2003; 44(6):2442-9

Danial NN, Gramm CF, Scorrano L, Zhang CY, Krauss S, Ranger AM, Datta SR, Greenberg ME, Licklider LJ, Lowell BB, Gygi SP, Korsmeyer SJ. BAD and glucokinase reside in a mitochondrial complex that integrates glycolysis and apoptosis. *Nature*. 2003; 21; 424(6951):952-6

Da-Silva WS, Gomez-Puyou A, Gomez-Puyou MT, Moreno-Sanchez R, De Felice FG, Davidson JF, Whyte B, Bissinger PH, Schiestl. Oxidative stress is involved in heat-induced cell death in Saccharomyces cerevisiae. *PROC NAT ACAD SCI*. 1996; 93:5116-5121

Day DA, Tuite MF. Post-transcriptional gene regulatory mechanisms in eukaryotes: an overview. *J Endocrinol*. 1998; 157(3):361-71

Debonneville C, Staub O. Participation of the ubiquitin-conjugating enzyme UBE2E3 in Nedd4-2-dependent regulation of the epithelial Na+ channel. *Mol Cell Biol*. 2004; 24(6):2397-409

Deichmann M, Polychronidis M, Wacker J, Thome M, Naher H. The protein phosphatase 2A subunit Bgamma gene is identified to be differentially expressed in malignant melanomas by subtractive suppression hybridization. *Melanoma Res*. 2001; 11(6):577-85

Delmelle M. Retinal damage by light: possible implication of singlet oxygen. *Biophys Struct Mech*. 1977; 3(2):195-8

Demontis GC, Longoni B, Marchiafava PL. Molecular steps involved in light-induced oxidative damage to retinal rods. *Invest Ophthalmol Vis Sci*. 2002; 43(7):2421-7

Deutsch WA, Yacoub A, Jaruga P, Zastawny TH, Dizdaroglu M. Characterization and mechanism of action of Drosophila ribosomal protein S3 DNA glycosylase activity for the removal of oxidatively damaged DNA bases. *J Biol Chem*. 1997; 272(52):32857-32860

Dieter M, Palmada M, Rajamanickam J, Aydin A, Busjahn A, Boehmer C, Luft FC, Lang F. Regulation of glucose transporter SGLT1 by ubiquitin ligase Nedd4-2 and kinases SGK1, SGK3, and PKB. *Obes Res*. 2004; 12(5):862-70

DiFiore MSH. Atlas of human histology, third edition. Lea and Febiger, Buenos Aires, Argentina. 1967

Dinudom A, Harvey KF, Komwatana P, Jolliffe CN, Young JA, Kumar S, Cook DI. Roles of the C termini of alpha -, beta -, and gamma -subunits of epithelial Na+ channels (ENaC) in regulating ENaC and mediating its inhibition by cytosolic Na+. *J Biol Chem*. 2001; 276(17):13744-9

Discovery fund for eye research web-site. http://www.discoveryfund.org/anatomyoftheeye.html. 2004

Dithmar S, Sharara NA, Curcio CA, Le NA, Zhang Y, Brown S, Grossniklaus HE. Murine high-fat diet and laser photochemical model of basal deposits in Bruch membrane. *Arch Ophthalmol*. 2001; 119(11):1643-9

Donovan M, Carmody RJ, and Cotter TG. Light-induced photorecpetor apoptosis in vivo requires nNOS and guanylate cyclase activity and is caspase-3 independent. *J Biol Chem*. 2001; 276:23000-8

Donovan M, Cotter TG. Caspase-independent photoreceptor apoptosis in vivo and differential expression of apoptotic protease activating factor-1 and caspase-3 during retinal development. *Cell Death Differ*. 2002; 9(11):1220-31

Dowling JE, Sidman RL. Inherited retinal dystrophy in the rat. *J Cell Biol*. 1962; 14:73-109

Downes SM, Holder GE, Fitzke FW, Payne AM, Warren MJ, Bhattacharya SS, Bird AC. Autosomal dominant cone and cone-rod dystrophy with mutations in the guanylate cyclase activator 1A gene-encoding guanylate cyclase activating protein-1. *Arch Ophthalmol*. 2001; 119(1):96-105

Dryja TP, Hahn LB, Cowley GS, McGee TL, Berson EL. Mutation spectrum of the rhodopsin gene among patients with autosomal dominant retinitis pigmentosa. *Proc Natl Acad Sci U S A*. 1991; 88(20):9370-4

Du K, Herzig S, Kulkarni RN, Montminy M. TRB3: a tribbles homolog that inhibits Akt/PKB activation by insulin in liver. *Science*. 2003; 300(5625):1574-7.

Du L, Zhang X, Han YY, Burke NA, Kochanek PM, Watkins SC, Graham SH, Carcillo JA, Szabo C, Clark RS. Intra-mitochondrial poly(ADP-ribosylation) contributes to NAD+ depletion and cell death induced by oxidative stress. *J Biol Chem*. 2003; 278(20):18426-33

Dunaief JL, Dentchev T, Ying GS, Milam AH. The role of apoptosis in age-related macular degeneration. *Arch Ophthalmol*. 2002; 120(11):1435-42

Dunlop PC, Bodley JW. Biosynthetic labeling of Diphthamide in Saccharomyces cerevisiae. *J Bio Chem*. 1983; 258(8):4754-4758

Dunn R, Klos DA, Adler AS, Hicke L. The C2 domain of the Rsp5 ubiquitin ligase binds membrane phosphoinositides and directs ubiquitination of endosomal cargo. *J Cell Biol*. 2004; 165(1):135-44

Dureau P, Jeanny J-C, Clerc B, Dufier J-L, Courtois Y. Long term light-induced retinal degeneration in the miniature pig. *Mol Vis.* 1996; 2: 7-14

Edelmann W, Zervas M, Costello P, Roback L, Fischer I, Hammarback JA, Cowan N, Davies P, Wainer B, Kucherlapati R.: Neuronal abnormalities in microtubule-associated protein 1B mutant mice. *Proc Nat Acad Sci*. 1996; 93: 1270-1275

Elyaman W, Terro F, Wong NS, Hugon J. In vivo activation and nuclear translocation of phosphorylated glycogen synthase kinase-3beta in neuronal apoptosis: links to tau phosphorylation. *Eur J Neurosci*. 2002; 15(4):651-60

Eye Disease Case-Control Study Group. Antioxidant status and neovascular age-related macular degeneration. *Arch. Ophthalmol.* 1992; 111:104-109

Fain GL, Lisman JE. Photoreceptor degeneration in vitamin A deprivation and retinitis pigmentosa: the equivalent light hypothesis. *Exp Eye Res*. 1993; 57(3):335-40

Farber DB, Seager-Danciger J, and Organisciak DT. Levels of mRNA encoding proteins of the cGMP cascade as a function of light environment. *Exp. Eye Res*. 1991; 53:781-786

Farr GW, Scharl EC, Schumacher RJ, Sondek S, Horwich AL. Chaperonin-mediated folding in the eukaryotic cytosol proceeds through rounds of release of native and nonnative forms. *Cell*. 1997; 89(6):927-37

Fath T, Eidenmuller J, Brandt R. Tau-mediated cytotoxicity in a pseudohyperphosphorylation model of Alzheimer's disease. *J Neurosci*. 2002; 22(22):9733-41

Fauser S, Luberichs J, Schuttauf F. Genetic animal models for retinal degeneration. *Surv Ophthalmol*. 2002; 47(4):357-67

Fearnley IM, Carroll J, Shannon RJ, Runswick MJ, Walker JE, Hirst J. GRIM-19, a cell death regulatory gene product, is a subunit of bovine mitochondrial NADH:ubiquinone oxidoreductase (complex I). *J Biol Chem*.2001; 276(42):38345-8

Feng Z, Li L, Ng PY, Porter AG. Neuronal differentiation and protection from nitric oxide-induced apoptosis require c-Jun-dependent expression of NCAM140. *Mol Cell Biol.* 2002 Aug; 22(15):5357-66

Fiorentini C, Falzano L, Travaglione S, Fabbri A. Hijacking Rho GTPases by protein toxins and apoptosis: molecular strategies of pathogenic bacteria. *Cell Death Differ*. 2003; 10(2):147-52

Fischer U, Janicke RU, and Schulze-Osthoff K. Many cuts to ruin: a comprehensive update of caspase substrates. *Cell death and Differentiation*. 2003; 10:75-100

Fite KV, Bengston L, Donaghey B. Experimental light damage increases lipfuscin in the retinal pigment epithelium of Japanese quail. *Exp Eye Res.* 1993; 57: 449-460

Foley BT, Moehring JM, Moehring TJ. Mutations in the Elongation factor 2 gene which confer resistance to diphtheria toxin and Pseudomonas exotoxin A: Genetic and biochemical analysis. *J Bio Chem*. 1995; 270(39):23218-23225

Fotia AB, Ekberg J, Adams DJ, Cook DI, Poronnik P, Kumar S. Regulation of neuronal voltage-gated sodium channels by the ubiquitin-protein ligases Nedd4 and Nedd4-2. *J Biol Chem.* 2004; 279(28):28930-5

Foundation Fighting Blindness website, http://www.blindness.org/ July 2004

Frigerio JM, Berthezene P, Garrido P, Ortiz E, Barthellemy S, Vasseur S, Sastre B, Selezneff I, Dagorn JC, Iovanna JL. Analysis of 2166 clones from a human colorectal cancer cDNA library by partial sequencing. *Hum Mol Gen.* 1995; 4(1): 37-43

Frohlich K-U, Madeo F. Apoptosis in yeast- a monocellular organism exhibits altruistic behavior. *FEBS Lett*. 2000; 473:6-9

Furth PA, Bar-Peled U, Li M. Apoptosis and mammary gland involution: reviewing the process. *Apoptosis.* 1997; 2(1):19-24

Gao H, Hollyfield JG. Basic fibroblast growth factor: increased gene expression in inherited and light-induced photoreceptor degeneration. *Exp Eye Res*. 1996; 62(2):181-9

Garcia A, Cayla X, Guergnon J, Dessauge F, Hospital V, Rebollo MP, Fleischer A, Rebollo A. Serine/threonine protein phosphatases PP1 and PP2A are key players in apoptosis. *Biochimie*. 2003; 85(8):721-6

Gasch AP, Spellman PT, Kao CM, Carmel-Harel O, Eisen MB, Storz G, Botstein D, Brown PO Genomic expression programs in the response of yeast cells to environmental changes. *Mol Biol Cell* 2000; 11(12):4241-57

Gasman S, Chasserot-Golaz S, Bader MF, Vitale N. Regulation of exocytosis in adrenal chromaffin cells: focus on ARF and Rho GTPases. *Cell Signal*. 2003; 15(10):893-9

Gaston K, Jayaraman PS. Transcriptional repression in eukaryotes: repressors and repression mechanisms. *Cell Mol Life Sci*. 2003; 60(4):721-41

Gietz, R.D. and R.A. Woods. Transformation of Yeast by the LiAc/ss-carrier DNA/PEG method. *Methods in Enzymology*. 2002; 350: 87-96

Giordano A and Avantaggiati ML. P300 and CBP: partners for life and death. *J Cell Physiol*. 1999; 181:218-230

Goldstone SD, Lavin MF. Isolation of a cDNA clone, encoding the ribosomal protein S20, downregulated during the onset of apoptosis in a human leukaemic cell line. *Biochem Biophy Res Com*. 1993; 196(2):619-623

Gonzalez-Billault C, Jimenez-Mateos EM, Caceres A, Diaz-Nido J, Wandosell F, Avila J. Microtubule-associated protein 1B function during normal development, regeneration, and pathological conditions in the nervous system. *J Neurobiol*. 2004; 58(1):48-59

Goodman RH and Smolik S. CBP/p300 in cell growth, transformation and development. *Genes Dev*. 2000; 14: 1553-1577

Goodrich JA, Cutler G, Tjian R. Contacts in context: promoter specificity and macromolecular interactions in transcription. *Cell*. 1996; 84(6):825-30

Gordon WC, Casey DM, Lukiw WJ, Bazan NG. DNA damage and repair in light-induced photoreceptor degeneration. *Invest Ophthalmol Vis Sci*. 2002; 43(11):3511-21

Gorgels TG, van Norren D. 1992. Spectral transmittance of the rat lens. *Vision Res*. 32(8):1509-12

Graham BH, Waymire KG, Cottrell B, Trounce IA, MacGregor GR, Wallace DC. A mouse model for mitochondrial myopathy and cardiomyopathy resulting from a deficiency in the heart/muscle isoform of the adenine nucleotide translocator. *Nat Genet.* 1997; 16(3):226-34 .

Green CD, Simons JF, Taillon BE, Lewin DA. Open systems: panoramic views of gene expression. *J Immunol Methods*. 2001 Apr; 250(1-2):67-79

Greenhalf W, Stephan C, Chaudhuri B. Role of mitochondria and C-terminal membrane anchor of Bcl-2 in Bax induced growth arrest and mortality in Saccharomyces cerevisiae. *FEBS Lett*. 1996; Feb 12; 380(1-2):169-75

Gregg D, de Carvalho DD, Kovacic H. Integrins and coagulation: a role for ROS/redox signaling? *Antioxid Redox Signal*. 2004; 6(4):757-64

Grewal R., Stepczynski J., Kelln R., Erickson T., Darrow R., Barsalou L., Patterson M., Organisciak D., Wong P. Co-ordinated changes in classes of ribosomal proteins gene expression is associated with light-induced retinal degeneration. *IOVS*. 2004; 45(11):3885-3895

Griffith TB, Brunner T, Fletcher SM, Green DR, Ferguson TA. Fas ligand-induced apoptosis as a mechanism of immune privilege. *Science*. 1995; 270:1189-1192
Grimm C, Wenzel A, Hafezi F, Remé CE. Gene expression in the mouse retina: the effect of damaging light. *Mol Vis*. 2000; 6:252-60

Grimm C, Remé CE, Rol PO, Williams TP. Blue light's effects on rhodopsin: photoreversal of bleaching in living rat eyes. *Invest Ophthalmol Vis Sci*. 2000a; 41(12):3984-90

Grimm C, Wenzel A, Hafezi F, Yu S, Redmond TM, Remé CE. Protection of Rpe65-deficient mice identifies rhodopsin as a mediator of light-induced retinal degeneration. *Nat Genet*. 2000b; 25(1):63-6

Grimm C, Wenzel A, Williams T, Rol P, Hafezi F, Remé C. Rhodopsin-mediated blue-light damage to the rat retina: effect of photoreversal of bleaching. *Invest Ophthalmol Vis Sci*. 2001; 42(2):497-505

Grimm C, Wenzel A, Groszer M, Mayser H, Seeliger M, Samardzija M, Bauer C, Gassmann M, Remé CE. HIF-1-induced erythropoietin in the hypoxic retina protects against light-induced retinal degeneration. *Nat Med.*2002; 8(7):718-24

Grosshans J, Wieschaus E. A genetic link between morphogenesis and cell division during formation of the ventral furrow in Drosophila. *Cell*. 2000; 101(5):523-31

Guise S, Braguer D, Remacle-Bonnet M, Pommier G, Briand C. Tau protein is involved in the apoptotic process induced by anti-microtubule agents on neuroblastoma cells. *Apoptosis*. 1999; 4(1):47-58

Gygi SP, Rochon Y, Franza BR, Aebersold R. Correlation between protein and mRNA abundance in yeast. *Mol Cell Biol.* 1999 Mar; 19(3):1720-30

Habas R, Kato Y, He X. Wnt/Frizzled activation of Rho regulates vertebrate gastrulation and requires a novel Formin homology protein Daam1. *Cell.* 2001 Dec 28; 107(7):843-54

Haeseleer F, Jang GF, Imanishi Y, Driessen CA, Matsumura M, Nelson PS, Palczewski K. Dual-substrate specificity short chain retinol dehydrogenases from the vertebrate retina. *J Biol Chem.* 2002; 277(47):45537-46

Hafezi F, Marti A, Munz K, Remé CE. Light-induced apoptosis: differential timing in the retina and pigment epithelium. *Exp Eye Res.* 1997a; 64(6):963-70

Hafezi F, Steinbach JP, Marti A, Munz K, Wang ZQ, Wagner EF, Aguzzi A, Remé CE. The absence of c-fos prevents light-induced apoptotic cell death of photoreceptors in retinal degeneration in vivo. *Nat Med.* 1997b; 3(3):346-9

Hafezi F, Grimm C, Wenzel A, Abegg M, Yaniv M, Remé CE. Retinal photoreceptors are apoptosis competent in the absence of JunD/AP-1. *Cell Death Differ.* 1999a; 6:934-6

Hafezi F, Marti A, Grimm C, Wenzel A, Remé CE. Differential DNA binding activities of the transcription factors AP-1 and Oct-1 during light-induced apoptosis of photoreceptors. *Vision Res.* 1999b; 39(15):2511-8

Ham WT Jr, Mueller HA, Sliney DH. Retinal sensitivity to damage from short wavelength light. *Nature.* 1976; 260(5547):153-5

Ham WT Jr, Mueller HA, Ruffolo JJ Jr, Guerry D 3rd, Guerry RK. Action spectrum for retinal injury from near-ultraviolet radiation in the aphakic monkey. *Am J Ophthalmol.* 1982; 93(3):299-306

Hao W, Wenzel A, Obin MS, Chen CK, Brill E, Krasnoperova NV, Eversole-Cire P, Kleyner Y, Taylor A, Simon MI, Grimm C, Remé CE, Lem J. Evidence for two apoptotic pathways in light-induced retinal degeneration. *Nat Genet.* 2002; 32(2):254-60

Harada T, Harada C, Sekiguchi M, Wada K. Light-induced retinal degeneration suppresses developmental progression of flip-to-flop alternative splicing in GluR1. *J Neurosci.* 1998; 18(9):3336-43

Harada T, Harada C, Nakayama N, Okuyama S, Yoshida K, Kohsaka S, Matsuda H, Wada K. Modification of glial-neuronal cell interactions prevents photoreceptor apoptosis during light-induced retinal degeneration. *Neuron.* 2000; 26(2):533-41

Harding HP, Zhang Y, Zeng H, Novoa I, Lu PD, Calfon M, Sadri N, Yun C, Popko B, Paules R, Stojdl DF, Bell JC, Hettmann T, Leiden JM, Ron D. An integrated stress response regulates amino acid metabolism and resistance to oxidative stress. *Mol Cell.* 2003; 11(3):619-33

Harris HR. On the rapid conversion of haematoxylin into haematein in staining reactions. *J Appl Microsc*. 1900; 3:777-80

Harrison TJ, Boles RG, Johnson DR, LeBlond C, Wong LJ. Macular pattern retinal dystrophy, adult-onset diabetes, and deafness: a family study of A3243G mitochondrial heteroplasmy. *Am J Ophthalmol*. 1997; 124(2):217-21

Hart WM. Radiometry and Photometry. *Adlers Physiology of the Eye, 9th Edition*, Mosby Year Book, St. Louis, MI, 1992

Hart WM. Visual Adaptation. *Adlers Physiology of the Eye, 9th Edition*, Mosby Year Book, St. Louis, MI, 1992

Harvey KF, Harvey NL, Michael JM, Parasivam G, Waterhouse N, Alnemri ES, Watters D, Kumar S. Caspase-mediated cleavage of the ubiquitin-protein ligase Nedd4 during apoptosis. *J Biol Chem*. 1998; 273(22):13524-30

Harvey KF, Kumar S. Nedd4-like proteins: an emerging family of ubiquitin-protein ligases implicated in diverse cellular functions. *Trends Cell Biol*. 1999 May; 9(5):166-9

He CH, Gong P, Hu B, Stewart D, Choi ME, Choi AM, Alam J. Identification of activating transcription factor 4 (ATF4) as an Nrf2-interacting protein. Implication for heme oxygenase-1 gene regulation. *J Biol Chem.* 2001; 276(24):20858-65

He L, Poblenz AT, Medrano CJ, Fox DA. Lead and calcium produce rod photoreceptor cell apoptosis by opening the mitochondrial permeability transition pore. *J Biol Chem*. 2000; 275:12175-84

Hecht, E. Optics. 2nd Ed, Addison Wesley, Boston, MA. 1987

Henke G, Maier G, Wallisch S, Boehmer C, Lang F. Regulation of the voltage gated K+ channel Kv1.3 by the ubiquitin ligase Nedd4-2 and the serum and glucocorticoid inducible kinase SGK1. *J Cell Physiol*. 2004; 199(2):194-9

Hettmann T, Barton K, Leiden JM. Microphthalmia due to p53-mediated apoptosis of anterior lens epithelial cells in mice lacking the CREB-2 transcription factor. *Dev Biol*. 2000; 222(1):110-23

Hilz H, Wielckens K, Bredehorst R. ADP-ribosylation reactions, eds. Hayaishi O and Ueda K. *Academic Press*, New York, NY. 1982

Horino K, Hiroshi N, Ohsako T, Shibuya Y, Hiraoka T, Kitamura N, Yamamoto TA monocyte chemotactic factor S19 ribosomal protein dimmer, in phagocytic clearance of apoptotic cells. *Lab Invest*. 1998; 78(5):603-617

Horton HR, Moran LA, Ochs RS, Rawn JD, Scrimgeour KG. Glycolysis and oxidative phosphorylation. *Principles of biochemistry*. Neil Patterson Publishers, Prentice Hall, Englewood Cliffs NJ, 1993

Hsu SH, Lee MJ, Hsieh SC, Scaravilli F, Hsieh ST. Cutaneous and sympathetic denervation in neonatal rats with a mutation in the delta subunit of the cytosolic chaperonin-containing t-complex peptide-1 gene. *Neurobiol Dis*. 2004; 16(2):335-45

Huang H, Li F, Alvarez RA, Ash JD, Anderson RE. Downregulation of ATP synthase subunit-6, cytochrome c oxidase-III, and NADH dehydrogenase-3 by bright cyclic light in the rat retina. *Invest Ophthalmol Vis Sci*. 2004; 45(8):2489-96

Humphries MM, Rancourt D, Farrar GJ, Kenna P, Hazel M, Bush RA, Sieving PA, Sheils DM, McNally N, Creighton P, Erven A, Boros A, Gulya K, Capecchi MR, Humphries P. Retinopathy induced in mice by targeted disruption of the rhodopsin gene. *Nat Genet*. 1997; 15(2):216-9

Humphries P, Kenna P, Farrar GJ. New dimensions in macular dystrophies. *Nat Genet*. 1994; 8(4):315-7

Hynes RO. Integrins: versatility, modulation, and signaling in cell adhesion. *Cell*. 1992; 69(1):11-25

Iglewski WJ, Lee H, Muller P. ADP-ribosyltransferase from beef liver which ADP-ribosylates Elongation factor-2. *FEBS Lett*. 1984; 173(1):113-8

Ikeda K, Kawakami K. DNA binding through distinct domains of zinc-finger-homeodomain protein AREB6 has different effects on gene transcription. *Eur J Biochem*. 1995; 233(1):73-82

Ink B, Zornig M, Baum B, Hajibagheri N, James C, Chittenden T, Evan G. Human Bak induces cell death in Schizosaccharomyces pombe with morphological changes similar to those with apoptosis in mammalian cells. *Mol Cell Biol*. 1997; 17(5):2468-74

Inoue H, Nojima H, and Okayama H. High efficiency transformation of Escherichia coli with plasmids. *Gene*. 1990; 96(1):23-8

Ito A, Koma YI, Watabe K. A mutation in protein phosphatase type 2A as a cause of melanoma progression. *Histol Histopathol*. 2003; 18(4):1313-9

Iwata E, Asanuma M, Nishibayashi S, Kondo Y, Ogawa N. Different effects of oxidative stress on activation of transcription factors in primary cultured rat neuronal and glial cells. *Brain Res Mol Brain Res.* 1997 Oct 15; 50(1-2):213-20

Jacobs GH, Neitz J, Deegan JF II. Retinal receptors in rodents maximally sensitive to unltraviolet light. *Nature*. 1991; 353:655-656

Jacobs GH, Fenwick JA, Williams GA. Cone-based vision of rats for ultraviolet and visible lights. *J Exp Biol.* 2001; 204: 2439-2446

James C, Gschmeissner S, Fraser A, Evan GI. CED-4 induces chromatin condensation in Schizosaccharomyces pombe and is inhibited by direct physical association with CED-9. *Curr Biol*. 1997; 7(4):246-52

Jiang Y, Liu YE, Goldberg ID, Shi YE. Gamma synuclein, a novel heat-shock protein-associated chaperone, stimulates ligand-dependent estrogen receptor alpha signaling and mammary tumorigenesis. *Cancer Res*. 2004; 64(13):4539-46

Joensuu T, Hämäläinen R, Yuan B, Johnson C, Tegelberg S, Gasparini P, Zelante L, Pirvola U, Pakarinen L, Lehesjoki A-E, de la Chapelle A, Sankila E-M. Mutations in a novel gene with transmembrane domains underlie Usher syndrome type 3. *Am J Hum Genet*. 2001; 69:673-684

Jomary C, Darrow RM, Wong P, Organisciak DT, Neal MJ, Jones SE. Lack of causal relationship between clusterin expression and photoreceptor apoptosis in light-induced retinal degeneration. *J Neurochem*. 1999; 72:1923-9

Jones SE, Jomary C, Grist J, Makwana J, Neal MJ. Retinal expression of gamma-crystallins in the mouse. *Invest Ophthalmol Vis Sci*. 1999; 40(12):3017-20

Joseph P, Lei YX, Whong WZ, Ong TM. Oncogenic potential of mouse translation Elongation factor-1 delta, a novel cadmium-responsive proto-oncogene. *J Biol Chem*. 2002; 277(8):6131-6

Kajimoto Y, Hashimoto T, Shirai Y, Nishino N, Kuno T, Tanaka C. cDNA cloning and tissue distribution of a rat ubiquitin carboxyl-terminal hydrolase PGP9.5. *J Biochem (Tokyo)*. 1992; 112(1):28-32

Kaldi I, Martin RE, Huang H, Brush RS, Morrison KA, Anderson RE. Bright cyclic rearing protects albino mouse retina against acute light-induced apoptosis. *Mol Vis*. 2003; 9:337-44

Kang JJ, Schaber MD, Srinivasula SM, Alnemri ES, Litwack G, Hall DJ, Bjornsti MA. Cascades of mammalian caspase activation in the yeast Saccharomyces cerevisiae. *J Biol Chem*. 1999; 274(5):3189-98

Katai N, Kikuchi T, Shibuki H, Kuroiwa S, Arai J, Kurokawa T, Yoshimura N. Caspase-like proteases activated in apoptotic photoreceptors of Royal College of Surgeons rats. *Invest Ophthalmol Vis Sci*. 1999; 40:1802-7

Katz ML, Stientjes HJ, Gao C-L, and Norberg M. Bright environmental light accelerates rhodopsin depletion in retinoid-deprived rats. *Invest Ophthalmol Vis Sci.* 1993; 34:2000-2008

Kaufman RJ. Regulation of mRNA translation by protein folding in the endoplasmic reticulum. *Trends Biochem Sci.* 2004; 29(3):152-8

Keller C, Grimm C, Wenzel A, Hafezi F, Remé C. Protective effect of halothane anesthesia on retinal light damage: inhibition of metabolic rhodopsin regeneration. *Invest Ophthalmol Vis Sci*. 2001; 42(2):476-80

Kenmochi N, Kawaguchi T, Rozen S, Davis E, Goodman N, Hudson TJ, Tanaka T, Page DC. A map of 75 human ribosomal protein genes. *Gen Res.* 1998; 8:509-523

Kerr, J.F.R. and Harmon, B.V. Definition and incidence of apoptosis: an historical perspective. in *Apoptosis, the molecular basis of cell death.* L.D.Tomei and F.O.Cope, editors. Cold Spring Harbor Laboratory Press, Plainsview, New York.1991

Kim J, Chubatsu LS, Admon A, Stahl J, Felous R, Linn S. Implication of mammalian ribosomal protein S3 in the processing of DNA damage. *J Biol Chem*. 1995; 20:13620-13629

Kim SH, Vlkolinsky R, Cairns N, Fountoulakis M, Lubec G. The reduction of NADH ubiquinone oxidoreductase 24- and 75-kDa subunits in brains of patients with Down syndrome and Alzheimer's disease. *Life Sci*. 2001; 68(24):2741-50

Kirsch M, Lee MY, Meyer V, Wiese A, Hofmann HD. Evidence for multiple, local functions of ciliary neurotrophic factor (CNTF) in retinal development: expression of CNTF and its receptors and in vitro effects on target cells. *J Neurochem.* 1997; 68(3):979-90

Kiss-Toth E, Bagstaff SM, Sung HY, Jozsa V, Dempsey C, Caunt JC, Oxley KM, Wyllie DH, Polgar T, Harte M, O'Neill LA, Qwarnstrom EE, Dower SK. Human tribbles: A protein family controlling mitogen activated protein kinase cascades. *J Biol Chem*. 2004 [Epub ahead of print]

Kobayashi, A.; Higashide, T.; Hamasaki, D.; Kubota, S.; Sakuma, H.; An, W.; Fujimaki, T.; McLaren, M. J.; Weleber, R. G.; Inana, G. HRG4 (UNC119) mutation found in cone-rod dystrophy causes retinal degeneration in a transgenic model. *Invest Ophthal Vis Sci.* 2000; 41: 3268-3277

Koegl M, Hoppe T, Schlenker S, Ulrich HD, Mayer TU, Jentsch S. A novel ubiquitination factor, E4, is involved in multiubiquitin chain assembly. *Cell.* 1999; 96(5):635-44

Kovtun Y, Chiu WL, Tena G, Sheen J. Functional analysis of oxidative stress-activated mitogen-activated protein kinase cascade in plants. *Proc Natl Acad Sci U S A.* 2000; 97(6):2940-5

Krishnamoorthy RR, Crawford MJ, Chaturvedi MM, Jain SK, Aggarwal BB, Al-Ubaidi MR, Agarwal N. Photo-oxidative stress down-modulates the activity of nuclear factor-kappa beta via involvement of caspase-1, leading to apoptosis of photoreceptor cells. *J Biol Chem.* 1999; 274:3734-43

Kubota S, Kobayashi A, Mori N, Higashide T, McLaren MJ, Inana G. Changes in retinal synaptic proteins in the transgenic model expressing a mutant HRG4 (UNC119). *Invest Ophthalmol Vis Sci.* 2002; 43(2):308-13

Kumar S, Harvey KF, Kinoshita M, Copeland NG, Noda M, Jenkins NA. cDNA cloning, expression analysis, and mapping of the mouse Nedd4 gene. *Genomics.* 1997; 40(3):435-43

Kurita R, Sagara H, Aoki Y, Link BA, Arai K, Watanabe S. Suppression of lens growth by alphaA-crystallin promoter-driven expression of diphtheria toxin results in disruption of retinal cell organization in zebrafish. Dev Biol. 2003; 255(1):113-27

Kutty, R.K., Kutty, G., Wiggert, B., Chader, G.J., Darrow, R.M., and Organisciak, D.T. Induction of heme oxygenase 1 in the retina by intense visible light: Suppression by the antioxidant dimethylthiourea. *Proc Natl Acad Sci. USA.* 1995; 92:1177-1181

Kuwabara T, and Masakazu F. Light effects on the synaptic organ of the rat. *Invest Ophthalmol Vis Sci.* 1976; 15(5):407-411

Lacal JC. Regulation of proliferation and apoptosis by Ras and Rho GTPases through specific phospholipid-dependent signaling. *FEBS Lett.* 1997; 410(1):73-7

Laemmli, U. K. Cleavage of structural proteins during the assembly of the head of bacteriophage T4. *Nature* 1970; 227:680–685

Lai MC, Lin RI, Tarn WY. Differential effects of hyperphosphorylation on splicing factor SRp55. *Biochem J.* 2003; 371(Pt 3):937-45

Lagali PS, MacDonald IM, Griesinger IB, Chambers ML, Ayyagari R, Wong PW. Autosomal dominant Stargardt-like macular dystrophy segregating in a large Canadian family. *Can J Ophthalmol.* 2000; 35(6):315-24

LaVail MM. Survival of some photoreceptor cells in albino rats following long-term expsoure to continuous light. *Invest Ophthalmol Vis Sci* 1976; 15 (1):64-70

LaVail MM. Eye pigmentation and constant light damage in the rat retina. In: *The effects of constant lights on visual processes*. Editors Williams TP, Baker BN. Plenum Press, New York, NY. 1980

LaVail MM, Gorrin GM, Repaci MA, Thomas LA, and Ginsberg HM. Genetic Regulation of Light Damage to Photoreceptors. *Invest Ophthalmol Vis Sci.* 1987; 28;1048-1987

Lavail MM, Li L, Turner JE, Yasumura D. Retinal pigment epithelial cell transplantation in RCS rats: normal metabolism in rescued photoreceptors. *Exp Eye Res*. 1992a; 55(4):555-62

LaVail MM, Unoki K, Yasumura D, Matthes MT, Yancopoulos GD, Steinberg RH. Multiple growth factors, cytokines, and neurotrophins rescue photoreceptors from the damaging effects of constant light. *Proc Natl Acad Sci U S A.* 1992b; 89(23):11249-53

LaVail MM, Gorrin GM, Yasumura D, Matthes MT. Increased susceptibility to constant light in nr and pcd mice with inherited retinal degenerations. *Invest Ophthalmol Vis Sci*. 1999; 40(5):1020-4

Lawwill T. Effects of prolonged exposure of rabbit retina to low intensity light. *Invest Ophthalmol Vis Sci.* 1973; 12: 45-51

Lay, A. J, Jiang, X.-M, Kisker, O, Flynn, E, Underwood, A, Condron, R, Hogg, P. J. Phosphoglycerate kinase acts in tumour angiogenesis as a disulphide reductase. *Nature*. 2000; 408: 869-873

Leao C, van Uden N. Transport of lactate and other short-chain monocarboxylates in the yeast Candida utilis. *Appl Microbiol Biotechnol.* 1986; 23:389-393

Lee H, Iglewski WJ. Cellular ADP-ribosyltransferase with the same mechanism of action as diphtheria toxin and Pseudomonas toxin A. *Proc Natl Acad Sci U S A*. 1984; 81(9):2703-7

Lee JW, Juliano R. Mitogenic signal transduction by integrin- and growth factor receptor-mediated pathways. *Mol Cells.* 2004; 17(2):188-202

Lee RH, Brown BM, Lolley RN. Light-induced dephosphorylation of a 33K protein in rod outer segments of rat retina. *Biochemistry*. 1984; 23(9):1972-7

Lee SJ, Montell C. Suppression of constant-light-induced blindness but not retinal degeneration by inhibition of the rhodopsin degradation pathway. *Curr Biol*. 2004; 14(23):2076-85

Levin B. Genes V. Oxford University Press, New York, NY. 1993.

Li F, Cao W, Anderson RE. Alleviation of constant-light-induced photoreceptor degeneration by adaptation of adult albino rat to bright cyclic light. *Invest Ophthalmol Vis Sci*. 2003; 44(11):4968-75

Li L, Dowling JE. Zebrafish visual sensitivity is regulated by a circadian clock. *Vis Neurosci.* 1998; 15: 851-857

Li Z-Y, Tso MOM, Wang H-M, Organisciak DT. Amerlioration of photic injury in rat retina by ascorbic acid: histopathologic study. *Invest Ophthalmol Vis Sci.* 1985; 26:1589-98

Ligr M, Madeo F, Frohlich E, Hilt W, Frohlich KU, Wolf DH. Mammalian Bax triggers apoptotic changes in yeast. *FEBS Lett.* 1998; 438(1-2):61-5

Lisman J, Fain G. Support for the equivalent light hypothesis for RP. *Nat Med.* 1995; 1(12):1254-5

Liu C, Li Y, Peng M, Laties AM, Wen R. Activation of caspase-3 in the retina of transgenic rats with the rhodopsin mutation s334ter during photoreceptor degeneration. *J Neurosci*. 1999; 19:4778-85

Liu G, Wu M, Levi G, Ferrari N. Down-regulation of the Diphthamide Biosynthesis protein 2-like gene during retinoid-induced differentiation and apoptosis: implications against its tumor-suppressor activity. *Int J Cancer*. 2000; 88:356-362

Liu M, Regillo CD. A review of treatments for macular degeneration: a synopsis of currently approved treatments and ongoing clinical trials. *Curr Opin Ophthalmol*. 2004; 15(3):221-6

Lolley RN, Rong H, Craft CM. Linkage of photoreceptor degeneration by apoptosis with inherited defect in phototransduction. *Invest Ophthalmol Vis Sci*. 1994; 35:358-62

Long X, Goldenthal MJ, Wu GM, Marin-Garcia J. Mitochondrial Ca2+ flux and respiratory enzyme activity decline are early events in cardiomyocyte response to H2O2. *J Mol Cell Cardiol*. 2004; 37(1):63-70

Los M, Stroh C, Janicke RU, Engels IH, Schulze-Osthoff K. Caspases: more than just killers? *Trends Immunol*. 2001; 22(1):31-4

Ludovico P, Sousa MJ, Silva MT, Leao C, Corte-Real M. Saccharomyces cerevisiae commits to a programmed cell death in response to acetic acid. *Microbio*. 2001; 147:2409-2415

Luna J, Tobe T, Mousa SA, Reilly TM, Campochiaro PA. Antagonists of integrin alpha v beta 3 inhibit retinal neovascularization in a murine model. *Lab Invest.* 1996; 75(4):563-73

Luo, X.; Budihardjo, I.; Zou, H.; Slaughter, C.; Wang, X. Bid, a Bcl2 interacting protein, mediates cytochrome c release from mitochondria in response to activation of cell surface death receptors. *Cell.* 1998; 94: 481-490

MacDonald B. Differential gene expression in LIRD in rats: focus on the cyrstallins. M.Sc. thesis. University of Alberta, Edmonton, AB. 2003

MacDonald IM, Hebert M, Yau RJ, Flynn S, Jumpsen J, Suh M, Clandinin MT. Effect of docosahexaenoic acid supplementation on retinal function in a patient with autosomal dominant Stargardt-like retinal dystrophy. *Br J Ophthalmol.* 2004; 88(2):305-6

MacFarlane M, Cain K, Sun XM, Alnemri ES, Cohen GM. Processing/activation of at least four interleukin-1beta converting enzyme-like proteases occurs during the execution phase of apoptosis in human monocytic tumor cells. *J Cell Biol.* 1997; 137:469-79

Madeo F, Frohlich E, Frohlich KU. A yeast mutant showing diagnostic markers of early and late apoptosis. *J Cell Biol*. 1997;139(3):729-34

Madeo F, Frohlich E, Ligr M, Grey M, Sigrist SJ, Wolf DH, Frohlich K-U. Oxygen stress: A regulator of apoptosis in yeast. *J Cell Bio.* 1999; 145(4):757-767

Madeo F, Engelhardt S, Herker E, Lebmann N, Maldener C, Proksch A, Wissing S, Frohlich K-U. Apoptosis in yeast: a new model system with applications in cell biology and medicine. *Curr Genet.* 2002; 41:208-216

Madeo F, Herker E, Maldener C, Wissing S, Lachelt S, Herlan M, Fehr M, Lauber K, Sigrist S, Wesselborg S, Frohlich K-U. A caspase-related protease regulates apoptosis in yeast. *Mol Cell*. 2002; 9:911-917

Madi A, Pusztahelyi T, Punyiczki M, Fesus L. The biology of the post-genomic era: the proteomics. *Acta Biol Hung*. 2003; 54(1):1-14

Madisen L, Hoar DI, Holroyd CD, Crisp M, Hodes ME. DNA banking: the effects of storage of blood and isolated DNA on the integrity of DNA. *Am J Med Genet*. 1987; 27(2):379-90

Maekawa, M, Ishizaki, T, Boku, S, Watanabe, N, Fujita, A, Iwamatsu, A, Obinata, T, Ohashi, K, Mizuno, K, Narumiya, S. Signaling from Rho to the actin cytoskeleton through protein kinases ROCK and LIM-kinase. *Science.* 1999; 285: 895-898

Mah DY, Wong PW, Edwars A, MacDonald IM. Recent advances in the genetics of macular dystrophies. *Can J Ophthalmol.* 1998; 33:35-43

Magabo KS, Horwitz J, Piatigorsky J, Kantorow M. Expression of betaB(2)-crystallin mRNA and protein in retina, brain, and testis. *Invest Ophthalmol Vis Sci.* 2000; 41(10):3056-60

Majewski N, Nogueira V, Robey RB, Hay N. Akt inhibits apoptosis downstream of BID cleavage via a glucose-dependent mechanism involving mitochondrial hexokinases. *Mol Cell Biol*. 2004; 24(2):730-40

Majji AB, Cao J, Chang KY, Hayashi A, Aggarwal S, Grebe RR, De Juan E Jr. Age-related retinal pigment epithelium and Bruch's membrane degeneration in senescence-accelerated mouse. *Invest Ophthalmol Vis Sci*. 2000; 41(12):3936-42

Mandal MN, Ambasudhan R, Wong PW, Gage PJ, Sieving PA, Ayyagari R. Characterization of mouse orthologue of ELOVL4: genomic organization and spatial and temporal expression. *Genomics*. 2004; 83(4):626-35

Mansergh FC, Millington-Ward S, Kennan A, Kiang AS, Humphries M, Farrar GJ, Humphries P, Kenna PF. Retinitis pigmentosa and progressive sensorineural hearing loss caused by a C12258A mutation in the mitochondrial MTTS2 gene. *Am J Hum Genet*. 1999; 64(4):971-85

Marmor MD, Yarden Y. Role of protein ubiquitylation in regulating endocytosis of receptor tyrosine kinases. *Oncogene*. 2004; 23(11):2057-70

Martin KJ, Pardee AB. Identifying expressed genes. *Proc Natl Acad Sci U S A*. 2000; 97(8):3789-91

Marzo I, Brenner C, Zamzami N, Jurgensmeier JM, Susin SA, Vieira HL, Prevost MC, Xie Z, Matsuyama S, Reed JC, Kroemer G. Bax and adenine nucleotide translocator cooperate in the mitochondrial control of apoptosis. *Science*. 1998; 281(5385):2027-31

Massin P, Guillausseau PJ, Vialettes B, Paquis V, Orsini F, Grimaldi AD, Gaudric A. Macular pattern dystrophy associated with a mutation of mitochondrial DNA. *Am J Ophthalmol*. 1995; 120(2):247-8

Matt T, Martinez-Yamout MA, Dyson HJ, Wright PE. The CBP/p300 TAZ1 domain in its native state is not a binding partner of MDM2. *Biochem J*. 2004; 381(Pt 3):685-91

Mattheakis LC, Shen WH, Collier RJ. Dph5, a methyltransferase gene required for diphthamide biosynthesis in Sacchromyces cerevisiae. *Mol Cell Biol*. 1992; 12(9):4026-4037

Mattheakis LC, Sor F, Collier RJ. Diphthamide synthesis in Saccharomyces cerevisiae: strucutre of the DPH2 gene. *Gene*. 1993; 132:149-154

Maxwell DP, Nickels R, McIntosh L. Evidence of mitochondrial involvement in the transduction of signals required for the induction of genes associated with pathogen attack and senescence. *Plant J.* 2002; 29(3):269-79

Mayumi-Matsuda K, Kojima S, Suzuki H, Sakata T. Identification of a novel kinase-like gene induced during neuronal cell death. *Biochem Biophys Res Commun.* 1999; 258(2):260-4

Mazure NM, Nguyen TL, Danan JL. Severe hypoxia specifically downregulates hepatocyte nuclear factor-4 gene expression in HepG2 human hepatoma cells. *Tumour Biol.* 2001; 22(5):310-7

McBee JK, Palczewski K, Baehr W, Pepperberg DR. Confronting complexity: the interlink of phototransduction and retinoid metabolism in the vertebrate retina. *Prog Ret Eye Res.* 2001; 20(4):469-529

McCallum CD, Do H, Johnson AE, Frydman J. The interaction of the chaperonin tailless complex polypeptide 1 (TCP1) ring complex (TRiC) with ribosome-bound nascent chains examined using photo-cross-linking. *J Cell Biol.* 2000; 149(3):591-602

McLaughlin JN, Thulin CD, Hart SJ, Resing KA, Ahn NG, Willardson BM. Regulatory interaction of phosducin-like protein with the cytosolic chaperonin complex. *Proc Natl Acad Sci U S A.* 2002; 99(12):7962-7

Meier-Ruge WA, Bertoni-Freddari C. Pathogenesis of decreased glucose turnover and oxidative phosphorylation in ischemic and trauma-induced dementia of the Alzheimer type. *Ann N Y Acad Sci.* 1997; 826:229-41

Milam AH, Li Z-Y. Retinal pathology in retinitis pigmentosa: considerations for therapy. In: Anderson RE, LaVail MM, Hollyfield JG eds. *Degenerative Diseases of the Retina*, New York, NY: Plenum Press. 1995

Miller LK. An exegesis of IAPs: salvation and surprises from BIR motifs. *Trends Cell Biol.* 1999; 9:323-8

Moehring JM, Moehring TJ and Dnaley DE. Posttranslational modification of Elongation factor 2 in diphtheria toxin-resistant mutants of CHO-K1 cells. *PROC NAT ACAD SCI.* 1980; 77(2):1010-1014

Moehring JM, Moehring TJ. The Post-translational Trimethylation of Diphthamide Studied in vitro. *J Bio Chem.* 1988; 263(8):3840-3844

Moehring TJ, Danley DE, Moehring JM. In vitro biosynthesis of diphthamide, studied with mutant Chinese Hamster Ovary cells resistant to diphtheria toxin. *Mol Cell Biol.* 1984; 4(4):642-650

Morey C, Avner P. Employment opportunities for non-coding RNAs. *FEBS Lett*. 2004; 567(1):27-34

Morimoto H, Bonavida B. Diphtheria toxin and Pseudomonas A toxin-mediated apoptosis. ADP Ribosylation of Elongation factor-2 is required for DNA fragmentation and cell lysis and synergy with Tumor Necrosis Factorα. *J Immunol*. 1992; 149:2089-2094

Morimura, H.; Fishman, G. A.; Grover, S. A.; Fulton, A. B.; Berson, E. L.; Dryja, T. P. Mutations in the RPE65 gene in patients with autosomal recessive retinitis pigmentosa or Leber congenital amaurosis. *Proc Nat Acad Sci*.1998; 95: 3088-3093

Moritz OL, Tom BM, Knox BE, Papermaster DS. Fluorescent photoreceptors of transgenic xenopres laevis imaged in vivo by two microscopy techniques. *Invest Ophthalmol Vis Sci*. 1999; 40:3276-80

Moss J, Vaughan M. Isolation of an avian erythrocyte protein possessing ADP-ribosyltransferase activity and capable of activating adenylate cyclase. *Proc Natl Acad Sci U S A*. 1978; 75(8):3621-4

Muller S, Straub A, Schroder S, Bauer PH, Lohse MJ. Interactions of phosducin with defined G protein beta gamma-subunits. *J Biol Chem*. 1996; 271(20):11781-6

Muller-Pillasch, F.; Zimmerhackl, F.; Lacher, U.; Schultz, N.; Hameister, H.; Varga, G.; Friess, H.; Buchler, M.; Adler, G.; Gress, T. M. Cloning of novel transcripts of the human guanine-nucleotide-exchange factor Mss4: in situ chromosomal mapping and expression in pancreatic cancer. *Genomics*. 1997; 46: 389-396

Munich information center for protein sequences (WIT/EMP/MPW pathway database). http://mips.gsf.de/genre/proj/ yeast/searchEntryActiondo?text=. 2004

Murakami S, Bodley JW, Livingston DM. Saccharomyces cerevisiae spheroplasts are sensitive to the action of diphtheria toxin. *Mol Cell Biol*. 1982; 2(5):588-92

Murdaca J, Treins C, Monthouel-Kartmann MN, Pontier-Bres R, Kumar S, Van Obberghen E, Giorgetti-Peraldi S. Grb10 prevents Nedd4-mediated vascular endothelial growth factor receptor-2 degradation. *J Biol Chem*. 2004; 279(25):26754-61

Naash MI, Al-Ubaidi MR, Anderson RE. Light exposure induces ubiquitin conjugation and degradation activities in the rat retina. *Invest Ophthalmol Vis Sci*. 1997; 38(11):2344-54

Naora H, Nishida T, Shindo Y, Adachi M, Naora H. Association of nbl gene expression and glucocorticoid-induced apoptosis in mouse thymus in vivo. *Immunology*. 1995; 85(1):63-8

Naora H, Takai I, Adachi M, Naora H. Altered cellular responses by varying expression of ribosomal protein gene: sequential coordination of enhancement and suppression of ribosomal protein S3a gene expression induces apoptosis. *J Cell Biol*. 1998; 141(3):741-753

Naora H, Naora H. Involvement of ribosomal proteins in regulating cell growth and apoptosis: translational modulation or recruitment for extraribosomal activity? *Immun Cell Biol*. 1999; 77:197-205

Neill S, Desikan R, Hancock J. Hydrogen peroxide signalling. *Curr Opin Plant Biol*. 2002; 5(5):388-95

Neumann F, Krawinkel U. Constitutive expression of human ribosomal protein L7 arrests the cell cycle in G1 and induces apoptosis in Jurkat T-lymphoma cells. *Experim Cell Res*. 1997; 230:252-261

Nicholls JG, Martin AR, Wallace BG. *From Neuron to Brain*, Third Edition. Sinauer Associates, Inc. Sunderland, MA. 1992

Nickells RW, and Zack DJ. Apoptosis in ocular disease: a molecular overview. *Poththalmic Genetics*. 1996; 17 (4): 145-165

Noell WK. Effects of environmental lighting and dietary vitamin A on the vulnerability of the retina to light damage. *Photochem. and Photobiol. 1979;* 29:717-723

Noell WK. Possible mechanisms of photoreceptor damage by light in mammalian eyes. *Vision Res*. 1980; 20(12):1163-71

Noell WK, Walker VS, Kang BS, and Berman S. Retinal damage by light in rats. *Invest Ophthalmol Vis Sci*. 1966; 5(5):450-473

Noell WK, Delmell MC, and Albrecht R. Vitamin A Deficiency effect on retina: Dependence on light. *Science*. 1971a; 172:72-76

Noell WK, and Albrecht R. Irreversible effects of visible light on the retina: Role of vitamin A. *Science*. 1971b; 172:76-80

Novoa I, Zhang Y, Zeng H, Jungreis R, Harding HP, Ron D. Stress-induced gene expression requires programmed recovery from translational repression. *EMBO J*. 2003; 22(5):1180-7

Obin M, Shang F, Gong X, Handelman G, Blumberg J, Taylor A. Redox regulation of ubiquitin-conjugating enzymes: mechanistic insights using the thiol-specific oxidant diamide. *FASEB J*. 1998; 12(7):561-9

Obin MS, Jahngen-Hodge J, Nowell T, Taylor A. Ubiquitinylation and ubiquitin-dependent proteolysis in vertebrate photoreceptors (rod outer segments). Evidence for ubiquitinylation of Gt and rhodopsin. *J Biol Chem.* 1996 ; 271(24):14473-84

Ohta S. A multi-functional organelle mitochondrion is involved in cell death, proliferation and disease. *Curr Med Chem.* 2003; 10(23):2485-94

Olah J, Orosz F, Keseru GM, Kovari Z, Kovacs J, Hollan S, Ovadi J. Triosephosphate isomerase deficiency: a neurodegenerative misfolding disease. *Biochem Soc Trans.* 2002; 30(2):30-8

Olshevskaya EV, Calvert PD, Woodruff ML, Peshenko IV, Savchenko AB, Makino CL, Ho YS, Fain GL, Dizhoor AM. The Y99C mutation in guanylyl cyclase-activating protein 1 increases intracellular Ca2+ and causes photoreceptor degeneration in transgenic mice. *J Neurosci.* 2004; 24(27):6078-85

Organisciak DT, Noell WK. The rod outer segment phospholipid/opsin ratio of rats maintained in darkness or cyclic light. *Invest Ophthalmol Vis Sci.* 1977; 16(2):188-90

Organisciak DT, Wang HM, Kou AL. Ascorbate and glutathione levels in the developing normal and dystrophic rat retina: effect of intense light exposure. *Curr Eye Res.* 1984; 3(1):257-67

Organisciak DT, Wang H-M, Li Z-Y, and Tso MOM. The protective effect of ascorbate in retinal light damage of rats. *Invest Ophthalmol Vis Sci.* 1985; 26:1580-1588

Organisciak DT, Jiang YL, Wang HM, Pickford M, Blanks JC. Retinal light damage in rats exposed to intermittent light. Comparison with continuous light exposure. *Invest Ophthalmol Vis Sci.* 1989; 30(5):795-805

Organisciak DT, Xie A, Wang HM, Jiang YL, Darrow RM, and Donoso LA. Adaptive Changes in Visual Cell Transduction Protein Levels: Effect of Light. *Exp Eye Res.* 1991; 53:773-779

Organisciak DT, Binknell IR, and Darrow RM. The effects of L- and D-ascorbic acid administration on retinal tissue levels and light damage in rats. *Current Eye Res.* 1992a; 11 (3):231-241

Organiscaik DT, Darrow RM, Jiang Y-I, Marak GE, and Blanks JC. Protection by dimethylthiourea against retinal light damage in rats. *Invest Ophthalmol Vis Sci.* 1992b; 33 (5):1599-1609

Organisciak DT, Winkler BS. Retinal light damage: Pratical and theoretical considerations. In: *Progress in retinal and eye research.* Osbourne NN. Chader GJ, eds Pergamon Press, Oxford, UK. 1994

Organisciak DT, Kutty RK, Leffak M, Wong P, Messing S, Wiggert B, Darrow RM, Chader GJ. Oxidative damage and responses in retinal nuclei arising from intense light exposure. In: Anderson RE, LaVail MM, Hollyfield JG eds. *Degenerative Diseases of the Retina*, New York, NY: Plenum Press. 1995

Organisciak DT, Darrow RM, Barsalou L, Darrow RA, Kutty RK, Kutty G, Wiggert B. Light history and age-related changes in retinal light damage. *Invest Ophthalmol Vis Sci.* 1998; 39(7):1107-16

Organisciak DT, Li M, Darrow RM, Farber DB. Photoreceptor cell damage by light in young Royal College of Surgeons rats. *Curr Eye Res.* 1999a; 19(2):188-96

Organisciak DT, Darrow RA, Barsalou L, Darrow RM, Lininger LA. Light-induced damage in the retina: differential effects of dimethylthiourea on photoreceptor survival, apoptosis and DNA oxidation. *Photochem Photobiol.* 1999b; 70(2):261-8

Organisciak DT, Darrow RM, Barsalou L, Kutty RK, Wiggert B. Circadian-dependent retinal light damage in rats. *Invest Ophthalmol Vis Sci.* 2000; 41(12):3694-701

Organisciak DT, Darrow RM Barsalou LS A guide to light-induced retinal degeneration and its prevention. In: *Ocular Neuroprotection* edited by Leonard A. Levin and Adriana Di Polo, Marcel Decker, Inc. New York, NY. 2003

Ornstein L. DISC electrophoresis I. Background and theory. *Ann N Y Acad Sci.* 1964; 121:321-49

O'Steen WK, Anderson KV, Shear CR. Photoreceptor degeneration in albino rats: dependency on age. *Invest Ophthalmol Vis Sci.* 1974; 13(5):334-9

O'Steen WK. Hormonal influences on retinal photodamage. In: *The effects of constant lights on visual processes*. Editors Williams TP, Baker BN. Plenum Press, New York, NY 1980

O-Steen WK and Donnelly JE. Antagonistic effects of adrenalectomy and ether/surgical stress on light-induced photoreceptor damage. *Invest Ophthalmol Vis Sci.* 1982; 22 (1):1-7

Osterberg, G. Topography of the layer of rods and cones in the human retina. *Acta Ophthal.* 1935; 6: 1-103

Oyster CW. The human eye: Structure and function. Sinauer Associates, Sunderland, MA. 1999

Pampulha ME, Loureiro V. Interaction of the effects of acetic acid and ethanol on inhibition of fermentation in Saccharomyces cerevisiae. *Biotechnol Lett.* 1989; 11:269-272

Pan HQ, Wang YP, Chissoe SL, Bodenteich A, Wang Z, Iyer K, Clifton SW, Crabtree JS, Roe BA. The complete nucleotide sequence of the SacBII Kan domain of the P1 pAD10-SacBII cloning vector and three cosmid cloning vectors: pTCF, svPHEP, and LAWRIST16. *Genet Anal Tech Appl.* 1994; 11(5-6):181-6

Papermaster DS, Windle J. Death at an early age. Apoptosis in inherited retinal degenerations. *Invest Ophthalmol Vis Sci.* 1995; 36(6):977-83

Pappenheimer AM Jr, Dunlop PC, Adolph KW, Bodley JW. Occurrence of diphthamide in archaebacteria. *J Bacteriol.* 1983; 153(3):1342-7

Paschen W. Shutdown of translation: Lethal or protective? Unfolded protein response versus apoptosis. *J Cerebral Blood Flow and Metabolism.* 2003; 23:773-779

Pastorino JG, Shulga N, Hoek JB. Mitochondrial binding of hexokinase II inhibits Bax-induced cytochrome c release and apoptosis. *J Biol Chem.* 2002; 277(9):7610-8

Pastorino JG, Hoek JB. Hexokinase II: the integration of energy metabolism and control of apoptosis. *Curr Med Chem.* 2003; 10(16):1535-51

Payne AM, Downes SM, Bessant DA, Taylor R, Holder GE, Warren MJ, Bird AC, Bhattacharya SS. A mutation in guanylate cyclase activator 1A (GUCA1A) in an autosomal dominant cone dystrophy pedigree mapping to a new locus on chromosome 6p21.1. *Hum Mol Genet.* 1998; 7(2):273-7

Pedersen AG, Baldi P, Chauvin Y, Brunak S. The biology of eukaryotic promoter prediction--a review. *Comput Chem.* 1999; 23(3-4):191-207

Penn JS, Baker BN, Howard AG, Williams TP. Retinal light-damage in albino rats: lysosomal enzymes, rhodopsin, and age. *Exp Eye Res.* 1985; 41(3):275-84

Penn JS, and Williams TP. Photostasis: Regulation of daily photon-catch by rat retinas in response to various cyclic illuminances. *Exp Eye Res.* 1986; 43:913-928

Penn JS, and Anderson RE. Effect of light history on rod outer-segemnt membrane composition in the rat. *Exp Eye Res.* 1987a; 44:767-778

Penn JS, Naash MI, and Anderson RE. Effects of light history on retinal antioxidants and light damage susceptibility in the rat. *Exp Eye Res.* 1987b; 44:779-788

Pepperberg DR, Okajima T-I.L, Wiggert B, Ripps H, Crouch RK, and Chader GJ. Interphotoreceptor retinoid-binding protein (IRBP), molecular biology and physiological role in the visual cycle of rhodopsin. *Molec Neurobiol.*1993; 7:61-84

Perentesis JP, Genbauffe FS, Veldman SA, Galeotti CL, Livingston DM, Bodley JW, Murphy JR. Expression of diphtheria toxin fragment A and hormone-toxin fusion proteins in toxin-resistant yeast mutants. *PROC NAT ACAD SCI.* 1988; 85: 8386-8390

Perentesis JP, Phan LD, Gleason WB, LaPorte DC, Livingston DM, Bodley JW. Saccharomyces cerevisiae Elongation factor 2: Genetic cloning and characterization of epxression, and G-domain modeling. *J Bio Chem.* 1992; 267(2):1190-1197

Phan LD, Perentesis JP, Bodley JW. Saccharomyces cerevisiae Elongation factor 2: Mutagenesis of the histidine precursor of diphthamide yields a functional protein that is resistant to diphtheria toxin. *J Bio Chem.* 1993; 268(12):8665-8668

Phillis RW, Goodwin S. *Biology of Cancer*. Benjamin Cummings, Pearson Education Inc., San Francisco, CA, 2003

Piatigorsky J, Wistow GJ. Enzyme/crystallins: gene sharing as an evolutionary strategy. *Cell.* 1989; 57(2):197-9

Pinol-Roma S. HnRNP proteins and the nuclear export of mRNA. *Semin Cell Dev Biol.* 1997; 8(1):57-63

Pogue-Geile K, Geiser JR, Shu M, Miller C, Wool IG, Meisler AI, Pipas JM, Ribosomal protein genes are overexpressed in colorectal cancer: isolation of a cDNA clone encoding the human S3 ribosomal protein. *Mol Cell Biol.* 1991; 11(8):3842-3849

Portera-Caillau C, Sung C-H, Nathans J, and Adler R. Apoptotic photoreceptor cell death in mouse models of retinitis pigmentosa. *PROC NAT ACAD SCI.* 1994; 91:974-978

Rabenstein MD, Zhou S, Lis JT, Tjian R. TATA box-binding protein (TBP)-related factor 2 (TRF2), a third member of the TBP family. *Proc Natl Acad Sci U S A.* 1999; 96(9):4791-6

Radlwimmer FB, Yokoyama S. Genetic analyses of the green visual pigments of rabbit (Oryctolagus cuniculus) and rat (Rattus norvegicus). *Gene.* 1998; 218(1-2):103-9

Rakoczy PE, Zhang D, Robertson T, Barnett NL, Papadimitriou J, Constable IJ, Lai CM. Progressive age-related changes similar to age-related macular degeneration in a transgenic mouse model. *Am J Pathol.* 2002; 161(4):1515-24

Rapp LM, and Williams TP. Damage to the albino rat retina produced by low intensity light. *Photochem. Photobiol.* 1979; 29: 731-733

Rapp LM, Williams TP. A parametric study of retinal light damage in albino and in pigmented rats. In The effects of constant lights on visual processes. Editors Williams TP, Baker BN. Plenum Press, New York, NY. 1980a

Rapp LM, Williams TP. The role of ocular pigmentation in protecting against retinal light damage. *Vision Res*. 1980b; 20(12):1127-31

Rapp LM, Talman BL, Dhindsa HS. Separate mechanisms for retinal damage by ultraviolet-A and mid-visible light. *Invest Ophthalmol Vis Sci*. 1990; 31(6):1186-1190

Rapp LM, and Smith SC. Morphologic comparison between rhodopsin-mediated and short-wavelength classes of retinal light-damage. *Invest Ophthalmol Vis Sci*. 1992; 33 (12):3367-3377

Redmond, T. M.; Yu, S.; Lee, E.; Bok, D.; Hamasaki, D.; Chen, N.; Goletz, P.; Ma, J.-X.; Crouch, R. K.; Pfeifer, K. Rpe65 is necessary for production of 11-cis-vitamin A in the retinal visual cycle. *Nature Genet*. 1998; 20: 344-351

Remé CE, Weller M, Szczesny P, Munz K, Hafezi F, Reinboth JJ, Clausen M. Light-induced apoptosis in the rat retina *in vivo*: morphologic features, threshold and time course. In *Degenerative Diseases of the Retina*. Plenum Press, New York, NY. 1995

Remé CE., Hafezi F, Marti A, Munz K, Reinboth JJ. Light damage to retina and pigment epithelium. In *The Retinal Pigment Epithelium: Function and disease*. Oxford University Press, New York, NY. 1998a

Remé CE, Grimm C, Hafezi F, Marti A, Wenzel A. Apoptotic cell death in retinal degenerations. *Prog Retin Eye Res*. 1998b; 17(4):443-64

Remé CE, Grimm C, Hafezi F, Iseli HP, Wenzel A. Why study rod cell death in retinal degenerations and how? *Doc Ophthalmol*. 2003; 106(1): 25-9

Remenyi A, Scholer HR, Wilmanns M. Combinatorial control of gene expression. *Nat Struct Mol Bio*l. 2004; 11(9):812-5

Ron D. Translational control in the endoplasmic reticulum stress response. *J Clin Invest*. 2002; 110(10):1383-1388

Ronai Z. Glycolytic enzymes as DNA binding proteins. *Int J Biochem*. 1993; 25(7):1073-6

Ross RS. Molecular and mechanical synergy: cross-talk between integrins and growth factor receptors. *Cardiovasc Res*. 2004; 63(3):381-90
Rotstein NP, Politi LE, German OL, Girotti R. Protective effect of docosahexaenoic acid on oxidative stress-induced apoptosis of retina photoreceptors. *Invest Ophthalmol Vis Sci*. 2003; 44(5):2252-9

Roybal CN, Yang S, Sun CW, Hurtado D, Vander Jagt DL, Townes TM, Abcouwer SF. Homocysteine increases the expression of vascular endothelial growth factor by a mechanism involving endoplasmic reticulum stress and transcription factor ATF4. *J Biol Chem*. 2004; 279(15):14844-52

Ruffolo JJ Jr, Ham WT Jr, Mueller HA, Millen JE. Photochemical lesions in the primate retina under conditions of elevated blood oxygen. *Invest Ophthalmol Vis Sci*. 1984; 25(8):893-8

Saari JC. The biochemistry of sensory transduction in vertebrate photoreceptors. *Adlers Physiology of the Eye, 9th Edition*, Mosby Year Book, St. Louis, MI, 1992

Sakaguchi H, Miyagi M, Darrow RM, Crabb JS, Hollyfield JG, Organisciak DT, Crabb JW. Intense light exposure changes the crystallin content in retina. Exp Eye Res. 2003; 76(1):131-3

Salinas PC. Wnt factors in axonal remodelling and synaptogenesis. *Biochem Soc Symp*. 1999; 65:101-9

Sambrook J, Fritsch EF, Maniatis T. Molecular Cloning: A Laboratory Manual. Second ed. Cold Spring Harbor Laboratory Press, Cold Spring Harbor, NY. 1989

Sanyal S, Hawkins RK. Development and degeneration of retina in rds mutant mice: effects of light in the rate of degeneration in albino and pigmented homozygous and heterozygous mutant and normal mice. *Vis Res*. 1986; 26:1177-1185

Sastry SK, Horwitz AF. Integrin cytoplasmic domains: mediators of cytoskeletal linkages and extra- and intracellular initiated transmembrane signaling. *Curr Opin Cell Biol*. 1993; 5(5):819-31

Savage JR, McLaughlin JN, Skiba NP, Hamm HE, Willardson BM. Functional roles of the two domains of phosducin and phosducin-like protein. *J Biol Chem*. 2000; 275(39):30399-407

Savolainen KM, Loikkanen J, Eerikainen S, Naarala J. Interactions of excitatory neurotransmitters and xenobiotics in excitotoxicity and oxidative stress: glutamate and lead. *Toxicol Lett*. 1998; 102-103:363-7

Scharschmidt E, Wegener E, Heissmeyer V, Rao A, Krappmann D. Degradation of Bcl10 induced by T-cell activation negatively regulates NF-kappa B signaling. *Mol Cell Biol*. 2004; 24(9):3860-73

Schwerk C, Schulze-Osthoff K. Non-apoptotic functions of caspases in cellular proliferation and differentiation. *Biochem Pharmacol*. 2003; 66(8):1453-8

Scortegagna M, Galdzicki Z, Rapoport SI, Hanbauer I. Activator protein-1 DNA binding activation by hydrogen peroxide in neuronal and astrocytic primary cultures of trisomy-16 and diploid mice. *Brain Res Mol Brain Res*. 1999; 73(1-2):144-50

Seher TC, Leptin M. Tribbles, a cell-cycle brake that coordinates proliferation and morphogenesis during Drosophila gastrulation. *Curr Biol.* 2000; 10(11):623-9

Semple-Rowland SL, and Dawson WW. Cyclic light intensity threshold for retinal damage in albino rats raised under 6 lx. *Exp Eye Res.* 1987; 44: 643-661

Sergeev YV, Hejtmancik JF, Wingfield PT. Energetics of domain-domain interactions and entropy driven association of beta-crystallins. *Biochemistry.* 2004; 43(2):415-24

Seshadri T, Uzman JA, Oshima J, Campisi J. Identification of a transcript that is down-regulated in senescent human fibroblasts. *J Biol Chem.* 1993; 268(25):18474-18480

Shaham S, Shuman MA, Herskowitz I. Death-defying yeast identify novel apoptosis genes. *Cell.* 1998; 92:425-427

Shahinfar S, Edward DP, Tso MO. A pathologic study of photoreceptor cell death in retinal photic injury. *Curr Eye Res.* 1991; 10(1):47-59

Shang F, Gong X, Taylor A. Activity of ubiquitin-dependent pathway in response to oxidative stress. Ubiquitin-activating enzyme is transiently up-regulated. *J Biol Chem.* 1997; 272(37):23086-93

Sheline CT, Choi DW. Neuronal death in cultured murine cortical cells is induced by inhibition of GAPDH and triosephosphate isomerase. *Neurobiol Dis.* 1998; 5(1):47-54

Shikama NJ, Lyon J, and La Thangue NB. The p300/CBP family: integrating signals with transcription factors and chromatin. *Trends in Cell Biology*, 1997; 7:230-236

Shimada M, Nakadai T, Tamura TA. TATA-binding protein-like protein (TLP/TRF2/TLF) negatively regulates cell cycle progression and is required for the stress-mediated G(2) checkpoint. *Mol Cell Biol.* 2003; 23(12):4107-20

Shinoda K, Nakamura Y, Matsushita K, Shimoda K, Okita H, Fukuma M, Yamada T, Ohde H, Oguchi Y, Hata J, Umezawa A. Light induced apoptosis is accelerated in transgenic retina overexpressing human EAT/mcl-1, an anti-apoptotic bcl-2 related gene. *Br J Ophthalmol.* 2001; 85(10):1237-43

Siegmund KD, Klink F. Production of an antiserum specific to the ADP-ribosylated form of Elongation factor 2 from archaebacteria and eukaryotes. *FEBS Lett.* 1992; 312(2-3):139-42

Sim AT, Baldwin ML, Rostas JA, Holst J, Ludowyke RI. The role of serine/threonine protein phosphatases in exocytosis. *Biochem J.* 2003; 373(Pt 3):641-59

Simons K. Artificial light and early-life exposure in age-related macular degeneration and in cataractogenic phototoxicity. *Arch Ophthalmol.* 1993; 111:297-298

Singh M, Savitz SI, Hoque R, Gupta G, Roth S, Rosenbaum PS, Rosenbaum DM. Cell-specific caspase expression by different neuronal phenotypes in transient retinal ischemia. *J Neurochem*. 2001; 77:466-75

Skaper SD. Poly(ADP-Ribose) polymerase-1 in acute neuronal death and inflammation: a strategy for neuroprotection. *Ann N Y Acad Sci*. 2003; 993:217-28

Slee EA, Harte MT, Kluck RM, Wolf BB, Casiano CA, Newmeyer DD, Wang HG, Reed JC, Nicholson DW, Alnemri ES, Green DR, Martin SJ. Ordering the cytochrome c-initiated caspase cascade: hierarchical activation of caspases-2, -3, -6, -7, -8, and -10 in a caspase-9-dependent manner. *J Cell Biol*. 1999; 144:281-92

Smith JA. *Current Protocols in Molecular Biology*. John Wiley and Sons, Inc. Winston-Salem, NC.1995

Smith PK, Krohn RI, Hermanson GT, Mallia AK, Gartner FH, Provenzano MD, Fujimoto EK, Goeke NM, Olson BJ, Klenk DC. Measurement of protein using bicinchoninic acid. *Anal Biochem*. 1985; 150(1):76-85

Smith SB, Bora N, McCool D, Kutty G, Wong P, Kutty RK, and Wiggeert B. Photoreceptor Cells in the Vitiligo Mouse Die by Apoptosis. *Invest Ophthalmol Vis Sci*. 1995; 36 (11):2193-2201

Specht S, Leffak M, Darrow RM, Organisciak DT. Damage to rat retinal DNA induced in vivo by visible light. *Photochem Photobiol*. 1999; 69(1):91-8

Sperling HG. Prolonged intense spectral light effects on Rhesus retina. In: *The Effects of Constant Light on Visual Processes*. Plenum Press, New York, NY. 1980a

Sperling HG. Are ophthalmologists exposing their patients to dangerous light levels? *Invest Ophthalmol Vis Sci*. 1980b; 19(9):989-90

Sperling HG, Johnson C, Harwerth RS. Differential spectral photic damage to primate cones. *Vision Res*. 1980; 20(12):1117-25

Spillantini MG, Schmidt ML, Lee VM, Trojanowski JQ, Jakes R, Goedert M. Alpha-synuclein in Lewy bodies. *Nature*. 1997; 388(6645):839-40

Stamnes M. Regulating the actin cytoskeleton during vesicular transport. *Curr Opin Cell Biol*. 2002; 14(4):428-33

Steele FR. Shedding light on inherited blindness: the genetics of Retinitis pigmentosa. *J NIH Res*. 1994; 6:58-62

Stepczynski J. Defining the molecular phenotype of the rat retina during the commitment phase of LIRD: a model of human retinal degenerative disease. M.Sc. thesis. University of Alberta, Edmonton, AB. 2001

Stocker R. Induction of heme oxygenase as a defense against oxidative stress. *Free Radical Res Commun.* 1990; 9:101-112

Strachan T, Read AP. *Human Molecular Genetics*, Second edition. Bios Scientific Publishing, Abingdom, Oxfordshire, Gt. Britian, 1999.

Suda T, Nagata S. Purification and characterization of the Fas-ligand that induces apoptosis. *J Exp Med.* 1994; 179:873-9

Sun HB, Zhu YX, Yin T, Sledge G, and Yang Y-C. MRG1, the product of a melanocyte-specific gene related gene, is a cytokine-inducible transcription factor with transforming activity. *PROC NAT ACAD SCI.* 1998; 95:13555-13560

Swerdlow RH, Parks JK, Miller SW, Tuttle JB, Trimmer PA, Sheehan JP, Bennett JP Jr, Davis RE, Parker WD Jr. Origin and functional consequences of the complex I defect in Parkinson's disease. *Ann Neuro*l. 1996; 40(4):663-71

Syntichaki P, Tavernarakis N. Death by necrosis. Uncontrollable catastrophe, or is there order behind the chaos? *EMBO Rep.* 2002; 3(7):604-9

Szczesny PJ, Munz K, Remé CE. 1995. Light damage in the rat retina: Patterns of acute lesions and recovery. In *Cell and tissue protection in Ophthalmology.* Hippokrates Verlag, Stuttgart. 1995

Szel, A. and Rohlich, P. 1992. Two cone types of rat retina detected by anti-visual pigment antibodies. *Exp Eye Res.* 55:47-52

Takahashi A, Masuda A, Sun M, Centonze VE, Herman B. Oxidative stress-induced apoptosis is associated with alterations in mitochondrial caspase activity and Bcl-2-dependent alterations in mitochondrial pH (pHm).*Brain Res Bull.* 2004; 62(6):497-504

Takeda A, Mallory M, Sundsmo M, Honer W, Hansen L, Masliah E. Abnormal accumulation of NACP/alpha-synuclein in neurodegenerative disorders. *Am J Pathol.* 1998; 152(2):367-72

Tanaka M, Schinke M, Liao HS, Yamasaki N, Izumo S. Nkx2.5 and Nkx2.6, homologs of Drosophila tinman, are required for development of the pharynx. *Mol Cell Biol.* 2001; 21(13):4391-8

Tanito M, Nishiyama A, Tanaka T, Masutani H, Nakamura H, Yodoi J, Ohira A. Change of redox status and modulation by thiol replenishment in retinal photooxidative damage. *Invest Ophthalmol Vis Sci.* 2002a; 43(7):2392-400

Tanito M, Masutani H, Nakamura H, Ohira A, Yodoi J. Cytoprotective effect of thioredoxin against retinal photic injury in mice. *Invest Ophthalmol Vis Sci.* 2002b; 43(4):1162-7

Taylor A, and Schalach W. Moderators of "nutrition and eye diseases". *Exp Eye Res.* 1992; 55:5152-5153

Taylor HR, Munoz B, West S, Bressler NM, Bressler SB, Rosenthal FS. Visible light and risk of age-related macular degeneration. *Trans Am Ophthalmol Soc.* 1990; 88:163-173

Thilmann R, Xie Y, Kleihues P, Kiessling M. Persistent inhibition of protein synthesis precedes delayed neuronal death in postischemic gerbil hippocampus. *Acta Neuropathol* (Berl). 1986; 71(1-2):88-93

Thornton S, Anand N, Purcell D, Lee J. Not just for housekeeping: protein initiation and Elongation factors in cell growth and tumorigenesis. *J Mol Med.* 2003; 81(9):536-48

Thulin CD, Howes K, Driscoll CD, Savage JR, Rand TA, Baehr W, Willardson BM. The immunolocalization and divergent roles of phosducin and phosducin-like protein in the retina. *Mol Vis.* 1999; 5:40

Thulin CD, Savage JR, McLaughlin JN, Truscott SM, Old WM, Ahn NG, Resing KA, Hamm HE, Bitensky MW, Willardson BM. Modulation of the G protein regulator phosducin by Ca2+/calmodulin-dependent protein kinase II phosphorylation and 14-3-3 protein binding. *J Biol Chem.* 2001; 276(26):23805-15

Tian G, Lewis SA, Feierbach B, Stearns T, Rommelaere H, Ampe C, Cowan NJ. Tubulin subunits exist in an activated conformational state generated and maintained by protein cofactors. *J Cell Biol.* 1997; 138(4):821-32

To K, Adamian M, Dryja TP, Berson EL. Retinal histopathology of an autopsy eye with advanced retinitis pigmentosa in a family with rhodopsin Glu181Lys. *Am J Ophthalmol.* 2000; 130(6):790-2

Tonin P, Shanske S, Miranda AF, Brownell AK, Wyse JP, Tsujino S, DiMauro S. Phosphoglycerate kinase deficiency: biochemical and molecular genetic studies in a new myopathic variant (PGK Albert). *Neurol.* 1993; 43:387-391

Tso MOM, Woodford BJ, Lam K-W. Distribution of ascorbate in normal primate retina and after photic injury: a biochemical, morphological correlated study. *Current Eye Res.* 1984; 3 (1):181-191

Tso MOM, Zhang C, Abler AS, Chang C-J, Wong F, Chang G-Q, and Lam TT. Apoptosis Leads to Photoreceptor Degeneration in Inherited Retinal Dystrophy of RCS Rats. *Invest Ophthalmol Vis Sci.* 1994; 35:2693-2699

Tucker RP. The roles of microtubule-associated proteins in brain morphogenesis: a review. *Brain Res Brain Res Rev*. 1990; 15(2):101-20

Ueda N, Shah SV. Endonuclease-induced DNA damage and cell death in oxidant injury to renal tubular epithelial cells. J Clin Invest. 1992; 90(6):2593-7

van den Ouweland JM, Lemkes HH, Ruitenbeek W, Sandkuijl LA, de Vijlder MF, Struyvenberg PA, van de Kamp JJ, Maassen JA. Mutation in mitochondrial tRNA(Leu)(UUR) gene in a large pedigree with maternally transmitted type II diabetes mellitus and deafness. *Nat Genet*. 1992; 1(5):368-71

Vander Heiden MG, Plas DR, Rathmell JC, Fox CJ, Harris MH, Thompson CB. Growth factors can influence cell growth and survival through effects on glucose metabolism. *Mol Cell Biol*. 2001; 21(17):5899-912.

van Driel R, Fransz PF, Verschure PJ. The eukaryotic genome: a system regulated at different hierarchical levels. *J Cell Sci*. 2003; 116(Pt 20):4067-75

Van Hoof C, Goris J. Phosphatases in apoptosis: to be or not to be, PP2A is in the heart of the question. *Biochim Biophys Acta*. 2003; 1640(2-3):97-104

Van Hoof C, Goris J. PP2A fulfills its promises as tumor suppressor: which subunits are important? *Cancer Cell*. 2004; 5(2):105-6

Van Ness BG, Howard JB, Bodely JW. Isolation and properties of the trypsin-derived ADP-ribosyl peptide from diphtheria toxin-modified yeast Elongation factor 2. *J Bio Chem*. 1978; 253(24):8687-8690

Van Ness BG, Howard JB, Bodley JW. ADP-Ribosylation of Elongation factor 2 by diphtheria toxin. NMR spectra and proposed structures of ribosyl-diphthamide and its hydrolysis products. *J Bio Chem*. 1980a; 255(22):10710-10716

Van Ness BG, Howard JB, Bodley JW. ADP-ribosylation of Elongation factor 2 by diphtheria toxin: Isolation and properties of this novel ribosyl-amino acid and its hydrolysis products. *J Bio Chem*. 1980b; 255(22):10717-10720

Vander Heiden MG, Plas DR, Rathmell JC, Fox CJ, Harris MH, Thompson CB. Growth factors can influence cell growth and survival through effects on glucose metabolism. *Mol Cell Biol*. 2001; 21(17):5899-912

Vardi A, Berman-Frank I, Rozenberg T, Hadas O, Kaplan A, Levine A. Programmed cell death of the dinoflagellate Peridinium gatunense is mediated by CO(2) limitation and oxidative stress. *Curr Biol*. 1999; 9(18):1061-4

Vaughan DK, Nemke JL, Fliesler SJ, Darrow RM, Organisciak DT. Evidence for a circadian rhythm of susceptibility to retinal light damage. *Photochem Photobiol.* 2002; 75(5):547-53

Vaughan DK, Coulibaly SF, Darrow RM, Organisciak DT. A morphometric study of light-induced damage in transgenic rat models of retinitis pigmentosa. *Invest Ophthalmol Vis Sci.* 2003; 44(2):848-55

Vazquez-Prado J, Casas-Gonzalez P, Garcia-Sainz JA. G protein-coupled receptor cross-talk: pivotal roles of protein phosphorylation and protein-protein interactions. *Cell Signal.* 2003; 15(6):549-57

Wahl S, Barth H, Ciossek T, Aktories K, Mueller BK. Ephrin-A5 induces collapse of growth cones by activating Rho and Rho kinase. *J Cell Biol.* 2000; 149(2):263-70

Walker AK, Shi Y, Blackwell TK. A extensive requirement for Transcription Factor II-D specific TAF-1 in Caenorhabiditis elegans embryonic transcription. *J Biol Chem.* 2004; 279(15):15339-15347

Wang M, Lam TT, Tso MO, Naash MI. Expression of a mutant opsin gene increases the susceptibility of the retina to light damage. *Vis Neurosci.* 1997; 14(1):55-62

Watson KL, Konrad KD, Woods DF, Bryant PJ. Drosophila homologue of the human S6 ribosomal protein is required for tumor suppression in the hematopoietic system. *PROC NAT ACAD SCI USA.* 1992; 89:11302-11306

Wegmann D, Hess P, Baier C, Wieland FT, Reinhard C. Novel isotypic gamma/zeta subunits reveal three coatomer complexes in mammals. *Mol Cell Biol.* 2004; 24(3):1070-80

Wellington CL, Ellerby LM, Gutekunst C-A, Rogers D, Warby S, Graham RK, Loubser O, van Raamsdonk J, Singaraja R, Yang Y-Z, Gafni J, Bredesen D, Hersch SM, Leavitt BR, Roy S, Nicholson DW, Hayden MR. Caspase cleavage of mutant huntingtin preceeds neruodegeneration in Huntingtin's Disease. *J Neurosci.* 2002; 22(18):7862-7872

Weng J, Mata NL, Azarian SM, Tzekov RT, Birch DG, Travis GH. Insights into the function of Rim protein in photoreceptors and etiology of Stargardt's disease from the phenotype in abcr knockout mice. *Cell.* 1999; 98(1):13-23

Wenzel A, Grimm C, Marti A, Kueng-Hitz N, Hafezi F, Niemeyer G, Remé CE. c-fos controls the "private pathway" of light-induced apoptosis of retinal photoreceptors. *J Neurosci.* 2000; 20(1):81-8

Wenzel A, Remé CE, Williams TP, Hafezi F, Grimm C. The Rpe65 Leu450Met variation increases retinal resistance against light-induced degeneration by slowing rhodopsin regeneration. *J Neurosci.* 2001a; 21(1):53-8

Wenzel A, Grimm C, Seeliger MW, Jaissle G, Hafezi F, Kretschmer R, Zrenner E, Remé CE. Prevention of photoreceptor apoptosis by activation of the glucocorticoid receptor. *Invest Ophthalmol Vis Sci*. 2001b; 42(7):1653-9

Wenzel A, Grimm C, Samardzija M, Remé CE. The genetic modifier Rpe65Leu(450): effect on light damage susceptibility in c-Fos-deficient mice. *Invest Ophthalmol Vis Sci*. 2003; 44(6):2798-802

West S, Vitale S, Hallfrisch *et al*, Are antioxidants or supplements protective for age-related macular degeneration? *Arch Ophthalmol*. 1994; 112:222-227

Westlin WF. Integrins as targets of angiogenesis inhibition. *Cancer J*. 2001; 7 Suppl 3:S139-43

Wiegand, R.D., Giusto, N.M., Rapp, L.M., and Anderson, R.E. Evidence for rod outer segment lipid peroxidation following constant illumination of the rat retina. *Invest Ophthalmol Vis Sci*. 1983; 24:1433-1435

Wilkie SE, Li Y, Deery EC, Newbold RJ, Garibaldi D, Bateman JB, Zhang H, Lin W, Zack DJ, Bhattacharya SS, Warren MJ, Hunt DM, Zhang K. Identification and functional consequences of a new mutation (E155G) in the gene for GCAP1 that causes autosomal dominant cone dystrophy. *Am J Hum Genet*. 2001; 69(3):471-80

Wilkinson KD. Roles of ubiquitinylation in proteolysis and cellular regulation. *Annu Rev Nutr*. 1995; 15:161-89

Williams JG. The preparation and screening of a cDNA clone bank in Genetic Engineering 1, Ed Williamson, R.Academic Press, London, Gt. Britian. 1981

Williams TP, and Howell WL. Action Spectrum of Retinal Light-Damage in Albino Rats. *Invest Ophthalmol Vis Sci*. 1983; 24:285-287

Wilson AS, Hobbs BG, Speed TP, Rakoczy PE. The microarray: potential applications for ophthalmic research. *Mol Vis*. 2002; 8:259-70
Wilson SE. Stimulus-specific and cell type-specific cascades: emerging principles relating to control of apoptosis in the eye. *Exp Eye Res*. 1999; 69:255-66

Wittenhagen LM, Kelley SO. Impact of disease-related mitochondrial mutations on tRNA structure and function. *Trends Biochem Sci*. 2003; 28(11):605-11

Wolf BB, Green DR. Suicidal tendencies: apoptotic cell death by caspase family proteinases. *J Biol Chem*. 1999; 274:20049-52

Wolfrum U, Schmitt A. Rhodopsin transport in the membrane of the connecting cilium of mammalian photoreceptor cells. *Cell Motil Cytoskeleton*. 2000; 46(2):95-107

Wong P. Lateral genetics: An approach to the cloning of potential human chorio-retinal X-linked genes. Ph.D. thesis. University of Ottawa, Ottawa, Ontario, Canada, 1991.

Wong P. Apoptosis, retinitis pigmentosa, and degeneration. *Biochem Cell Biol*. 1994; 72: 489-498

Wong P, Borst DE, Farber D, Danciger JS, Tenniswood M, Chader GJ, and van Veen T. Increased TRPM-2/clusterin levels during the time of retinal degeneration in mouse models of retinitis pigmentosa. *Biochem Cell Biol.* 1994a; 72:439-446

Wong P, Kutty RK, Darrow RM, Shivaram S, Kutty G, Fletcher RT, Wiggert B, Chader G, and Organisciak DT. Changes in clusterin expression associated with light-induced retinal damage in rats. *Biochem Cell Biol.* 1994b; 72 (11 and 12):499-503

Wong P, Ulyanova T, Organisciak DT, Bennett S, Lakins J, Arnold JM, Kutty RK, Tenniswood M, vanVeen T, Darrow RM, and Chader G. Expression of multiple forms of clusterin during light-induced retinal degeneration. *Current Eye Research*. 2001; 23(3): 157-165

Wool IG, Chan YL, Gluck A. Structure and evolution of mammalian ribosomal proteins. *Biochem Cell Biol*. 1995; 73(11-12): 933-947

Wool IG. Extraribosomal functions of ribosomal proteins. *Trend Biochem Sci.* 1996; 21(5): 164-165

WordIQ online dictionary, July, 2004. (http://www.wordIQ.com/dictionary).

Wu J, Gorman A, Zhou X, Sandra C, Chen E. Involvement of caspase-3 in photoreceptor cell apoptosis induced by in vivo blue light exposure. *Invest Ophthalmol Vis S*ci. 2002; 43(10):3349-54

Wu T, Chen Y, Chiang SK, Tso MO. NF-kappaB activation in light-induced retinal degeneration in a mouse model. *Invest Ophthalmol Vis Sci.* 2002; 43(9):2834-40

Wu T, Chiang SK, Chau FY, Tso MO. Light-induced photoreceptor degeneration may involve the NF kappa B/caspase-1 pathway in vivo. *Brain Res*. 2003; 967(1-2):19-26

Xu L, Ma J, Seigel GM, Ma JX. l-Deprenyl, blocking apoptosis and regulating gene expression in cultured retinal neurons. *Biochem Pharmacol*. 1999; 58(7):1183-90

Xu J, Wu D, Slepak VZ, Simon MI. The N terminus of phosducin is involved in binding of beta gamma subunits of G protein. *Proc Natl Acad Sci* U S A. 1995; 92(6):2086-90

Yamaizumi M, Mekada E, Uchida T, Okada Y. One molecule of diphtheria toxin fragment A introduced into a cell can kill the cell. *Cell*. 1978; 15(1):245-50

Yamao F. Ubiquitin system: selectivity and timing of protein destruction. *J Biochem (Tokyo)*. 1999; 125(2):223-9

Yamashita H, Horie K, Yamamoto T, Nagano T, and Hirano T. Light-Induced Retinal Damage in Mice: Hydrogen peroxide production and superoxide dismutase activity in the retina. *Retina*. 1992; 12:59-66

Yang E, Zha J, Jockel J, Boise LH, Thompson CB, Korsmeyer SJ. Bad, a heterodimeric partner for Bcl-XL and Bcl-2, displaces Bax and promotes cell death. *Cell*. 1995; 80(2):285-91

Yokota S, Yanagi H, Yura T, Kubota H. Cytosolic chaperonin-containing t-complex polypeptide 1 changes the content of a particular subunit species concomitant with substrate binding and folding activities during the cell cycle. *Eur J Biochem*. 2001; 268(17):4664-73

Yonish-Rouach E, Deguin V, Zaitchouk T, Breugnot C, Mishal Z, Jenkins JR, May E. Transcriptional activation plays a role in the induction of apoptosis by transiently transfected wild-type p53. *Oncogene*. 1995; 11(11):2197-205

Yoshizawa K, Nambu H, Yang J, Oishi Y, Senzaki H, Shikata N, Miki H, Tsubura A. Mechanisms of photoreceptor cell apoptosis induced by N-methyl-N-nitrosourea in Sprague-Dawley rats. *Lab Invest*. 1999; 79:1359-67

Yoshizawa K, Yang J, Senzaki H, Uemura Y, Kiyozuka Y, Shikata N, Oishi Y, Miki H, Tsubura A. Caspase-3 inhibitor rescues N -methyl- N -nitrosourea-induced retinal degeneration in Sprague-Dawley rats. *Exp Eye Res*. 2000; 71:629-35

Yu, S.-W.; Wang, H.; Poitras, M. F.; Coombs, C.; Bowers, W. J.; Federoff, H. J.; Poirier, G. G.; Dawson, T. M.; Dawson, V. L. Mediation of poly(ADP-ribose) polymerase-1-dependent cell death by apoptosis-inducing factor. *Science*. 2002; 297: 259-263

Zarbin MA. Current concepts in the pathogenesis of age-related macular degeneration. *Arch Ophthalmol*. 2004; 122(4):598-614

Zhang K, Kniazeva M, Han M, Li W, Yu Z, Yang Z, Li Y, Metzker ML, Allikmets R, Zack DJ, Kakuk LE, Lagali PS, Wong PW, MacDonald IM, Sieving PA, Figueroa DJ, Austin CP, Gould RJ, Ayyagari R, Petrukhin K. A 5-bp deletion in ELOVL4 is associated with two related forms of autosomal dominant macular dystrophy. *Nat Genet*. 2001; 27(1):89-93

Zhang W, Hawse J, Huang Q, Sheets N, Miller KM, Horwitz J, Kantorow M. Decreased expression of ribosomal proteins in human age-related cataract. *Invest Ophthalmol Vis Sci*. 2002; 43(1);198-204

Zhang XM, Yang Z, Karan G, Hashimoto T, Baehr W, Yang XJ, Zhang K. Elovl4 mRNA distribution in the developing mouse retina and phylogenetic conservation of Elovl4 genes. *Mol Vis.* 2003; 9:301-7